FERMILAB-PROPOSAL-0822

March 19, 1991

Proposal for

A Long Baseline Neutrino Oscillation Experiment Using the Soudan 2 Neutrino Detector

P822 collaboration

W.W.M. Allison[3], G.J. Alner[1], D.S. Ayres[1], L. Balka[1], W.L. Barrett[1], R.E. Blair[1], P. Border[2], C.B. Brooks[3], J.H. Cobb [3], D.J.A. Cockerill[4], H. Courant [2], J. Dawson[1], B. Ewen[5], T.H. Fields[1], C. García-García[9] G. Giller[3], M.C. Goodman[1], R. Gray[2], N. Hill[1], D.J. Jankowski[1], K. Johns[6], T. Kafka[5], S. Kasahara[2], J. Kochocki[8], W. Leeson[5], P.J. Litchfield[4], N. Longley[2], F. Lopez[1], M. Lowe[2] W. A. Mann[5], M. L. Marshak[2], E.N. May[1], L. McMaster[5], R. Milburn[5], W. Miller[2], A. Napier[5], W. Oliver[5], G.F. Pearce[1], D.H.Perkins[3], E.A. Peterson[2], L.E. Price[1], J. Repond[1], D. Roback[2], K. Ruddick[2], D. Schmid[2], J. Schneps[5], P. Schoessow[1], M. Shupe[6], N. Sundaralingam[5], R. Talaga[1], M.A. Thomson[3], J. Thron[1], H. J. Trost[1], G. Villaume[2], S. Werkema[7] and N. West[3]

Argonne[1] - Minnesota[2] - Oxford[3] - Rutherford[4] - Tufts[5]

[6]Arizona
[7]Fermilab
[8]Notre Dame
[9]Valencia

Contents

Abstract

We propose a long baseline neutrino oscillation experiment using a fine-grained calorimeter which is appropriate to the study of neutrino interactions. The high flux from the Main Injector neutrino beams, coupled with moderate neutrino energies and the long distance from Fermilab to Soudan Minnesota, will combine to provide unprecedented sensitivity to several possible modes of neutrino oscillation. The high spatial resolution and good energy resolution of the Soudan 2 detector make it well suited to study leptons and hadrons in neutrino interactions. Our key measurements will will involve the neutral current to charged current ratio and will not depend upon a knowledge of the absolute flux. However, we will simultaneously measure the absolute flux with a near detector, which will provide important consistency checks on any observed signals.

1 Introduction

A long baseline neutrino oscillation experiment using the Fermilab main injector and the sensitive Soudan 2 fine grained calorimeter would be able to probe an important and large new area of parameter space for the mode $\nu_\mu \rightarrow \nu_\tau$. The capabilities of the detector are such that a number of independent tests of the oscillation hypothesis can be made. The experiment will either discover neutrino oscillations in a compelling way (if they exist in the sensitive region of parameter space), or rule them out.

A long baseline neutrino oscillation experiment was first suggested for Fermilab in 1977[1]. A sensitive new experiment is considered in this proposal and is motivated by five factors:

- The possible observation of atmospheric ν_μ oscillations by the Kamiokande measurement of an anomalous ν_μ/ν_e ratio.[2]
- The interpretation of the missing solar neutrino problem as evidence for matter-induced $\nu_e \rightarrow \nu_\mu$ oscillations.[3]
- The near completion of the 1 kiloton Soudan 2 nucleon decay detector and its demonstrated capability in neutrino detection.[4]
- The planned new Main Injector at Fermilab which could be a source of large neutrino fluxes with relatively low energy.[5][6] and
- The design of a double horn high intensity neutrino beam which could be targeted on a remote North American underground detector such as Soudan 2[7].

In a nine month run with a 120 GeV proton beam and a conventional double horn neutrino beam aimed at the Soudan 2 detector 800 km away, a search could be made for neutrino oscillations with particular emphasis on the most likely oscillation mode $\nu_\mu \rightarrow \nu_\tau$. If evidence for oscillations is not found, new limits would be set extending the Δm^2 excluded region from 0.3 eV^2 to 0.0025 eV^2 for mixing angles $\sin^2(2\theta) > 0.06$ at 90% confidence level. We will show that Soudan 2 could set the limits which are shown in figure 1. We plan to use a number of Soudan 2 modules as a near detector at Fermilab in order to keep systematic errors at a low level.

The physics motivation for a long baseline neutrino experiment is discussed in section 2. The issues covered include the present status of the search for neutrino oscillations as well as the interest in a particular region of parameter space (Δm^2 vs $\sin^2(2\theta)$) which is based on the reported atmospheric ν_μ and solar ν_e deficits mentioned above.

The properties of the Soudan 2 detector are covered in section 3, and the double horn neutrino beam is discussed in section 4. The physics capabilities of the Soudan 2 detector with a Fermilab beam are covered in section 5. The expectation for ν_μ disappearance and ν_τ appearance experiments are included, as well as a number of other ν experiments that we could carry out. Performance and calibration of the Soudan 2 detector are discussed in section 6. In section 7 we discuss the requests of the P822 collaboration from Fermilab for this proposal.

A long baseline neutrino oscillation experiment, carried out in Soudan 2 and concentrating on Δm^2 of 1.0 to $10^{-3} eV^2$ for the mode $\nu_\mu \rightarrow \nu_\tau$, well complements the proposed Fermilab

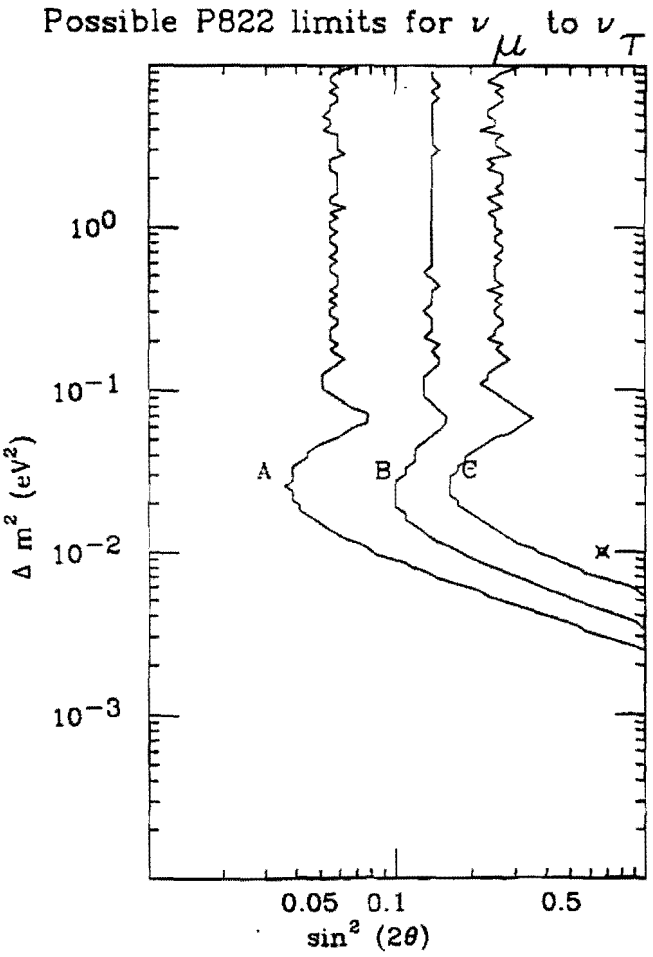

Figure 1: 90%CL Limits on $\nu_\mu \rightarrow \nu_\tau$ oscillations attainable by Soudan. Curve A is based on the $R_{near/far}$ test using the Soudan 2 shield. B is based on the $R_{"\nu e"/"cc"}$ test, and C is based on $R_{"\nu e"/"cc"}$ test in the calorimeter. The point is Kamioka's "best fit". These tests are described in section 5.

P803 emulsion experiment with its search for $\nu_\mu \rightarrow \nu_\tau$ at higher Δm^2 and lower mixing angle.

2 Physics Motivation for Long Baseline Neutrino Experiments

In this section we discuss some of the previous neutrino oscillation searches. These searches have been motivated by the possible existence of a weak mixing matrix analogous to the quark mixing (CKM) matrix. We then discuss two recent experimental results which specifically motivate an interest in the region of parameter space which this proposal could explore. The first is a result on the flavor composition of atmospheric neutrinos which can be explained by $\nu_\mu \rightarrow \nu_\tau$ (or $\nu_\mu \rightarrow \nu_e$) oscillations in a particular region of parameter space ($\sin^2(2\theta) > 0.1, \Delta m^2 \sim 10^{-2}$ eV^2). The other is the widely discussed explanation of the solar neutrino problem as matter enhanced $\nu_e \rightarrow \nu_\mu$ oscillation (MSW effect) which, when coupled with a see-saw mechanism[8] for the mass hierarchy of lepton families, again leads to $(\Delta m^2) \sim 10^{-1}$-$10^{-2}$ eV^2 for $\nu_\mu \rightarrow \nu_\tau$.

2.1 Status of accelerator searches for $\nu_\mu \rightarrow \nu_\tau$

During the last two decades there have been a number of experiments which have searched for neutrino oscillations[10]. These experiments have hypothesized the possible existence of nonzero neutrino mass and lepton number violation. Although lepton number seems to be a conserved quantum number in experimental physics thus far, this does not reflect any known fundamental dynamical conservation law.

If the neutrino mixing matrix is similar to the quark mixing matrix, $\nu_\mu \rightarrow \nu_e$ oscillations might be expected with a large mixing angle and $\nu_\mu \rightarrow \nu_\tau$ oscillations with a smaller mixing angle. More general considerations, however, would lead us to search for all possible values of a "weak" CKM matrix, in which elements might be expected to be 0.001 or larger. If Δm^2 is small, previous accelerator searches for ν_μ oscillations would not have found evidence for any such oscillations.

The present limits on $\nu_\mu \rightarrow \nu_\tau$ oscillations from accelerators are shown in figure 2. The two curves are from Fermilab Experiment 531, which used a 23 liter emulsion stack as the target in a wide band horn beam with mean effective energy of $\sim$ 20 GeV[11], and CDHS, which used two detectors in a high energy neutrino beam at CERN[12]. The technique in the E531 experiment is similar to the proposed P803 emulsion experiment at the Main Injector.

A large number of experiments have searched for evidence of neutrino oscillations at several laboratories[10]. Several of the experiments were only sensitive to $\nu_\mu \rightarrow \nu_e$ oscillations. Many searches have ruled out portions of parameter space in figure 2 that were already excluded using different techniques. Other experiments have looked for other less favored modes of neutrino oscillation, such as $\nu_e \rightarrow \nu_\tau$ or $\nu_\mu \rightarrow \overline{\nu}_\mu$.

In order to improve existing limits at accelerators, experiments must either achieve better statistical precision, to be sensitive to lower $\sin^2(2\theta)$, or go to larger distances from the neutrino source, to be sensitive to lower values of Δm^2.[1] This is precisely what a paired short and long baseline experiment at the Main Injector could accomplish.

[1] See equation 2. The ν_τ charged current energy threshold is 3.9 GeV, so an appearance experiment could not be done at lower energy.

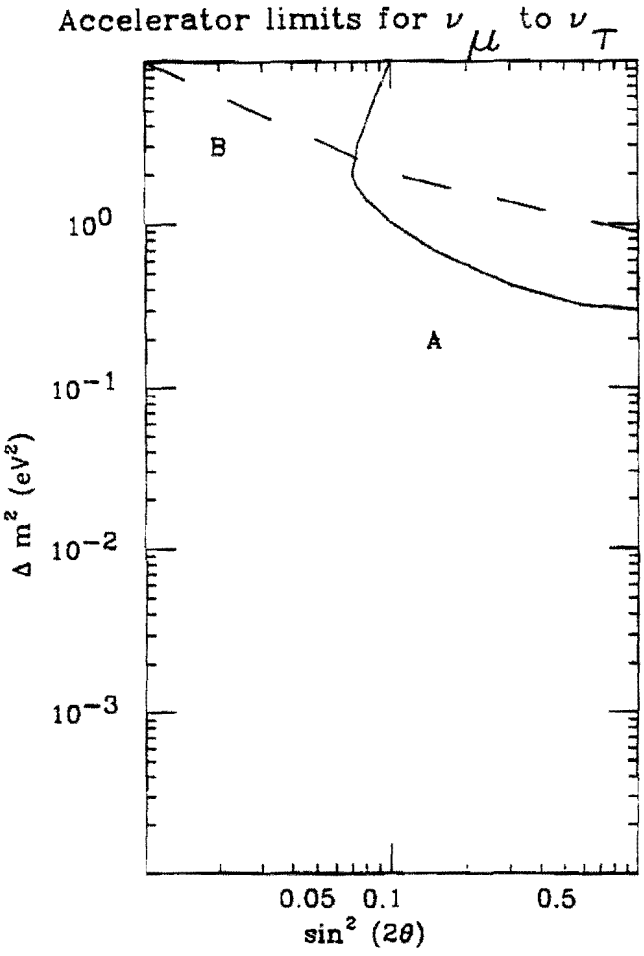

Figure 2: Parameter space excluded by accelerator experiments in the mode $\nu_\mu \rightarrow \nu_\tau$. Curve A is from CDHS and B from FNAL 531.

2.2 Atmospheric neutrino results and outlook

Searches for neutrino oscillations are being conducted in underground detectors using the atmospheric neutrino flux. These neutrinos result mainly from the decays of pions and muons produced in cosmic ray showers in the earth's atmosphere. Neutrino oscillations would affect the expected flux, flavor composition, angular distribution and energy distribution of the underground neutrino flux. To examine the flavor composition, we consider the ratio:

$$r \equiv \frac{(\nu_\mu/\nu_e)_{measured}}{(\nu_\mu/\nu_e)_{predicted}} \qquad (1)$$

A measurement of r different from 1 is an indication that neutrino oscillations exist, probably in the mode $\nu_\mu \rightarrow \nu_\tau$ or $\nu_\mu \rightarrow \nu_e$. Oscillations in these two modes would affect the ratio differently. In the absence of oscillations, it is claimed[14] that the denominator in equation 1 can be calculated to ± 0.01 independent of possible variation in the atmospheric ν flux with solar cycle[15]. However, the earliest calculations ignored the muon polarization, which affects the denominator in r by 10%.

This ratio has been measured in the last few years by Kamiokande, Frejus and IMB-3. Kamiokande[2] reported the ratio $r = 0.71 \pm 0.08$. The error is the combination of statistical and estimated systematic effects. More recently, IMB-3[13] presented a result from which r can be calculated to be 0.67 ± 0.18 (following an earlier report of a deficit of muon decay signals in IMB-1). Frejus[16] reported 1.01 ± 0.10[17] with the most recent analysis of all of their data, but Frejus obtained 0.87 ± 0.15 with their contained events. (It seems possible that the Frejus uncontained events may be contaminated by cosmic ray muons.) NUSEX[18], an experiment similar to Frejus with much lower statistics, obtained a value of r consistent with unity but does not rule out the lower values. Taken together, the results of these experiments statistically suggest that there is a deficit of ν_μ neutrinos, perhaps of about 30%. However, possible systematic errors involved in separating low energy electron and muon events in a water Cerenkov counter may not be adequately understood.

Kamiokande's result is evidence in favor of neutrino oscillations. The best fit of their data to the hypothesis $\nu_\mu \rightarrow \nu_\tau$ is for $\sin^2(2\theta) = .69$ and $\Delta m^2 = 10^{-2} eV^2$. This point is shown in figure 3 and several other figures. The area of *allowed* parameter space at 90%CL is shown between the two solid lines in figure 3. The 90% CL limit from the analysis of all the Frejus data is also shown. The region *allowed* by all atmospheric and accelerator experiments at 90%CL is outlined.

Also shown in figure 3 is another limit that IMB-1 has set using the ratio of upward going to downward going atmospheric neutrinos[19]. If neutrino oscillation parameters were in this small area of parameter space, the oscillation length would be close to the radius of the earth, and the number of upward and downward going neutrinos would not be the same. A recent analysis of the Kamiokande data excluded the part of Δm^2 below $10^{-3} eV^2$[20] which an earlier analysis said was allowed[21]. At Δm^2 of $3.0\ 10^{-3} eV^2$, the oscillation length of atmospheric neutrinos is comparable to the radius of the earth. That region of parameter space is more sensitive to the angular distribution of the Kamiokande data, and the fact that the zenith angle distribution of the Kamiokande data is flat suggests Δm^2 is above $3.0\ 10^{-3} eV^2$. If the Kamiokande effect continues to be confirmed by further evidence from Kamiokande, IMB, and Soudan, then either neutrino oscillations can be detected by our

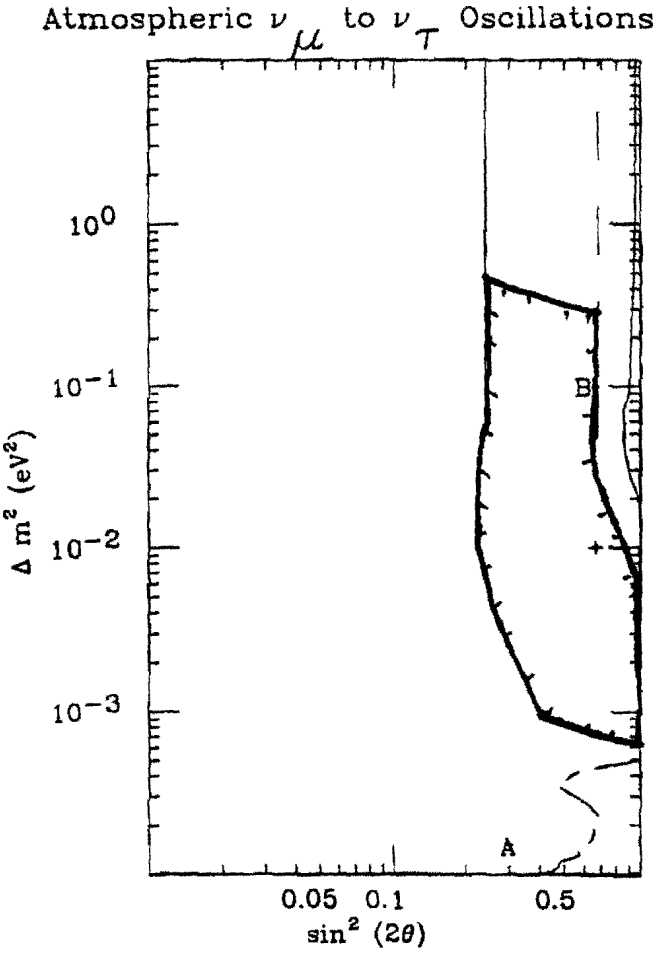

Figure 3: Regions of parameter space *allowed* by one Kamiokande analysis for $\nu_\mu \rightarrow \nu_\tau$ (between lines) and excluded by IMB-1(A) and Frejus (B). The point is Kamioka's best fit. The area allowed by all experiments at 90% CL is outlined

proposed Fermilab experiment, or the angular distribution of the atmospheric events should become inconsistent with flat, as better statistics are obtained. We note that after 5 kiloton years of running, Soudan 2 may be able to rule out most of the "allowed" region if we measure the flavor ratio expected in the absence of neutrino oscillations.

We consider these atmospheric ν measurements to be related to possible long baseline oscillation experiments for two reasons. First, if atmospheric neutrino studies have their systematic errors under control, they can study the same $\Delta m^2 - \sin^2 2\theta$ space for which long baseline experiments are sensitive. And secondly, if the result published by Kamiokande is correct, an accurate accelerator experiment to measure in the same parameter space region is highly desirable. We note that the E/L distributions are very close for atmospheric neutrinos and our proposed long baseline experiment.

2.3 Solar neutrino puzzle

The solar neutrino deficit was discovered by the Davis chlorine experiment[22]. A similar deficit has recently been measured by the Kamiokande[23] detector. The deficit represents a lower measured neutrino flux than would be expected based on standard solar model calculations[24]. Both experiments have detected only about half of the predicted neutrino flux in their acceptance region, $E_\nu > 7MeV$. Recently SAGE, a new gallium experiment which is sensitive to lower energy neutrinos produced in the main solar cycle, showed preliminary results which also indicate a deficit of the neutrino flux[33]. All of these results on solar neutrinos, if taken at face value, leave us the choice that either there is a mechanism making ν_e's undetectable or models of the sun's energy generation process are wrong. One popular hypothesis is the Mikheyev-Smirnov-Wolfenstein (MSW) mixing mechanism, [25] which can explain the observed solar neutrino flux depletion if there is a small mass difference ($\Delta m^2 \sim 10^{-4} - 10^{-7} eV^2$) between ν_e and ν_μ. The MSW effect is the name given to the resonant enhancement, by matter in the sun, of the probability that a ν_e created in the solar interior oscillates into another species. The effect is due to the fact that $\nu_e e$ elastic scattering can proceed by both neutral and charged current amplitudes, while other species would scatter on electrons only by the neutral current.

The solar neutrino situation is relevant to long baseline neutrino experiments for three reasons:

- It is a requirement of the MSW effect that nonzero neutrino mass and vacuum neutrino oscillations exist.

- If parameters ($\Delta m^2 \sim 10^{-6} eV^2$) suggested by the MSW effect are applicable for $\nu_\mu \rightarrow \nu_e$ oscillations, one could reasonably expect the existence of $\nu_\mu \rightarrow \nu_\tau$ oscillations at a higher Δm^2. This would be a consequence of requiring the three generations of neutrinos to have the same mass hierarchy as the lepton and quark generations, a plausible though not mandatory requirement.

- If there is a see-saw mechanism which is responsible for fermion masses,[8] and if the MSW solution to the solar neutrino problem using $\nu_\mu \rightarrow \nu_e$ oscillations is correct, then we expect $\nu_\mu \rightarrow \nu_\tau$ oscillations in just the region of Δm^2 accessible to this proposal.

2.4 Modes of neutrino oscillations

Which modes of neutrino oscillation are most likely? In analogy with the quark mixing matrix, $\nu_\mu \rightarrow \nu_e$ and $\nu_\mu \rightarrow \nu_\tau$ are expected to be more likely than $\nu_e \rightarrow \nu_\tau$. It is possible to search for other modes, such as $\nu_\mu \rightarrow \overline{\nu}_\mu$ and $\nu_\mu \rightarrow \nu_R$.[2] These are discussed briefly in section 5.

In this proposal we concentrate on the search for $\nu_\mu \rightarrow \nu_\tau$. This is motivated by the discussions of the last three sections. If $\nu_\mu \rightarrow \nu_e$ oscillations are related to the solar neutrino puzzle, they would not manifest themselves in any Fermilab long baseline experiment, since the oscillation length for the likely set of parameters is on the order of 10^7 km. We will discuss our capability to search for $\nu_\mu \rightarrow \nu_e$ oscillations in section 5.5, and in fact the possible limits that could be set in the absence of oscillations are better than those for $\nu_\mu \rightarrow \nu_\tau$. However, compared to previous limits set in reactor experiments.[26] our $\nu_\mu \rightarrow \nu_e$ limits would not represent a large improvement.

[2] ν_R represents a right handed sterile neutrino, which does not interact with nuclei.

3 The Soudan 2 Detector

3.1 Detector description

The Soudan 2 experiment uses a currently operating detector in an underground laboratory 710 m (2090 meters water-equivalent) beneath Soudan, Minnesota. When it is completed, the detector will consist of a 1030-ton fine-grained tracking calorimeter surrounded on all sides by a two-layer active shield of proportional tubes. Its primary goal is to search for nucleon decay in modes which may be dominated by neutrino-interaction background in other experiments. It is well suited to be a neutrino detector for the average energies of a Main Injector neutrino beam, and is in fact similar in resolution and size to neutrino detectors which have been used in past experiments at Fermilab and CERN.

The performance of the calorimeter modules has also been studied using cosmic ray muon tracks, both on the surface and underground. Results of module performance studies are presented in section 6 of this proposal. A charged particle test beam, at the Rutherford Laboratory ISIS accelerator, has been used to study detector response to low energy particles. The test beam studies have provided the energy calibration for electromagnetic showers and tracks, and have measured the ability of Soudan 2 to identify muon charge and direction.

The completed Soudan 2 detector [27] will consist of 240 identical 4.3 ton calorimeter modules, which are constructed at Argonne National Laboratory and the Rutherford Appleton Laboratory. One hundred fifty two modules are taking data in the Soudan mine at present. The modules are placed in a rectangular parallelepiped 2 modules high x 8 modules in the east-west direction x 15 modules along the axis of the cavity (north-south direction), yielding a dimension for the full detector of 5x8x15 m^3. This layout is illustrated in figure 4.

Each module is composed of 240 layers of $1m$ x $1m$ x 1.6 mm corrugated steel sheets interleaved with an insulated "bandolier" assembly of 1 m long x 0.5 mm thick x 15 mm diameter resistive Hytrel drift tubes (see figure 5). The insulation consists of two layers of 125 μm mylar, laminated together with long pockets to accommodate the drift tubes, and 0.5 mm thick polystyrene inserts which are vacuum formed to fit the steel corrugation. The steel sheets and the bandolier are stacked in 240 layers (2.5 m) by fanfolding the bandolier back and forth with steel sheets interleaved. The stack is then compressed with about 15 tons of force. Each module is enclosed in a gas-tight sheet steel enclosure consisting of welded sideskins to maintain compression and removable covers to allow access to the wireplanes and stack faces.

The basic detector element of the experiment is shown in figure 6. It is a resistive ($\sim 4x10^{12}\Omega - cm$) plastic Hytrel tube (made by DuPont Corporation). Each module contains 7560 drift tubes. A linearly graded electric field is applied by 21 1.5 mm wide copper electrodes (see figure 5). These have a voltage of -9 kV at the middle of the tube and 0 V at the two ends. The resistive tube then grades the voltage between electrodes, creating a uniform axial drift field of 180 $volt/cm$ inside the tube. The modules are filled with a very pure drift gas mixture of 85% argon, 15% CO_2 and 0.4% of H_2O (from the plastic). When a charged particle passes through the tube it ionizes the gas; the liberated electrons then drift (with a velocity of 0.6 $cm/\mu sec$) up to 50 cm to the ends of the tube where they are collected and amplified on a 50 μm diameter anode wire.

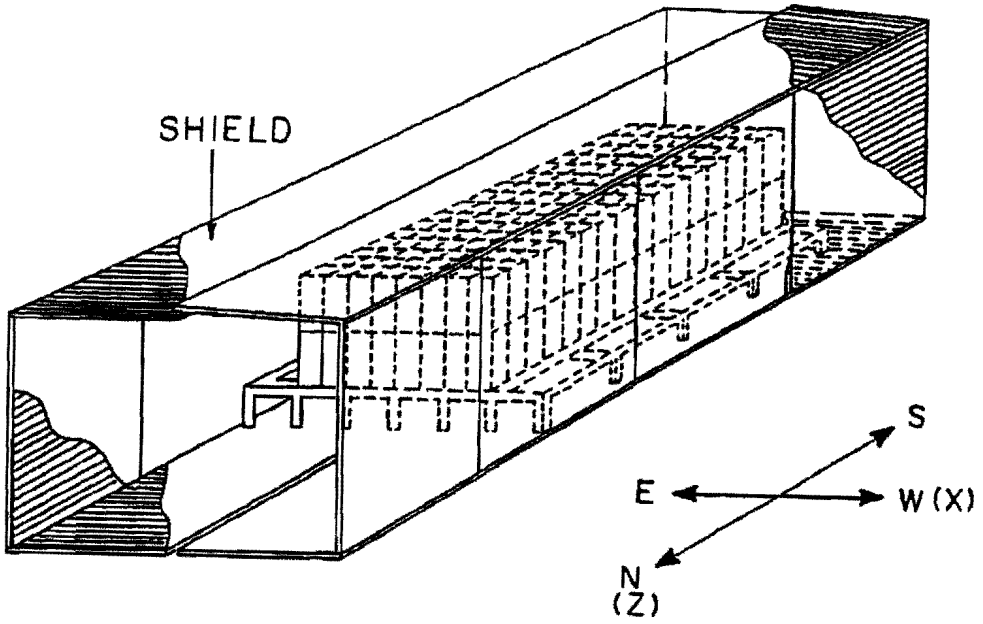

Figure 4: Soudan 2 main detector and active shield layout.

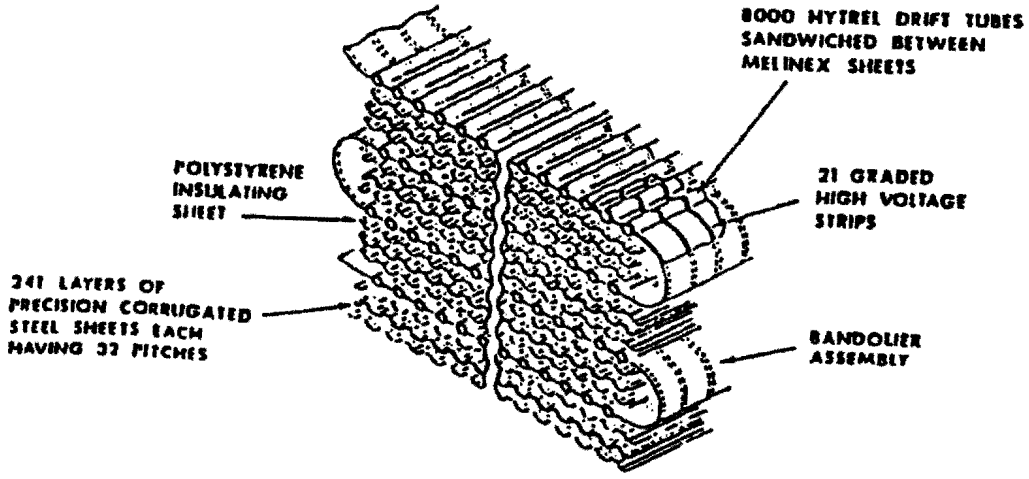

Figure 5: *Bandolier*, insulation sheets (inserts) and corrugated steel assembly (stack).

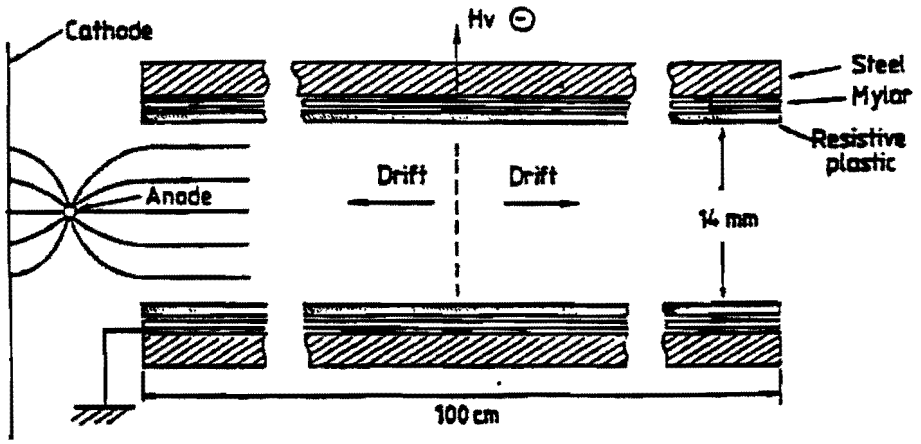

Figure 6: A single drift tube. The drift field is generated by the application of graded voltages on a series of 21 copper electrodes

The tubes are arranged in a close-packed hexagonal array as shown in figure 5. The anode wires run vertically in a plane 10 mm from the tube ends and are spaced every 15 mm so that they are aligned with the centers of the tubes. Cathode pads are connected in horizontal strips orthogonal to the anode wires 5 mm behind them, and are aligned with the tubes. Thus it is possible to identify which tube a signal came from, since the anode wires and cathode pads form a grid centered on the tube ends. The position along the tube length is obtained from drift-time information. Three correlated spatial coordinates and a dE/dx measurement are recorded for every charged particle crossing of a drift tube.

The raw data pulse patterns at the ADC inputs are continuously compared with programmable trigger conditions to detect localized clusters of hits in the drift tubes. Since every readout channel contributes equally, the trigger requirement is uniform throughout the detector volume. Efficiency is high for muons above 230 MeV/c and falls linearly to zero at 90 MeV/c (for muons which do not have a visible decay). The electron (shower) triggering threshold is about 50 MeV. The rate of random triggers from natural radioactivity is less than 0.5 Hz in the full detector under these conditions. The trigger efficiency for neutrino events produced by the Fermilab beam will be essentially 100%.

The main detector is surrounded on all sides by a 2-layer array of extruded aluminum proportional tubes [28]. This active shield is mounted against the cavity walls to signal the presence of cosmic ray events in the cavity and the surrounding rock. Cosmic ray muons can create contained event candidates by entering the detector through the spaces between main detector modules, or by creating neutrons, photons and K_L^0's in the nearby rock which penetrate to the interior without leaving tracks. Such neutral particle production is almost always associated with charged particles which are detected in the shield. Because the 1700 m^2 shield has nearly 3.5 times the area of the main detector in the direction of Fermilab, it can also be used to increase the effective area for the measurement of the flux of muons from ν interactions in the rock upstream of Soudan 2.

Some advantages of the Soudan 2 detector for detecting and identifying neutrino events are:

- The fine granularity gives much better track and vertex resolution than water Čerenkov counters. The result is high quality pictorial event information, comparable to that from standard electronic and heavy liquid bubble chamber neutrino experiments. The spatial resolution is 1 cm or better in all three spatial coordinates.
- The ionization measurement yields particle identification information (e.g. proton/pion-muon separation) not available in some other detectors.
- μ^- absorption in iron gives a track charge information not available in a water Čerenkov detector. (about 2/3 of stopped μ^+'s decay visibly in Soudan 2.)
- In a moderate density iron calorimeter, high energy muon/hadron separation is easy.
- The energy threshold of the trigger for muons is lower than in any other underground ν detector.
- The observation of shower development yields better low energy electron-muon separation than in water Čerenkov detectors.
- The modularity of the detector has allowed detailed test beam calibration studies.
- The modularity of the detector will allow us to operate an almost identical type of near detector at Fermilab.

The particular features which make this detector quite powerful for the proposed neutrino experiment are the excellent pattern recognition and particle identification of hadrons, muons and electrons. This capability will enable reliable separation of charged and neutral current events and the identification of the flavor of the final state lepton.

3.2 Detector operation

The complete detector will be read out by 32256 anode wires and 122880 cathode pads through 5888 electronics channels. The reduction in the number of channels is accomplished in two stages. Groups of 8 modules are stacked 2 high by 4 across to form a halfwall. The complete detector will consist of 30 halfwalls. The two large faces of each halfwall contain 8 wireplanes. Anode signals from the upper modules are bussed to the lower modules and cathode signals are bussed across the halfwall to give an equivalent readout plane which is 5m high x 1m wide and is known as a *loom*. Each loom consists of 256 anode channels and 480 cathode channels. The preamplifier signals from each anode are then multiplexed 8-fold by connecting the anode channels from 8 separate looms to one digitization crate. The preamplifier signals from each cathode pad are also multiplexed 8-fold, but in a distinct manner, ensuring that the looms served by one anode crate are served by different cathode crates. Since any one loom is served by a unique anode crate and cathode crate combination, a tube anywhere in the detector may be located by matching the anode and cathode pulses. A total of 24 digitization crates are used in the experiment.

To prompt the Soudan 2 detector to read out and store an event, it is necessary for the event to satisfy the trigger requirements. The primary trigger requirement in the Soudan 2 detector is the "edges" trigger. A detailed description of the edge trigger will not be given here, for a complete account, see reference 29. Compton electrons produced by photons interacting in the endplane of a module are a primary element of the noise rate in the detector. The edges trigger was designed to reject these events, so an event must have some minimum extent in the drift direction to satisfy this trigger. The trigger efficiency for events associated with the Fermilab beam would be near 100%. The deadtime will be less than 1%.

The readout electronics are CAMAC based. A serial CAMAC highway is used that allows the readout of all crates on a single highway controller. A Jorway Model 411 CAMAC interface is used between the serial highway and the host computer, a Digital Equipment Corporation VAXstation 3200 running under VMS. Kinetic Systems L2 Serial Crate Controllers are used to control each of the crates on the highway. Prior to readout, an 8086 microprocessor controls the compaction of the data from each 6 bit flash ADC-based 16 channel digitization card, only passing on a channel only if the signal from it is above a preset threshold. The digitization and trigger electronics are MULTIBUS based.

An example of part of a cosmic ray muon track is shown in figure 7. The fine detail of a few pulses can be seen. This shows both the pulse shape information and the 200ns digitization time. The result of the fit to that part of the track in relationship to the pattern of the stack is also shown. A complete muon track traversing the detector is shown in figure 8. Comparing the two figures, the large amount of information that is available for each event is apparent.

Data at the Soudan site is stored on disk in runs of length 1-2 hours, and is processed immediately after the run ends on a local Vaxcluster with an analysis package SOAP (Soudan Offline Analysis Program). SOAP performs noise rejection, pulse matching, track reconstruction, and sorting of events into various categories of physics interest, such as muons, multimuons, monopole candidates, (contained) neutrino candidates, and semi-contained events. Muons from neutrino interactions in the rock from the direction of Fermilab would all be found in the muon sample. Neutrino events would be in either the contained or semi-contained event classifications. An additional processor would be written to flag events that were in time with a Fermilab beam pulse and have the correct spatial orientation. This event sample would be compared with the contained and semi-contained event samples to ensure that all Fermilab events were being found with high efficiency.

3.3 Detector status

The Soudan 2 detector has been operational since July 1988 when the first 275 tons of detector was turned on. Data are taken while the detector is being constructed: currently 655 tons of detector is in operation and 0.43 kton years of exposure has been obtained. Reconstruction and filtering of contained neutrino events and cosmic ray muons is performed at the Soudan site immediately after data acquisition. Detailed analysis has been completed on all data taken before December 1990. The detector is now in routine operation about 70% of the time. The major down-time is associated with the addition of new modules to the detector and will cease with the completion of the detector in 1992. The performance of the detector has been remarkably reliable and stable over the past two years of operation. We

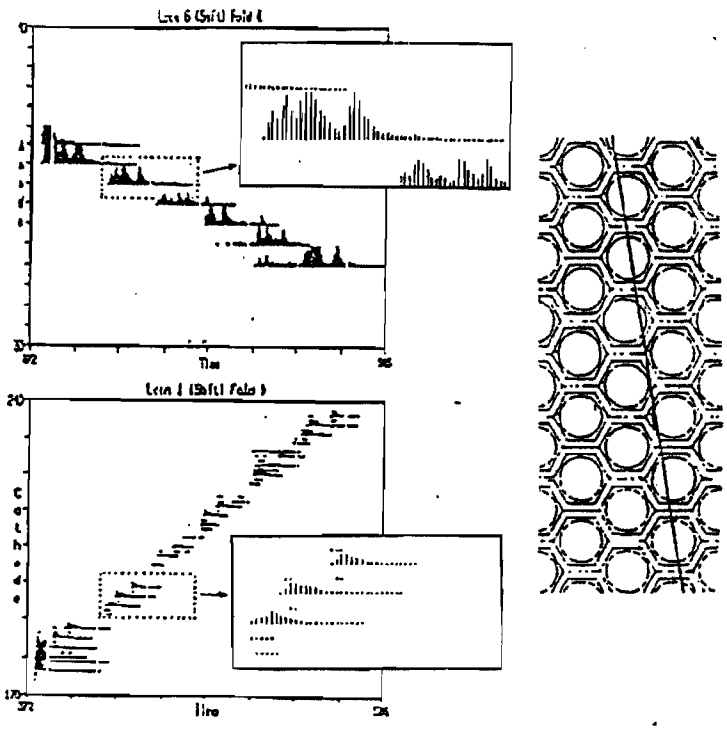

Figure 7: Segment of a muon track and fit

do not anticipate any problems with continuing operation through the time period when a neutrino beam might be available. We are in any case committed to running Soudan 2 at least until 1995 to obtain a proton decay exposure of 3 kiloton years. The detector performance is entirely consistent with the original Soudan 2 proposal and more than adequate to perform the experiment (see section 6).

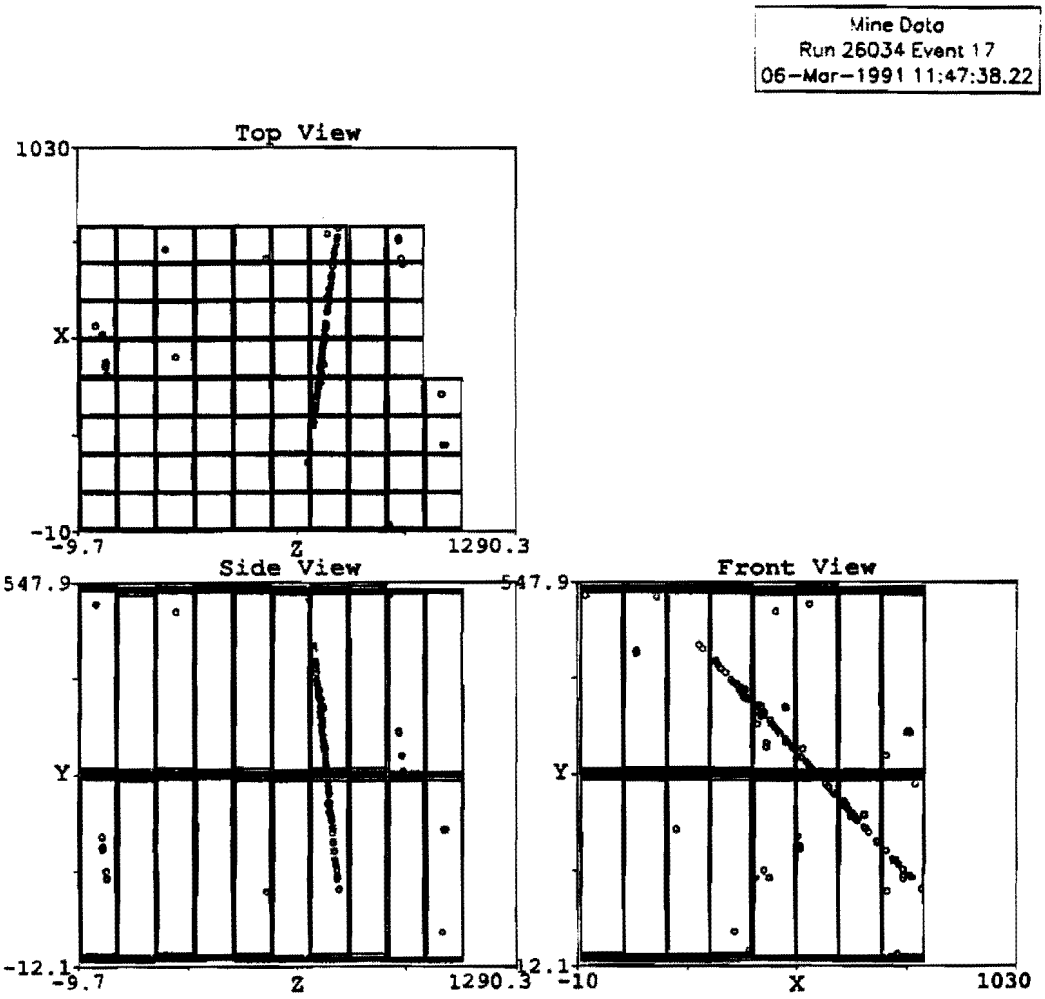

Figure 8: A cosmic ray muon in the Soudan 2 detector. The anode-time (x), cathode-time (y), and matched (z) views are shown

4 The Double Horn Neutrino Beam

The present plan for Fermilab neutrino beams from the injector is to use 120 GeV primary protons and a double horn similar to the one used by many previous Fermilab wide band beam neutrino experiments. The Fermilab neutrino beam simulator, NUADA, has been run for a Soudan 2 sized detector located 800 km from Fermilab. The resulting neutrino flux and event rate are shown as functions of energy in figures 9 and 10. Note that at this distance from Fermilab, the flux scales simply as $\frac{1}{r^2}$. The present "run" that we are using for illustrative purposes is 4×10^{13} protons per pulse every 2.0 seconds, and 100 hours of beam per week for nine months. This corresponds to 2.1×10^{20} protons on target. Unlike an experiment on the surface, we could use "pings" on a slow spill, and would not need one turn extraction.

There will be small contaminations of the ν_μ beam by ν_e's, $\overline{\nu_e}$'s, and $\overline{\nu}_\mu$'s. These come predominantly from K decay, and have been calculated as a function of energy[6]. In general, they are of the order of 1% of the beam or less. They will require some minor corrections for the tests described in section 5, but no conclusions are affected by this level of background. There is no significant source of ν_τ or $\overline{\nu}_\tau$ in the double horn itself. Less than 10^{-4} events are expected from the process $pN \rightarrow D_s X; D_s \rightarrow \tau X; \tau \rightarrow \nu_\tau X$ in the proton dump for the entire run.

Flux estimates calculated from beam design parameters may only be accurate to $\pm 20\%$. A better value can be measured from contained neutrino events in the detector and would give an estimate of the neutrino flux good to $\pm 4\%$. Information from a P822 near detector, as well as P803 and beam monitors should allow us to determine the beam flux as well as 2%. Either P803 or P822's measurement of the beam flux would be limited by systematic and not statistical factors. A 35 ton P822 near detector would record over 5 million events. Possible systematic errors due to uncertainties in the energy and angular distributions are discussed in the section on the near station data.

Geography There is room on the Fermilab site for a neutrino beam pointing true north after the switchyard (to the left of the meson beams). An initial bend to the north will be required, for which 40 main ring dipoles and 10 quadrupoles are needed; thereafter the beam is as described in the **Conceptual Design Report: Main Injector Neutrino Program**[7](CDR). We will not repeat the description of the beam given in that document. We only note that the design criteria for that beam make it a very good match to our proposed experiment:

- Maximum neutrino flux in the forward direction.
- Sufficient flux above ν_τ threshold to make a ν_τ appearance experiment feasible.
- Little variation of the energy spectrum of the beam as a function of angle from the beam direction.

We recognize that there will be a number of conflicting demands on the 120 GeV proton beam, including injection into the Tevatron, $\overline{p}$ production, and other possible fixed target experiments studying Kaon properties. It will be important to look at the compatibility of various experiments, both those needing the 120 GeV beam, and those using Tevatron

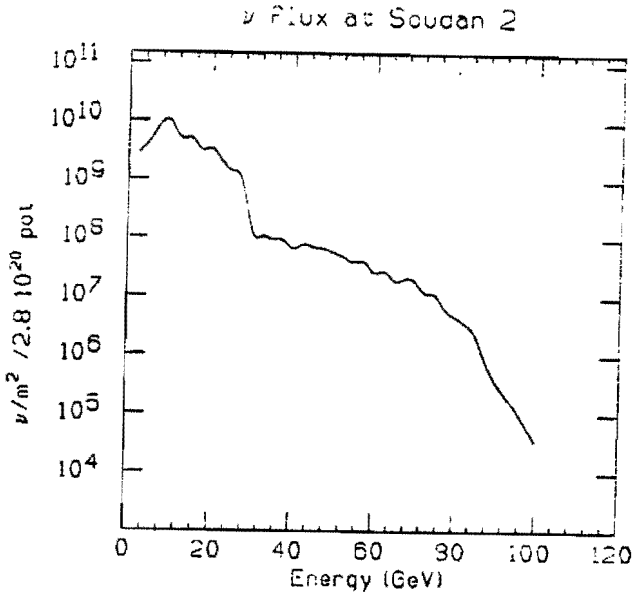

Figure 9: Expected neutrino flux from a 120 GeV Main Injector beam and a conventional double horn neutrino beam.

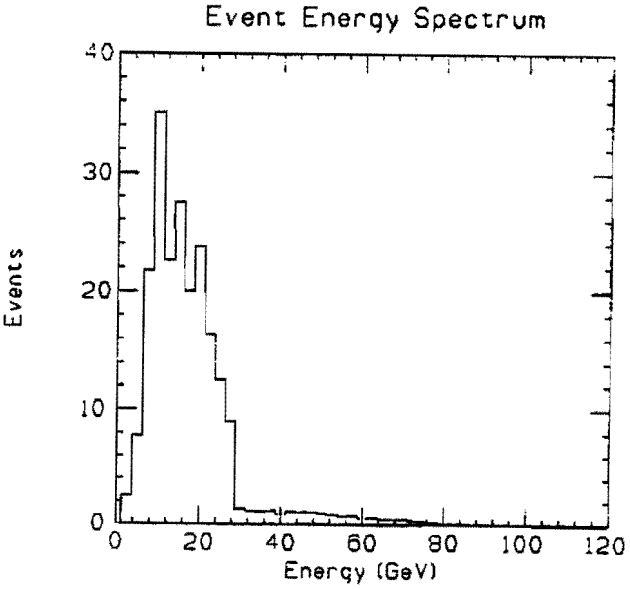

Figure 10: Event rate in the Soudan 2 detector as a function of energy.

extracted fixed target beam. As a remote experiment which is continuously operating, we are completely flexible about beam usage schedules.

The CDR also looks in detail at the costs of constructing the beam, including the additional costs required for our proposal. The estimate for P822 was $7 million more than for the cost of P803 alone, including engineering and contingency. We will continue to work with Fermilab engineers to find less expensive ways to construct the beam.

5 Physics Potential of P822

5.1 General considerations

We will be able to study $\nu_\mu \rightarrow \nu_\tau$ oscillations in a significant large new area of parameter space. This is because of the combination of large oscillation distance, moderate beam energy, and very high ν flux compared to any previous experiment.

If neutrino oscillations exist, the probability (P) of oscillation is:

$$P_{\nu_a - \nu_b} = \sin^2(2\theta)\ \sin^2(1.27\,\Delta m^2\,\frac{L}{E_\nu}) \tag{2}$$

with Δm^2 in eV^2, L in km and E_ν in GeV. $\Delta m^2 = |m^2_{\nu_a} - m^2_{\nu_b}|$ and θ is the mixing angle of ν_a and ν_b neutrinos. In order that the energy be high enough for clean identification of the flavor through observing charged current events, and to explore the very small mass differences which appear to be interesting, a large distance for oscillation is required. The Soudan 2 baseline of 800 km extends the Δm^2 sensitivity downward by two orders of magnitude from all previous accelerator experiments. Without the large neutrino flux from the Main Injector, experiments at this distance would have only a handful of events: a "similar" experiment using the Tevatron would have eight hundred times fewer events and would thus not be sufficiently sensitive. Only the Main Injector combines the high flux with the right energy range for this experiment.

The sensitivity to mixing angle depends on statistics and control of systematic errors[30]. One of the most important ways of minimizing systematic error will be understanding the neutrino beam itself to sufficient accuracy. There are three important characteristics of the beam that need to be measured and monitored:

1. The absolute direction of the center of the beam.

2. The width of the beam at the detector.

3. The change in the energy distribution as a function of angle from the center of the beam direction.

An important tool in understanding the long baseline beam will be measurements done in the same beam by a number of Soudan 2 modules in a near detector at Fermilab. Useful information would also be available from the short baseline experiment, Fermilab P803.

Any underground neutrino detector away from the Fermilab site can record neutrinos interacting either inside the detector (contained vertex signal) or in the material upstream of the detector ("rock" muons). The size of the contained vertex signal is proportional to detector mass and the rock μ signal is proportional to the detector surface area facing the neutrino beam front. Both signals are inversely proportional to the square of the distance separating neutrino source and detector. For example, Soudan 2 is at a distance of 800 km from Fermilab, while IMB (P805) is at 570 km. This results in a reduction of a factor of 2 in the neutrino flux, but lowers the limit on Δm^2 that can be reached.

The detector will search for a decrease in the ν_μ flux due to oscillations. The ν_μ's interacting in the earth will create muons that have a range which is almost linearly proportional

to muon energy. As muons range out, new ones are created by charged current interactions, so at any point along the beam there will be a constant muon flux (#/sr), which is nearly independent of rock density. The long range of muons from high energy neutrinos provides an effective target mass which is larger than the mass of the detector. This effective target mass is a function of energy and is larger for high energy muons.

As a large highly segmented detector, there are a number of ways that Soudan 2 could look for neutrino oscillations. Both appearance and "disappearance" experiments are possible. In the next three sections, we describe three independent ratios that are sensitive to the existence of $\nu_\mu \rightarrow \nu_\tau$ oscillations:

- $R_{"nc"/"cc"}$ which requires the separation of neutral current and charged current contained vertex events.
- $R_{\frac{\mu}{\nu}}$ which compares the rate of rock muon events to contained vertex neutrino events.
- $R_{near/far}$ which compares the rate of events in the near detector to the rate in the detector at the Soudan mine.

In the subsequent sections, we describe additional measurements and other neutrino oscillation modes.

5.2 $R_{"nc"/"cc"}$ test to detect ν_τ appearance

If ν_μ's oscillate into ν_τ's, this will affect the apparent ratio of neutral current events to charged current events. In the absence of oscillations, we expect[31]

$$R \equiv \frac{number\ of\ events\ without\ a\ muon}{number\ of\ events\ with\ a\ muon} = 0.31 \pm 0.01 \tag{3}$$

Then for N events,

$$n_{cc} = N \times \frac{1}{1+R}\ and\ n_{nc} = N \times \frac{R}{1+R} \tag{4}$$

If there is a probability, P, for ν_μ to oscillate into ν_τ, then the resulting ν_τ neutral current events would be indistinguishable from the ν_μ neutral current events. However, most (83%) of the ν_τ charged current events have no muon and would therefore be classified as neutral current events. We would measure

$$n_{"cc"} = \frac{N(1-P+\eta BP)}{1+R}\ and\ n_{"nc"} = \frac{N(R+\eta(1-B)P)}{1+R} \tag{5}$$

where B = 0.17 is the branching fraction for $\tau^- \rightarrow \mu^- X$ and η is the ratio of the ν_τ charged current cross section to the ν_μ charged current cross section. The notation "cc" distinguishes events classified as charged current due to the presence of a muon in the final state from the actual charged current events, which for an incoming ν_e or ν_τ would be incorrectly classified as nc events.

$$R_{"nc"/"cc"} = \frac{n_{"nc"}}{n_{"cc"}} = \frac{R+\eta(1-B)P}{1-P+\eta BP} \tag{6}$$

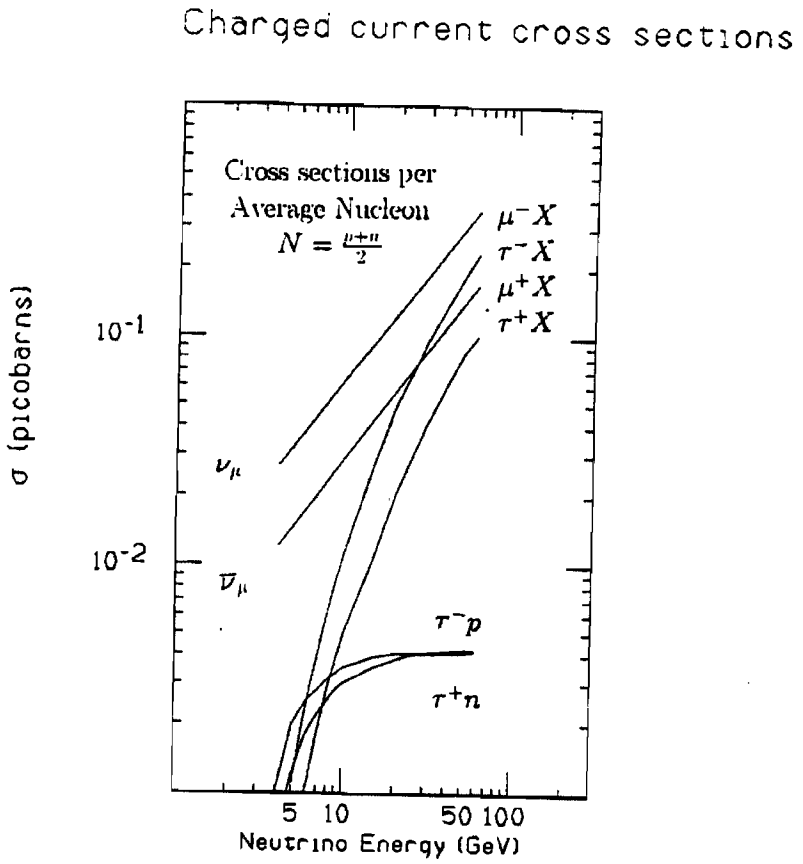

Figure 11: Calculated ν_τ total and quasi-elastic cross section

The ratio η has been calculated as a function of energy by Roger Phillips at the Rutherford Lab[37]. The relevant cross sections are shown in figure 11. η also has been calculated by the Ohio State P803 group[32] with a similar result. Integrated over the neutrino spectrum in figure 9, $\eta = 0.24$. By contrast, the neutral current cross sections for ν_τ and ν_μ are equal. The signal of an oscillation thus consists of a value of $R_{\text{"nc"}/\text{"cc"}}$ that is too large. If our measurement yields the known $R_{\text{"nc"}/\text{"cc"}}$, ratio for ν_μ allows a limit on the probability of oscillation can be deduced.

The expected number of contained vertex events in the Soudan 2 detector can be written as:

$$N = n_{cc} + n_{nc} = n_{\text{"cc"}} + n_{\text{"nc"}} = \int \sigma_{tot}(E) \frac{d\sigma_\nu(E)}{dE} N_t dE \qquad (7)$$

where N_t is the number of target nucleons and $\phi(E)$ is the neutrino flux. Using an assumed injector beam with 4×10^{13} protons every 2.0 seconds and 100 hours of beam per week for nine months, we compute from equation 7 that the entire Soudan 2 detector would record 678 events with a contained production vertex.

We have performed a Monte Carlo calculation to generate these events uniformly through-

out the volume of the Soudan 2 detector. We conclude that $(64 \pm 7)\%$ of the events will have their hadronic showers well contained in the active volume of Soudan 2. (The error is based on the statistics of Monte Carlo events that we have studied so far, and does not represent a systematic error for the experiment.) We have therefore chosen a restricted Soudan 2 fiducial volume in which there is close to 100% separation between neutral current and charged current topologies for these 434 events. The distinctive topologies of neutral and charged current events are illustrated in figures 12 and 13 respectively. Figure 12shows the neutral current event at the same scale as the charged current event, and one view on a magnified scale. The high spatial resolution of the detector makes identification of charged and neutral current events rather straightforward on an event by event basis, similar to what has been done in Fermilab E594[34]. We further note that with the external muon identifier described in section 5.9, the acceptance would rise to over 90%.

The presence or absence of a muon from the main vertex is a powerful signature, and the fine granularity of Soudan 2 makes it well suited to detect this signature. The average event energy will be 16 GeV, so for most of the y region, the separation will be straightforward. For very low y, a correction will have to be made for muons which do not come out of the shower. A small correction will also be needed for neutral current events which are mistakenly classified as having an exiting track. It should be possible to accurately make these corrections with the help of a Monte Carlo, as has been done by all previous ν experiments at Fermilab and CERN. Note that this correction is not needed if we compare $R_{"nc"/"cc"}$ as measured at Soudan with that measured in our near detector. The 90% confidence level limit we could set in the absence of oscillations is shown in figure 1 in the curve labeled "C". Only statistical errors are included: systematic errors will be negligible compared with the statistical errors.

5.3 $R_{\frac{\mu}{\nu}}$ tests using muons from the rock

We plan to measure $R_{\frac{\mu}{\nu}}$, the ratio of muons from the rock to neutrino events with vertices inside the Soudan 2 detector. We define the ratio $R_{\frac{\mu}{\nu}}$ as the ratio of incoming (muon) events from the rock in front of the detector, to the number of contained vertex (neutrino) events. Systematic errors due to beam pointing, knowledge of the energy distribution of the beam, the geometry of the detector and properties of the surrounding matter have been considered. No effects have been identified which would introduce uncertainties larger than 1% in the measurement of $R_{\frac{\mu}{\nu}}$. An overall systematic accuracy in the measurement of this parameter of the order of 2% is expected. Note that the beam flux normalization (or time variability) does not affect $R_{\frac{\mu}{\nu}}$.

The rate of muons entering the detector from ν_μ charged current interactions in the rock is:

$$n_\mu = 1.0 \times 10^{-12} GeV^{-2} \int_0^\infty dE_\nu E_\nu^2 n(E_\nu) \tag{8}$$

The two E_ν factors come from the cross section and muon range, both proportional to the neutrino energy. The Fermilab beam would enter the detector (in the plan view) pointing 26.4°W of North. The long axis of Soudan 2 is oriented along the N-S direction. The effective area of Soudan 2 viewed from the direction of Fermilab is then 94 m^2 for the main detector and 275 m^2 for the shield. For the main detector, using the existing trigger, we would expect

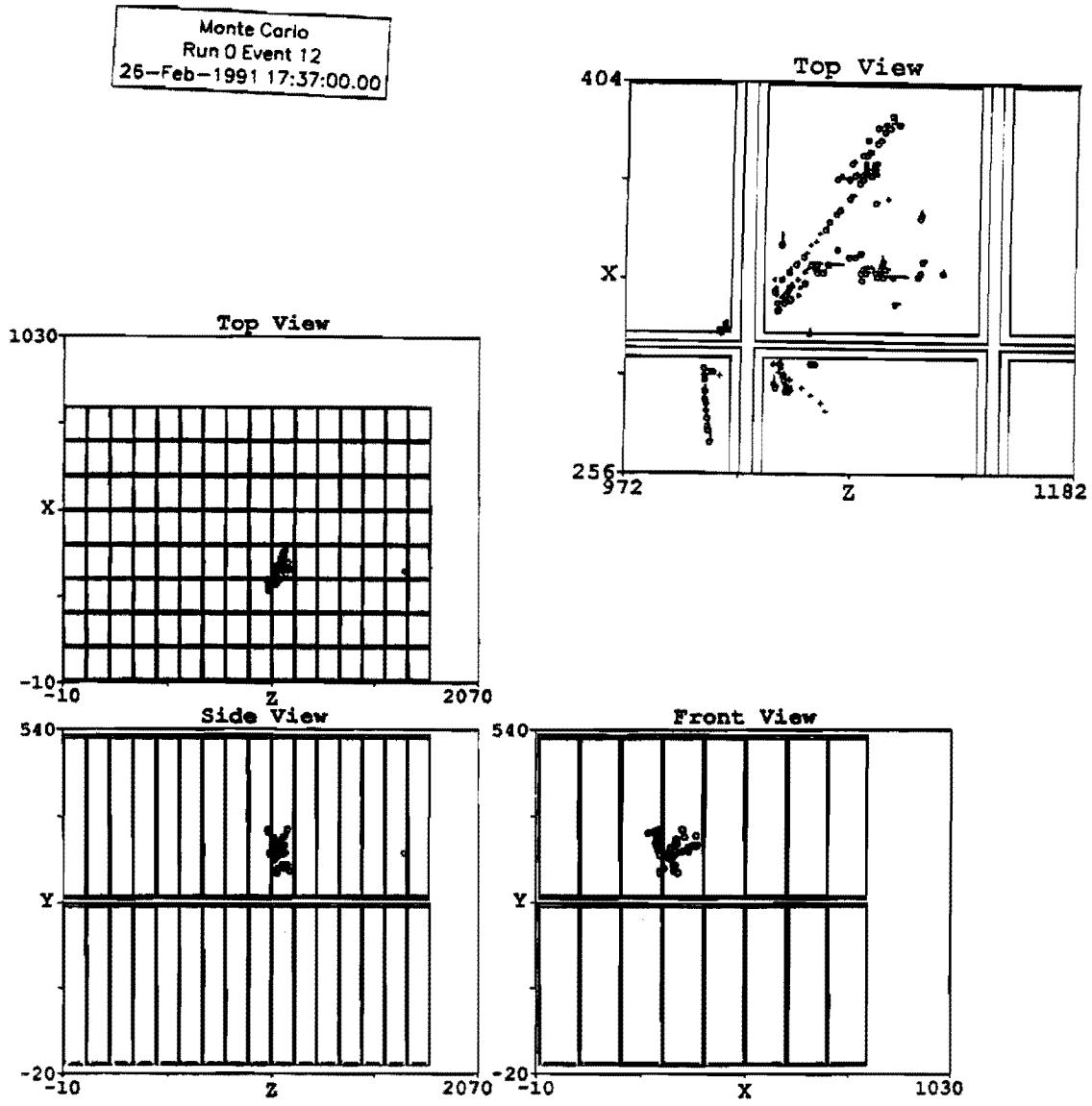

Figure 12: Simulated neutral current neutrino event in Soudan 2. One view is shown in a magnified scale.

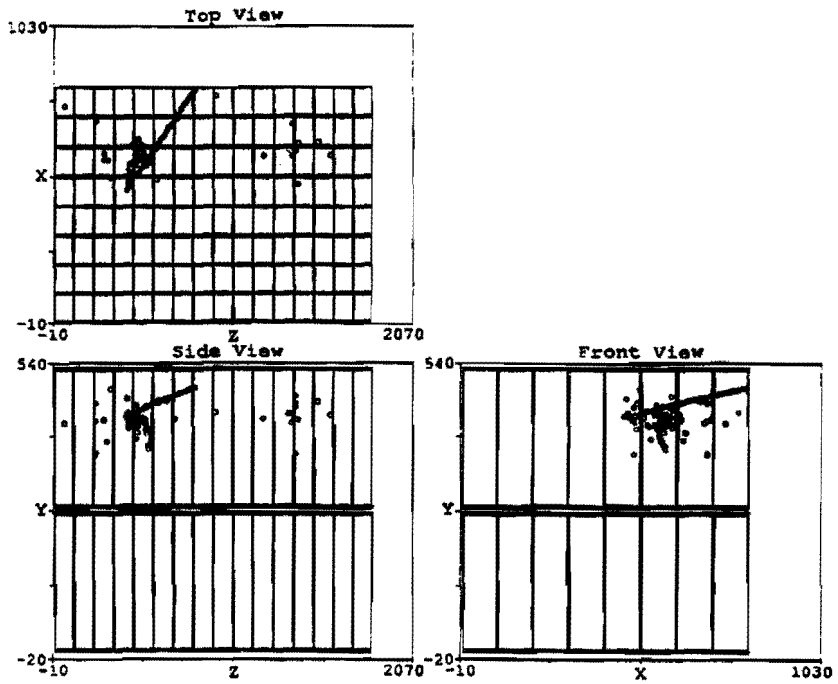

Figure 13: Simulated charged current neutrino event in Soudan 2

to detect 2150 muons from the rock for the entire exposure. Our trigger and reconstruction efficiencies will be near unity.

Using these muons, an additional neutrino oscillation experiment can be done. We would look for a decrease from the expected number of muons n_μ^{ex} due to $\nu_\mu \rightarrow \nu_\tau$ oscillation:

$$n_\mu = n_\mu^{ex}(1 - P + P\eta B) \tag{9}$$

In the absence of such a decrease, a limit on the oscillation probability, P, could be set. This is the curve labeled "B" in figure 1. The limit is dominated by the statistical error for n_μ^{ex}. Note that the full number of such events can be used in this calculation, whether or not they are in the fiducial volume required for distinguishing between neutral and charged current interactions.

The calculation of n_μ^{ex} depends not only on the measured number of contained vertex events but also on knowledge of the energy dependence of the ν_μ flux. To first order, the density of the rock in which the muons are made does not affect the muon flux. In any case, the rock in the vicinity of the Soudan mine has been well measured. In contrast to the $R_{"nc"/"cc"}$ ratio, we will be comparing the observed ratio $R_{\frac{\mu}{\nu}}$ to a calculated ratio, with the rock muon rate having one extra power of E_ν in the numerator.

5.4 $R_{near/far}$ test using Soudan 2 modules at Fermilab

The Soudan 2 detector is very modular. Main detector modules have been operated in the Rutherford ISIS test beam, and on cosmic ray test stands at Argonne and Rutherford-Appleton Laboratories. Thus we are able to carry out a two station experiment, using Soudan 2 modules near the P803 detector at Fermilab. The experiment will need eight meters of space along the beam direction.

We propose to bring eight modules to Fermilab. in a 2 (wide) by 4 (deep) configuration. This corresponds to 31.1 tons of detector and over 40 million neutrino interactions in the nine month run. The trigger will require a vertex in the front two modules. giving about one trigger per spill. Although the muon flux should be modest (a requirement of P803). it would be helpful to have a "veto" scintillation counter in front of our near detector.

These neutrino events will be used to measure $R_{"nc"/"cc"}$ in the near detector. Selecting electron. muon and tau charged current events in the same way in the near and far detectors. and measuring the ratio of each type to the total number of interactions will yield information on all types of oscillation. Although containment issues would not be identical in the two detectors. these can be corrected using Monte Carlo techniques. This approach will greatly lower the level of systematic errors in the NC/CC ratio.

In addition. the near station will give us data which we will use to normalize the beam flux. The muon rate at Soudan can be normalized to the rate that is measured by the near detector. We call this the $R_{near/far}$ test. Since the statistical accuracy of the near detector is enormous. the main intrinsic limitations will be from the statistical accuracy of the far detector and the ability to accurately estimate the muon rate due to uncertainties in the energy distribution as a function of angle. Computer studies done on the proposed neutrino beam[36] show that as long as the angle from the beam axis is less than 0.25 mr the systematic error on the expected muon rate is less than 1.2%. This requirement is straightforward to satisfy and has been achieved by other Fermilab neutrino exposures. Effects that we have not yet identified may limit our knowledge of the absolute flux by 1.0%. Therefore we expect that our near station will give us knowledge of the neutrino flux at our Soudan detector with a systematic error of about 2.0%.

This flux measurement can be used in at least two different ways. It can be used to normalize the muon rates in the detector to search for both $\nu_\mu \rightarrow \nu_\tau$ and $\nu_\mu \rightarrow \nu_R$. The latter mode represents the oscillation of ν_μ into a right handed neutrino. which would be "sterile" and not interact so that both the neutral current cross section and charged current cross section are zero. In the absence of oscillations. the limits that can be set in this way are shown in figure 14. Using the normalized flux from the near station with the rock muons increases the precision of the oscillation test from that shown in curve "B" of figure14. In section 5.7. we discuss how the Soudan 2 active shield can be used to obtain curve "A" in figure1 1.

Another possible use of a near station would be to bring the detectors into a low energy (5-25GeV) hadron beam. This would allow an additional check on the neutral current to charged current separation. The near detector would be moved into a charged particle test beam at Fermilab. A modest amount of running time would suffice for such calibrations.

5.5 $\nu_\mu \rightarrow \nu_e$ oscillations

Soudan 2 can also search for neutrino oscillations in the mode $\nu_\mu \rightarrow \nu_e$. although we note that present limits on $\nu_\mu \rightarrow \nu_e$ in the relevant parameter space range already exist from certain reactor experiments. The limit from the Gosgen experiment. which is the most sensitive. is shown in figure 15. Also. the Δm^2 sensitivity does not approach that which is relevant to solar neutrino experiments. We can search for possible $\nu_\mu \rightarrow \nu_e$ oscillations using the $R_{"nc"/"cc"}$ test. the $R_{\frac{\mu}{\nu}}$ test and the $R_{near/far}$ test. For the $R_{"nc"/"cc"}$ test. equation 6 should

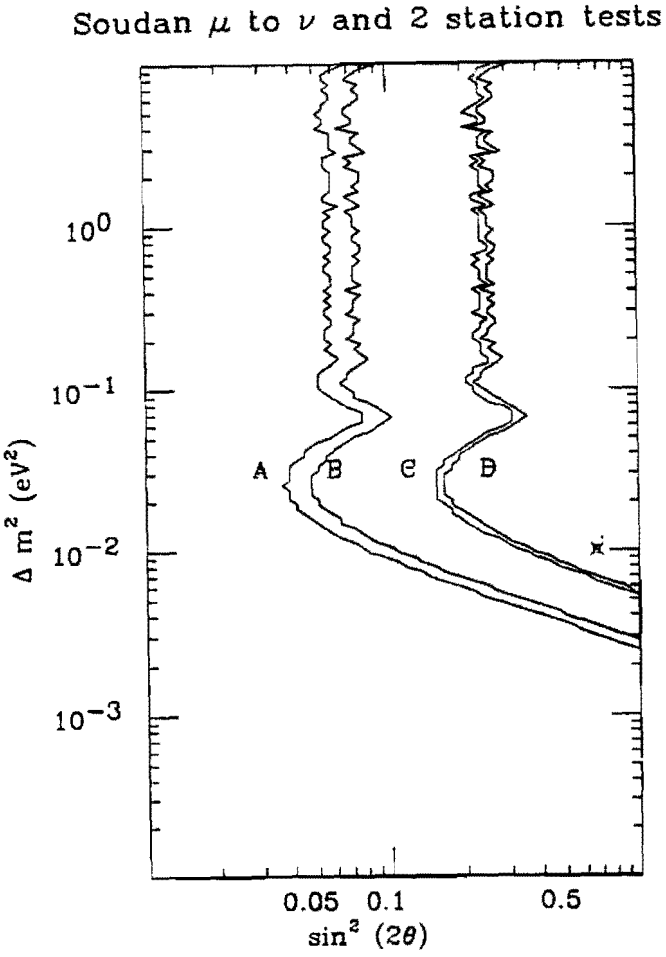

Figure 11: 90% CL limits using the $R_{near/far}$ test (A,B) and the $R_{\frac{\mu}{\nu}}$ test (C,D). Each pair uses the rate of muons in the shield(8150) and the calorimeter (2150). The point is Kamioka's best fit.

be used with $B = 0$ and $\eta = 1$ so that the search would be more sensitive than that for $\nu_\mu \rightarrow \nu_\tau$. Limits that can be reached are plotted in figure 15.

Another analysis strategy for ν_e's is to try to separate charged current ν_e and ν_μ events on an event by event basis. This is something that Soudan 2 can do for atmospheric neutrinos with $< E > \sim 1GeV$. Preliminary studies indicate that for the deep inelastic events with 5 times that energy, it is likely that hadronic showers would be confused with the electrons a significant fraction of the time. However, electromagnetic showers above about 10GeV will be relatively uncontaminated by π^0 showers from the hadronic vertex[35]. We will continue to investigate this possibility. Soudan 2 is well suited to be able to measure the electromagnetic energy fraction as a function of event energy. A large fraction of events with over 20 GeV electromagnetic energy may be a signal for $\nu_\mu \rightarrow \nu_e$ oscillation.

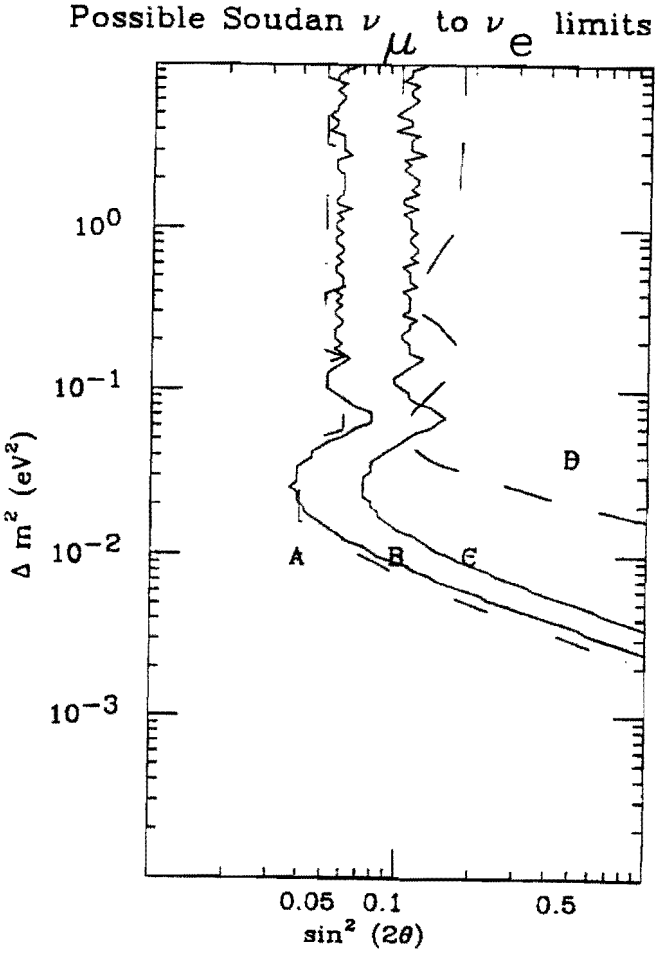

Figure 15: 90% CL limits on $\nu_\mu \rightarrow \nu_e$ oscillations attainable by Soudan 2. Curve A(dot-dash) uses the $R_{"nc"/"cc"}$ test, B is based on the $R_{near/far}$ test and C on the $R_{\frac{e}{\mu}}$ test. Curve D is the presently excluded region from Gosgen reactor.

5.6 Stopping muons

Approximately 500 of our 2150 muons emerging from the rock are expected to stop in the detector. We have studied the response of our detector to stopping muons both in surface cosmic ray events and in the Rutherford ISIS test beam. We have measured the ionization rise at the end of the track and have observed the decay electrons from stopping μ^+'s. Visible decays are strongly suppressed in iron for stopping μ^-'s. This μ^+/μ^- discrimination will enable us to search for oscillations in the mode $\nu_\mu \rightarrow \overline{\nu}_\mu$ using the μ^+/μ^- ratio. The rate of stopping muons has a different energy dependence than the total rate of rock muons. The energy dependence of several processes which we will measure is listed in Table 1. Whether a neutrino oscillation signal is present or absent, P822 should measure a consistent number of events for these processes. The ability to measure a number of different processes will be an important confirmation that the energy dependence of the flux is understood.

Table 1
Energy dependence of various processes

Neutrino flux	$\phi_\nu(E)$
Contained vertex events	$E\phi_\nu(E)$
Rock muons	$E^2\phi_\nu(E)$
Quasi-elastic contained events	$\phi_\nu(E)$
stopping muons	$E\phi_\nu(E)$

5.7 Larger area muon detection

In addition to the 2150 μ's entering the main detector, we expect 8150 μ's (based on $275m^2$ normal to the direction of the beam[3]) entering the south and east shield wall. It would not be expensive to enhance the front shield wall with a crossed layer of proportional tubes, in order to trigger on the extra 6000 muons. Within the present configuration of the shield, there would be four tube crossings for each muon traversing the Soudan 2 shield. We propose to enhance this to at least six. With six tube crossings, we will both get an acceptable trigger rate, and be able to fully reconstruct the angle of the muon to the $\sim 2^\circ$ angular resolution of the shield[38]. After reconstruction, there would be essentially no background for muons at this angle, even before event timing in coincidence with the Fermilab beam is imposed. The limit that could be set if the expected number of muons is observed is given in figure 1 curve "A".

Besides enhancing the existing "shield", several other parts of the Soudan mine could be instrumented with crossed proportional tubes. A significant area of tubes in a variety of locations throughout the Soudan mine, and/or on the surface, would again increase the statistics and allow some information about the radial extent of the beam to be measured. This would require the building of additional equipment. However, the relative cost of these detectors compared to either the main calorimeter or the neutrino beam itself would be

[3]This area is comparable to the area of the IMB detector (P805).

small. It is seen from figure 14 that the physics value of an increased number of muons using the R_μ test is quite marginal. This is because the statistical power of the test is dominated by the number of vertex contained events that are measured. However, increased statistics of muons would allow important systematic studies to be performed, and would provide a consistency check on any possible signal with an independent data sample. In conjunction with the $R_{near/far}$ test, the enhancement of the shield is more valuable. This can also be seen in figure 14. The most sensitive $\nu_\mu \rightarrow \nu_\tau$ search that we could perform requires both a two station experiment and the enhancement of the shield.

The ν beam exits the earth about 20 miles north of the Soudan mine. One could install four sets of $10m^2$ tube planes, 6 layers each of muon detectors here, doubling the effective area of the experiment for a modest cost. The four sets could measure the lateral spread of the beam. Since the telescope would aim almost horizontally, cosmic ray background should be manageable.

5.8 ν_τ event identification

As already pointed out, ν_τ charged current (CC) interactions in which the τ decays into hadrons plus a ν_τ will be classified as neutral current (NC) interactions. However, they are expected to have a significantly different kinematic configuration than the ν_μ neutral current events. We have made a Monte Carlo study using the proposed neutrino beam spectrum to see if this difference can be exploited to identify ν_τ events. The method we use is the multivariant discriminant analysis. This method finds clusters corresponding to the three classes of events, CC, NC, and ν_τ, in a multidimensional space of kinematic variables. We found that a significant portion of the ν_τ region was not overlapped by the NC or CC regions (in any case CC's will be identified by their muons). Therefore for oscillation probabilities greater than P=.06 we could expect to identify on the order of half of the τ events in the Soudan central detector. For the near detector part of the experiment, we need further study since we would be dealing with much smaller values of P and need to carefully see how the tails of the NC cluster reach into the τ region. We intend to continue this study, increasing our Monte Carlo statistics and folding in detector properties. Of course, such analyses can be made only in detectors which yield information about individual tracks from complex events.

Another signal that Soudan 2 can search for is quasi-elastic ν_τ scattering ($\nu_\tau n \rightarrow \tau^- p$). The calculated ν_τ quasi-elastic cross section as a function of energy is given in figure 11. In 65% of τ decays, the tau will show up as one to five charged pions, plus neutral energy. Events containing tightly collimated high energy pions are expected to have a characteristic signature in Soudan 2, but would be difficult to identify in water Cerenkov detectors. We are now carrying out Monte Carlo studies on simulated quasi-elastic ν_τ events to quantitatively estimate our event identification capability for ν_τ events.

In the other 35% of the quasi-elastic events, the τ would decay into a single electron or muon. Single leptons at small but nonzero angles from the Fermilab beam direction would be rather unlikely in the absence of oscillations, and a positive result for ν_τ's in the appearance (nc/cc) and/or disappearance part of the experiment should be accompanied by such events. For the electron channel, this will rely on our ability to reject hadrons versus single electrons near 20 GeV, which will be better than 100 to 1 for exclusive electron

events[39]. Coherent π^0 production off the nucleus and neutrino electron elastic scattering would be small backgrounds in this channel. Here again, we are carrying out Monte Carlo studies.

5.9 External muon identifier

We believe that the installation of an external muon identification system would constitute a valuable addition to this experiment. It would increase by 50% the fiducial mass of the detector which can be used for the $R_{"nc"/"cc"}$ tests. About half of the muons from ambiguous nc or cc events deep in the detector will exit the north wall, while the other half will exit towards the west. On the north side, there is ample space to instrument an external muon identification system, and to place material to absorb hadrons from neutrino events deep in the calorimeter.

In addition, magnetized iron as part of the external muon identifier would give us information about the muon momentum for many events. We have just started exploring the advantages that an external muon identifier would give using Monte Carlo simulations. No result shown in this proposal relies on external muon identification, but all those dependent on the number of identified events in the main detector would be improved. We expect to submit an addendum to this proposal at a later date which will discuss both the possible improvements in physics reach that this enhancement would provide, and the possible design and costs of such a system.

5.10 Additional enhancements to the Soudan 2 detector

This proposal for the long baseline neutrino beam is one that would require a substantial investment on the part of Fermilab. Completion of the Main Injector and the proposed wide band neutrino beam are at least four years in the future. It is reasonable to examine what other possibilities exist for enhancing this experiment that have not yet been thoroughly considered. Anti-neutrino running is one possibility.

The Soudan site contains three times the volume of excellent laboratory space than will be occupied by the Soudan 2 detector. This gives us considerable flexibility to:

1. Add additional modules to the Soudan 2 detector.
2. Expand the shield
3. Add distributed dead mass within the existing detector to increase the contained vertex ν event rate at low cost.
4. Add an external muon identifier system.
5. Move an additional existing detector into the Soudan Laboratory
6. Build a new detector.

5.11 Summary of oscillation measurements

We have considered a number of different ways to study potential neutrino oscillations. The following list summarizes the different processes which Soudan 2 can observe.

- the neutral current rate
- the charged current rate
- the contained vertex rate
- the rock muon rate in the detector
- the rock muon rate in the shield
- the stopping muon rate
- the stopping muon charge ratio
- the quasi-elastic muon rate
- all of the above rates in a near detector at Fermilab.

Neutrino oscillation tests involve measuring the ratios of these various rates. Of course not all of the ratios would be independent tests. We have discussed in some detail the $R_{"nc"/"cc"}$, $R_{\frac{\mu}{e}}$, and $R_{near/far}$ tests. We try to summarize in table 2 the most important tests we can do. In the table we distinguish four modes of neutrino oscillation ($\nu_\mu \rightarrow \nu_\tau, \nu_\mu \rightarrow \nu_e, \nu_\mu \rightarrow \nu_R, \nu_\mu \rightarrow \overline{\nu}_\mu$) and those independent tests that could be used in each mode.

In table 3 we give some example event rates for different assumed values of the oscillation probability. This way is not precisely correct because the probability is a function of energy, but it gives the reader a feeling for the statistical power of the various tests.

Table 2
Neutrino Oscillation Tests

mode	test	note
$\nu_\mu \rightarrow \nu_\tau$	$R_{\text{"nc"}/\text{"cc"}}$	
$\nu_\mu \rightarrow \nu_\tau$	$R_{\frac{\mu}{\nu}}$	detector μ
$\nu_\mu \rightarrow \nu_\tau$	$R_{\frac{\mu}{\nu}}$	shield μ
$\nu_\mu \rightarrow \nu_\tau$	$R_{near/far}$	two station
$\nu_\mu \rightarrow \nu_\tau$	$R_{near/far}$	shield, two station
$\nu_\mu \rightarrow \nu_\tau$	stopping muon rate	two station
$\nu_\mu \rightarrow \nu_e$	$R_{\text{"nc"}/\text{"cc"}}$	
$\nu_\mu \rightarrow \nu_e$	$R_{\frac{\mu}{\nu}}$	detector μ
$\nu_\mu \rightarrow \nu_e$	$R_{near/far}$	two station
$\nu_\mu \rightarrow \nu_e$	$R_{near/far}$	shield, two station
$\nu_\mu \rightarrow \nu_e$	$R_{\frac{\mu}{\nu}}$	shield μ
$\nu_\mu \rightarrow \nu_R$	two detector	
$\nu_\mu \rightarrow \overline{\nu}_\mu$	$\frac{\mu^-}{\mu^+}$	stopping muons

Table 3--Example event rates

	P = 0	P = 0.1	P = 0.2	P = 0.345
$R_{\text{"nc"}/\text{"cc"}}$	$\frac{103}{331} = .31 \pm .03$	$\frac{109}{299} = .37 \pm .04$	$\frac{116}{268} = .43 \pm .05$	$\frac{126}{222} = .57 \pm .06$
$R_{\frac{\mu}{\nu}}$	$\frac{2150}{678} = 3.17 \pm .14$	$\frac{1939}{639} = 3.04 \pm .14$	$\frac{1729}{599} = 2.88 \pm .14$	$\frac{1423}{542} = 2.62 \pm .13$
$R_{near/far}$	$\frac{10^6}{8150} = 123 \pm 2.5$	$\frac{10^6}{7351} = 136 \pm 2.7$	$\frac{10^6}{6553} = 153 \pm 3.1$	$\frac{10^6}{5395} = 185 \pm 3.7$

Table 3: Expected ratios for several example probabilities of oscillation (.345 corresponds to the Kamiokande value at high L/E)

6 Performance and Calibration

6.1 Module performance

The response of the detector is continuously monitored by analysing the data from the cosmic ray muons which trigger the experiment at a rate of about 0.3 Hz. A sample of tracks accumulated over several weeks is used to measure the detailed response in the region of nucleon decay or neutrino interaction candidate events. In order to optimize the operating parameters (e.g. gas and electronic gains), a few modules were initially operated on the surface where the cosmic ray flux is high enough to do high statistics studies rapidly. Some of the results on detector performance of the modules operated on the surface are presented in this section.

For the study of tube efficiency the cosmic ray muon trajectories were fitted. By comparing the number of hit tubes crossed by the trajectory with the number predicted to be hit, the tube efficiency is determined. Such a definition not only considers if the tube is working, it also includes the anode-cathode matching efficiency and the track fitting efficiency. Moreover, the efficiency will be decreased due to deviations of the actual tube position from its nominal position, and random scattering of the muon from a smooth trajectory. In the case of perfect geometry, for Monte Carlo data, the tube efficiency is 85%. Under actual operating conditions the mean tube efficiency is of the order of 75%. The mean tube efficiency is very uniform throughout a module, as is shown in figure 16, where the efficiency is plotted along the cathode direction. The variations seen in figure 16 are correlated with the pulse height variations along the cathode direction. The maximum tube efficiency that is reached is 80% for very high pulse heights, but the modules were operated at the knee of the efficiency plateau to remain in the proportional gain region.

Typical drift attenuation lengths are of the order of 70 cm. For the pulse height distribution shown in figure 17 the attenuation lengths for the two 50 cm drift regions are 71 and 63 cm. Such attenuation is well understood in terms of electron diffusion during drifting and electron attachment due to O_2 contamination at the few ppm level. Some variations from module-to-module can be observed, even with the same gas composition, due to imperfections in the electric field which show up as a difference in the effective radii of the tubes. In the absence of oxygen attachment, attenuation lengths are expected to be about 70 cm. The spatial resolution is determined by the anode and cathode spacing, the drift time digitization unit and the drift velocity. The spatial resolution is obtained from the RMS of the residual distributions, calculated by fitting cosmic ray muon tracks. The spatial resolution in the vertical (y) direction is 0.47 ± 0.10 cm , compatible with the expectations from cathode separation. A result consistent with anode separation is obtained in the horizontal (x) direction. The spatial resolution in the drift (z) direction is 1.04 ± 0.24 cm.

One of the main characteristics of the Soudan 2 detector is its ability to yield pulse height information for track direction determination and particle identification. To make maximum use of this information, the pulse height variation between modules must be smaller than Landau fluctuations (20%). Typical pulse height fluctuations along the wire plane are of the order of 30%, while in the drift direction, due to pulse height attenuation, a 50% reduction in pulse height can be observed (see figure 17). However, these variations are corrected by calibrating out the effects of measured pulse height attenuation, wire plane nonuniformities,

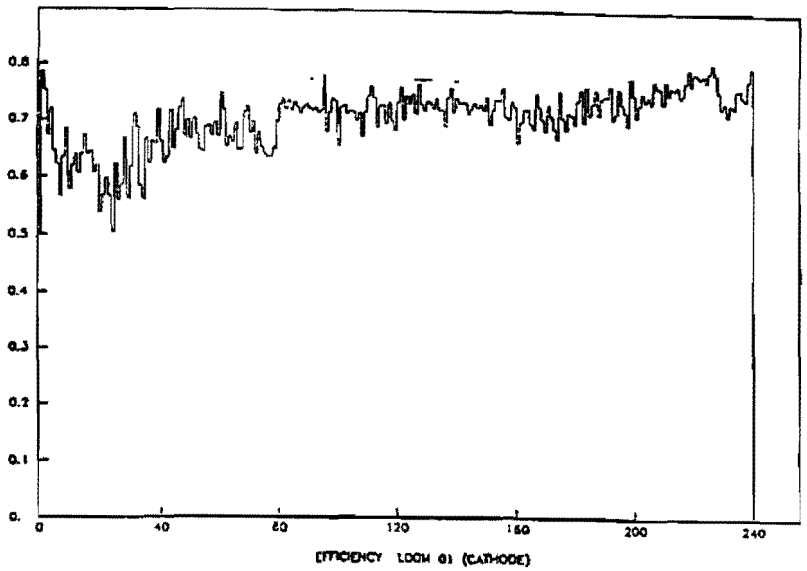

Figure 16: Typical mean tube efficiency variation with cathode numbers.

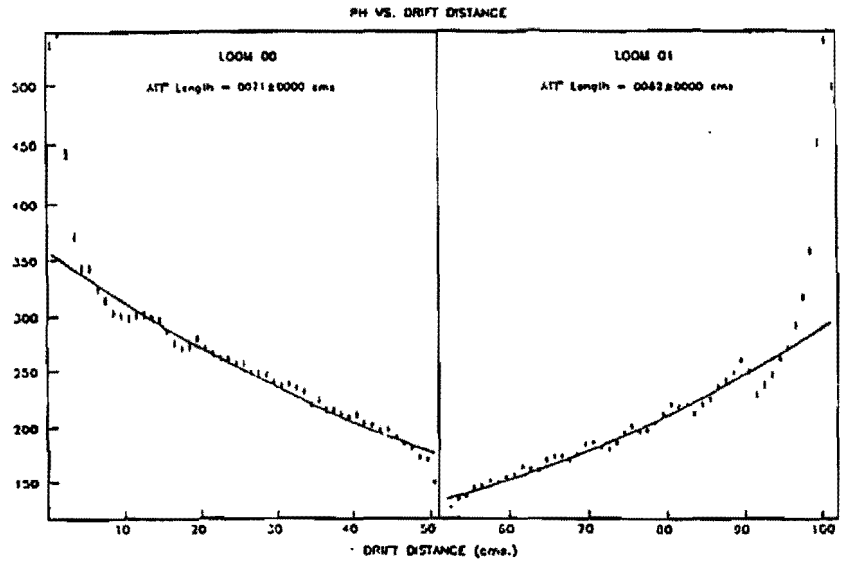

Figure 17: Typical pulse height variation along the drift direction.

module-to-module variations, atmospheric pressure, and gas composition. After pulse height calibration, a 10% variation is obtained.

6.2 Module calibration

At the Rutherford Laboratory's ISIS pulsed neutron source, a Soudan 2 calorimeter module was exposed to beams of positive and negative pions, muons, and electrons at momenta between 140 and 400 MeV/c, and protons at 700 and 830 MeV/c, for several angles of incidence. Analysis of the data is in progress but preliminary results are available on the detector resolution, ionization response, and particle identification. These studies have confirmed that the detector modules are performing as expected, and also have provided detailed response parameters which can be used in the Monte Carlo detector simulation.

The electromagnetic shower energy is determined by counting tube crossings (hits). Figure 18 shows the number of tube crossings as a function of the electron beam energy, for ISIS and Monte Carlo data. The non-linear dependence upon the energy reflects the high density of tube crossings at high energy. The measured energy resolution can be represented as in figure 19.

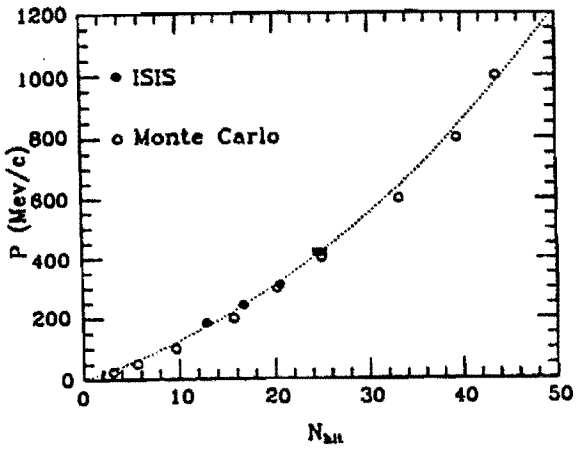

Figure 18: Electron shower energy versus number of hits from ISIS data and Monte Carlo simulations.

Although the Soudan 2 detector is designed to be relatively isotropic, its geometry is not completely uniform. This fact will affect, at some level, the number of hits counted for shower energy measurement. Figure 20a shows the number of hits observed for different vertical incidence angles of the beam, for tracks perpendicular to the tubes. The maximum variation (8%) is obtained for small vertical angles. This variation is easily calibrated. The total pulse height is independent of the vertical incidence angle as is shown in figure 20b. When the dependence upon horizontal angle (angle with the z direction) was measured, a variation of the number of hits was observed where the beam is almost parallel to the tubes (see figure 20c). The total pulse height does not vary with horizontal angle (figure 20d).

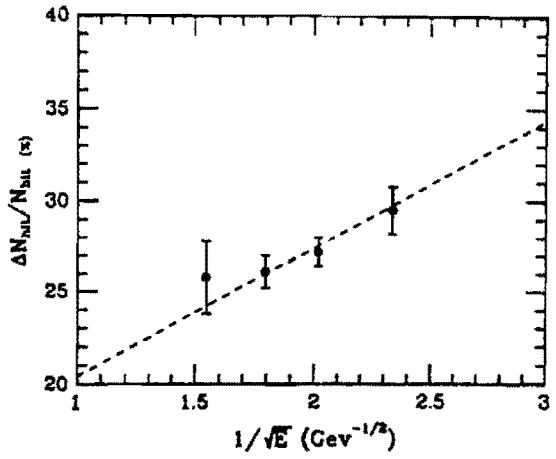

Figure 19: Energy resolution for electron showers.

Therefore, the Soudan 2 detector is isotropic after some small corrections. The small detector anisotropy observed is confirmed with the Monte Carlo and does not compromise the energy resolution.

A sample of π^0's produced in charged pion interactions has been reconstructed. The events were selected by scanning for events with two well separated showers. The π^0 peak is centered at $136 \pm 3\ MeV/c^2$ and has an RMS of $40\ MeV/c^2$ (see figure 21). When the production vertex is known it is possible to distinguish electrons from photons by measuring the distance between the vertex and the first hit (conversion length). If the distance is smaller than $4\ cm$ the relative probability to be $e : \gamma$ is $8 : 1$, for a distance larger than $1\ cm$ the shower is more likely a photon with $e : \gamma$ a probability of $1 : 14$.

Muon momentum is calculated from the range obtained by measurement of the muon track length (L) and using a mean detector density ($1.6\ g/cm^3$). The average length for $245\ MeV/c$ muons is $40.6\ cm$, with $\frac{\Delta L}{L} = 20\%$, giving a momentum resolution of 8%. This resolution is independent of momentum for the ISIS energies.

Soudan 2 can distinguish between stopping positive and negative muons because most negative muons are captured by iron nuclei and do not decay visibly. The decay positrons from positive muons are usually detected. Figure 22 shows the number of extra hits at the ends of tracks for samples of negative and positive muons. Two or more shower hits are observed at the end of 85% of the positive muon tracks. No hits are observed for 75% of the negative muon tracks.

The expected ionization response of a slowing muon is observed. Figure 23 shows the mean pulse height along the muon trajectory measured from the end of the track. Crude measurement of the track direction (choosing the end with the higher mean ionization on the last 5 hits as the stopping end) yields the correct direction 80% of the time.

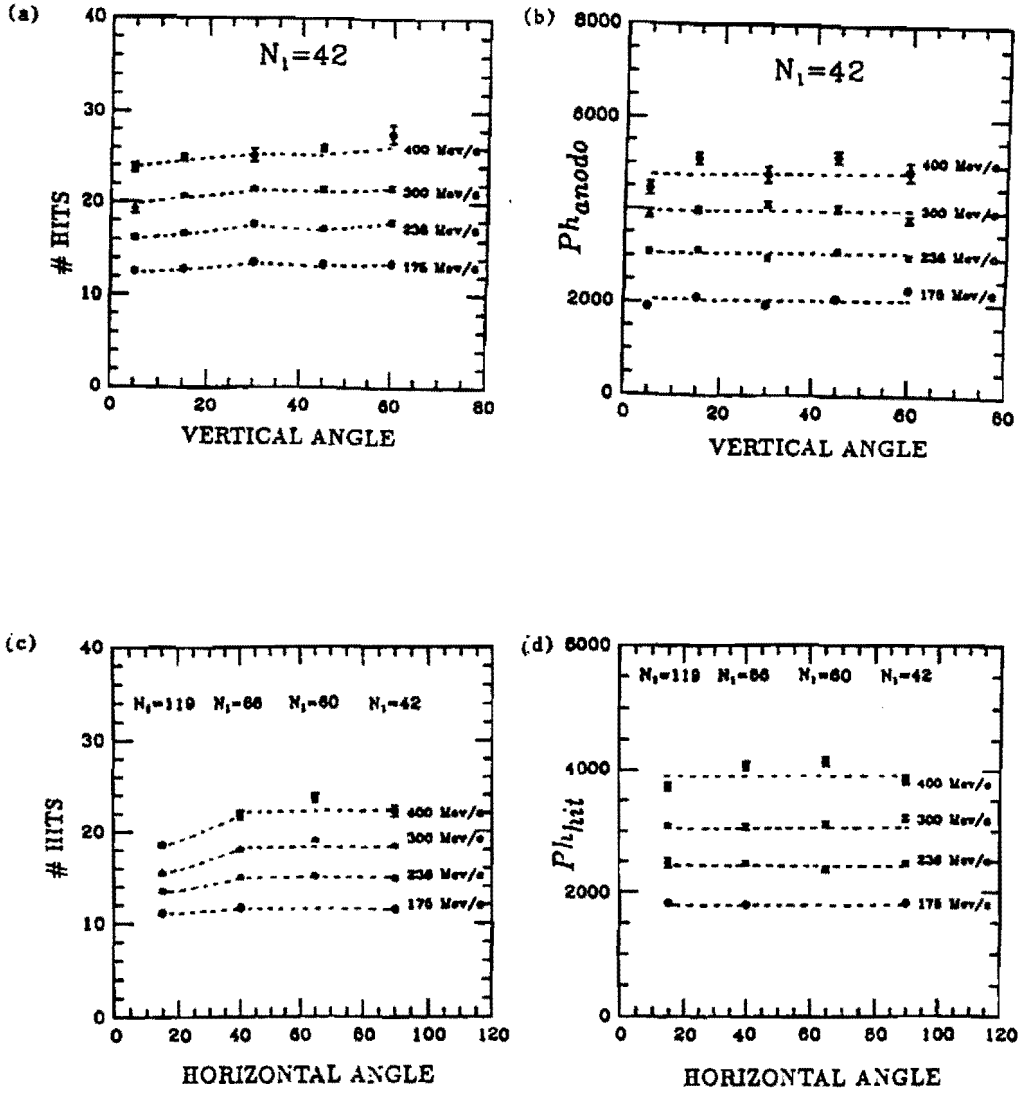

Figure 20: Mean number of hits (a) and mean total pulse height (b) for different beam momenta versus the vertical angle, and mean number of hits (c) and mean total pulse height (d) versus the horizontal angle.

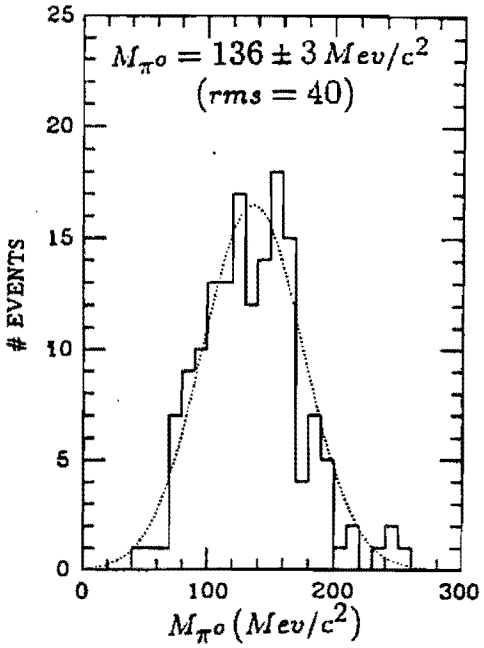

Figure 21: Invariant mass distribution for two shower events in the $\pi^{\pm}$ beam.

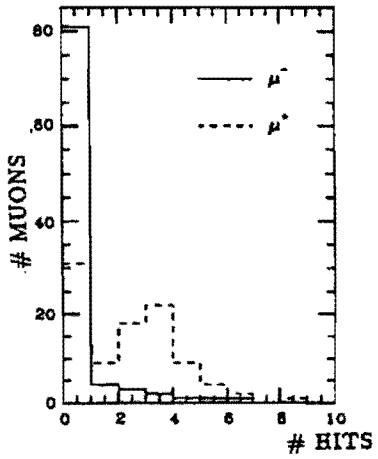

Figure 22: Number of shower hits at the end of $\mu+$ and $\mu-$ tracks.

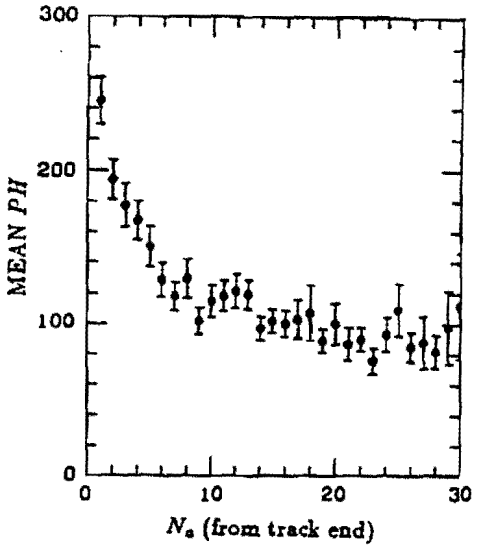

Figure 23: Mean pulse height versus anode number (measured from the last anode in the μ trajectory).

7 Requests of Fermilab

7.1 Clock

To enhance the purity of the neutrino signal it is important to know the timing of the events seen at Soudan relative to the Fermilab beam spill. In order to achieve the required timing of $<\sim 1ms$, it will be necessary to have clocks at each end which are accurate at this level and synchronized with each other. This can be achieved by using clocks which lock onto the WWVB shortwave radio timing signals. An absolute synchronization and a continuing check can be achieved at the microsecond level by using television synchronization signals as broadcast by any of the geosynchronous satellites.

At Soudan, we would write, as part of the data record, the time of every trigger. At Fermilab we would write the time of each spill as well as any other information available (e.g. spill intensity, targeting information....). There is a data link between the two sites and at the end of each run the Fermilab disk file would be sent to Soudan where an offline correlation would be done to match up events with beam spills. At this time an integrated exposure could be calculated, based on beam intensity and targeting.

In addition, if necessary for the shield-only events, we could use the Soudan clock to generate a trigger gate for the expected beam arrival time. Clearly this would have to be regularly checked against the actual accelerator clock by sending information on the data link, particularly when the spill period or phase is changed.

7.2 Beam monitoring

It will be very important to monitor the primary and secondary beams with great precision and with redundant systems. For secondary flux measurements in the horn, we would want beam toroids and secondary emission monitors, as well as a calibration system to study the particle content in the horn. For the proton beam, a series of precise segmented wire ionization chambers will be required to record the position where the beam hits its target on a pulse by pulse basis. Downstream of the dump, scintillation counter arrays would be used for both flux and targeting comparisons, as muon rates are extremely sensitive to these parameters.

7.3 Near detector

Our collaboration will provide the modular detectors and the electronics for the near station experiment. However, about 8 m of space which does not interfere with Fermilab P803 will be required, in addition to a data acquisition system, and full access to beam monitoring information.

7.4 Detector cost estimates

We estimate that the necessary additional equipment, such as a WWVB clock and communications system, a veto counter system for the near detector, beam monitoring equipment, a platform for near station modules, and a data acquisition system will cost about $250,000. A

major upgrade, such as the external muon identification system at Soudan, would certainly be much more expensive. However, the largest cost is certainly the construction of the beam as described in the Fermilab Neutrino Conceptual Design Report.

7.5 Computing requirements

The primary off-line analysis for Soudan 2 is now done at the Soudan site. At Fermilab, we would require processing for the large event sample from the near detector, and for Monte Carlo and summary tape analysis. We request

1. 7 Vaxstation 3200 equivalents for 9 months at the time of the ν exposure.
2. 1 Vax 3200 equivalent for 2 years (the year before and the year after) for Monte Carlo and summary tape analysis.
3. Access to Fermilab computing resources before the exposure for beam design Monte Carlo, etc.

8 Concluding remarks

8.1 Personnel issues

Our collaboration includes all institutions which are currently carrying out the Soudan 2 proton decay experiment: Argonne National Laboratory, the University of Arizona, the University of Minnesota, Tufts University, the University of Oxford and Rutherford-Appleton Laboratory. Considerable support will continue to be provided by those institutions for P822. Members of our collaboration have extensive experience on neutrino experiments, having worked on E594 and CCFR at Fermilab, and on Argonne 12', Fermilab 15' and CERN BEBC neutrino experiments, as well as Los Alamos neutrino exposures, τ studies at SLAC's HRS, and atmospheric neutrino studies.

8.2 Conclusion

The Soudan 2 detector is an excellent target for a long baseline ν beam from the Fermilab Main Injector. The detailed event reconstruction capabilities of Soudan 2 and our ability to perform a two station experiment will give very good control of potential systematic errors. We can also uniquely perform an important ν_τ appearance experiment by using the clearly distinguishable patterns of charged current and neutral current events. This is more important than the added statistical power one achieves in an experiment closer to Fermilab without such pattern recognition capability. Our experiment could discover compelling evidence for neutrino oscillations. If $\nu_\mu \rightarrow \nu_\tau$ and $\nu_\mu \rightarrow \nu_e$ oscillations do not exist in this large new region of parameter space, important new limits on neutrino properties can be set.

List of Figures

References

[1] A.K. Mann & H. Primakoff. Phys. Rev. **D15**. (1977) 655.

[2] K. S. Hirata *et al.*, Physics Letters **B205**. (1988) 416 .

[3] S.P. Mikheyev and A. Yu. Smirnov Sov. J. Nucl. Phys., **42**. (1986) 913; Nuovo Cimento. **9C**. (1986) 17.

[4] D. S. Ayres, "The Soudan 2 Experiment", Proceedings of the 10th Workshop on Grand Unification, Chapel Hill, North Carolina, April 1989.

[5] Proceedings of the Workshop on the Main injector, May 16-18, 1989, S. Holmes and B. Winstein, editors.

[6] P803, Proposal for an Experiment to improve limits for $\nu_\mu \rightarrow \nu_\tau$ neutrino oscillations, R. Lipton *et al.*, p10.

[7] Conceptual Design Report: Main Injector Neutrino Program, 1991.

[8] M. Gell-Mann, P. Raymond, and R. Slansky, 1979 in *Supergravity*, edited by P. Van Nieuwenhuizen and D. Z. Freedman (North-Holland, Amsterdam), p. 315; T. Yanagida, 1979, Proceedings of the Workshop on Unified Theory and Baryon Number of the Universe, Tsukuba, Ibaraki, Japan, unpublished.

[9] T. K. Gaisser, T. Stanev, S. A. Bludman, and H. Lee, Phys. Rev. Lett. **51** (1983) 223; J. L. Osborne, S. S. Said, and A. W. Wolfendale, Proc. Phys. Soc. **86** (1965) 93; A. C. Tam and E. C. M. Young, in: Proc. Eleventh Intern. Conf. on Cosmic rays (Budapest, 1969), Acta Phys. Hungaricae **29**, Supp. 4 (1970) 307; E. C. M. Young, Cosmic Rays at ground level (Adam Hilger, London, (1973), p. 105; K. Mitsue, Y. Minorikawa, and H. Komori, Nuovo Cimento **9 C** (1986) 995; E. V. Bugaev, G. V. Domogatsky, and V.A. Naumov, Proc. Japan-USA Seminar, Cosmic ray muon and neutrino physics/astrophysics using deep underground/underwater detectors, eds. Y. Ohashi and V. Z.Peterson (Institute for Cosmic Ray Research, University of Tokyo, June 1986) p. 232.

[10] See for example, M. Shaevitz, proceedings of the conference on New Directions in Neutrino Physics at Fermilab, September 1988; and F. Vannucci, Proceedings of Neutrino '88, Boston (1988).

[11] N. Ushide *et al.*, Phys. Rev. Lett. 57, (1986) 2897.

[12] F. Dydak *et al.*, Phys. Lett. 134B, (1984) 34.

[13] D. Casper *et al.*, "Measurement of Atmospheric Neutrino Composition with IMB", BU preprint 90-23, (1990), submitted to Phys. Rev. Lett.

[14] G. Barr, T.K. Gaisser and T. Stanev; Phys. Rev. **D39** (1989), 3532.

[15] S. Barr, T.K. Gaisser, P. Lipari and S. Tilav; Phys. Lett. **B214** (1988) 147.

[16] Ch. Berger *et al.*, Phys. Lett. **B245** (1990) 305.

[17] Ch. Berger *et al.*, Phys. Lett. **B227** (1989) 489.

[18] M. Aglietta *et al.*, Europhys. Lett. **8** (1989) 611.

[19] LoSecco *et al.*, Phys. Rev. Lett. **55**, (1985) 2299, Nucl. Physics B (Proc. Suppl.) **14A** (1990) 119.

[20] Luciano Moscoso, Saclay preprint DPhPE 90-14, submitted to the proceedings of Neutrino '90, CERN, June 1990.

[21] J. G. Learned, S. Pakvasa, and T. J. Weiler, Physics Letters **B207** (1988) 79, M. Takita, University of Tokyo Ph. D. Thesis (1989).

[22] J. K. Rowley, B. T. Cleveland, and R. Davis, Jr., in Solar Neutrinos and Neutrino Astronomy, eds: M. L. Cherry, W. A. Fowler, and K. Lande, AIP Conf. Proc. No. 126, p. 1, (1985); R. Davis Jr., in Proc. of the Seventh Workshop on Grand Unification, ICOBAN '86, ed: J. Arafune (World Scientific), p. 237 (1987); R. Davis, Jr., in Proc. of the 19th Int'l Conf. on Neutrino Physics and Astrophysics, "Neutrino '88," eds: J. Schneps *et al.* (World Scientific) p. 518 (1989).

[23] K. S. Hirata *et al.*, Phys. Rev. Lett. **65** (1990) 1297.

[24] Neutrino Astrophysics, John N. Bahcall, Cambridge University Press, 1989.

[25] J. N. Bahcall and H. A. Bethe, Phys. Rev. Lett. **65**, (1990) 2233; S. P. Mikheyev and A. Yu. Smirnov, Sov. Phys. Usp., **30** (1987) 759; L. Wolfenstein, Phys. Rev. **D 17** (1978) 2369; T. K. Kuo and J. Pantaleone, Rev. Mod. Phys. **61** (1989) 937-979; S. J. Parke, Resonant Neutrino Oscillations, Fermilab-Conf-86/131-T (1986).

[26] V Zacek *et al.*, Phys Lett. **164B** (1985) 193, and J. F. Cavaignac *et al.*, Phys. Lett. **148B** (1984) 387.

[27] J. L. Thron, Nucl. Instr. and Methods **A283** (1989) 642.

[28] W. P. Oliver *et al.*, *A rugged 1700 m^2 Proportional Tube Array*, Nucl. Instr. and Methods **A276** (1989) 371.

[29] Steve Werkema, Ph. D. thesis, Monte Carlo Evaluation of the Atmospheric Neutrino Background to Nucleon Decay in the Soudan 2 Detector University of Minnesota 1989.

[30] A. J. Parke, Terrestrial Long-Baseline Neutrino Oscillation Experiments, FNAL internal note, July 24, 1990; R. Bernstein, Long-Baseline Neutrino Oscillation Experiments at the Fermilab Main Injector, FNAL internal note, June 11, 1990.

[31] D. Bogert *et al.*, Phys. Rev. Lett. **55**, (1985) 1969.

[32] N. Reay, Report from the Short Baseline neutrino oscillations Group, p 159, Proceedings of the Workshop on the Main Injector, 1989; also N. Stanton, private communication.

[33] J. Wilkerson, Proceedings of 1990 Snowmass summer study on Future Directions in Particle Physics. To be published.

[34] D. Bogert *et al.*, IEEE Trans. Nucl. Sci., **NS-29**, No. 1 (February 1981). D. Bogert *et al.*, Phys. Rev. Lett. **55**, (1985) 574; and D. Bogert *et al.*, Phys Rev. Lett. **55**, (1985) 1969.

[35] A Proposal for a Long Baseline Oscillation Experiment Using A High Intensity Neutrino Beam from the Fermilab Main Injector to the IMB Water Čerenkov Detector (P805) October 1990.

[36] Conceptual Design Report: Main Injector Neutrino Program, 1991, p122.

[37] Roger Phillips, private communication.

[38] Joe Kochocki, "An underground search for an excess muon flux from the direction of Cygnus X-3", Ph.D. Thesis Tufts University, May 1989; and Kochocki *et al.*, Phys. Rev. **D42** (1990), 2967.

[39] We will be able to take advantage of all of the techniques used in Fermilab Experiment 594. They are described in "A measurement of the elastic scattering cross section $\nu_\mu + e^- \rightarrow \nu_\mu + e^-$" by Michael Tartaglia, Ph.D. thesis, Massachusetts Institute of Technology, 1984.

Progress Report and Revised P–822 Proposal for a Long Baseline Neutrino Oscillation Experiment from Fermilab to Soudan 12 October 1993

W.W.M. Allison[6], G.J. Alner[7], D.S. Ayres[1], L. Balka[1], W.L. Barrett[11], R.H. Bernstein[2], R.E. Blair[1], C. Bode[5], D. Bogert[2], P. Border[5], C.B. Brooks[6], V.A. Chechin[4], N. Christiansen[5], J.H. Cobb [6], D.J.A. Cockerill[7], R. Cotton[7], H. Courant [5], J. Dawson[1], D. Demuth[5], B. Ewen[10], T.H. Fields[1], H. Gallagher[1], G. Giller[6], S. Giron[5], M.C. Goodman[1], K. Heller[5], N. Hill[1], D.J. Jankowski[1], D. Johnson[2], T. Kafka[10], S. Kasahara[5], G. Koizumi[2], D. Krakauer[1], E.P. Kuznetesov[4], W. Leeson[10], P.J. Litchfield[7], F. Lopez[1], W. A. Mann[10], D. Maxam[5], M. L. Marshak[5], E.N. May[1], L. McMaster[10], R. Milburn[10], W. Miller[5], L. Mualem[5], A. Napier[10], W. Oliver[10], G.F. Pearce[7], D.H.Perkins[6], E.A. Peterson[5], L.E. Price[1], J. Repond[1], D. Roback[5], R. Rusack[5], K. Ruddick[5], D. Schmid[8], J. Schneps[10], P. Schoessow[1], N. Sundaralingam[10], R. Talaga[1], J. Thron[1], T. Toohig[8], H. J. Trost[9], I. Trostin[3], V. Tsarev[4], G. Villaume[5], J. Volk[2], S. Werkema[2], and N. West[6]

Argonne[1] - Fermilab[2] - ITEP[3] - Lebedev[4]

Minnesota[5] - Oxford[6] - Rutherford[7] - SSC Lab[8]

Texas A&M[9] - Tufts[10] - Western Washington[11]

Progress Report and Revised P–822 Proposal for a Long Baseline Neutrino Oscillation Experiment from Fermilab to Soudan 12 October 1993

Contents

Abstract

The atmospheric muon neutrino deficit suggests that ν_τ mass and mixings could be measured with a long baseline neutrino oscillation experiment from Fermilab's Main Injector. We are proposing such an experiment from Fermilab to Soudan, Minnesota using a double horn neutrino beam and the 120 GeV Main Injector. The experiment concentrates on the mode $\nu_\mu \rightarrow \nu_\tau$. The experiment would make use of the existing Soudan 2 detector and a smaller near detector located behind the short baseline experiment P–803. The systematically cleanest signal for this mode is a change in the apparent neutral-current to charged-current ratio. In two nine month runs, we are sensitive to $\sin^2 2\theta \geq 5.0 \times 10^{-2}$ and $\Delta m^2 \geq 2 \times 10^{-3} eV^2$. This experiment will conclusively confirm or refute the exciting possibility that neutrino oscillations are causing the atmospheric ν_μ deficit.

1 Introduction

1.1 Historical Context

The solar neutrino deficit, atmospheric neutrino deficit, and the missing mass problem offer three separate hints that the neutrino may possess mass. Neutrino oscillations are a natural consequence of neutrino mass. For the last several years, there has been increasing evidence that the Δm^2 range from 0.001 to 1 eV^2 is the range of interest for neutrino oscillation searches. ($\Delta m^2 = \mid m_1^2 - m_2^2 \mid$) In this range there is a very strong hint for neutrino oscillations from the atmospheric neutrino deficit. Independently, if the solar neutrino deficit is due to $\nu_\mu \rightarrow \nu_e$ oscillations, this range is a strong candidate for $\nu_\mu \rightarrow \nu_\tau$ oscillations. Finally, if the dark matter includes a 10 eV ν_τ, this range is a strong candidate for $\nu_\mu \rightarrow \nu_e$ oscillations. It is this range of 0.001 to 1 eV^2 to which a long baseline ($\sim$ 700 km) neutrino experiment from Fermilab's Main Injector is sensitive.

The P–822 Proposal for the long baseline neutrino oscillation experiment from Fermilab to Soudan was submitted in March 1991. The overall physics motivation and capabilities of the experiment to study neutrino oscillations remain essentially the same.

Several aspects of our original proposal will be updated in this document. A discussion of the double horn beam was presented to Fermilab in June 1991 through a Conceptual Design Report.[1] That beam did not point at the Soudan 2 detector; a new beam design and cost estimate are being prepared by the FermiLab Facilities Engineering Services (FES). A number of important physics and detector issues have been documented in some detail in the Proceedings of the Long Baseline Workshop at Fermilab in late 1991.[2] We have addressed those aspects of long baseline neutrino physics which we regard as most crucial in this revised proposal. We are also working on other concepts, which are identified at the end of the proposal.

The P–822 proposal was discussed by two neutrino review panels which were convened at

Fermilab in May 1991 and June 1993. In August our collaboration was given questions from the PAC June 1993 Aspen meeting. They require much detailed work to provide complete answers which we have not yet finished to our full satisfaction. However we do present in this document our progress towards full answers. Since we expect further questions from the PAC at the November meeting, we anticipate giving more complete answers to all these questions at the next presentation cycle.

1.2 What we are proposing

We believe that the prospect of a convincing discovery of $\nu_\mu \rightarrow \nu_\tau$ oscillations justifies a major neutrino oscillation program at Fermilab. This document discusses several options to broaden the capabilities of a long baseline experiment from Fermilab to Soudan. Although several such improved capabilities are referred to within this revised proposal, we regard the essence of our proposal as the following:

1. We request that Fermilab build a wide band neutrino beam at the Main Injector pointed in the direction of Soudan 2, together with a detector hall to be shared with P-803.

2. We will use the existing Soudan 2 calorimeter and a similar but smaller near detector to measure neutrino interactions.

3. We are proposing to build a muon toroid system and an enhanced shield, in order to add to the systematic reliability of the experiment.

4. We propose to run for two years with the full upgraded Main Injector proton flux of 9.4×10^{20} protons per year.

If the experiment is approved, we are confident we will be able to determine whether or not the apparent atmospheric neutrino deficit is due to neutrino oscillations.

An important upgrade to the Soudan 2 detector would be to take advantage of the empty space next to it. An approximately 8 kiloton "cavity filler" could be constructed there. Using one of several possible conventional techniques, such a detector could be constructed in a straightforward fashion, though its size would make it relatively costly. We are working to determine its costs and capabilities. We will keep Fermilab appraised of the progress of these studies, and should we decide such capabilities offer compelling advantages, we will propose an additional detector at Soudan or revise this proposal as appropriate.

In Section 3, we compare the capabilities of a long baseline experiment with and without a cavity filler. Some preliminary thoughts about construction and cost of a cavity filler are presented in Section 5. However, we wish to make clear that the cavity filler is not yet a part of this (P-822) proposal. Although it would greatly increase the statistics, it would significantly add to the costs; the tradeoffs must be carefully studied. For example,

additional detector mass would be of great value if several years should be required to reach design intensity in the Main Injector. The tradeoffs in "cavity filler" cost versus granularity, resolution, density, and other capabilities will depend on Monte Carlo simulations which are underway but not yet completed.

This proposal for a long baseline neutrino oscillation experiment depends on the construction of a wide band neutrino beam with the Main Injector, and also on the existence of a short baseline experiment such as P–803.[3] As will be described later, we would rely on the P–803 spectrometer for high resolution measurements of the neutrino beam energy spectrum and composition.

1.3 Organization of Revised Proposal

Since many of the PAC members are new since our first proposal[4] we repeat in this version the essential elements of the physics justification and experimental method to avoid the necessity for constant cross reference between the two documents.

The organization of this document is as follows: In Section 2 we review the physics motivation for a long baseline neutrino oscillation experiment. In Section 3 the experimental capabilities of this proposal are reviewed. In Section 4, we provide preliminary answers to the questions posed by the PAC. We note that we have been unable to answer to our satisfaction all of the questions posed by the PAC but we believe we are headed in the right direction, have made substantial progress and will be able to give more complete answers to the rest of the questions at the next presentation cycle. In Section 5 we discuss the possibilities for a new cavity filler detector in the Soudan facility. In Section 6 we compare the capabilities of this proposal to other searches for $\nu_\mu \rightarrow \nu_\tau$. These include several possible and/or approved short and long baseline experiments. Section 7, describing future work, discusses our efforts on a "cavity-filler design" and sets out our plans for continued analysis. Appendix A discusses the derivation of limits in Δm^2 versus $\sin^2 2\theta$ space for different neutrino oscillation tests. Appendix B describes the existing Soudan detector and calibration. In Appendix C we offer a consistent definition of appearance and disappearance neutrino oscillation experiments. Because we have found differing uses of these terms to be widespread, it is necessary to define and distinguish them.

Where appropriate, cost estimates are included within the relevant Section. All cost estimates are in 1993-94 dollars, with no estimate for inflation.

2 Physics Motivation

2.1 Atmospheric Neutrinos

When our P–822 proposal was submitted in 1991, we argued that the possible atmospheric neutrino deficit was a strong motivation for a long baseline neutrino oscillation experiment. At that time, the evidence for an atmospheric ν_μ deficit was based on 2.8 kiloton years of Kamioka data, and IMB had not publicly presented its μ versus e ring analysis. Now, the same deficit is seen in over 13 kiloton years of H_2O Čerenkov data. It is reviewed here only briefly.

Several underground experiments which can measure the ratio of ν_μ to ν_e in the atmospheric neutrino flux see an apparent deficit of ν_μ compared to expectation. We define a ratio of ratios :

$$R \equiv \frac{(\nu_\mu/\nu_e)_{measured}}{(\nu_\mu/\nu_e)_{predicted}} \tag{1}$$

The experimental situation is summarized in Table 1.[5] We note that the following measurements of contained atmospheric neutrinos are all consistent with a 30-40% deficit of ν_μ normalized to the measured ν_e rate.

- IMB-1 (3.8 kton-year): muon decay fraction[6]
- Kamiokande (6.2 kton-year): muon decay fraction[7]
- Kamiokande (6.2 kton-year): ring analysis[7]
- IMB-3 (7.7 kton-year): muon decay fraction[8]
- IMB-3 (7.7 kton-year): ring analysis[8]
- Kamiokande (2.7 kton-year): ring analysis with inelastics taken into account.[9] This is not independent of the second item above, but uses different analysis techniques and includes more information about the total event sample.
- Frejus (2.0 kton-year): contained events.[10] An analysis of their data including the uncontained events does not favor the existence of a deficit, however. The limit based on this analysis is included on the plot of Figure 1.
- Soudan 2 (1.0 kton-year): preliminary result with contained events.[11] The statistics of the Soudan 2 observation is small, but it is quite intriguing to us that the value is on the low side.

Ascribing the atmospheric deficit to neutrino oscillations defines an allowed region in $\Delta m^2, \sin^2 2\theta$ space. The allowed region (at 90%CL) for $\nu_\mu \rightarrow \nu_\tau$ is shown in Figure 1, together with accelerator limits. The data are taken from an analysis of the first 2.76 kt-year of the Kamioka data. The statistical significance for $R \neq 1$ has increased as Kamioka

has taken more data and more sharply defined the allowed values. IMB has not publicly presented an oscillation analysis, but the results are expected to be similar. A large mixing angle is required to explain the entire effect as $\nu_\mu \rightarrow \nu_\tau$. The entire area shown in Figure 1 is larger than the region of parameter space which is statistically allowed by Kamiokande at 90% CL. However, given the current spectrum of experimental results, and plausible systematic errors, it represents the relevant area of interest for the atmospheric neutrino deficit.

Limits on $\nu_\mu \rightarrow \nu_\tau$ have been presented based on the rate of upward throughgoing muons.[12] However, any limits based on upward going muons must include large systematic uncertainties in the absolute flux of cosmic rays and hence ν's.[13], [14] In our view, such muon measurements have not reliably excluded any of the allowed region in Figure 1. Limits have also been presented by IMB based on upward going stopping muons. This result depends on knowledge of the energy spectrum and on the absence of background, such as hadron backscatter. A background of only 10 such events would invalidate this limit.

Experiment	Exposure	R'
Kamiokande	6.10 kton-year	$0.60^{+0.07}_{-0.05} \pm 0.05$
IMB 3	7.70	$0.54 \pm 0.02 \pm 0.07$
Frejus	2.00	0.87 ± 0.19
NUSEX	≈ 0.4	0.99 ± 0.40
PRELIMINARY		
Soudan 2	1.00	$0.69 \pm 0.19 \pm 0.09$

Table 1: Atmospheric neutrino exposures and results.

2.2 Why Concentrate on $\nu_\mu \rightarrow \nu_\tau$?

We first the define relevant notation. If neutrinos of one species oscillate into at most one other species, the probability is given by

$$P_{\nu_a \rightarrow \nu_b} = \sin^2 2\theta \, \sin^2(1.27 \, \Delta m^2 \, \frac{L}{E_\nu}) \tag{2}$$

with Δm^2 in eV^2, L in km and E_ν in GeV. $\Delta m^2 = |m^2_{\nu_a} - m^2_{\nu_b}|$ and θ is the mixing angle between ν_a and ν_b neutrinos. The masses and mixing angles are unknowns. An experiment

which fails to find neutrino oscillations can set a limit in the Δm^2 versus $\sin^2 2\theta$ parameter space.

Several neutrino oscillation experiments and proposals have been run or are being considered within the high energy physics and nuclear physics communities. Since the observed width of the Z boson permits only three flavors of light neutrinos,[15] it is reasonable to concentrate attention on the three possible modes $\nu_\mu \rightarrow \nu_e$, $\nu_\mu \rightarrow \nu_\tau$ and $\nu_e \rightarrow \nu_\tau$. A long baseline experiment with a primarily ν_μ beam can look for the oscillation modes $\nu_\mu \rightarrow \nu_\tau$ and $\nu_\mu \rightarrow \nu_e$.

What motivates an expensive, difficult search for oscillations? A skeptic can reasonably ask the following question:

> *The parameter space for neutrino oscillations is three semi-infinite plots of Δm^2 versus $\sin^2 2\theta$. Dozens of experiments have searched for and failed to find evidence for neutrino oscillations. Why should any new expensive experiment be built which can only exclude another finite area in parameter space?*

There are two sets of answers to this question. The first set is based on the experimental evidence of the atmospheric and solar deficits. The second combines this evidence with some theoretical considerations to justify a search in a particular channel, and in a definite region in mass and mixing space.

The $\nu_\mu \rightarrow \nu_\tau$ channel deserves a careful search because of two experimental observations:

- The atmospheric neutrino ν_μ deficit is naturally explained by $\nu_\mu \rightarrow \nu_\tau$ oscillations in the parameter region accessible to P–822. This is the strongest argument for a new neutrino oscillation experiment in general and for P–822 in particular. The combined data yield a statistically compelling effect. There is no reason to disbelieve the result but the natural interpretation, that we have discovered a violation of lepton family number, is so important that a definitive experiment *must* be carried out. The accelerator community cannot ignore or downplay the result merely because the techniques are unfamiliar; rather, it should use the considerable advantages of neutrino beams to definitively confirm or refute the effect.
- The solar neutrino data can be explained by $\nu_\mu \rightarrow \nu_e$ oscillations with the MSW effect.[16] This range of Δm^2 for $\nu_\mu \rightarrow \nu_e$ cannot be reached with any proposed accelerator experiment, yet serves as a strong motivation for the notion of neutrino mass and mixing. The solar-implied range of Δm^2 for $\nu_\mu \rightarrow \nu_e$ together with the expected neutrino mass hierarchy implies a m_{ν_τ} heavier than $\sqrt{\Delta\ m^2\ (\nu_\mu - \nu_e)} \approx 10^{-3} eV$. This could be accessible to either the short baseline proposal P–803 at small mixing angle and Δm^2 above a few eV^2, or to P–822 at larger mixing angle and Δm^2 down to below $10^{-2} eV^2$.

A second set of arguments are more speculative and model-based but point toward P–822.

The solar and atmospheric deficits are linked by our theoretical expectations. If the neutrino masses have the same generational hierarchy as the other quarks and leptons, and if the lepton version of the KM matrix has the same nearly diagonal structure as the quark KM matrix, then $\nu_\mu \rightarrow \nu_\tau$ is a natural candidate for accelerator-based experiments based on the following chain of reasoning:

- The sum of the three neutrino masses are likely to be less than 10–100 eV or they would overclose the Universe. It is also interesting to note that if global symmetries are broken at the Planck scale, this implies a lower limit of m_ν of $10^{-5} eV$.[17]

- Within this range, there would be three neutrino masses, m_{ν_e}, m_{ν_μ} and m_{ν_τ}. The quarks and leptons all exhibit a generational mass hierarchy, $m_u < m_c < m_t$; $m_d < m_s < m_b$; and $m_e < m_\mu < m_\tau$. Therefore it is plausible that $m_{\nu_e} < m_{\nu_\mu} < m_{\nu_\tau}$. We point out that in specific models which have been published in the literature most seem to have this feature.[18] If no pair of neutrino masses is near-degenerate, we would have

$$\begin{aligned} \Delta m^2(\nu_\mu - \nu_\tau) &= m^2_{\nu_\tau} \\ \Delta m^2(\nu_e - \nu_\tau) &= m^2_{\nu_\tau} \\ \Delta m^2(\nu_e - \nu_\mu) &= m^2_{\nu_\mu} \equiv \epsilon_1^2 m^2_{\nu_\tau} \end{aligned} \tag{3}$$

  This last relation defines ϵ_1; which is smaller than 1.

  Again with guidance from the quark sector, a lepton Kobayashi Maskawa Matrix is expected to have the following general form:

$$\begin{array}{ccc} \sim 1 & \epsilon_2 & \epsilon_2^2 \\ \epsilon_2 & \sim 1 & \epsilon_2 \\ \epsilon_2^2 & \epsilon_2 & \sim 1 \end{array}$$

  with ϵ_2 small compared to 1.

- To date, no evidence has been found for oscillations at accelerator experiments, so P is small. If we imagine increasing L/E and repeating those experiments, then as we increase L and decrease E, we may find oscillations with $P \approx \theta^2 1.27 \Delta m^2 L/E$. If we now compare the probability of oscillation for the three modes for experiments at a fixed distance and energy, we find

$$\begin{aligned} P_{\nu_\mu \rightarrow \nu_\tau} &\propto \epsilon_2^2 \\ P_{\nu_e \rightarrow \nu_\tau} &\propto \epsilon_2^4 \\ P_{\nu_\mu \rightarrow \nu_e} &\propto \epsilon_2^2 \epsilon_1^2 \end{aligned} \tag{4}$$

  With these rather general assumptions, the mode $\nu_\mu \rightarrow \nu_\tau$ is the most likely mode to be observable with accelerator neutrinos.

2.3 See-Saw models

The see-saw mechanism[19] naturally explains both the low neutrino masses and the mass hierarchy in equation 4. If the solar neutrino problem is explained by the MSW effect, then $m_{\nu_\tau} > 10^{-3} eV$. Depending on whether the see-saw mechanism is implemented with quark masses or lepton masses, and whether a linear or quadratic mechanism is used, a m_{ν_τ} from 0.01 to 10 eV is predicted.[20] If the $m_{\nu_\tau} \approx 10\ eV$ and the mixing angle is smaller than E531 limits, then CHORUS, NOMAD and the more powerful P-803 could discover $\nu_\mu \rightarrow \nu_\tau$ in that parameter space. This scenario is favored by "mixed dark matter" proponents who have come forward since the anisotropies of COBE have been seen.[21] But neutrino mass, even without direct cosmological implications, is interesting and important. $m_{\nu_\tau} \approx 0.1\ eV$, which is also allowed by see-saw models, is favored as an explanation of the atmospheric neutrino deficit.[22] Recent reports of MACHO's,[23] massive compact halo objects (such as Jupiter, but filling the galactic halo region), offer alternative dark matter explanations and leave the neutrino sector accessible to solar, atmospheric, and long baseline accelerator experiments. A suggestion that the see-saw mechanism might be accompanied by enhanced mixing[24] also favors this scenario.

2.4 $\nu_\mu \rightarrow \nu_e$

This proposal concentrates on the oscillation mode $\nu_\mu \rightarrow \nu_\tau$. However, it is also possible that the atmospheric anomaly is due to $\nu_\mu \rightarrow \nu_e$. P-822 would confirm that. If the ν_τ were heavier than 1 eV, with a mixing angle below the limits of FNAL E531, then the atmospheric neutrino problem could be explained with $\nu_\mu \rightarrow \nu_e$ oscillations. Reactor experiments have limited some, but not all of this $\nu_\mu \rightarrow \nu_e$ parameter space. In this scenario, the MSW effect cannot explain the Solar neutrino deficit. However, a solar neutrino deficit equal to the atmospheric deficit would be expected in Homestake, Gallex and SAGE, with a slightly smaller deficit in the Kamiokande solar data.[17]

2.5 The NUMI Program

The NUMI program at Fermilab, by combining the short baseline P-803 and the long baseline P-822 offers a unique opportunity to study neutrino oscillations. The availability of a neutrino beam using the Main Injector will provide an extremely large neutrino flux capable of giving large event rates at long distances, with a substantial fraction of the beam above ν_τ charged-current threshold. Both appearance and disappearance experiments can be run simultaneously.

There are three possible indications of neutrino mass: the missing mass problem, for which the heaviest neutrino mass of 1-10eV is needed if hot dark matter is a significant part of the answer; the atmospheric neutrino problem which needs a high mixing angle and Δm^2 of $10^{-2} eV^3$ to $10^0 eV^2$, and the solar neutrino problem, which might be explained by

Reference	m_{ν_μ} (eV)	m_{ν_τ} (eV)	Does it explain? Solar deficit	Atmospheric deficit	Dark Matter	P–803?	P–822?
Standard Model	0	0	NO	NO	NO	NO	NO
Pakvasa[22]	10^{-3}	10^{-1}	YES	YES	NO	YES	YES
Hall[25]	10^{-3}	10	YES	NO	YES	YES	NO
Akhmedov[17]	10^{-1}	10	NO	YES	YES	YES	YES
GINO[26]	0	0	YES	YES	NO	NO	YES
Caldwell[27]	3	3	YES	YES	YES	YES	YES
Wolfenstein B[28]	$3\ 10^{-4}$	$3\ 10^{-3}$	YES	NO	NO	NO	NO
"Just So"	10^{-5}	10^{-5}	YES	NO	NO	NO	NO

Table 2: Several theoretical neutrino mass scenarios

$\nu_\mu \rightarrow \nu_e$ oscillations and the MSW effect. Neutrino oscillations cannot naturally explain all three effects, but could naturally explain any two of them. Table 2 lists a number of neutrino mass scenarios. Most of them have been designed to "explain" one or more of the three hints. It is seen that the NUMI program, consisting of a short baseline experiment P–803 and a long baseline experiment P–822 is well positioned to find neutrino oscillations or greatly constrain the neutrino physics explanations of these three important phenomena.

3 Discovering Neutrino Oscillations with P–822

3.1 Neutrino flux and event rates

The design and capabilities of a wide band neutrino beam using the Main Injector were spelled out in the Fermilab Conceptual Design Report for the Main Injector Neutrino Program.[1] The specifics for extraction and beam design in the direction of Soudan 2 have been worked out by the Fermilab Main Injector groups and Research Division and will not be addressed in this document. A map of the beam and a cartoon sketch of a profile of the earth are shown in Figure 2. The neutrino beam will go through the short baseline detector P–803 and also a $\approx$ 50 ton near version of the long baseline detector at the Fermilab site. It will then traverse 730 km to the Soudan mine.

The Soudan 2 detector has a mass of 960 tons. The cavity in the Soudan hall is $72m \times 14m \times 11m$, and we estimate that, depending on the required granularity, another detector of up to 8 kton could be constructed behind Soudan 2 with a similar capability for measuring NC/CC in the Fermilab beam.

Since the original proposal was written, the expected intensity for the Main Injector has increased from 4 10^{13} protons per pulse every 2 seconds to 10^{14} protons per pulse every 1.5

seconds. This increases the neutrino event rate in the existing Soudan detector by a factor of 3.3, as shown in Table 3. We assume two nine-month runs with 100 hours per week of running. ***All of the rates and limits given in this document apply to this base running assumption, unless otherwise noted.*** In Table 4 we show the event rate which could be obtained in two nine month runs if we also build an 8 kiloton cavity filler.

It is useful to be able to compare different scenarios for a long baseline experiment with the double horn beam from the Fermilab Main Injector. Starting with our base assumptions we can scale the mass, distance and running time and intensity as follows:

$$N = 6000 \times (\frac{M}{900tons})(\frac{730km}{L})^2(\frac{protons\ on\ target}{2 \times 9.4 \times 10^{20}}) \quad (5)$$

	P = 0	P = 0.1	P = 0.2	P = 0.345
$R_{"nc"/"cc"}$	$\frac{1060}{3440} = .310 \pm .011$	$\frac{1130}{3110} = .365 \pm .013$	$\frac{1200}{2780} = .433 \pm .015$	$\frac{1300}{2300} = .566 \pm .020$
$R_{\mu/\nu}$	$\frac{17600}{6000} = 2.93 \pm .04$	$\frac{15800}{5650} = 2.80 \pm .04$	$\frac{14100}{5300} = 2.66 \pm .04$	$\frac{11500}{4800} = 2.40 \pm .04$
$R_{near/far}$	$\frac{10^8}{44000} = 2270 \pm 45$	$\frac{10^8}{39600} = 2530 \pm 51$	$\frac{10^8}{35200} = 2840 \pm 57$	$\frac{10^8}{28800} = 3470 \pm 69$

Table 3: Expected ratios for several probabilities of oscillation (.345 corresponds to the Kamiokande value at large L/E). Rates are for two calendar year (nine month) runs using the existing Soudan Detector. The errors are statistical only for $R_{"nc"/"cc"}$ and $R_{\mu/\nu}$ tests and are dominated by 2% systematic errors for the $R_{near/far}$ test. These numbers are not corrected for ν_e and NC/CC misidentification. Those corrections, which are discussed in the text, will change the values of the ratios, but will not greatly affect the statistical significances shown in this Table.

3.2 Neutrino Oscillation Tests

The expected event rate as a function of neutrino energy is shown in Figure 3. The rates for quasi-elastic, resonance production, and deep inelastic are shown separately. The bulk of events are deep inelastic, with several pions in the final state.

The most powerful test we have for neutrino oscillations, the $R_{"nc"/"cc"}$ test is the most independent of precise knowledge of the beam flux or energy spectrum. Several other statistically independent tests can also be used. All require more work, but any of these

	P = 0	P = 0.1	P = 0.2	P = 0.345
$R_{"nc"/"cc"}$	$\frac{9600}{30900} = .310 \pm .004$	$\frac{10200}{28000} = .365 \pm .004$	$\frac{10800}{25000} = .433 \pm .005$	$\frac{11700}{20700} = .566 \pm .007$
$R_{\mu/\nu}$	$\frac{35000}{54000} = .65 \pm .004$	$\frac{31500}{50900} = .62 \pm .004$	$\frac{28000}{47700} = .59 \pm .004$	$\frac{20700}{43200} = .53 \pm .004$
$R_{near/far}$	$\frac{5\times10^8}{132000} = 3790 \pm 76$	$\frac{5\times10^8}{119000} = 4210 \pm 84$	$\frac{5\times10^8}{106000} = 4730 \pm 95$	$\frac{5\times10^8}{86000} = 5780 \pm 116$

Table 4: Rates are for two calendar year runs (9 months) with an 8 kiloton cavity filler.

statistically-independent tests described below would provide a clear and convincing signal in the Kamioka-allowed region for the atmospheric deficit.

- $R_{"nc"/"cc"}$ test, the ratio of neutrino events without a clear muon to the number with a clear muon. We will directly compare the ratio measured at Soudan to that measured in the same beam at the near detector and in P–803.
- $R_{\mu/\nu}$ test, the ratio of muons coming from ν_μ charged-current interactions in the rock upstream of Soudan 2, to the rate of neutrino interactions in Soudan 2.
- $R_{near/far}$ test, the ratio of numbers of events seen in the near and far detectors.

P–822 can search for $\nu_\mu \rightarrow \nu_e$ as well. A small intrinsic ν_e/ν_μ rate would enable us to search for $\nu_\mu \rightarrow \nu_\tau$ or $\nu_\mu \rightarrow \nu_e$ by direct detection of electrons. Soudan 2 can identify low energy electrons with high efficiency, although we have not yet determined the efficiency with which we can separate electrons from hadrons at higher energy or multiplicity. Using the decay channel $\tau \rightarrow e\nu_e\nu_\tau$ (branching fraction = 18%) as signal the background is then $\kappa N_{\nu_\mu} + N_{\nu_e}$. κ is the probability that a hadron shower will be misidentified as an electron. A multivariate analysis has been performed for P–803 to separate ν_τ events from neutral-current background. Some of these variables, such as the angle of the muon with respect to the hadrons, can be measured in a fine-grained calorimeter such as Soudan 2. This may lead to additional power to distinguish ν_τ's, particularly if mixing angles are large.

Finally, we expect 4300 events in which there will be an incoming muon from a charged current interaction in the rock which stops in the detector. This event rate will be particularly sensitive to the lowest energy neutrinos, and hence to neutrino oscillations. In the presence of ν oscillation, the stopping muon rate would decrease in a way that is more sensitive to low values of Δm^2 than the throughgoing muon rate. Knowledge of the beam spectrum is important for this test, particularly at the low energy part of the spectrum.

We have calculated the event rates and limit curves for the first three tests listed. The limit curves which can be obtained using the three tests for our base running conditions, and assuming 2% systematic error, are shown in Figure 4. For comparison, the limit curves for the three tests discussed in the original proposal are shown in Figure 5. Restricting ourselves to the $R_{"nc"/"cc"}$ test, we compare the effects of systematic and statistical errors in Figure 6. That figure compares the limits with and without an eight kiloton cavity filler, with and without a 2% assumed systematic error in σ_R/R; $(R = R_{"nc"/"cc"})$.

With a fine grained short baseline detector, and the running experience of the P–803 and E–770/E-815 experiments, we estimate that we may be able to achieve σ_R/R of $<$ 2%.[2, 29][1]Limit curves for the $R_{\mu/\nu}$ test are shown in Figure 7.

Limit curves give one description of the sensitivity of a search, but a worthwhile experiment must be capable of seeing a positive signal. This is illustrated in Tables 3 and 4. In Table 3 we show the expected event rates under the assumption of no neutrino oscillations (P=0), and assuming that the average probability is 0.1, 0.2 and 0.345. The latter value corresponds to the mean of the atmospheric ν_μ deficit. If P = 0.345, we will see a 13 σ result in $R_{"nc"/"cc"}$, and independently an 13 σ result in $R_{\mu/\nu}$ and a 17 sigma result in $R_{near/far}$. (We approximate the errors as Gaussian for illustrative purposes.) The latter result is dominated by a 2% systematic error. All three results are statistically independent. It is important to note that although this experiment *intends* to measure R absolutely, the oscillation test only requires that the systematic error on the change in the *measured* R is small; recall that the central Kamioka value would cause a shift in the measured R of 0.566, so P–822 would still measure a significant result with an unknown systematic error as big as 5%.

Table 4 shows the statistical errors on event rates for two nine-month runs with an 8 kiloton cavity filler. As an example, if P = 0.1, we could obtain an 14 σ result in $R_{"nc"/"cc"}$, a 7 σ result in $R_{\mu/\nu}$, a 5 σ result in $R_{near/far}$. These independent measurements provide a strong handle on whether any anomaly might be due to neutrino oscillations.

In tables 3 and 4, we have compared the NC/CC ratio to the world average of 0.310. However, there are uncertainties in the expected ratio in the energy region around charm threshold.[30] This experiment is operating in that energy region. The Soudan 2 detector is very modular. Main detector modules have been operated in the Rutherford ISIS test beam, and on cosmic ray test stands at Argonne and Rutherford-Appleton Laboratories. Thus we are able to carry out a two station experiment, using Soudan 2 modules near the P–803 detector at Fermilab.

The configuration of the near detector is discussed in Section 4, Question 3. The near detector will provide a systematic check of the measurement in Soudan 2 modules of $R_{"nc"/"cc"}$, and in addition, provide high statistics information about the neutrino beam. Our expectations for the $R_{"nc"/"cc"}$ test will be normalized to the measured NC/CC ratio in the near detector. On the other hand the check that, after correction,the near detector measures the expected NC/CC ratio, up to uncertainties due to charm thresholds, will provide a valuable test of our systematic errors. This empirical ratio will be measured with high statistical

[1]E-770 has already achieved $\sigma(R)/R < 1.2\%$.

accuracy (millions of events) which will allow us to compare the ratio in the near and far detector to a greater accuracy than $R_{"nc"/"cc"}$ is presently known at these energies.

The energy dependence of different event rates varies as shown in Table 5. While $R_{\mu/\nu}$ depends on knowledge of the energy spectrum of the beam, and $R_{near/far}$ on the absolute rate, $R_{"nc"/"cc"}$ is much less dependent on either. In the next three Sections, these tests are discussed in more detail:

Table 5: Energy dependence of various processes

Neutrino flux	$\phi_\nu(E)$
Contained vertex events	$E\phi_\nu(E)$
Rock muons	$E^2\phi_\nu(E)$
Quasi-elastic contained events	$\phi_\nu(E)$
stopping muons	$E\phi_\nu(E)$

3.2.1 $R_{"nc"/"cc"}$ Test to Detect ν_τ Appearance

If ν_μ's oscillate into ν_τ's, this will affect the apparent ratio of neutral-current events to charged-current events. In the absence of oscillations, we expect[31]

$$R^{obs}_{"nc"/"cc"} = R^{true} \equiv \frac{number\ of\ events\ without\ a\ muon}{number\ of\ events\ with\ a\ muon} = 0.31 \pm 0.01 \qquad (6)$$

Then for N events,

$$n_{cc} = N \times \frac{1}{1+R^{true}} \quad and \quad n_{nc} = N \times \frac{R^{true}}{1+R^{true}} \qquad (7)$$

If there is a probability, P, for ν_μ to oscillate into ν_τ, then the resulting ν_τ neutral-current events would be indistinguishable from the ν_μ neutral-current events. However, most (83%) of the ν_τ charged-current events have no muon and would therefore be classified as neutral-current events. We would measure

$$n_{"cc"} = \frac{N(1-P+\eta BP)}{1+R^{true}} \quad and \quad n_{"nc"} = \frac{N(R^{true}+\eta(1-B)P)}{1+R^{true}} \qquad (8)$$

where B = 0.17 is the branching fraction for $\tau^- \to \mu^- X$ and η is the ratio of the ν_τ charged-current cross-section to the ν_μ charged current cross-section. (See equation 16). The notation "cc" distinguishes events classified as charged-current due to the presence of a muon from the actual charged-current events. For an incoming ν_e or ν_τ, most charged current events would be incorrectly classified as NC events.

$$R^{obs}_{"nc"/"cc"} = \frac{n_{"nc"}}{n_{"cc"}} = \frac{R^{true}+\eta(1-B)P}{1-P+\eta BP} \qquad (9)$$

Integrated over the neutrino spectrum from the Main Injector, $\eta = 0.24$. By contrast, the neutral-current cross-sections for ν_τ and ν_μ are equal. The signal of an oscillation thus consists of a value of $R_{\text{"nc"}/\text{"cc"}}$ that is larger than expected. If our measurement yields the known $R_{\text{"nc"}/\text{"cc"}}$ ratio for ν_μ, this allows a limit on the probability of oscillation to be deduced.

In general, ν_e contamination of the beam will cause $R^{obs}_{\text{"nc"}/\text{"cc"}}$ to increase. Both ν_e neutral-current and charged-current events will be classified as neutral current. A 1% ν_e contamination will cause a 4% increase in $R^{obs}_{\text{"nc"}/\text{"cc"}}$. ν_e's in the beam mostly come from K_{e3} decay, and the K's decay at the beginning of the decay pipe. Monte Carlo calculations confirm that the spectrum of ν_e's is not a strong function of angle. This background is discussed further in the answer to Question 2.

The expected number of contained vertex events in the Soudan 2 detector can be written as:

$$N^{ee}_{tot} = n_{\text{"cc"}} + n_{\text{"nc"}} = \int \sigma_{tot}(E) \frac{d\phi_\nu(E)}{dE} N_t dE \tag{10}$$

where N_t is the number of target nucleons and $\phi(E)$ is the neutrino flux. Using an assumed injector beam with 10^{14} protons every 1.5 seconds and 100 hours of beam per week for two nine month runs, we compute from equation 10 that the entire Soudan 2 detector would record 6000 events with a contained production vertex.

Implementation of the $R_{\text{"nc"}/\text{"cc"}}$ test is discussed extensively in Section 4 in the answer to Question 2.

3.2.2 $R_{\mu/\nu}$ Tests Using Muons from the Rock

We plan to measure $R_{\mu/\nu}$, the ratio of muons from the rock to neutrino events with vertices inside the Soudan 2 detector. We define the ratio $R_{\mu/\nu}$ as the ratio of incoming (muon) events from the rock in front of the detector, to the number of contained vertex (neutrino) events. The rate of muons entering the detector from ν_μ charged-current interactions in the rock is:

$$N_\mu = 1.0 \times 10^{-12} GeV^{-2} \int_0^\infty dE_\nu E_\nu^2 n(E_\nu) \tag{11}$$

The two E_ν factors come from the cross-section and muon range, both proportional to the neutrino energy. The Fermilab beam would enter the detector (in the plan view) pointing 26.4°W of North. The long axis of Soudan 2 is oriented along the N-S direction. The effective area of Soudan 2 viewed from the direction of Fermilab is then 94 m^2 for the main detector and 275 m^2 for the shield.

Using these muons from the rock, an additional neutrino oscillation experiment can be done. We would look for a decrease from the expected number of muons N^{ee}_μ due to $\nu_\mu \rightarrow \nu_\tau$ oscillation:

$$N_\mu = N^{ee}_\mu (1 - P + P\eta B) \tag{12}$$

In the absence of such a decrease, a limit on the oscillation probability, P, could be set. The limit depends on the statistical error on N_μ and the systematic error on N_μ^{ex}. Note that the full number of such events can be used in this calculation, whether or not they are in the fiducial volume required for distinguishing between neutral and charged-current interactions.

The calculation of N_μ^{ex} depends not only on the measured number of contained vertex events but also on knowledge of the energy dependence of the ν_μ flux. To first order, the density of the rock in which the muons are made does not affect the muon flux. In any case, the rock in the vicinity of the Soudan mine has been well measured. In contrast to the $R_{"nc"/"cc"}$ ratio, we will be comparing the observed ratio $R_{\mu/\nu}$ to a calculated ratio, with the rock muon rate having one extra power of E_ν in the numerator. Systematic errors due to beam pointing, knowledge of the energy distribution of the beam, the geometry of the detector and properties of the surrounding matter have been considered. No effects have been identified which would introduce uncertainties larger than 1% in the measurement of $R_{\mu/\nu}$. An overall systematic accuracy in the measurement of this parameter of the order of 2% is expected. Note that the beam flux normalization (or time variability) does not affect $R_{\mu/\nu}$.

3.2.3 $R_{near/far}$ Test Using Soudan 2 Modules at Fermilab

The near station will give us data which we will use to normalize the beam flux. The muon rate at Soudan can be normalized to the rate measured by the near detector. We call this the $R_{near/far}$ test.

The statistical accuracy is that of the far detector. The systematic error is dominated by our ability to accurately estimate the muon rate due to uncertainties in the energy distribution as a function of angle. Computer studies done on the proposed neutrino beam[1] show that as long as the angle from the beam axis is less than 0.25 mr the systematic error on the expected muon rate is less than 1.2%; the energy and rate as a function of angle are shown in Figure 8. This requirement is straightforward to satisfy and has been achieved by other Fermilab neutrino beamlines. Effects that we have not yet identified may limit our knowledge of the absolute flux by 1.0%. Therefore we expect that our near station will give us knowledge of the neutrino flux at our Soudan detector with a systematic error of about 2.0%.

This flux measurement can be used to normalize the muon rates in the detector to search for both $\nu_\mu \rightarrow \nu_\tau$ and $\nu_\mu \rightarrow \nu_s$. The latter mode represents the oscillation of ν_μ into a right handed neutrino, which would be "sterile", i.e. both the neutral-current and charged-current cross-sections would be zero. Recent cosmological arguments related to the primordial Helium abundance preclude this mode in our area of sensitivity, however.[32]

3.2.4 Using the Tests for the Mode $\nu_\mu \rightarrow \nu_e$

In P–822, the $\nu_\mu \rightarrow \nu_e$ sensitivity is actually better than the $\nu_\mu \rightarrow \nu_\tau$ sensitivity using the $R_{"nc"/"cc"}$ test, because $\eta = 1.0$ and B = 0. P_{min}, and hence $\sin^2 2\theta$ is lower by a factor of 2.6 for $\nu_\mu \rightarrow \nu_e$. ($P_{min}$ is defined in Section 4.1.) If the atmospheric neutrino anomaly is due to this mode of oscillation, we would expect a large and consistent effect in the $R_{"nc"/"cc"}$, $R_{\mu/\nu}$ and $R_{near/far}$ tests. These limits are shown in Figure 9. In the event that a signal for ν oscillation is measured in P–822, the $R_{"nc"/"cc"}$ test and the hadronic energy distribution could be used to separate whether the oscillations were due to $\nu_\mu \rightarrow \nu_e$ or $\nu_\mu \rightarrow \nu_\tau$.

3.3 Hadron Beam calibration at Fermilab

To properly understand the response of the calorimeter to hadrons with energies up to 8 GeV the modules must be tested in a particle beam for two reasons. First, the "length" of hadronic showers as a function of energy must be measured so that we can distinguish charged from neutral-currents as in E–770. Second, the response of the detector *vs.* energy is required so that we can measure the hadronic energy distribution; combined with the information from the toroid (discussed below in Sec. 4.7), we can compare the observed neutrino energy spectrum to predictions and check the observed y-distribution. Both are necessary to provide a believable signal. As a natural choice the modules could be tested at FNAL, *e.g.* in the NK beamline in Lab F.

The NK beamline was initially designed as a muon beam for Experiment 782 at Lab F. It is being modified by Experiment 815 to serve as a hadron calibration beam. The NK beamline optics will allow for the selection of production angles and beam momenta and is equipped with collimators to adjust the beam rate and to removed off-momentum particles. In this beamline 800 GeV/c protons from the Tevatron are delivered to a target in Enclosure NE8 at a typical rate of 3×10^{11} protons per accelerator cycle. NK secondary beam is capable of transporting a negative beam with a momenta between approximately 10 GeV and 200 GeV/c. The modified NK beam consists of pions with an admixture of electron, muons and antiprotons. The particle mixture depends very strongly on the momentum selected. The particle types can be identified on an event by event basis with a Cerenkov counter between Enclosure NEB and NKC (π, K, and antiproton separation), transition radiation detector (e) in Enclosure NKC, and a backing calorimeter from the Experiment 815 (μ). Given that the distance from the target in Enclosure NE8 to Lab F is approximately 450 m, low energy hadrons produced at the target will not be able to reach the P–822 calorimeter modules in Lab F. An effort is presently underway to design a tertiary beam. Since Enclosure NKC is less than 100 m from Lab E (and even less to Lab F), low energy hadrons produced in Enclosure NKC will be able to reach the modules to be calibrated. The details of what the tertiary been will look like has not been finalized but will involve the transport of highest energy secondary beam (the highest momentum presently capable of being transported through Enclosure NEB is 200 GeV/c) to the new tertiary target station in Enclosure NKC. The basic design in Enclosure NKC will consist of a target, a dipole, a dump

and a dipole. A similar design tertiary beam was successfully used in the NW beam during the 1991 fixed target run. Since Enclosure NKC will be approximately 65' long after the planned Experiment 815 modifications to it are done there should be adequate space within Enclosure NKC. Cerenkov counters, quadrapoles and additional bends for good momentum resolution could be installed within Lab F upstream of the modules to be calibrated. The shielding around Enclosure NKC will be 3' thick and should be adequate for the needs of the tertiary beam target. The modified NK hadron calibration beam will be utilized to check the energy calibration of the modules for hadrons, the mapping of the detector response at the boundaries of the modules, and to study muon identification probability. These calibration runs are expected to require about six months excluding the initial set-up time.

3.4 Event simulation

In order to demonstrate the power of P–822 to study neutrino oscillations, we have run a Monte Carlo simulation of ν_μ and ν_τ events in our detector. We have calculated the ν_μ spectrum at the far detector using the program NUADA, the fraction of other neutrinos using a program developed by P–803, and simulated $\mu's, e's, \tau's$ and hadronic interactions in our detector with a Monte Carlo developed in Soudan 2. The Soudan 2 Monte Carlo was written within the collaboration and has been used for a number of years to simulate the wide variety of physical processes that are studied with the Soudan 2 detector. It has played a crucial role in our analysis of nucleon decay and atmospheric neutrinos. The event generation component of the Monte Carlo includes quasi-elastic scattering and resonance production in addition to deep inelastic scattering. Cross-sections for ν_τ interactions have also been carefully studied. The detector simulation component of the Monte Carlo is very comprehensive: particle tracking in an exact detector geometry, energy deposition in gas, digitization and electronics readout are all simulated. It utilizes the SLAC EGS routines for electromagnetic interactions and the GEISHA routines for hadronic interactions. It produces electronics readout in a format indistinguishable from real data.

Calculation of ν_τ event rates is complicated by the fact that most standard calculations of cross-sections neglect terms proportional to the lepton mass. For ν_τ charged-current interactions the contributions from such terms can be significant. Cross-sections for quasi-elastic scattering that include terms proportional to lepton mass have been calculated by C. Llewelyn-Smith.[33] Here one must include the usually neglected pseudo-scalar form factor F_p, and make some assumption as to its functional form. Following Llewelyn-Smith we take

$$F_p(q^2) = \frac{2M^2 F_A(q^2)}{m_\pi^2 - q^2} \tag{13}$$

which follows from the condition that the axial current would be conserved if m_π were zero.[33] The inclusion of F_p in the quasi-elastic cross-section for ν_τ has the net effect of further reducing the cross-section (by about 4% for energies around 15 GeV). One must undertake a similar procedure for the resonance production cross-sections. In addition to the usual phase space reduction we further reduce the cross-sections by the same factor as

the quasi-elastic cross-sections. Our cross-sections for resonance production are taken from the work of Rein and Seghal.[34]

For deep inelastic scattering (DIS), we use the expression for the differential cross-section calculated by Albright and Jarlskog.[35]

$$\frac{d^2\sigma^{\nu,\bar{\nu}}}{dxdy} = \frac{G^2ME}{\pi}\{(xy + \frac{m^2}{2ME})yF_1 + [(1-y) - (\frac{M}{2E}xy + \frac{m^2}{4E^2})]F_2 \pm [xy(1-\frac{y}{2}) - \frac{m^2}{4ME}y]F_3 \pm \frac{m^2}{M^2}[(\frac{M}{2E}xy + \frac{m^2}{4E^2})F_4 - \frac{M}{2E}F_5]\} \quad (14)$$

We are now faced with the task of finding an appropriate form for F_4 and F_5. Following Albright and Jarlskog, we take $F_4 = 0$ and $xF_5 = F_2$ which are consequences of the assumptions $2xF_1 = F_2$ and $xF_3 = F_2$. The DIS ν_τ cross-sections we have calculated in this fashion have been compared to an independent calculation carried out by Roger Phillips of RAL. Phillip's calculation follows from first principles of the quark model. Despite the different approximations involved, the two calculations are in good agreement. The form factors F_2 and xF_3 are then computed from the parton distributions in a standard fashion. Our charged-current and neutral-current DIS routines employ the CTEQ1M parton distributions.[36] Figure 10 shows the quasi-elastic and deep inelastic ν_τ cross-sections we have calculated.

Figures 11-13 show a representative ν_μ neutral-current, ν_μ charged current, and ν_τ charged-current event respectively. Each event is shown with the whole detector view, and with one view magnified around the event vertex. The τ event, which had the decay $\tau^- \rightarrow \pi^-\pi^o\pi^o\nu_\tau$, looks topologically like the neutral-current events, just as we would expect. In Figure 14 is shown a ν_e charged-current event. This also has the appearance of a neutral-current event in our detector.

3.5 Shield Upgrade

We propose to augment the present Soudan 2 active shield with additional proportional tube panels to convert the shield to a stand-alone detector of muons emerging from the upstream rock. The 275 m^2 shield cross-section (as viewed from Fermilab) is nearly three times larger than the cross-section of the central detector. The correspondingly larger yield of rock muon events will improve the statistical accuracy of the numerator in the $R_{\mu/\nu}$ test. The $R_{\mu/\nu}$ test, while prone to more systematic error than the $R_{"nc"/"cc"}$ test, provides an important check of our understanding of the neutrino beam energy distribution since the rate for emergent muons includes E_ν factors both for the neutrino cross-section and for the range of the muons in the rock. An enhanced shield, capable of triggering on rock muons alone, would also provide an electronics path for measuring the intensity of the Fermilab neutrino beam, which is independent of the electronics of the calorimeter.

The active shield consists of panels of two-layer proportional tubes (constructed at Tufts) arranged to form a 13.4 m × 9.5 m × 31 m rectangular parallelopiped which surrounds

the central detector. Some augmentation of this base shield has already been performed. Five panels of single-layer proportional tubes (obtained from the Harvard-Purdue-Wisconsin experiment) have been placed on the ceiling. The HPW tubes are oriented at 90° to the Tufts tubes to enable particle tracking. We have already in the Soudan mine enough HPW tubes to complete the double coverage of the entire ceiling and floor. In addition we have available in the mine 900 m^2 of single-layer proportional tubes obtained from the TASSO experiment at PETRA.

Our experience with the performance of the active shield as presently constituted allows us to determine the level of enhancement required to convert the shield to a stand-alone detector. The principal problem is that the shield must be equipped with a stand-alone trigger. The single-layer panels now available are not adequate to produce such a trigger. It is essential to have additional panels of two-layer tubes to cover the two side walls (north and west) of the shield which are opposite to Fermilab. The tubes in the add-on panels would be oriented at 90° to the tubes in the adjacent Section of the base shield. The great utility of the two-layer tubes arises from the ability to form a coincidence between the two layers. Measurements in the mine show that the two-layer coincidence rate is only 1% of the single-layer rate. Both rates are primarily the result of radioactivity. We would build the additional two-layer tubes and associated electronics in precisely the same fashion as for our original shield. Since only a continuation of earlier effort is required we can accurately estimate costs. Panels sufficient to double cover both the north and west walls would cost $200K.

The signature for a through-going muon emerging from the rock would be the triple coincidence of two-layer coincidences. Two of the coincidences would come from overlapping panels on either the north or west walls and the third would come from any of the panels on the remaining four walls of the shield.

The trigger rate expected due to radioactivity is calculated to be 0.006 Hz. This rate is negligible and is of even less concern if the experiment is gated on only during the Fermilab beam spill.

The expected rate of cosmic ray muons passing through the shield at various zenith angles can be calculated from rates already measured in the Soudan 2 experiment for nearly vertical muons and from muon angular distributions measured previously in the nearby Soudan 1 detector. Any through-going muon which passes through the north or west walls will satisfy the trigger requirement. The flux of vertical muons in the Soudan 2 cavity is measured to be $0.0010 m^{-2} s^{-1} sr^{-1}$. The angular distribution measured in Soudan 1 is used to calculate the flux through a vertical surface of muons with zenith angle θ greater than a specified minimum value. The results are $0.0003 m^{-2} s^{-1}$ for θ greater than 50°, $0.0001 m^{-2} s^{-1}$ for θ greater than 60°, and $0.00001 m^{-2} s^{-1}$ for θ greater than 70°. The flux of nearly horizontal ($\theta > 70°$) cosmic ray muons through the 420 m^2 area of the north and west walls over a 9-month run is then expected to be roughly 100,000. This background can be reduced substantially by an azimuthal angle cut which requires the muon to have come from the direction of Fermilab but it is clear that the Fermilab duty cycle (1 ms/1.5 s) information is required to reduce the background to a tolerable level of less than 50 muons.

The muon tracking capability (x,y measurement on each of the six walls) would be completed by installing the TASSO panels on the east and south walls. The spatial resolutions of the various proportional tubes are 20 cm for Tufts, 15 cm for HPW and 4 cm for TASSO. The path length within the shield would be typically more than 10 m so we may expect an angular resolution of roughly 1 ° for the stand-alone shield.

The expected costs of the upgrade are given below in 1994 dollars

Equipment costs (tubes and electronics):	\$400K
Installation (6 FTE x 3 years x \$35K):	\$560K
Support structure:	\$ 40K
Contingency (20%):	\$200K
Total	\$1,200K

3.6 Operation of the Laboratory

Plans call for the Soudan 2 detector to operate through 1998, well before the operation of this long baseline experiment. We estimate future operating costs in Table 6.

Item	Present Soudan 2	Soudan 2 + toroid	Soudan 2 + toroid + 8 kton CF detector
Mine crew FTE	6	8	10
Hours of access/week	50	66	96
Mine crew salaries	\$240K	\$320K	\$400K
DNR (hoist, electricity,overtime)	\$ 50K	\$ 70K	\$200K
Gas	\$ 50K	\$100K	\$150K
Supplies, misc.	\$110K	\$150K	\$200K
Total/year	\$450K	\$640K	\$950K

Table 6: Steady state laboratory operations costs (1994 \$)

4 Answers to Questions of June 1993

4.1 Question 1a –Limit Curves

What specifically limits the $\sin^2 2\theta$ and Δm^2 range?

In general, the minimum $\sin^2 2\theta$ detectable by any experiment depends on the sensitivity of the test employed. The minimum Δm^2 depends on both the sensitivity and L/E , the distance the neutrino has travelled and the energy of the beam. The sensitivity of a test depends on the statistical and the systematic errors. The derivation of the limit curves is given in Goodman and Snyder.[37] The complicated shapes are due to energy integrals. It is instructive to consider straight line approximations to the limit curves, following Parke and Bernstein,[38] which are then easy to scale for various other assumptions. A detailed comparison of various parameters and how they affect the limits is given in appendix A. Here we focus on the neutral current to charged current limits for the case $\nu_\mu \rightarrow \nu_\tau$.

The oscillation probability is given by

$$P_{\nu_\mu \rightarrow \nu_\tau} = \frac{R^{obs}_{\text{"nc"}/\text{"cc"}} - R^{true}}{\eta(1-B) + R^{obs}_{\text{"nc"}/\text{"cc"}}(1 - B\eta)} \tag{15}$$

where R^{true} is the expected neutral-current to charged current ratio, $R^{obs}_{\text{"nc"}/\text{"cc"}}$ is the measured ratio, B = 0.17 is the branching fraction $\tau \rightarrow \mu X$, and

$$\eta \equiv \frac{\int \sigma_{\nu_\tau}(E)\phi_\nu(E)dE}{\int \sigma_{\nu_\mu}(E)\phi_\nu(E)dE} = 0.24 \tag{16}$$

using the Main Injector neutrino spectrum. η takes into account the fact that the ν_τ charged-current cross-section is lower than the ν_μ charged-current cross-section throughout this energy region.

In the absence of oscillation, an experiment can set a limit on P in equation 15, defining P_{min}. At 90% confidence level, $R^{obs}_{\text{"nc"}/\text{"cc"}} - R^{true} = 1.29\ \sigma_R$ (for a one-sided Gaussian). Putting this into equation 15,

$$P_{min} = 2.56\sigma_R \tag{17}$$

σ_R is a combination of systematic and statistical error:

$$(\frac{\sigma_R}{R})^2 = (\frac{\sigma_R^{stat}}{R})^2 + (\frac{\sigma_R^{syst}}{R})^2 \tag{18}$$

Keeping just the statistical error,

$$P_{min} = \frac{1.87}{\sqrt{N}} \tag{19}$$

where N is the number of events. For a two year run, P–822 should see 6000 events in the existing one kiloton detector with 4500 events in the fiducial volume. Thus $P_{min} = 0.020$,

and we get limits $\sin^2 2\theta = 0.040$ and $\Delta m^2 = 0.0019\ eV^2$ as shown in Figure 15. A systematic error of 2% added in quadrature with this statistical error leads to a $P_{min} = 0.032$, and limits $\sin^2 2\theta = 0.064$ and $\Delta m^2 = 0.0025\ eV^2$. For our base running assumption, the statistical errors and systematic effects will each contribute a similar amount to our sensitivity. A run with lower intensity or time than we have assumed will be dominated by statistical errors.

We can compare these limits with those that could be obtained with an 8 kiloton cavity filler in addition to Soudan 2 under the same running conditions. The statistical limits would give $P_{min} = 0.0066$, and limits $\sin^2 2\theta = 0.013$ and $\Delta m^2 = 0.0011\ eV^2$. However, adding a 2% systematic error in quadrature would lead to $P_{min} = 0.018$, and limits $\sin^2 2\theta = 0.037$ and $\Delta m^2 = 0.0019\ eV^2$. The burden on a cavity filler design is not only to keep costs low, but also to keep possible sources of systematic error in σ_R/R to below 0.5%.

Our studies of systematic effects discussed in the following answers make us confident that we can maintain a systematic error of 2% or less using the Soudan 2 detector, thus ensuring that the systematic error is less than the statistical error. Extensive Monte Carlo and beam studies are still necessary to determine whether systematic errors of 0.5% or less, necessary to justify the increased statistics of a cavity filler detector, can be achieved.

4.2 Question 1b –Thresholds

Provide an outline of the analysis procedure including discussion of thresholds, smearing effects, acceptance corrections, etc.

- Thresholds

  The Trigger threshold in the Soudan 2 detector is 50% efficient for a neutrino energy of 300 MeV. Thus except for a fraction of the $\nu_\mu p$ elastic scattering events, Soudan 2 will trigger on virtually all of the Main Injector neutrino beam events which interact in the detector. The Soudan 2 trigger is discussed in detail elsewhere,[39], but is basically 7 or 8 local hits, depending on geometry. Most triggers are due to throughgoing muons which enter from the ceiling and leave through the floor. About 30% of the triggers are due to random radioactivity. We measure about 75 events per year of atmospheric neutrino interactions and a similar number of neutral particles coming out of the rock accompanied by other shower particles in our active shield. These latter showers are presumably all due to cosmic ray muons. Our simulation shows that we trigger on 97% of neutrino interactions from Fermilab which interact anywhere in the detector. Thus the P–822 proposal could proceed with no change in trigger.

- Backgrounds

  The two important kinds of beam associated events are the throughgoing muons from the direction of Fermilab, and neutrino events with a vertex in the detector. For both categories of events, we have calculated the rate of background cosmic ray events and found it to be acceptably low (2-5 events over two years). We have not yet estimated

the backgrounds for incoming showers and incoming stopping muons but those events are not used in any limits described in this proposal. The backgrounds for all of these classes can be measured using the present Soudan 2 data sample. This analysis is currently under way to confirm our predictions.

- Analysis procedure

Preliminary event processing would be similar to present practice described in Appendix B2. Events associated with the Fermilab beam spill will be collected on separate tapes for further analysis. The most straightforward analysis tasks are to identify the presence of a vertex and the presence or absence of a long track. Track finding algorithms in the Soudan detector exist.[40] To date, vertex recognition has been accomplished by scanning.[41]. For orientation, a charged current Monte Carlo event is shown in Figure 16. Based solely on the track and vertex information, events will be categorized as follows:

1. A throughgoing muon. Tracks are expected to enter the south or east wall and exit the north or west wall and their angle will be within 10° of the Fermilab beam direction.
2. An incoming stopping muon. Tracks will enter the south or east wall and stop in the detector.
3. An incoming shower. Segments of showers will appear on the south or east side of the shield and detector. There may also be a track associated with the shower.
4. Contained vertex event. Contained vertex events should have no shield hits on the south and east walls. Our goal is to distinguish the neutral and charged-current events. First we present a simple analysis algorithm:
   - If the event has a non-interacting track longer than 3 meters ($480 g/cm^2$), it is classified as charged-current.
   - Among the events left, if the event has a track from the vertex which exits the detector, the event is classified as outside acceptance.
   - The remaining events are classified as neutral current.

The 3 meter cut has not been optimized. The length of the muon tracks in an (infinite) Soudan detector is shown in Figure 17. The angle of the muon tracks with respect to Fermilab (the neutrino direction) is shown in Figure 18. Also, the distribution of track lengths in the detector for p's, π's and μ's is shown in Figure 19.

When scanning the events, it is clear that this simple algorithm does not take advantage of all the information. Other event characteristics useful for NC/CC separation are: straight tracks from the vertex along the beam direction, hadron energy deposition, interactions along the tracks, quasielastic (and hence low hadron energy) event topologies, event ionization (for μ/p separation), hits in the shield, and unusual geometrical effects, such as tracks which leave the detector and reenter it. Many 1-3 meter tracks from the vertex will be muons. Using additional information during scanning, more events will be accepted and classified than with the simple algorithm. In order to take advantage of this information, more sophisticated pattern recognition software

must be developed since the events are in general much larger and more complicated than are dealt with in the current Soudan 2 software. In this document, we present an analysis using the simple algorithm and by scanning.

- Acceptance corrections

  In Section 4.4 we discuss the NC/CC confusion matrix and the acceptance for the two methods described in the last Section. The result is that the acceptance is 66%±2% for the simple algorithm and 74% ±3% for the scanning. The quoted errors are statistical Monte Carlo errors, which will be negligible when the experiment runs.

- smearing effects

  Hadronic energy resolution does not affect the event classifications listed above. However, hadron energy resolution and e/π separation are useful additional measurements to complement the $R_{"nc"/"cc"}$ test. This is discussed further in the answer to Question 5.

4.3 Question 1c –Calibration

Outline the strategy to determine the detector calibration and resolution and their implications for the measurement of the hadron energy spectrum and the neutrino energy spectrum.

Soudan 2 modules have been calibrated in low energy lepton and hadron beams as discussed in appendix B. Tests in higher energy hadron beams would be required for this experiment, and are briefly described in Sections 3.3 and costs are included in 4.5. Detectors in situ are monitored using cosmic ray muons. The number of cosmic ray muon events is about 10 million per year.

The major purpose for the hadron beam calibration would be to permit the measurement of hadronic showers which fake charged-current events. The two components of this misidentification would be long penetrating hadrons and decays of π's and K's in the hadronic shower into muons. Both contributions could be studied with sufficient statistics to check our Monte Carlo simulations, and verify the corrections that are required. Running the detector at a variety of angles, and using different energy hadrons will increase the reliability of that comparison.

The implications for measurement of the hadron energy spectrum are discussed together with the muon momentum measurement in the answer to Question 5.

4.4 Question 2 –NC/CC Identification

Question 2a How big is the correction to charged-current events from muons that are not separated from the hadron shower? How well is this correction likely to be known?

Question 2b How big is the correction to the NC event rates for exiting tracks that lead to classification as CC events? How well is this correction likely to be known?
Question 2c Are there other contributions to the NC/CC misidentification matrix? What are they and how much do they contribute to the systematic uncertainty in R?
Question 2d In general what are the magnitudes and uncertainties in the various contributions to the observed NC/CC ratio in the near and far detectors? Simulation with expected detector resolutions, thresholds, and cuts should be used in this analysis.

These four questions all address the issue as to how well the NC/CC test can be used to look for oscillations. With perfect event identification we would expect to measure R to be 0.31 in the absence of oscillations. In a fine grained calorimeter such as Soudan 2, the track length is a powerful criterion to separate muon tracks from hadrons.

We define a charged-current event to be one with a non-interacting track of three meters or more emanating from the primary vertex. Elements of misidentification in the "confusion matrix" are shown in Table 7. One key question is the fraction of charged-current events in which the muon does not get out of the hadron shower. In a Monte Carlo run of 7601 charged-current ν_μ events, 450 had a range of less than $480 g/cm^2$. At that range, they would fail to travel 3 meters in the Soudan 2 detector. This is $6.0 \pm 0.3\%$ of the charged current events, where the error is statistical based on that Monte Carlo statistics. Soudan 2 will contain only a very small fraction of these muons. The fraction of muons which stop in the detector (presently based on a smaller statistics simulation, 22/308) is 7.1%.

In general, charged current events with a track shorter than 3 meters will be classified as neutral current events. However many events with short muons will be low energy events with only small numbers of hadrons produced, and it may be possible to identify them correctly with more detailed selection criteria. In a sample of 310 neutral current events, the longest track went more than 3 meters in 9 cases.

A bigger problem than the misidentification of low energy muons is the classification of events near the edges of the detector whose tracks exit with a potential path length of less than 3 meters. One choice is to restrict the fiducial volume. Such a strategy is not optimum in a long baseline experiment which is limited by statistics. At the expense of some increase in misidentification, we keep and classify events throughout the detector. If an event has tracks which exit the detector before it can be determined whether they are hadrons or muons they are classified as "outside acceptance". These events can not be used for the $R_{"nc"/"cc"}$ test but they are still useful for the $R_{\mu/\nu}$ test.

In order to study the systematic errors to $R_{"nc"/"cc"}$ we have studied simulations of NC and CC events in our detector, using the beam spectra discussed in Section 4.5. Events were fully simulated in the total mass of the detector. We have not yet finalized our best analysis strategy and thus the statistics of the Monte Carlo studies are at present small. Two physicists each scanned 489 events, and then compared their classification to the Monte

Carlo "truth". Events were classified in 3 categories:

1. Charged-current (CC);
2. Neutral-current (NC);
3. Outside acceptance;

Factors which affected the classification included multiple scattering of the longest track, other interactions along the tracks, geometrical considerations, kinks along tracks, and energy flow with respect to the direction of Fermilab. The result of the scan is in Table 8. It is seen that the scanners were correct 91% and 93% of the time. The acceptance, i.e. the fraction of events useful for the $R_{"nc"/"cc"}$ test was found to be 74%.

We note there are modest asymmetries between NC and CC in the events rejected as "outside acceptance". If there is an event near the edge with hadrons which exit the detector, a long μ may still be visible and the event is a clear CC. Had such an event been a neutral current one, it would have been classified as "outside acceptance". Neutral current events located near the edge of the detector may have all of the tracks from the primary vertex interact before leaving the detector. Had an event like this been charged current, the muon would not have been long enough, so it would have been classified as "outside acceptance". The first effect is somewhat bigger, leading to a higher fraction of charged current events in the acceptance for scanning. Of course, at the expense of statistics, these effects can be checked by defining a reduced fiducial volume which ensures hadronic containment.

A simple program was written which categorizes the longest track in the event. This program was correct in 93% of the cases in which it decided to make a choice. It found an acceptance of 66%. The program has not been optimized to use all events in the acceptance which carry useful information. Also, at present, it is not using reconstructed track lengths for the comparison. We expect there needs to be considerable program development until the program can be as good as a scanner.

Although our study is by no means complete, the number of off-diagonal, misidentified events is small. The misidentification will be corrected by applying the same algorithm to the Monte Carlo events, leading to an error on the correction which is a small fraction of the error itself. In addition of course the ratio in the far detector will be compared to that measured in the near detector with very similar experimental biases. Even with this small statistical sample, we find that the σ_R/R from event misidentification, after corrections based on applying the same algorithm to the Monte Carlo events, will be less than the 2% required to better the statistical accuracy. There is also the potential that further Monte Carlo studies could lead to a smaller misidentification.

Events from ν_e charged current interactions will appear to be neutral-current events in all of our tests. The correct fluxes of each neutrino type are included in the simulation. The fluxes are well understood and will be checked in the near detector, as is discussed in the next Section. The ν_e events will be less than 2% of the event totals, and the uncertainty on

that fraction will be less than 20%. Therefore we do not expect the systematic error from the ν_e's (or $\bar{\nu}_e$'s) in the beam to contribute to our measured $R_{"nc"/"cc"}$ ratio, after correction.

The largest present uncertainty in the NC/CC misidentification is the differences between the edge effects in the near and far detectors. This issue is addressed again in the next Section.

	Apparent CC	Apparent NC
True CC	correct	low energy muons cracks ν_e events edge effects
True NC	hadron punch through edge effects	correct

Table 7: Contributions to the CC/NC confusion matrix.

	CC	NC	outside acceptance
Scanner 1:			
True CC	244	20	101
True NC	6	82	22
ν_e	0	4	0
Scanner 2:			
True CC	244	14	108
True NC	16	69	20
ν_e	0	4	0

Table 8: CC/NC confusion matrix by scanning

	CC	NC	outside acceptance
True CC	727	64	484
True NC	9	301	83
ν_e	0	5	0

Table 9: CC/NC confusion matrix by program

4.5 Question 3. –Near Detector

Provide details on how to determine and handle the difference between the near detector and far detector geometry and analy-

sis. In particular, what are the following parameters: angular divergence, electron neutrino component, antineutrino component, and energy spectrum, for the beams in the near and far locations? What are the contributions to the final error from uncertainties in these effects?

We have used the Fermilab neutrino Monte Carlo NUADA to calculate the energy spectra of the ν_μ neutrino events at the near and far detector. The event spectra at the location of the near detector for 5 radial slices of the beam is shown in Figure 20. In Figure 21 we show the event energy spectrum at the far detector location (730 km) and have normalized it to the central radial slice at the near detector, $r < 0.25m$. It is seen that there is little difference, despite the huge differences in the five near spectra. The central 25 cm of the beam at the near detector represents the beam at the far detector.

In order to estimate the $\nu_e, \bar{\nu}_\mu$ and $\bar{\nu}_e$ event energy spectra, we have used this P-803 Monte Carlo.[3] Restricting ourselves to the central 0.25 meters of the beam, we get the neutrino fluxes shown in Figure 22. We obtain the following flux ratios: $\nu_\mu : \nu_e : \bar{\nu}_\mu : \bar{\nu}_e = 116,110 : 781 : 1749 : 122$. It is seen that the ν_e's are less than 1% of the beam, and $\bar{\nu}_\mu$'s are less than 2%.

At a distance from Fermilab which is large compared to the length of the decay pipe, the neutrinos appear to come from a point source. In Figure 23, we show the event energy spectra from various neutrinos for a detector at 10 km. (It is not practical to run this Monte Carlo at 730 km.) The neutrino ratios are: 13724:73:247:18. Again, the conclusion that the central part of the beam at the near detector matches the beam at the far detector is valid.

The near detector will be much smaller and have much larger statistics than the far detector. However, the geometry will be different, which will lead to different acceptance corrections. We estimate 12 modules in the near detector (1 *high* × 3 *wide* × 4 *deep*) versus 224 in the far detector (2 *high* × 8 *wide* × 14 *deep*) at an angle of 27°. We will run the near detector at the same angle as the far detector (see Figure 24). For some analyses, we will restrict the events in the near detector to those in a radius of 0.25 meters from the center of the beam, in order to match the energy spectrum at the far detector.

For the $R_{\text{"nc"}/\text{"cc"}}$ test, restricting ourselves to the 4% acceptance that matches the far detector beam, we will still have over 10^6 events to use. This would correspond to an error on $R_{\text{"nc"}/\text{"cc"}}$ (statistics only) of $\sigma_R/R = 7.3 \times 10^{-4}$. We would use the full acceptance and compare our answer in the near detector to E-815's result, which will be $\sigma_R/R = 0.002$. We would expect, after acceptance corrections, to match that answer to 0.01 or better. Without a cavity filler, the statistical error in the far detector would be greater.

A neutral current event in the near detector geometry is shown in figure 25. A charged current event in that size detector is shown in figure 26.

Since the event rate in the near detector is very high we can restrict the target volume for comparison with the far detector to the central 25 cm of the beam and to the first module in the stack. This ensures long potential lengths for all tracks from the vertex. We will, in the

near future, repeat the analysis described in question 4.4 in the near detector. We estimate at present that a near detector of the size described here will be adequate to keep geometrical differences to a size that can be corrected by the Monte Carlo to leave systematic errors of less than 2%. If detailed analysis should show this not to be true, then the size of the near detector could be increased without seriously increasing the costs or affecting the operation of the far detector. The following checks will also be available.

- The statistics in the near detector is large. We will be able to study not only millions of events in the part of the beam similar to the long baseline energy spectrum, but millions more with a similar range of energies closer to the edge of the detector.
- We may choose to run part of the time with the near detector offset with respect to the beam axis, in order to sample more geometrical effects with the central 0.25 m radius of the beam.
- These effects can be studied in considerable detail during the hadron calibration running.

There is a potential problem from pileup using Soudan 2 as a near detector. The Soudan 2 drift times is about 86 microseconds, and the total window to record drifting events is about 200 microseconds. With the high Main Injector fluxes that are anticipated, and using a 50 ton near detector, we could expect 15 events per 2 millisecond spill. Thus the neutrino events themselves would not be a large problem. We note that with existing electronics, we can trigger only on one event per spill. Depending on their rate, throughgoing muons from upstream interactions (such as in the P–803 magnet) might present a pileup problem. A high efficiency active veto counter upstream of Soudan 2 would alleviate this if it turns out to be a problem. Other scintillation counters will be used in a trigger where required.

The twelve modules will be arranged in a 4 m x 3.5 m x 2.5 m (high) structure, weighing 50 tons. These modules will be removed from the Soudan 2 detector, and will be calibrated in a charged particle test beam at Fermilab before it is moved into the P-822/P-803 neutrino beam. Many of the electronics and gas system components needed to operate them already exist.

We estimate the following timetable for these test beam exposures:

Set up detector in charged particle test beam:	6 months
Check out operation and performance:	3 months
Charged particle test beam exposure:	3 months
Move to neutrino beam:	6 months
Neutrino beam exposure:	2 years

We have made the following preliminary cost estimate:

Electronics, High voltage, data acquisition equipment:	\$200K
Gas, tapes, supplies	\$ 30K
Mine crew travel/living at Fermilab	\$ 70K
Contingency (20%):	\$ 60K
Total	\$360K

We will request the following help from Fermilab:

- Steel detector support structure
- 2 man years technician effort
- 0.5 man years engineering effort
- Computing facilities

4.6 Question 4 –803

Would a muon identifier help in the near detector? If so, what kind of muon detectors have you considered? If it would not help, why not? What information from P–803 is needed in the analysis?

As we have discussed in detail elsewhere in this proposal, the fine grain and large size of Soudan 2 allows precise reliable classification of events into CC and NC (i.e. having or not having a muon). For the near detector, our intent is to deploy enough Soudan detector modules to be able to achieve the same high precision event classification as at Soudan 2. Therefore a muon identifier is not needed for the near detector. The related issue of the importance of making a muon momentum measurement at the near detector is discussed in our answer to Question 5.

We expect to rely on P–803 for the following information:

- The ν_μ, ν_e, $\bar{\nu_\mu}$, and $\bar{\nu_e}$ components of the beam, as a check on the beam composition Monte Carlos.
- The radial dependence of the energy spectrum compared to that predicted by the beam Monte Carlos, particularly the muon energy spectrum.
- A beam flux measurement which can serve as a check upon our own measurements.
- Hadron energy distribution for CC and NC events. This will serve as a check on our own rather precise measurements of these two spectra in our near detector.

- A high statistics measurement of NC/CC for neutrino interactions in this energy range, and an estimate of the contribution of neutrino induced charm production just above threshold.

4.7 Question 5 –Muon Toroid

The Panel recognizes that the observed CC events are not those which oscillated. However, the Panel continues to believe that a measurement of the neutrino spectrum at the far location is important for controlling the systematics. Discuss measurement of the muon momentum in this context.

The principal reason for measuring the muon momentum spectrum at the far detector is to verify that the observed distribution is consistent with expectations based upon the neutrino beam design, the best-fit oscillation parameters measured using the other methods described herein, and the muon spectrum measured by P–803 at the near detector. For most values of Δm^2 and $\sin^2 2\theta$ in the range over which this experiment will be sensitive, only small changes in the muon spectrum at Soudan will be caused by the oscillation. Nonetheless, at the lower end of our Δm^2 range, a measurable change in the muon spectrum could occur (at its low momentum end).

There are two ways to make a muon momentum measurement, by range and with a magnetic deflection measurement. A small fraction of the muons, about 7%, will range out in the Soudan 2 detector, yielding a momentum measurement for those events. One such muon from our Monte Carlo is shown in Figure 27. The momentum of this 2.3 GeV muon can be determined from its range to 11%.

There are several kinds of apparatus enhancements which can give range measurements for a larger fraction of the muon events. A passive dense absorber followed by muon detectors could increase the 7% to perhaps 15% or greater, using the existing space around the Soudan 2 detector. Another, less promising, idea which we are exploring is to instrument the rock for range measurements, using holes in the wall and placing detectors in them. Of course, all of these range measurements will be confined to the muons of relatively low momentum.

To measure muon momentum by magnetic deflection, we would place a 1 meter thick iron toroid on the north end of the Soudan 2 detector. This location would result in a toroid muon acceptance of about 50%. With drift chambers before and after the toroid, we could achieve a muon momentum resolution of about 20% throughout the entire muon spectrum. (This toroid would also act as a passive absorber, increasing our range measurement capability. Such an absorber also functions as a muon identifier and will allow some increase in the usable neutrino interaction fiducial volume of Soudan 2.)

This toroid, shown in Figure 28, is a substantial object of approximately octagonal shape, standing 8.5 meters high and weighing 600 tons. Because of the underground location, it

would be made of many pieces of iron and probably would be magnetized by a superconducting coil. Overall, the toroid and drift chambers could be quite similar to the forward toroids which have been designed and costed for the SDC. Based on the SDC work [SDC-92-201], we estimate the following costs:

Iron		\$1300K
Drift chamber system		500K
Coil system		400K
Installation		200K
	Total	\$2400K

Table 10: Toroid Costs (1994 dollars)

There is another important issue to consider in deciding whether to add muon momentum measurement capability to Soudan 2. That is the fact that by measuring the hadronic energy spectrum of NC and CC events in Soudan 2, we will already have accurate and important spectral information of the type discussed above.

The measurement of the muon momentum is related to the measurement of the hadron energy spectrum. Measurement of the hadron energy spectrum is important for two reasons:

- Comparison of the hadron energy spectrum for charged-current events is an important check that the near and far detectors are measuring the same region of the neutrino beam.
- Comparison of the hadron energy spectrum for neutral-current events is an additional test for $\nu_\mu \rightarrow \nu_\tau$ oscillations, to the $R_{"nc"/"cc"}$, $R_{\mu/\nu}$ and $R_{near/far}$ tests. In the presence of $\nu_\mu \rightarrow \nu_\tau$ (or $\nu_\mu \rightarrow \nu_e$) oscillations, there would be more high hadron energy events in the far detector.

In order to study the value of the muon toroid, we have used our Monte Carlo to compare the energy distributions which could be measured in the near and far detectors. The true muon momenta have been smeared with:

$$\frac{\Delta p_\mu}{p_\mu} = 20\% \tag{20}$$

and the hadronic energy has been smeared with[42]:

$$\frac{\Delta E}{E} = \frac{40.0}{\sqrt{E}} \tag{21}$$

We have used the central 0.5 m of the beam for the energy spectrum at the near detector. The smeared E_μ, E_{had} and $E_{total} = E_\mu + E_{had}$ distributions for charged-current events in

the near detector are shown in Figure 29. The distributions using the far energy spectrum, and the statistics of our base assumptions, is shown in Figure 30. The acceptance for containing the hadronic shower will be about 80% of the acceptance for neutral-current-charged-current separation. The toroid acceptance will further reduce the acceptance for the E_{tot} measurement by a factor of two.

The two smeared total energy plots are shown together in Figure 31. It can be seen that our measurement of the charged-current event energy is sensitive to the difference in the two spectra. We will certainly measure any shift in the energy spectrum which is larger than the difference between our two assumed plots. The difference between the neutral current to charged-current ratio for the two energy spectra will be less than 1%. Given the measurement of the expected energy distribution in Figure 30, it will be possible to correct for some of that difference.

A muon toroid system clearly adds to the reliability of this experiment, and is included as part of this proposal. The addition of this system to the proposal requires additional simulation which is not yet included in our Monte Carlo. We expect to repeat these studies with the full detector Monte Carlo of the toroid system, and include the additional information in the NC/CC separation, and report to the PAC in the spring of 1994.

4.8 Question 6 –Expanded detector

How much, and at what cost can the detector be expanded in its present location?

A floor plan of the Soudan laboratory is given in Figure 32. The amount of space that can be utilized for the detector has been estimated at about 3/4 of the space not presently utilized by the Soudan 2 detector. We believe that filling the remaining space with Soudan modules would be quite expensive. There is room for 3 kilotons of Soudan 2 in the cavity. Based upon our experience in building Soudan 2 modules, we can accurately estimate the costs in Table 11.

The Soudan 2 detector is a high resolution pictorial device. Costs and space constraints would prohibit the building of 10 kton with a similar resolution. The aim of such a cavity filler would be to identify muons from charged-current events by range, and measure the hadronic energy in a calorimetric fashion. This can only be achieved by an increase in the thickness of the passive material from 3mm to 1-2 cm. The threshold for neutral-current events in such a detector would be 1 GeV or more, much higher than the Soudan 2 threshold.

Design considerations of a cavity filler are discussed in the next Section. An element of such a detector is illustrated in Figure 33. We define the steel thickness s, the detector wall thickness a, and the gas thickness g. For a steel thickness s and density $d_s = 7.8 g/cm^3$, with 2a = 5 mm and g = 10 mm, and $d_a = 3 g/cm^3$ (like aluminum), we could put 4 to 11 kilotons of detector in a space $8 \times 10 \times 25 m^3$, depending on s. This is shown in Table 12.

Modules	\$14520K	
Module Assembly Manpower	1560K	
Module Installation	1560K	
Module Support Structure	1748K	
Gas System	60K	
Electronics and High Voltage	4700K	
Total (1993 \$'s)	\$24148K	or \$24M

Table 11: Costs for tripling the size of Soudan 2

s mm	m g/cm^3	8 x 8 x 24 kton	8 x 8 x 24 chambers	8 x 10 x 25 kton	8 x 10 x 25 chambers
5	2.70	4.10	48000	5.4	56250
10	3.75	5.76	38400	7.5	45000
15	3.75	5.76	38400	8.8	37500
20	4.8	7.49	27400	9.76	32109
25	5.25	8.06	24000	10.5	28125
30	5.53	8.49	21320	11.1	24984

Table 12: Density versus size of cavity filler options.

5 Cavity Filler

Preliminary studies have begun to define a detector that could be constructed in the currently unused space in the Soudan laboratory which would give up to an order of magnitude higher statistics than can be obtained with Soudan 2 alone. This would yield a factor of roughly three smaller errors. The detector has to be designed to keep losses and event misidentification to a minimum, as these effects have to be corrected by Monte Carlo. The criteria we have adopted are

1. A planar geometry for simplicity of construction and optimum event definition given a known beam direction.
2. Steel target plates for compactness and precision of construction to obtain the maximum detector density.
3. Event losses and misidentifications should be less than 20%. These can be corrected to give less than 1% errors on $\sin^2 2\theta$ using the near-far detector comparison and a not very demanding Monte Carlo simulation.
4. Detecting elements must also be compact and cheap.

Table 13 shows the results of a simulation using the expected neutrino beam spectrum at the far detector for various steel thicknesses and trigger conditions.

	1 cm iron	2 cm iron	4 cm iron
% events crossing less than 5 planes	10%	17%	53%
% events < 6 hits in hadron shower	11%	15%	36%
% events with muon contained within the hadron shower	12%	7%	10%

Table 13: Steel thickness options showing event length

Table 13 shows that our criteria are satisfied with 2 cm steel plates and we have adopted this thickness.

We have studied two options for detecting elements; resistive plate chambers (RPC) and drift chambers with diamond shaped cathode readout similar to the OPAL muon chambers.

A resistive plate chamber, obtained from the Italian manufacturers, is working at RAL and performs according to the advertised characteristics. Tests of the cathode-readout drift chambers have been carried out in Oxford. The resistive plate chambers have the advantages of speed, compactness and cheapness since they do not require electronic amplification. However they work best with flammable gases which may cause problems in the mine. The very large number of channels is another disadvantage. We have not yet made a final decision between the two options.

A preliminary engineering study has been carried out assuming use of RPC's. Figure 34 shows a possible layout. In this scheme a 8 kton detector could be built in the currently available space. We would strongly advocate running Soudan 2 and the new detector in parallel, at least at the beginning of the experiment, to take advantage of the much higher granularity of Soudan 2. At this early stage it is difficult to make reliable cost calculations but preliminary estimates are that the 8 kton detector would cost between \$25M and \$35M. One prospect for keeping the costs down that we are pursuing is to use steel at the low prices available in Russia to our collaborators from Lebedev Institute and the Institute for Theoretical and Experimental Physics (ITEP).

As the statistical precision of the detector increases the systematic errors become much more critical. Detailed Monte Carlo simulations of the beam at the near and far locations have only recently become available and much work remains to be done to ensure that the systematics of the proposed system can match the statistical precision.

A massive detector of this granularity could not do the traditional underground proton decay physics. However there would be a significant rate of high energy (> 2 GeV) atmospheric neutrino interactions in the detector ≈ 500/year). With the fast timing of the RPC it should be possible to define a large fraction as being produced inside the detector even though the high energy muon may not be contained within the detector. A measurement of the muon to electron ratio at these high energies will be very interesting to complement the Kamioka/IMB/Soudan 2 measurements at lower energies. At these energies the correlation of muon/electron direction and energy with those of the neutrino is much tighter thus enabling a more precise oscillation analysis to be performed. Monte Carlo studies of the reach of this detector in the $\sin^2 2\theta, \Delta m^2$ plot for atmospheric neutrinos will be performed in the near future.

The decision about the value of the "cavity filler" must balance the square root of mass improvement in statistical precision which can be attained versus the costs of that detector and the required systematic controls. On the one hand, larger statistics in a new more massive "cavity filler" detector would allow greater study of systematic effects. On the other hand, to take advantage of the higher statistics in setting neutrino oscillation limits a smaller systematic uncertainty would be required.

6 Comparison with Other Experiments

There are a variety of new and proposed neutrino oscillation experiments at accelerators around the world. Since the search for $\nu_\mu \rightarrow \nu_\tau$ oscillations is motivated in part by atmospheric neutrino experiments, and the time scale for running P–822 is long, in this Section we shall also consider the capabilities of new and proposed underground experiments to study atmospheric neutrinos.

We divide the consideration of other proposals/experiments into three classes; atmospheric neutrino experiments, "long baseline" accelerator experiments aimed at sensitivity to smaller values of Δm^2, and "short baseline" accelerator experiments designed to probe small mixing angles.

Between now and 1995, the only experiment likely to shed new light on the atmospheric flavor ratio is Soudan 2. Additional Kamiokande running will not reduce their statistical uncertainty significantly over the next several years. IMB, Frejus, and Kamiokande may further analyze aspects of their existing data to see if they are consistent with a neutrino oscillation hypothesis. In two years, there will be a beam test of a water Cerenkov detector at KEK using both Kamiokande and IMB tubes. This will measure the trigger and pattern recognition efficiencies used in their analyses. The angular and energy distributions of atmospheric neutrinos will be important in distinguishing possible neutrino oscillation interpretations of the data.[2]

Later in this decade, Superkamiokande will greatly increase the number of contained ν events. At present, it seems unlikely that the atmospheric ν_μ deficit seen by Kamiokande and IMB can be explained away as a statistical aberration. However, improved statistics will be useful in studying systematic effects.

A few proposals are directly competitive with the goals of P–822, i.e. to search for $\nu_\mu \rightarrow \nu_\tau$ at low mass differences. Brookhaven experiment 889 would be a disappearance experiment along a 20km beam on Long Island. CERN is thinking about aiming beams at Superkamiokande or the Gran Sasso laboratory. Existing detectors at Gran Sasso are not suitable for $\nu_\mu \rightarrow \nu_\tau$, so proposals are being considered for ICARUS, a liquid argon detector, and GENIUS, a planar calorimeter. A comparison of Brookhaven, CERN and P–822 is made in Table 14 and Figure 35.

Also relevant to the question of possible atmospheric neutrino oscillations is the flux of upgoing muons, and the angular distribution of that flux. In addition to IMB and Kamiokande, this can be measured at MACRO, LVD, Baksan, and when they start to take data, at DUMAND and AMANDA. At the present time, uncertainty in the prediction of the upward going neutrino flux makes it difficult to obtain reliable limits or signals from this technique.

Several experiments and proposals at accelerators emphasize other modes and other regions of parameter space than P–822. At CERN, Chorus and Nomad will improve $\nu_\mu \rightarrow \nu_\tau$ limits at small mixing angle. If it gets significant running at Los Alamos, LSND could improve $\nu_\mu \rightarrow \nu_e$ limits at small mixing angle.

To summarize, we think that the P-822/P-803 combination offers the best ability to observe neutrino oscillations if they are responsible for existing anomalies. Although a large fraction of this collaboration is actively involved in the study of atmospheric neutrinos, we regard it as unlikely that these experiments will conclusively prove or rule out neutrino oscillations, with the statistics and systematic errors which are required for such a demonstration. The short baseline experiments are searching for neutrino oscillations in regions of parameter space which are complementary to the region we are focusing on. In the NUMI program, we will run concurrently with the best such experiment. Two major ideas which are directly competitive to this proposal are the experiments which could be done at Brookhaven and CERN. The major disadvantage of doing this physics at Brookhaven is that the beam energy is below ν_τ charged-current threshold. They are exclusively relying on ν_μ disappearance with the incumbent systematic challenge of understanding the neutrino flux calculations. The CERN proposals do not have the potential high neutrino fluxes which will be available from the Main Injector. We feel that coupling the existing fine grained Soudan detector with the Main Injector, which is presently under construction, offers a unique opportunity to address the exciting possibility of neutrino mass and mixing.

	Soudan 2 as is	P-822 cavity filler	BNL889
event rate far detector	6000 ν 17600 μ (from rock)	54,000 ν 35,000 μ	18,300 quasi
event rate near detector	500×10^6	0.5×10^9	638,000
date to completion	$\sim$ 2003	$\sim$ 2003	$\sim$ 2000
distances	1km 730 km	1km 730 km	1 km 3 km 20 km
masses	1. 50 ton, 2. 900 ton	1. 100 ton 2. 8 kton	1. 400 ton 2. 400 ton 3. 4.6 kton
mean energy	16 GeV	16 GeV	1 GeV
run time	2-9 month runs	2-9 month runs	1-4 month run
type of experiment	appearance	appearance	disappearance
neutral-current	yes	yes	$(\nu N \rightarrow \nu \pi^o N)$ (?)
$\nu_\tau CC$	yes	yes	no
detector	calorimeter	calorimeter	H_2O Cerenkov
site	underground	underground	surface
accelerator requirement	Main Injector	Main Injector	upgraded AGS
beam	new beam	new beam	new beam

Table 14: Comparison Fermilab P-822 and Brookhaven 889

7 Work in Progress

This proposal remains incomplete in several aspects. In this section, we identify the main tasks which are still required and describe our plan to complete them.

7.1 Cavity filler proposal

The optimal cavity filler proposal will depend on the energy resolution and triggering capability that is required, which in turn requires extensive Monte Carlo work. This has been started,[43] but has not been carried out in enough detail to choose an optimal detector design. .

Other work is in progress to study the suitability of diamond cathode pad chambers and RPC's for a new detector. In addition, the engineering requirements on getting flat yet inexpensive steel to place between chambers is receiving attention.

7.2 Further Simulations

Considerable simulation work remains to be done. These jobs include:

1. Complete a higher statistics analysis of NC/CC separation issues, and further optimize algorithms to get the highest possible acceptance with low misidentification.
2. Extend the Monte Carlo into the upstream rock and generate the rock muons for the $R_{\mu/\nu}$ test.
3. Perform a high statistics simulation of the proposed near detector and optimize the near detector configuration and mass.
4. Incorporate the toroid, which was discussed in answer to Question 5, in our detector simulation.
5. Calculate the hadron energy resolution for high energy neutrino events, both for P–822 and for high energy atmospheric neutrinos.
6. Study particularly the quasi-elastic neutrino events, as a clean potential source of ν_τ signatures.
7. Study ν_τ simulated events and devise low background signatures.
8. Study the possibility to identify $\nu_\mu \rightarrow \nu_\tau; \tau \rightarrow e\nu\nu$. This depends on electron hadron separation, and we note that Soudan 2's high granularity make it well suited for such a search, if it is possible in an iron calorimeter.

9. Study the backgrounds and signal for stopping muons coming out of the rock, which are sensitive to the lowest energy, and hence low values of Δm^2.

10. Study of Soudan 2 data to confirm that backgrounds to Fermilab beam events are low.

7.3 Other Ideas

We list here some of the other ideas which are being considered to enhance the experiment. Some of these ideas will be further developed over the next year:

- The anti-proton (AP2) beam line was considered as a source of pions and muons for P–860. The same beam might be used to aim a new neutrino beam at Soudan 2 with a long decay pipe.
- Beam profile counters could be placed on the surface or other areas of the the Soudan mine. These would measure the radial distribution of the flux of rock muons and ensure that the horn is correctly aligned with respect to the mine.
- Holes could be drilled into the west wall, and counters placed in them. This would serve as an external muon identifier for Soudan 2, and would also increase the target mass for the highest energy charged-current events.
- Iron absorber could be added on the west side of the detector to increase the acceptance for muon identification, using the existing shield as a muon identifier.

7.4 Timeframes

The P–822 collaboration is committed to document to Fermilab the capabilities and possible limitations of this proposal. By the spring of 1994, we expect to have most of the simulation work referred to in this Section completed. This has become the major time commitment of several members of the collaboration, as well as graduate students from Minnesota and Oxford. In the same time period, we expect to work with Fermilab to gain a realistic appraisal of the costs of building the beam. Other collaboration members are working on understanding the required capabilities and costs of a major new detector at Soudan. We expect more detailed questions about our proposal from the Fermilab Program Advisory Committee, and to provide answers in the spring.

The collaboration is actively working to enlarge its size in order to work out many of the detailed issues facing our experiment. Uncertainties in the time frame for the Main Injector hamper some groups from making such a commitment. We recognize the necessity that a successful experiment requires more collaborators than we have at present.

8 Summary

We believe that the question of possible neutrino mass requires a major effort to search for neutrino oscillations in the region of parameter space where this proposal is sensitive. The granularity of Soudan 2, its distance from Fermilab, the neutrino energy spectrum and fluxes possible from the Main Injector, and the Δm^2 range of the atmospheric neutrino deficit together provide a fortuitous opportunity to make a major discovery. We are confident that Soudan 2 is the right detector to use in such a search.

We have not identified any systematic effect which would cause σ_R/R to be larger than 2%. The (uncorrected) event rates expected and the ability to measure oscillations based on R can be seen in Table 3. Let us suppose for example that neutrino oscillations $\nu_\mu \rightarrow \nu_\tau$ exist with $\Delta m^2 = 10^{-2}$ and $\sin^2 2\theta = 0.4$. (This point is conservatively chosen on the low $P_{\nu_\mu \rightarrow \nu_\tau}$ side of the allowed atmospheric neutrino deficit solution.) Convincing evidence from this experiment for a positive and consistent neutrino oscillation signal would consist of the following:

- Measurement of an 8 σ effect in $R_{\text{"nc"}/\text{"cc"}}$.
- A measurement of R in the near detector, which statistically can be measured to $\sigma_R/R = 7.4 \times 10^{-4}$, but which will only need to agree with E815's measurement to better than 5%.
- A comparable measurement of R in P–803.
- Measurement of an independent 7 σ effect in $R_{\mu/\nu}$.
- Measurement of a 10 σ effect in $R_{near/far}$. if knowledge of the beam flux can be controlled to 2%.
- Confirmation of the expected $\nu_\mu, \bar{\nu}_\mu, \nu_e$, and $\bar{\nu}_e$ fluxes in P–803 to 2% for ν_μ and 20% for the others.
- A hadronic energy spectrum for charged-current events in the near detector which is consistent with the 803 spectrometer results.
- Calibration of the hadronic energy response in a hadron beam at Fermilab.
- Measurement of a comparable hadronic energy distribution for charged-current events at Soudan with the much larger statistics in the near detector, E_{had}.
- A μ momentum measurement in the muon toroid yielding the expected distribution.

A long baseline neutrino oscillation experiment also represents a risk. We believe that the prospects for a real and convincing signal are considerable. The NUMI program is uniquely positioned to lead the world's high energy physics community into a new study of the once elusive neutrino.

Appendices

A Long Baseline limit curves

A.1 Introduction

The limits in Figures 4 and 6 properly take into account the cross-section weighted energy integrals. However if we approximate using just the average energy at low Δm^2 and take the limit $\int(\sin 1.27\Delta m^2 L/E)^2 dE = 1/2$ at high Δm^2, we get straight line (log-log) parameter space plots. These are easy to calculate by hand, which is useful for comparing various experiments and assumptions about energy, detector size, running periods, statistics, distances, etc.

A.2 Types of Neutrino Oscillation Searches

Four kinds of neutrino oscillation signals can be considered for a neutrino oscillation search. They can be separated as follows:

1. Disappearance of some of the neutrinos in the beam. The measurement consists of comparing the number of observed neutrino interactions to the number predicted by other measurements. The solar neutrino experiments, the atmospheric neutrino experiments, Brookhaven E889 and the $R_{near/far}$ test in P-822 are examples of this kind of search.

2. Exclusive appearance experiments. Here the signal is a clear cut neutrino interaction(s) from a flavor not present in the original beam, with little or no background. P-803, CHORUS, and in principle NOMAD are examples of this kind of experiment.

3. $R_{"nc"/"cc"}$ test, or the Shrock-Albright test[44]. This is an appearance experiment, but since the background to the signal is large (all neutral-current events), one can not identify ν_τ events on an event-by-event basis. However, the test is sensitive to ν_τ appearance, and if $\nu_\mu \rightarrow \nu_{sterile}$ takes place, the test does not measure any change, so it is an appearance experiment.

4. Kinematic cuts. A signal such as electron appearance will have some large background rejection κ, but may still be dominated by background. Such a test will also have some efficiency for ν_τ's, ϵ_τ. If the rejection is sufficiently high, this could be a zero background test.

A.3 The Line Limit Approximation

There are several subtle aspects to the usual 90% confidence level plots which are used to characterize limits obtained by neutrino oscillation experiments. In order to make certain

scaling approximations and compare experiments more easily, it is useful to approximate the curves as two straight lines. The probability of oscillation is:

$$P = \sin^2(2\theta)\sin^2(1.27\frac{\Delta m^2 L}{E}) \tag{22}$$

where L is the distance in km, E the neutrino energy in GeV, and the unknown parameters are the mixing angle θ and the squared neutrino mass difference Δm^2. If an experiment is sensitive to neutrino oscillations, it can either measure P to some accuracy, or set a limit on P which we will call P_{min} for the usual 90% confidence level limit. An experiment with a sensitive test for neutrino oscillations could set a small P_{min}, a less sensitive test would lead to a larger P_{min} or no limit at all.

All limit curves which depend on a single variable P_{min} start at some Δm^2 with a slope -0.5 on a log log plot, oscillate, and approach a fixed mixing angle at high mass. We will therefore approximate the limit curves with two numbers, D_0, which is the Δm^2 at maximal mixing, and S, which is the $\sin^2 2\theta$ limit at high mass. We extend the curve from D_0 with a slope -0.5 until it crosses the other line at S, D_2. These are shown in Figure 36.

At maximal mixing, $\sin^2 2\theta = 1$ and we will set a limit when the second sine term in equation 22 is small:

$$\Delta m^2 \approx \frac{\bar{E} \times \sqrt{P_{min}}}{1.27L} \equiv \frac{F\bar{E} \times \sqrt{P_{min}}}{1.27L} \tag{23}$$

where $\bar{E}$ is the average neutrino event energy, and the factor F takes into account the fact that integrating over energy differs from using the average energy. For our limits, F = 0.80.

At high mass, the energy integral of $\sin^2 1/E$ averages to 0.5. We thus have three simple equations for s, D_0 and D_2:

$$S = 2P_{min} \tag{24}$$

$$D_0 = \frac{0.8\bar{E}\sqrt{P_{min}}}{1.27L} \tag{25}$$

$$D_2 = \frac{D_0}{\sqrt{S}} \tag{26}$$

A.4 Specific Neutrino Oscillation Tests

A.4.1 Neutral-Current to Charged-Current test

For the neutral-current to charged-current test in the presence of oscillations,[37]

$$P = \frac{(R^{obs}_{\nu_{nc}/\nu_{cc}} - R^{true})}{\eta(1-B) + R^{obs}_{\nu_{nc}/\nu_{cc}}(1-B\eta)} \tag{27}$$

where R^{true} is the expected neutral-current to charged-current ratio, $R^{obs}_{"nc"/"cc"}$ is the measured ratio, B is the branching fraction of the final state lepton to muons, and η is the event weighted charged-current cross-section of the final state lepton compared to that for muons.

$$\eta \equiv \frac{\int \phi_\nu(E)\sigma_{\nu_\tau}(E)dE}{\int \phi_\nu(E)\sigma\nu_\mu(E)dE} \tag{28}$$

For $\nu_\mu \rightarrow \nu_\tau$, B = 0.17 and $\eta = 0.25$. (For $\nu_\mu \rightarrow \nu_e$ B=0 and $\eta = 1.0$) For a 90% limit,

$$P_{min} = \frac{1.29\sigma_R}{\eta(1-B) + R^{true}(1-B\eta)} \tag{29}$$

which is 2.56 σ_R for $\nu_\mu \rightarrow \nu_\tau$ and .99 σ_R for $\nu_\mu \rightarrow \nu_e$. Thus the $\nu_\mu \rightarrow \nu_e$ limits are always 2.6 times to the left of the $\nu_\mu \rightarrow \nu_\tau$ limits for the same statistics. The factor 1.29 corresponds to the 90% confidence level, and is 3 for a 3 σ effect, 4 for a 4 σ effect, etc.

For the neutral-current to charged-current test,

$$\sigma_R = R\sqrt{\frac{1}{NC} + \frac{1}{CC}} = \frac{R(1+R)}{\sqrt{Nr}} = \frac{0.73}{\sqrt{N}} \tag{30}$$

where N is the total number of events. Thus for an experiment with full acceptance and efficiency, no other background or systematic error,

$$P_{min} = \frac{1.87}{\sqrt{N}} \tag{31}$$

We can also use these equations to study the effect of systematic error. If we express S in terms of σ_R/R, we get S = 1.59 σ_R/R. The PAC recommended that the experiment should reach a systematic uncertainty on the NC/CC ratio (or σ_R/R) of less than 0.02, which yields $S = 0.03$. We believe that we can exceed this goal, since we are only sensitive to the *change* in r and do not require an absolute measurement (although we will certainly do so as a check).

A.4.2 Low background appearance experiments

For a truly zero background appearance experiment, a long baseline detector has no advantage over a short baseline experiment.[45] The reason is that while for a low Δm^2 the probability of oscillation increases as L^2, the flux and event rate fall as $1/L^2$.

When there is background, the background falls as $1/L^2$. As one moves far away, the signal might go down slightly, but the signal to background greatly increases. Detectors like P-803 are very expensive per kiloton, and should be run at an accelerator first, and then only moved a long distance if there are backgrounds which are seen with possible signals.

Unlike the other tests, this limit goes linearly with statistics:

$$P_{min} = \frac{2.3}{N_{cc} \times \eta \times \epsilon} \tag{32}$$

where η takes into account the ν_τ charged current cross-section, and ϵ includes all other efficiencies. For P-803 in the Conceptual Design Report, $\epsilon = 0.06$.[1, 3] It is interesting to note that D_0 which is proportional to $\sqrt{P_{min}}/L$ is a constant as you move a given detector because $P_{min} \propto 1/N$ and $N \propto 1/L^2$. This is the same as the argument made above. For fixed statistics, $D_0 \propto 1/L$.

A.4.3 Muon disappearance experiments

ν_μ disappearance can be measured by seeing a decrease in the absolute rate of events at a far detector. Here the crucial element is the measurement of the flux in an identical (or similarly configured) detector. One could also predict the far detector event rate based on the proton flux hitting the target and a calculated neutrino flux, but the systematic errors in such a calculation are known to be large. Assuming that the statistical errors at the near detector are small, a limit can be set from:

$$P_{min} = \frac{1.29}{\sqrt{N_{cc}}(1 - \eta B)} \tag{33}$$

Strictly speaking, in a two detector disappearance experiment, one is looking for a difference between the two detectors, and the limit at high Δm^2 returns to maximal mixing. Both detectors would measure the neutrino flux which was maximally mixed. The two line approximation fails to take this into account. Since previous short baseline appearance experiments at accelerators have failed to see neutrino oscillations, this is unimportant.

A.4.4 Kinematic cuts, such as electron appearance

Using kinematic and topological cuts, it may be possible to identify τ events. The decay mode $\tau \rightarrow e\nu\nu$ is one particularly promising example. Let's assume we can identify electrons and perhaps π^o's. The number that you measure is:

$$N_{em} = \kappa N_\mu + N_\mu \varepsilon_\tau \eta P_{\nu_\mu \rightarrow \nu_\tau} \tag{34}$$

where κ is the background rejection factor for events which pass the cuts. We may be able to achieve $\kappa \approx 10^{-2}$. ε_τ is the fraction of signal which passes the cuts ≈ 0.50 and η is the cross-section factor, 0.18 .

With 90% CL, in the absence of oscillations, we measure less than $1.29\sqrt{\kappa N_\mu}$ events. Therefore, if we measure κN_μ, the expected rate, we can set a limit on P:

$$P_{min} = \frac{1.29\sqrt{\kappa N_\mu}}{\varepsilon_\tau \eta N_\mu} = \frac{1.43}{\sqrt{N_\mu}} \tag{35}$$

A.5 Using the equations to scale various experiments

Now we can ask what it would take to get to the curve actually shown in Figure 36. The stated PAC goal is shown at $\Delta m^2 = 0.01$, $\sin^2 2\theta = 0.01$. The parameters we calculate are $D_0 = 10^{-3}, D_2 = 10^{-2}, S = 10^{-2}, L = 713km$ (!) and N = 140,000 events. Using the high Main Injector flux from two nine-month runs, and scaling this event rate to the P-822 proposal with 100% acceptance at 730 km, leads to a requirement of a detector twenty times more massive than Soudan 2 with no systematic error. If we demand a 4 σ signal at the PAC point, it goes up to 1.33 Million events. If we consider the Δm^2 goal to be one for D_2 and the required distance would be 71 km, and the required statistics 140,000 events. A detector the size of Soudan 2 would be adequate, but we note that such an experiment does not address much of the Δm^2 region suggested by the atmospheric neutrino problem.

Another important point is the way that $\sin^2 2\theta$ and Δm^2 scale with statistics. Limits on the mixing angle will improve as the square root of the number of events, while limits on the mass will improve only as the one fourth power of the statistics. If one aimed a beam at a new detector at a moderate distance, such as 100 km, one could gain over this proposal with better limits on mixing angle at the expense of Δm^2 reach. However, it would be impractical to improve that situation with greater mass or running time. On the other hand, a detector located at 700 km would start with a better Δm^2 reach at the expense of mixing angle sensitivity. However, this could be more readily improved with an additional detector or more running time.

B The Soudan 2 Detector

B.1 Detector description

The Soudan 2 experiment uses a currently operating detector in an underground laboratory 710 m (2090 meters water-equivalent) beneath Soudan, Minnesota. The detector consists of a 963 metric ton fine-grained tracking calorimeter surrounded on all sides by a two-layer active shield of proportional tubes. Its primary goal is to search for nucleon decay in modes which may be dominated by neutrino-interaction background in other experiments. It is well suited to be a neutrino detector for the average energies of a Main Injector neutrino beam, and is in fact similar in resolution and size to neutrino detectors which have been used in past experiments at Fermilab and CERN.

The performance of the calorimeter modules has been studied using cosmic ray muon tracks, both on the surface and underground. A charged particle test beam, at the Rutherford Laboratory ISIS accelerator, has been used to study detector response to low energy particles. The test beam studies have provided the energy calibration for electromagnetic showers and tracks, and have measured the ability of Soudan 2 to identify muon charge and direction.

The Soudan 2 detector [39] consists of 224 identical 4.3 ton calorimeter modules, which

were constructed at Argonne National Laboratory and the Rutherford Appleton Laboratory. Two hundred and sixteen modules are taking data in the Soudan mine at present.(October 1993). The modules are placed in a rectangular parallelopiped 2 modules high x 8 modules in the east-west direction x 14 modules along the axis of the cavity (north-south direction), yielding a dimension for the full detector of 5x8x16 m^3. This layout is illustrated in Figure 37.

Each module is composed of 240 layers of $1m$ x $1m$ x 1.6 mm corrugated steel sheets interleaved with an insulated "bandolier" assembly of 1 m long x 0.5 mm thick x 15 mm diameter resistive Hytrel drift tubes (see Figure 38). The insulation consists of two layers of 125 μm mylar, laminated together with long pockets to accommodate the drift tubes, and 0.5 mm thick polystyrene inserts which are vacuum formed to fit the steel corrugation. The steel sheets and the bandolier are stacked in 240 layers (2.5 m high) by fanfolding the bandolier back and forth with steel sheets interleaved. The stack is then compressed with about 15 tons of force. Each module is enclosed in a gas-tight sheet steel enclosure consisting of welded sideskins to maintain compression and removable covers to allow access to the readout proportional wireplanes and stack faces. The assembled detector has a density 1.6 g/cm^3, a radiation length of 9.7 cm and a nuclear interaction length of $\sim$ 81 cm.

The basic detector element of the experiment is shown in Figure 39. It is a tube made of resistive ($\sim 2\text{x}10^{12}\Omega - cm$) plastic Hytrel (DuPont Corporation). Each module contains 7560 drift tubes. A linearly graded electric field is applied by 21 1.5 mm wide copper electrodes (see Figure 38). These have a voltage of -9 kV at the middle of the tube and 0 V at the two ends. The resistive tube grades the voltage between electrodes, creating a uniform axial drift field of 180 $volt/cm$ inside the tube. The modules are filled with a drift gas mixture of 85% argon, 15% CO_2 and 0.5% of H_2O (from the plastic). When a charged particle passes through the tube it ionizes the gas; the liberated electrons then drift (with a velocity of 0.6 $cm/\mu sec$) up to 50 cm to the ends of the tube where they are collected and amplified on a 50 μm diameter anode wire (gold plated tungsten). The gas is circulated through the modules and filtered to remove oxygen and hydrocarbons which absorb the drifting electrons.

The tubes are arranged in a close-packed hexagonal array as shown in Figure 38. The anode wires run vertically in a plane 10 mm from the tube ends and are spaced every 15 mm so that they are aligned with the centers of the tubes. Cathode pads are connected in horizontal strips orthogonal to the anode wires and 5 mm behind them, and are aligned with the tubes. Thus it is possible to identify which tube a signal came from, since the anode wires and cathode pads form a grid centered on the tube ends. The position along the tube length is obtained from drift-time information. Three correlated spatial coordinates and a dE/dx measurement are recorded for every charged particle crossing of a drift tube.

The main detector is surrounded on all sides by a 2-layer array of extruded aluminum proportional tubes [46]. This active shield is mounted against the cavity walls to signal the presence of cosmic ray events in the cavity and the surrounding rock. The tubes are up to 7 m long and 20 cm wide and have a time resolution of 1 μs. Cosmic ray muons can create contained event candidates by entering the detector through the spaces between main detector modules, or by creating neutrons, photons and K_L^0's in the nearby rock which penetrate to the interior without leaving tracks. Such neutral particle production is almost

always associated with charged particles which are detected in the shield. Because the 1700 m^2 shield has nearly 3.5 times the area of the main detector in the direction of Fermilab, it can also be used to increase the effective area for the measurement of the flux of muons from ν interactions in the rock upstream of Soudan 2.

B.1.1 Electronics Readout

The detector is read out by 28,224 anode wires and 107,520 cathode pads through 5,888 electronics channels. The reduction in the number of channels is accomplished in two stages. Groups of 8 modules are stacked 2 high by 4 across to form a halfwall. The detector consists of 28 halfwalls. The two large faces of each halfwall each contain 8 wireplanes. Anode signals from the upper modules are bussed to the lower modules and cathode signals are bussed across the halfwall to give an equivalent readout plane which is 5m high x 4m wide and is known as a *loom*. Each loom consists of 252 anode channels and 480 cathode channels. Preamplifier signals from 8 anodes are then summed together by connecting the anode channels from 8 separate looms to one digitization crate. The preamplifier signals from each cathode pad are also summed 8-fold, but in a different pattern, ensuring that the looms served by one anode crate are served by different cathode crates. Since any one loom is served by a unique anode crate and cathode crate combination, a tube anywhere in the detector may be located by matching the anode and cathode pulses.

The resulting 5888 channels of ionization signal are digitized by flash ADC's every 200 ns and stored in RAM. The digitization and data acquisition process occurs in a system of 24 parallel MULTIBUS crates each containing an Intel 80C86 microprocessor, which supervises a pipe-lined data compactor (which removes digitizations below a programmable threshold), and manages transfer of the compacted data via CAMAC to the host computer. Within each data crate there is a calibration card which, under local processor control, can be used to calibrate all the analog channels and verify the trigger logic within the data crate. The calibration card controls an array of pulsers which can send pulses to various combinations of the preamp inputs.

Digitization proceeds asynchronously in each of the 24 data crates with the RAM's used as circular data buffers. When a trigger decision is positive, the digitization is continued for an additional time beyond trigger time. This allows all the ionization for that event to drift out of the tubes so a complete drift history is stored for each channel.

To prompt the Soudan 2 detector to read out and store an event, it is necessary for the event to satisfy the trigger requirements. The raw data pulse patterns at the ADC inputs are continuously compared with programmable trigger conditions to detect localized clusters of hits in the drift tubes. The primary trigger requirement in the Soudan 2 detector is the "edge" trigger. A detailed description of the edge trigger will not be given here, for a complete account, see reference 47. Compton electrons produced by photons interacting in the endplane of a module are a primary element of the noise rate in the detector. The edge trigger was designed to reject these events, so an event must have some minimum extent in

the drift direction to satisfy this trigger. Since every readout channel contributes equally, the trigger requirement is uniform throughout the detector volume. Efficiency is high for muons above 230 MeV/c and falls linearly to zero at 90 MeV/c (for muons which do not have a visible decay). The electron (shower) triggering threshold is about 50 MeV. The rate of random triggers from natural radioactivity is less than 0.5 Hz in the full detector under these conditions. The trigger efficiency for neutrino events produced by the Fermilab beam will be essentially 100%. The deadtime will be less than 6%.

B.2 Detector Status and Operation

The Soudan 2 detector has been operational since July 1988 when the first 275 tons of detector was turned on. Data were taken while the detector was being constructed; currently (October 1993) 929 tons of detector are in operation and 1.5 kton-years of exposure has been obtained. Reconstruction and filtering of contained neutrino events and cosmic ray muons is performed at the Soudan site immediately after data acquisition. Detailed analysis has been completed on all data taken before November 1992 (1.0 fiducial kton-years). The detector is now in routine data taking operation more than 70% of the time. The major downtime is associated with the addition of new modules to the detector and will cease with the completion of the detector in late 1993. The performance of the detector has been reliable and stable over the past two years of operation. We do not anticipate any problems with continuing operation through the time period when a neutrino beam might be available. We are in any case committed to running Soudan 2 at least through 1998 to obtain a proton decay exposure of 5 fiducial kton-years. The detector performance is entirely consistent with the original Soudan 2 proposal and more than adequate to perform this experiment.

Data at the Soudan site are stored on disk in runs of $\sim$ 1 hour length, and is processed immediately after the end of a run on a local VAX Cluster with an analysis package SOAP (Soudan Offline Analysis Program). SOAP performs noise rejection, pulse matching, track reconstruction, and sorting of events into various categories of physics interest, such as muons, multimuons, monopole candidates, (contained) neutrino candidates, and semi-contained events. Muons from neutrino interactions in the rock from the direction of Fermilab would all be found in the muon sample. Neutrino events would be in either the contained or semi-contained event classifications. An additional processor would be established to flag events that were in time with a Fermilab beam pulse. This event sample would be compared with the contained and semi-contained event samples to ensure that all Fermilab events were being found with high efficiency.

The detector is monitored in several ways to assure that it is operating properly. The pulser system is used to inject signals into the preamp inputs. These signals then work their way through the readout chain and check the operation of the electronics. Pulser calibration runs are performed daily to find amplifiers with incorrect gain, disconnected cables, etc. The response of the detector (as well as the electronics) is continuously monitored by analysing the data from throughgoing cosmic ray muons. These muons trigger the experiment at a rate of about 0.3 Hz. One to two days of data is sufficient to detect larger effects such as

air leaking into a module or bad electrical connections inside a module. A sample of tracks accumulated over about one month is used to measure the detailed pulse height response at the level of individual drift tubes and can be used to correct the pulse heights in the region of nucleon decay or neutrino interaction candidate events.

An example of part of a cosmic ray muon track is shown in Figure 40. The fine detail of a few pulses can be seen. This shows both the pulse shape information and the 200ns digitization time. The result of the fit to that part of the track in relationship to the pattern of the stack is also shown. A complete muon track traversing the detector is shown in Figure 41. Comparing the two figures, the large amount of information that is available for each event is apparent.

To provide pulse height uniformity over time, the atmospheric pressure is monitored and the anode wire high voltage, for the modules and for the shield, is adjusted to compensate the effect of pressure changes on gas gain.

B.3 Performance and Calibration

B.3.1 Module performance

In order to optimize the operating parameters (e.g. gas and electronic gains), a few modules were initially operated on the surface where the cosmic ray flux is high enough to do high statistics studies rapidly. Some of the results on performance of the modules operated on the surface are presented in this Section.

For the study of tube efficiency the cosmic ray muon trajectories were fitted. By comparing the number of hit tubes crossed by the trajectory with the number predicted to be hit, the tube efficiency is determined. Such a definition not only considers if the tube is working, it also includes the anode-cathode matching efficiency and the track fitting efficiency. Moreover, the efficiency will be decreased due to deviations of the actual tube position from its nominal position, and random scattering of the muon from a smooth trajectory. In the case of perfect geometry, for Monte Carlo data, the tube efficiency is 85%. Under actual operating conditions the mean tube efficiency is of the order of 75%. The mean tube efficiency is very uniform throughout a module, as is shown in Figure 42, where the efficiency is plotted along the cathode direction. The variations seen in Figure 42 are correlated with the pulse height variations along the cathode direction. The maximum tube efficiency that is reached is 80% for very high pulse heights, but the modules were operated at the knee of the efficiency plateau to remain in the proportional gain region.

Typical drift attenuation lengths are of the order of 70 *cm*. For the pulse height distribution shown in Figure 43 the attenuation lengths for the two 50 *cm* drift regions are 71 and 63 *cm*. Such attenuation is well understood in terms of electron diffusion during drifting and electron attachment due to O_2 contamination at the few ppm level. Some variations from module-to-module can be observed, even with the same gas composition, due to imperfections in the electric field which show up as a difference in the effective radii of the tubes. In the absence of oxygen attachment, attenuation lengths are expected to be about 70 *cm*. The spatial resolution is determined by the anode and cathode spacing, the drift time digitization unit and the drift velocity. The spatial resolution is obtained from the RMS of the residual distributions, calculated by fitting cosmic ray muon tracks. The spatial resolution in the vertical (y) direction is 0.47 ± 0.10 *cm* , compatible with the expectations from cathode separation. A result consistent with anode separation is obtained in the horizontal (x) direction. The spatial resolution in the drift (z) direction is 1.04 ± 0.24 *cm*.

One of the main characteristics of the Soudan 2 detector is its ability to yield pulse height information for track direction determination and particle identification. To make maximum use of this information, the pulse height variation between modules must be smaller than Landau fluctuations (20%). Typical pulse height fluctuations along the wire plane are of the order of 30%, while in the drift direction, due to pulse height attenuation, a 50% reduction in pulse height can be observed (see Figure 43). However, these variations are corrected by calibrating out the effects of measured pulse height attenuation, wire plane nonuniformities, module-to-module variations, and gas composition. After pulse height calibration, a 10%

variation is obtained.

B.3.2 Module calibration

At the Rutherford Laboratory's ISIS pulsed neutron source, a Soudan 2 calorimeter module was exposed to beams of positive and negative pions, muons, and electrons at momenta between 140 and 400 MeV/c, and protons at 700 and 830 MeV/c, for several angles of incidence. Analysis of the data is in progress but preliminary results are available on the detector resolution, ionization response, and particle identification. These studies have confirmed that the detector modules are performing as expected, and also have provided detailed response parameters which can be used in the Monte Carlo detector simulation.

The electromagnetic shower energy is determined by counting tube crossings (hits). Figure 44 shows the number of tube crossings as a function of the electron beam energy, for ISIS and Monte Carlo data. The non-linear dependence upon the energy reflects the high density of tube crossings at high energy. The measured energy resolution can be represented as in Figure 45.

Although the Soudan 2 detector is designed to be relatively isotropic, its geometry is not completely uniform. This fact will affect, at some level, the number of hits counted for shower energy measurement. Figure 46a shows the number of hits observed for different vertical incidence angles of the beam, for tracks perpendicular to the tubes. The maximum variation (8%) is obtained for small vertical angles. This variation is easily calibrated. The total pulse height is independent of the vertical incidence angle as is shown in Figure 46b. When the dependence upon horizontal angle (angle with the z direction) was measured, a variation of the number of hits was observed where the beam is almost parallel to the tubes (see Figure 46c). The total pulse height does not vary with horizontal angle (Figure 46d). Therefore, the Soudan 2 detector is isotropic after some small corrections. The small detector anisotropy observed is confirmed with the Monte Carlo and does not compromise the energy resolution.

A sample of π^{0}'s produced in charged pion interactions has been reconstructed. The events were selected by scanning for events with two well separated showers. The π^0 peak is centered at 136 ± 3 MeV/c^2 and has an RMS of 40 MeV/c^2 (see Figure 47). When the production vertex is known it is possible to distinguish electrons from photons by measuring the distance between the vertex and the first hit (conversion length). If the distance is smaller than 4 cm the relative probability to be $e : \gamma$ is 8 : 1, for a distance larger than 4 cm the shower is more likely a photon with $e : \gamma$ a probability of 1 : 14.

Muon momentum is calculated from the range obtained by measurement of the muon track length (L) and using a mean detector density (1.6 g/cm^3). The average length for 245 MeV/c muons is 40.6 cm, with $\Delta L/L = 20\%$, giving a momentum resolution of 8%. This resolution is independent of momentum for the ISIS energies.

Soudan 2 can distinguish between stopping positive and negative muons because most

negative muons are captured by iron nuclei and do not decay visibly. The decay positrons from positive muons are usually detected. Figure 48 shows the number of extra hits at the ends of tracks for samples of negative and positive muons. Two or more shower hits are observed at the end of 85% of the positive muon tracks. No hits are observed for 75% of the negative muon tracks.

The expected ionization response of a slowing muon is observed. Figure 49 shows the mean pulse height along the muon trajectory measured from the end of the track. Crude measurement of the track direction (choosing the end with the higher mean ionization on the last 5 hits as the stopping end) yields the correct direction 80% of the time.

B.4 Detector Summary

Some advantages of the Soudan 2 detector for detecting and identifying neutrino events are:

- The fine granularity gives very good track and vertex resolution. The result is high quality pictorial event information, comparable to that from standard electronic neutrino experiments. The spatial resolution is 1 cm or better in all three spatial coordinates.
- The ionization measurement yields particle identification information (e.g. proton/pion-muon separation) not available in some other detectors.
- μ^- absorption in iron gives track charge information. (about 2/3 of stopped μ^+'s decay visibly in Soudan 2.)
- In a moderate density iron calorimeter, high energy muon/hadron separation is easy.
- The energy threshold of the trigger for muons is lower than in any other underground ν detector.
- The observation of shower development yields better low energy electron-muon separation than in water Čerenkov detectors.
- The modularity of the detector has allowed detailed test beam calibration studies. Detector modules will also be calibrated in a high energy charged particle test beam at Fermilab at energies appropriate for the P-822 proposal.
- The modularity of the detector will allow us to operate an almost identical type of near detector in the P-822 neutrino beam at Fermilab.

The particular features which make this detector powerful for the proposed neutrino experiment are the excellent pattern recognition and particle identification of hadrons, muons and electrons. This capability will enable reliable separation of charged and neutral current events and the identification of the flavor of the final state lepton.

C Definition of an appearance experiment

It is conventional to distinguish between two kinds of neutrino oscillation experiments, appearance and disappearance. In our definition, an appearance experiment is one in which we search for the presence of a neutrino species absent in the initial neutrino beam, or the increase in flux of a species. In order to measure such an appearance, particularly in the presence of any background, then the signal (the number of suitably selected events) should be greater than it would be in the absence of oscillations. In the $R_{"nc"/"cc"}$ test, that signal is the number of neutral-current events.

In a disappearance experiment, the search is for a decrease in the flux of a neutrino species which is present in the beam. The latter is often done by measuring the flux in similar detectors at two or more locations and search for a variation of L/E_ν. High energy accelerator neutrino beams are usually more than 95%ν_μ. Thus the appearance experiments can normally measure $\nu_\mu \rightarrow \nu_e$ or $\nu_\mu \rightarrow \nu_\tau$ while the disappearance ones measure the decrease of ν_μ, *e.g.* $\nu_\mu \rightarrow \nu_X$.

In the June 1993 PAC report, a different definition for an appearance experiment was chosen, "The Committee considers an appearance experiment one in which the definitive presence of the unexpected charged lepton (e.g. τ in the mode $\nu_\mu \rightarrow \nu_\tau$) is detected." An experiment which has little or no background is certainly to be preferred over an experiment with large backgrounds. Our "measurement" of the τ leptons by counting the neutral-current events has a large background, e.g. all ν_μ neutral-current events. This does not remove the important distinction, however, that our measurement is sensitive to, and is only sensitive to, the appearance in the beam of a neutrino species that was not initially present.

A crucial aspect of our experiment is the measurement of $R_{"nc"/"cc"}$ in both the near and far detectors. This aspect of the experiment can be distinguished from the disappearance versus appearance question. Every appearance experiment would be made better by having more than one detector measuring the strength of oscillations at more than one location.

Our disappearance test, $R_{near/far}$, is sensitive to ν_μ disappearance. It would be sensitive, for example, to oscillation of ν_μ into a right handed, and hence sterile, neutrino species. However, the $R_{"nc"/"cc"}$ and $R_{\mu/\nu}$ tests would be completely insensitive to such ν_μ disappearance. The ratio that we measure with these latter two tests is only changed by the appearance in the beam of a ν with a different flavor, ν_τ or ν_e.

References

[1] Conceptual Design Report: Main Injector Neutrino Program, 1991.

[2] Proceedings of the Workshop on Long-Baseline Neutrino Oscillation, Fermilab , 17-20 November 1991. Maury Goodman editor.

[3] FERMILAB PROPOSAL P–803, Muon Neutrino to Tau Neutrino Oscillations, Kodama *et al.*, October 1990 and revisions.

[4] FERMILAB PROPOSAL P–822, Proposal for a Long Baseline Neutrino Oscillation Experiment Using the Soudan 2 Neutrino Detector, W.W.M. Allison *et al.*, March 1991.

[5] K. S. Hirata *et al.*, *Phys. Lett.* **B280**, 146 (1992); D. Casper *et al.*, *Phys. Rev. Lett.* **66**, 2561 (1991); Ch. Berger *et al.*, *Phys. Lett.* **B227**, 489 (1989); M. Aglietta *et al.*, *Europhys. Lett.* **8**, 611 (1989); M. Goodman, Proceedings of the DPF conference, Fermilab 1992; H. Meyer, private communication.

[6] T. Haines *et al.*, Phys. Rev. D. **57** 1986 (1986).

[7] T. Kajita, in Proceedings of the Baton Rouge Workshop on Atmospheric Neutrinos, 6-8 may 1993, B. Svoboda, editor.

[8] S. Dye, in Proceedings of the Baton Rouge Workshop on Atmospheric Neutrinos, 6-8 may 1993, B. Svoboda, editor.

[9] Ed Frank, Ph.D. thesis, "A study of Atmospheric neutrino interactions in the Kamiokande-II Detector", University of Pennsylvania, 1992.

[10] H. Meyer, in Proceedings of the Baton Rouge Workshop on Atmospheric Neutrinos, 6-8 may 1993, B. Svoboda, editor.

[11] M. Goodman, in Proceedings of the Calgary Workshop on Atmospheric Neutrinos, 20 July 1993, M. Goodman editor.

[12] R. Svoboda *et al.*, LSU-HEPA-3-92.

[13] Frati *et al.*,UPR-218E, Dec 1992.

[14] Don Perkins, OUNP-93-03 (unpublished).

[15] Adeva *et al.*, Phys. Lett. **B237** (1990).

[16] J. N. Bahcall and H. A. Bethe, Phys. Rev. Lett. **65**, (1990) 2233; S. P, Mikheyev and A. Yu. Smirnov, Sov. Phys. Usp., **30** (1987) 759; L. Wolfenstein, Phys. Rev. **D 17** (1978) 2369; T. K. Kuo and J. Pantaleone, Rev. Mod. Phys. **61** (1989) 937-979; S. J. Parke, Resonant Neutrino Oscillations, Fermilab-Conf-86/131-T (1986).

[17] S. Pakvasa, private communication; Akhmedov *et al.* Phys. Lett. **69** 3013 (1992).

[18] Dimopoulous, Hall and Raby Phys. Rev. D47 R3697 (1993). ; K. S. Babu and R. N. Mohapatra, *Phys. Rev Let.* 70 2845 (1993).

[19] M. Gell-Mann, P. Raymond, and R. Slansky, 1979 in *Supergravity*, edited by P. Van Nieuwenhuizen and D. Z. Freedman (North-Holland, Amsterdam), p. 315; T. Yanagida, 1979, Proceedings of the Workshop on Unified Theory and Baryon Number of the Universe, Tsukuba, Ibaraki, Japan, unpublished.

[20] Carlo Rubbia, "The Renaissance of Experimental Neutrino Physics", CERN-PPE/93-08, presented at the Conversaciones de Madrid El Escorial, Madrid Spain.

[21] G. Smoot *et al.*, *Astrophys. J* **396**, 11(1992); E. Wright *et al.*, *Astrophys. J* **396**, L13 (1992).

[22] Learned, S. Pakvasa, and T. J. Weiler, Physics Letters **B207** (1988) 79

[23] Reported in the New York Times on September 21, 1993 by J. Wilford, on work done by Alcock *et al.*, from Lawrence Livermore Laboratory, and Spiro *et al.*, from the National Center for Scientific Research at Saclay.

[24] "See-Saw Enhancement of Lepton Mixing", by Alexei Yu. Smirnov, April 1993, submitted to *Phys. Rev. D.*

[25] S. Dimopoulos, L. Hall and Stuart Raby, *Phys. Rev.* **D47** (1993) R3697.

[26] Gravitationally Induced Neutrino Oscillations, GINO, J. Pantaleone, A. Halprin and C. Leung, UDHEP-10-92; also Butler, Nozawa, Malaney and Boothroyd, to be published in Phys. Rev. D.

[27] D. Caldwell and R. Mohapatra, SLAC-PUB-93-03, submitted to *Phys. Rev. Lett.*, April 1993.

[28] L. Wolfenstein, as reported at the Workshop on the many worlds of Neutrino Physics, Fermilab, October 1991.

[29] Proposal for the E–815 experiment, Fermilab, 1991.

[30] U. Amaldi *et al.*, Phys. Rev. **36D** (1987) 1385.

[31] D. Bogert *et al.*, Phys. Rev. Lett. **55**, (1985) 1969.

[32] Shi, Schramm and Fields, Fermilab pub-93/154A, (1993).

[33] C. Llewellyn-Smith, Physics Reports 3, no. 5 (1972) 261-379.

[34] Rein and Seghal, Annals of Physics (NY) 133 (1981) 79.

[35] Albright and Jarlskog, Nuclear Physics B 84 (1975) 467-492.

[36] Botts et. al., Physics Letters B 304 (1993) 159-166.

[37] Goodman and Snyder, Proceedings of the Workshop on Long Baseline Neutrino Oscillations, Fermilab, 1991.

[38] R. H. Bernstein and S. J. Parke, Phys Rev. D44 1991, (2069).

[39] J.L. Thron, Nucl. Instr. and Methods, A283 1989 (642).

[40] M. A. Thomson *et al.*, Phys. Lett. B, 269 1991 (220).

[41] Maury Goodman, Proceedings of the Fermilab DPF meeting, edited by Albright *et al.*, 1992 (1300).

[42] Proceedings of the First International Conference on Calorimetry in High Energy Physics, Ed. D.F. Anderson *et al.*, 1990, World Scientific (426).

[43] Peter Litchfield, Proceedings of the Workshop on Long baseline Neutrino Oscillations, October 1991.

[44] Albright, Shrock and Smith, *Phys. Rev.*, D20, p2177 (1979).

[45] Maury Goodman, Proceedings of the Workshop on Long BAseline Neutrino Oscillations, October 1991.

[46] W. P. Oliver *et al.*, *A rugged 1700 m^2 Proportional Tube Array*, Nucl. Instr. and Methods A276 (1989) 371.

[47] Steve Werkema, Ph. D. thesis, Monte Carlo Evaluation of the Atmospheric Neutrino Background to Nucleon Decay in the Soudan 2 Detector University of Minnesota 1989.

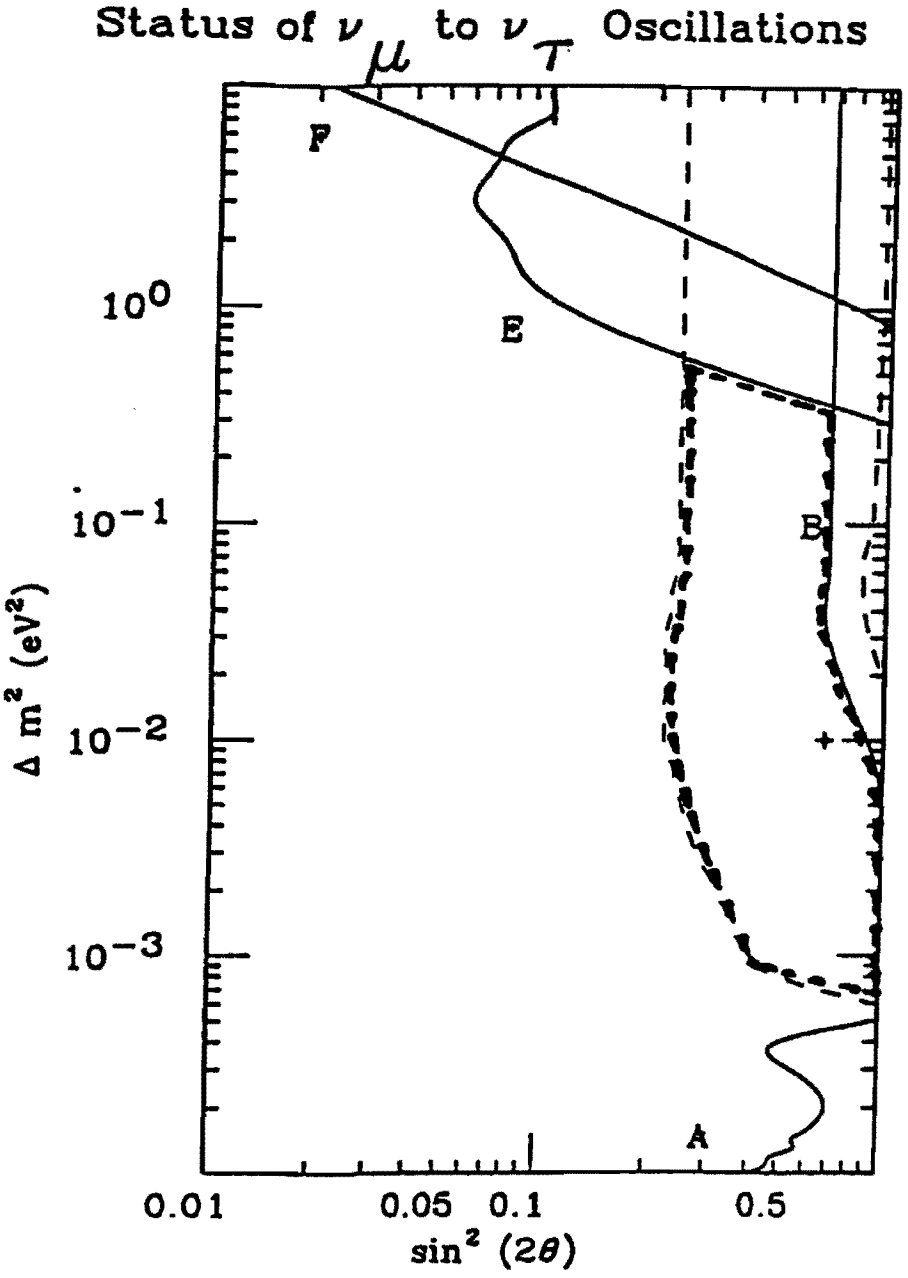

Figure 1: Atmospheric and Accelerator Limits for $\nu_\mu \rightarrow \nu_\tau$. The Allowed region from 2.7 kt-yr of Kamiokande is between the dashed lines. A and B are limits from IMB and Frejus data. E and F are accelerator limits from CDHS and Fermilab 531.

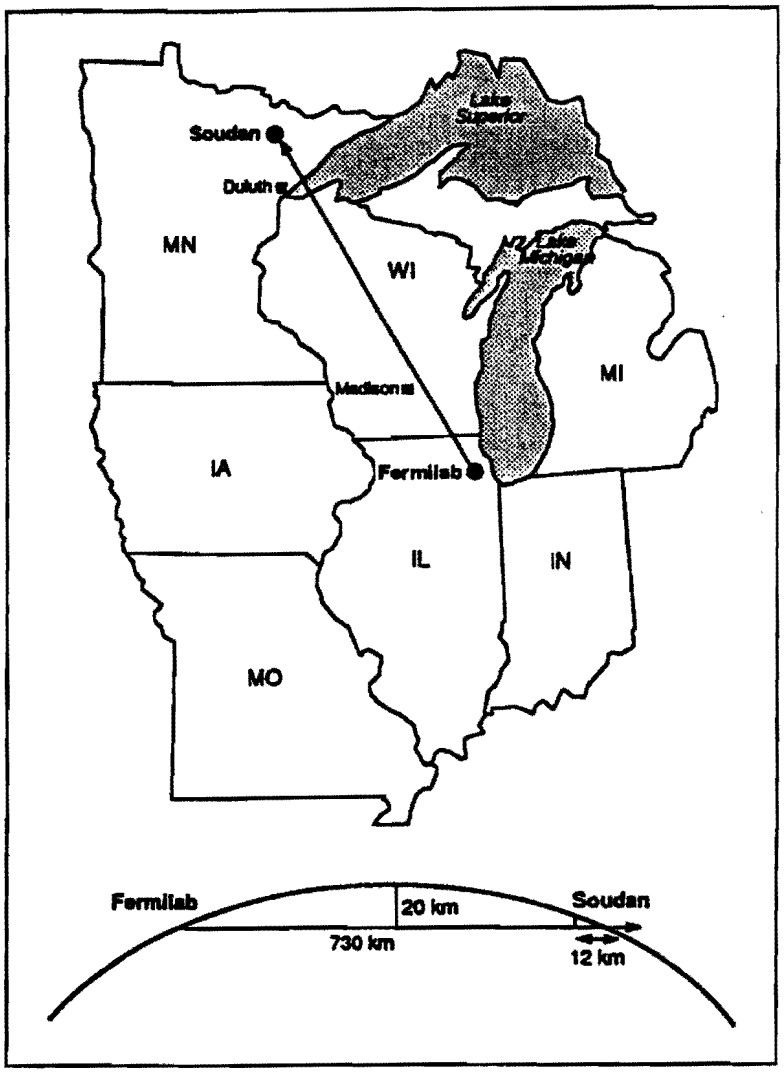

Figure 2: The neutrino beam from Fermilab to Soudan

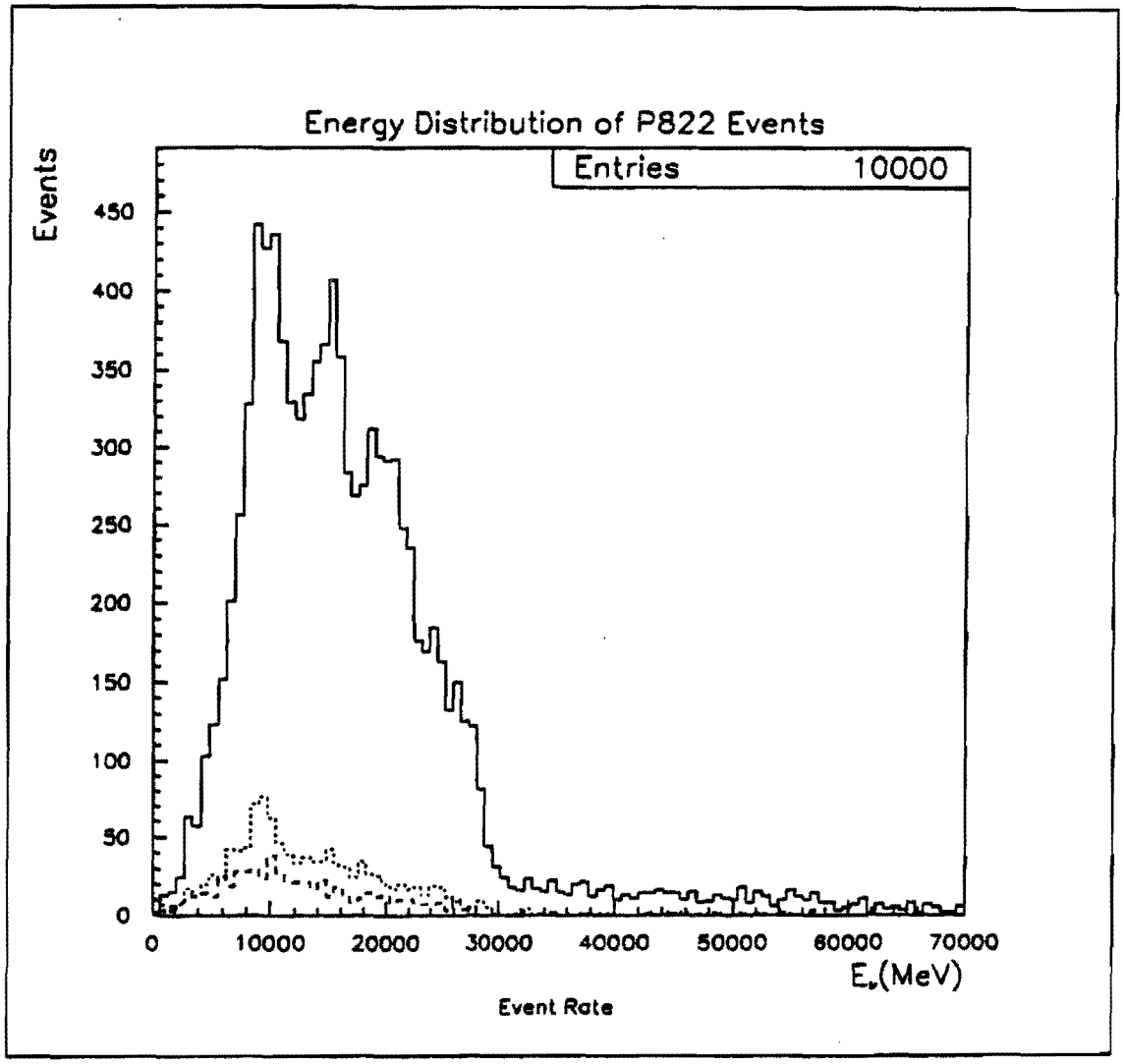

Figure 3: Event rate as a function of neutrino energy. The curves are for deep inelastic, quasi-elastic, and resonance (dashed) production

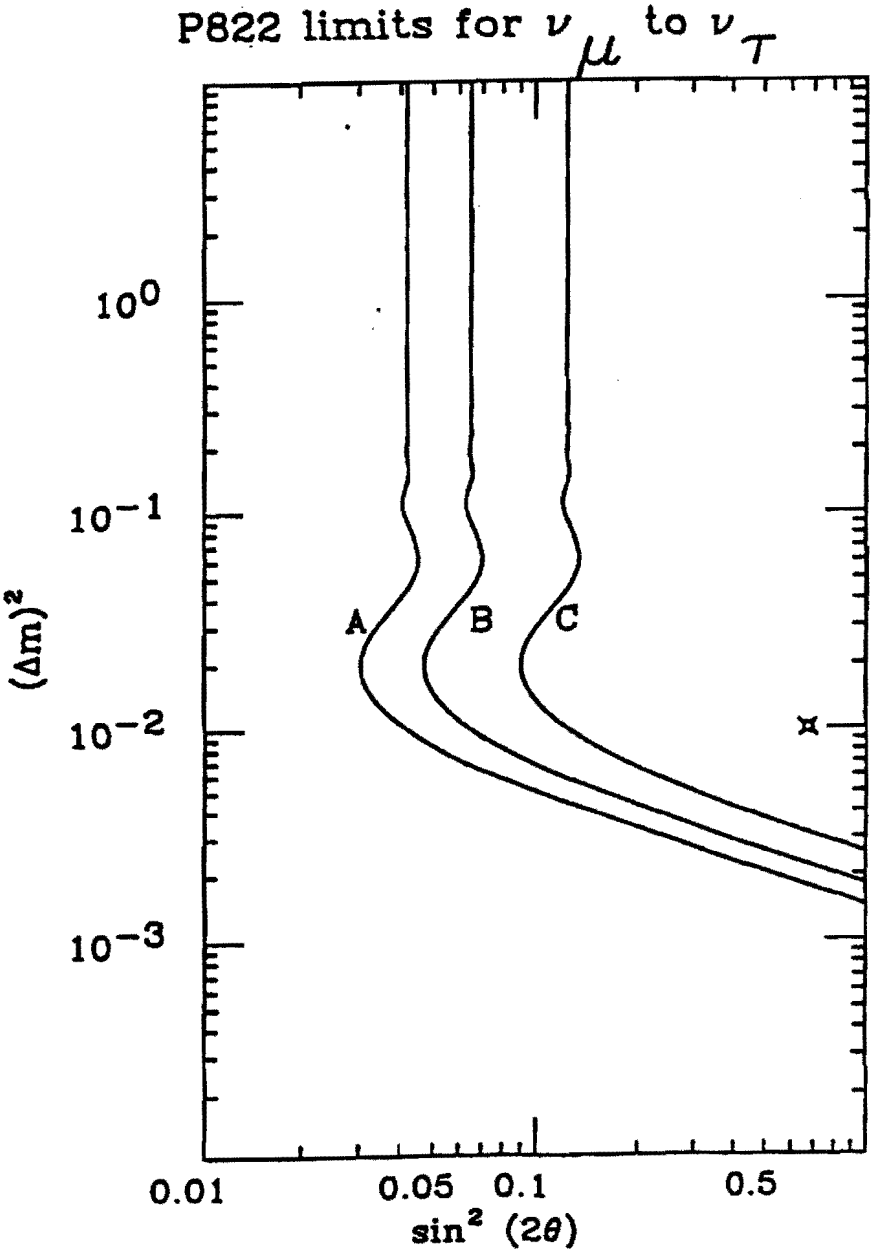

Figure 4: Limit curves for $\nu_\mu \rightarrow \nu_\tau$ using our base running assumption, A: $R_{near/far}$; B: $R_{"nc"/"cc"}$; C: $R_{\frac{e}{\mu}}$

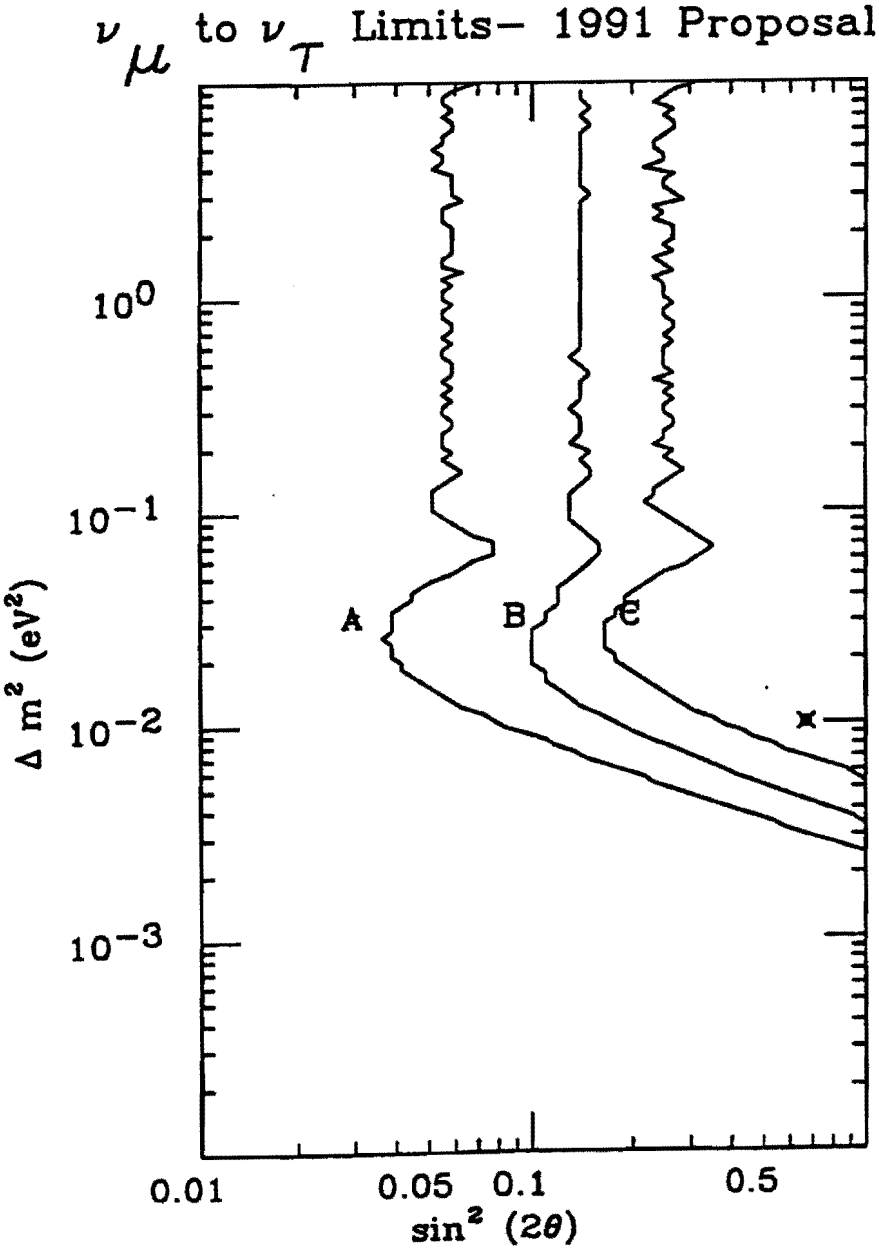

Figure 5: Limit curves for $\nu_\mu \rightarrow \nu_\tau$ from original proposal A: $R_{near/far}$; B: $R_{"nc"/"cc"}$; C: $R_{\frac{e}{\mu}}$

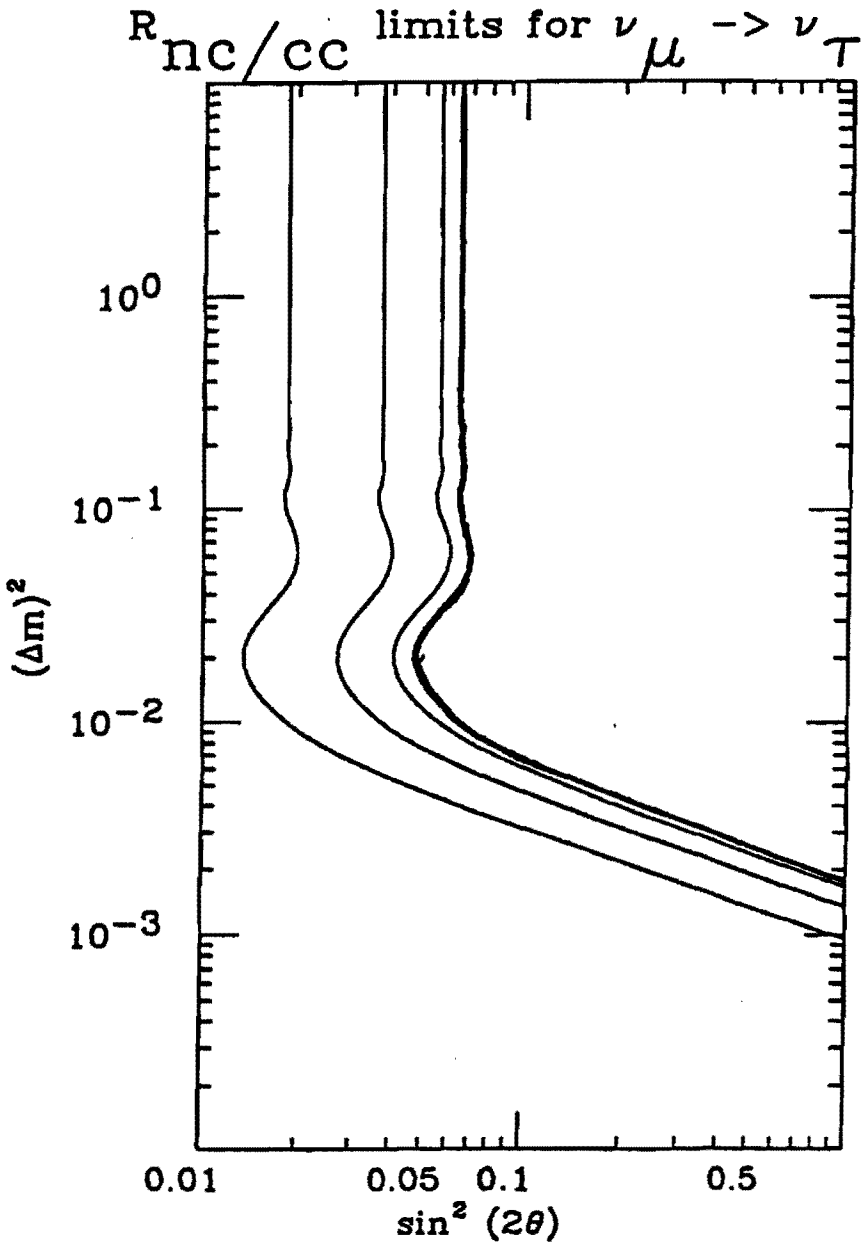

Figure 6: Effect of systematic error on the $R_{\text{"nc"}/\text{"cc"}}$ tests. From left to right the curves assume an 8 kiloton new detector and 0% systematic error, 8 kilotons and 2% systematic error, the existing detector with no systematic error, and the existing detector with 2% systematic error.

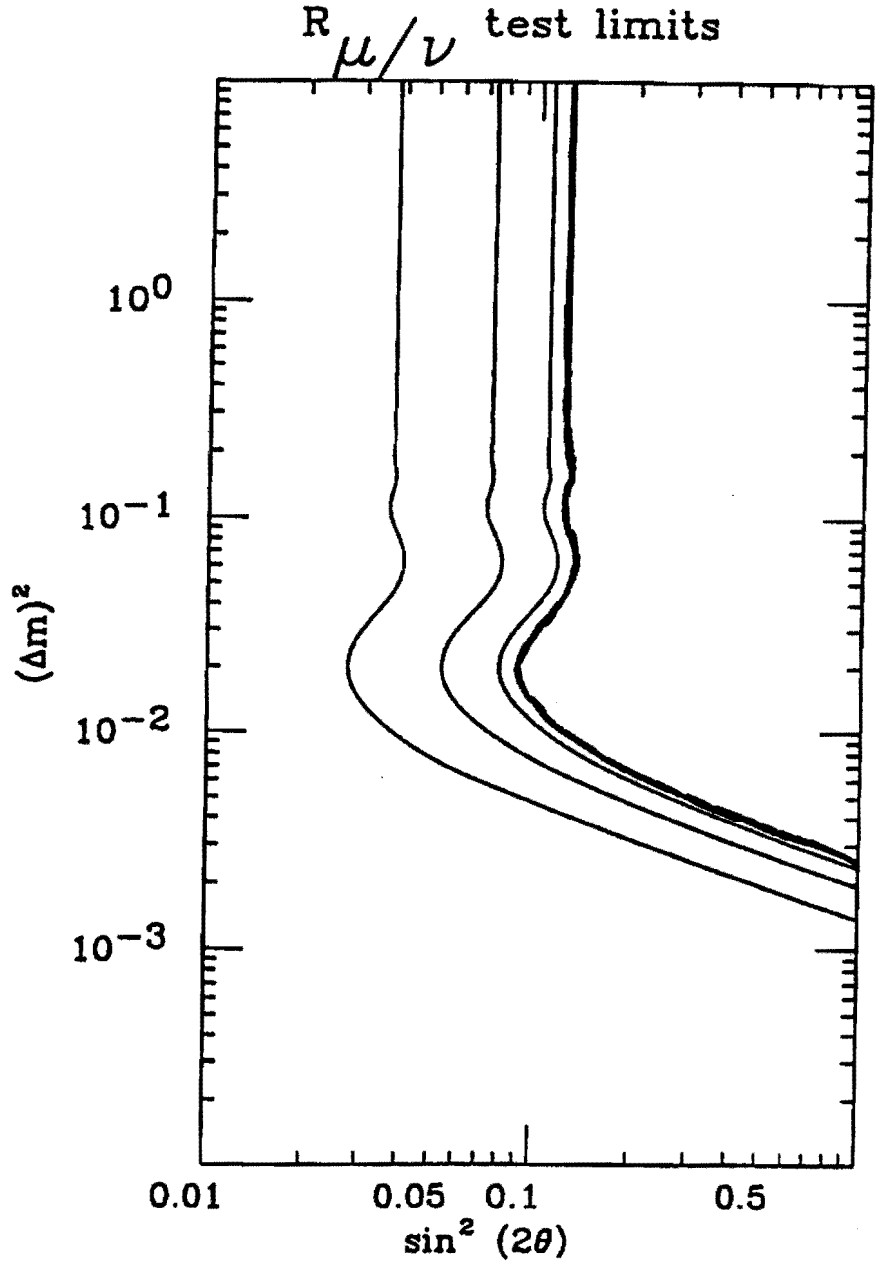

Figure 7: Potential 822 limits using $R_{\bar{\nu}}$. From left to right the curves assume an 8 kiloton new detector and 0% systematic error, 8 kilotons and 2% systematic error, the existing detector with no systematic error, and the existing detector with 2% systematic error.

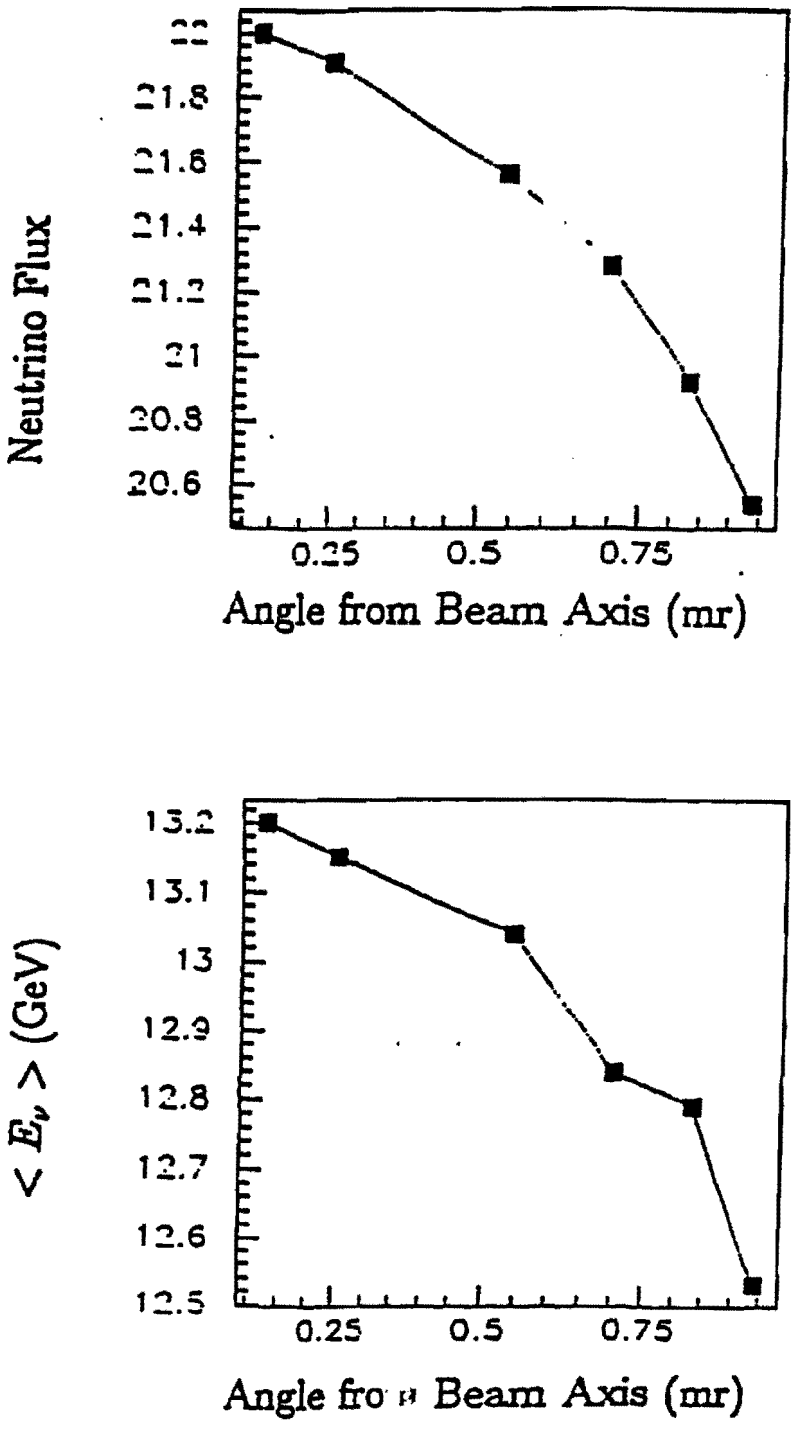

Figure 8: Energy and rate dependance of the neutrino beam versus angle

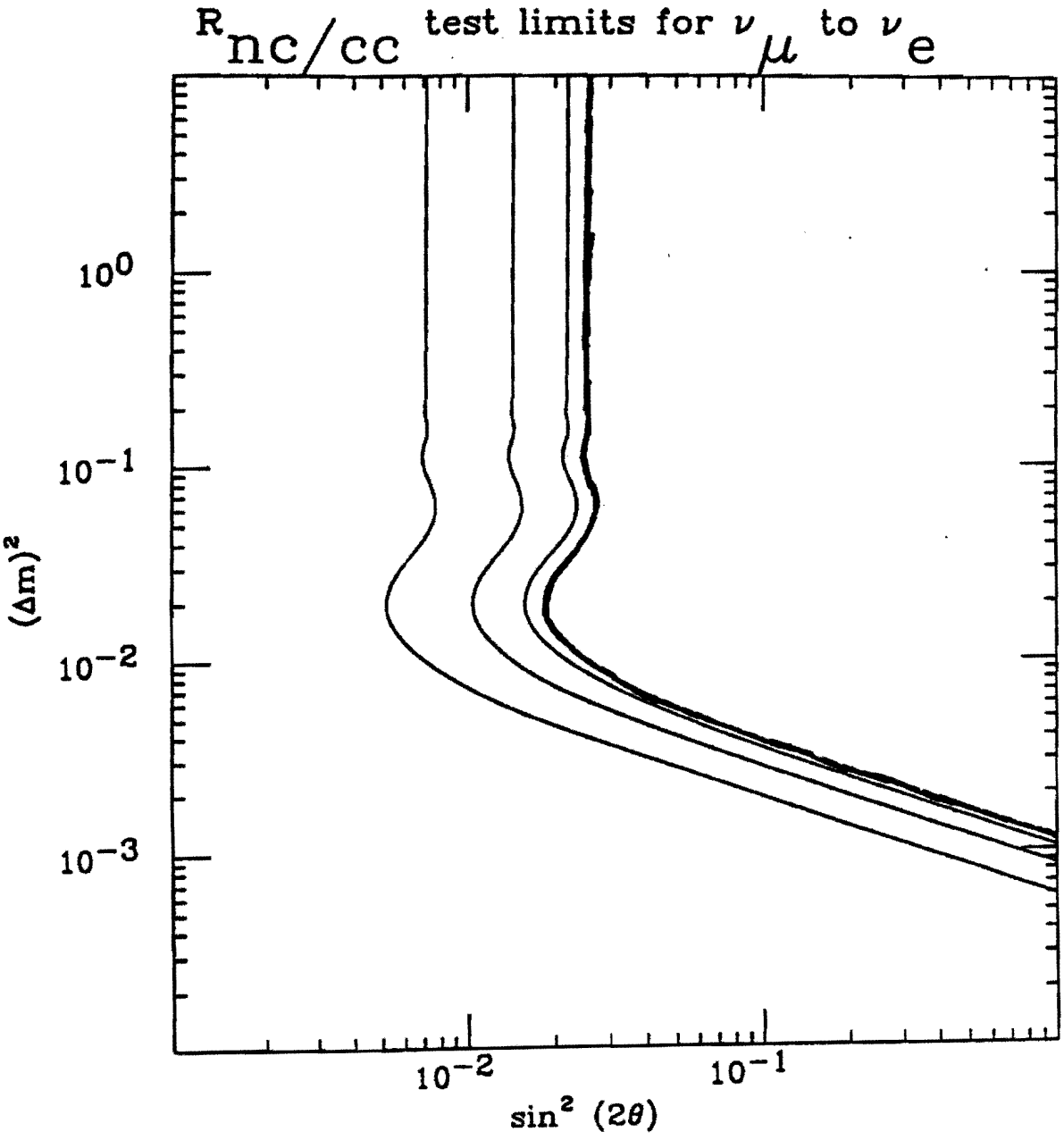

Figure 9: 822 limits for $\nu_\mu \rightarrow \nu_e$

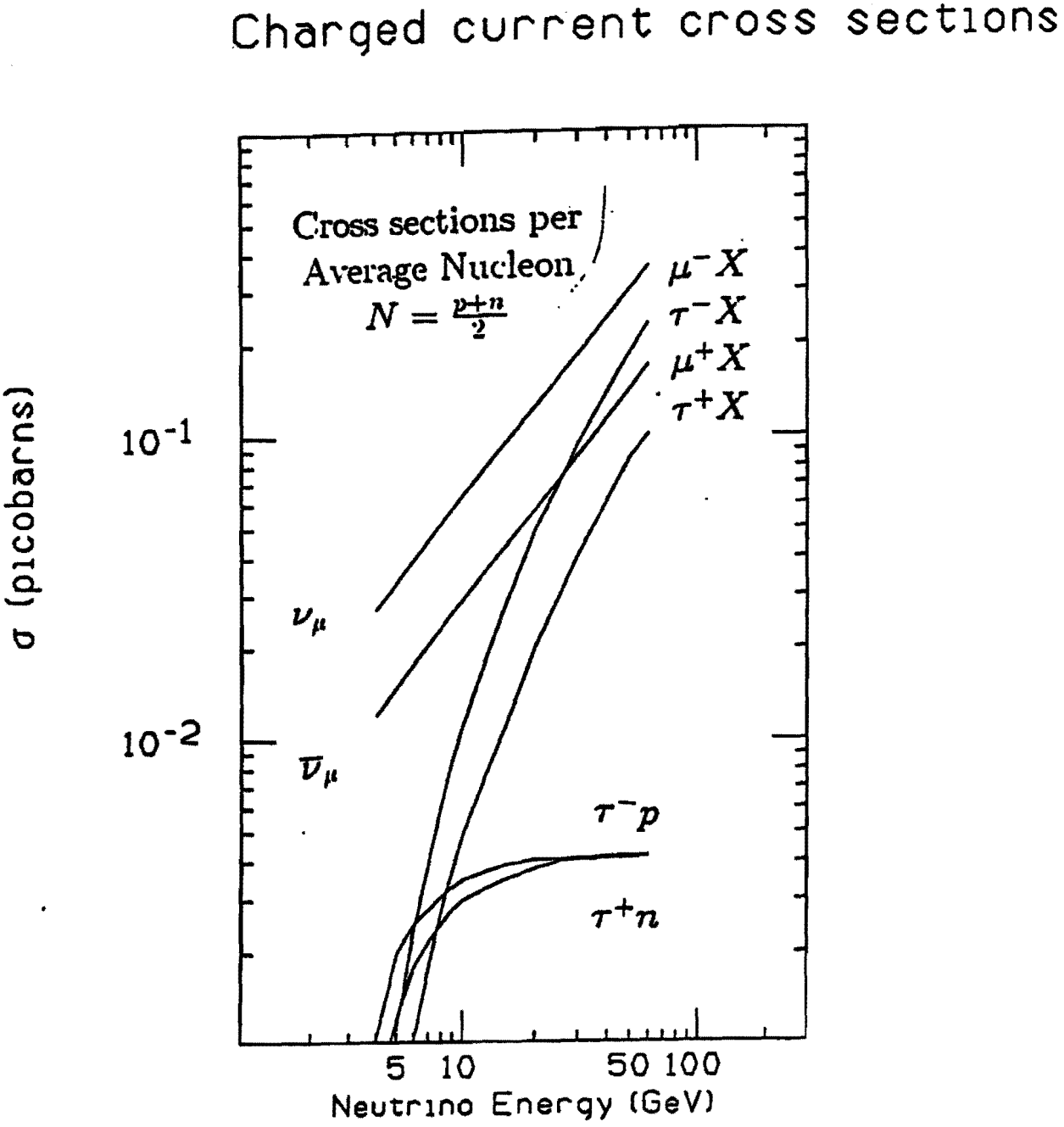

Figure 10: Calculated ν_τ cross sections

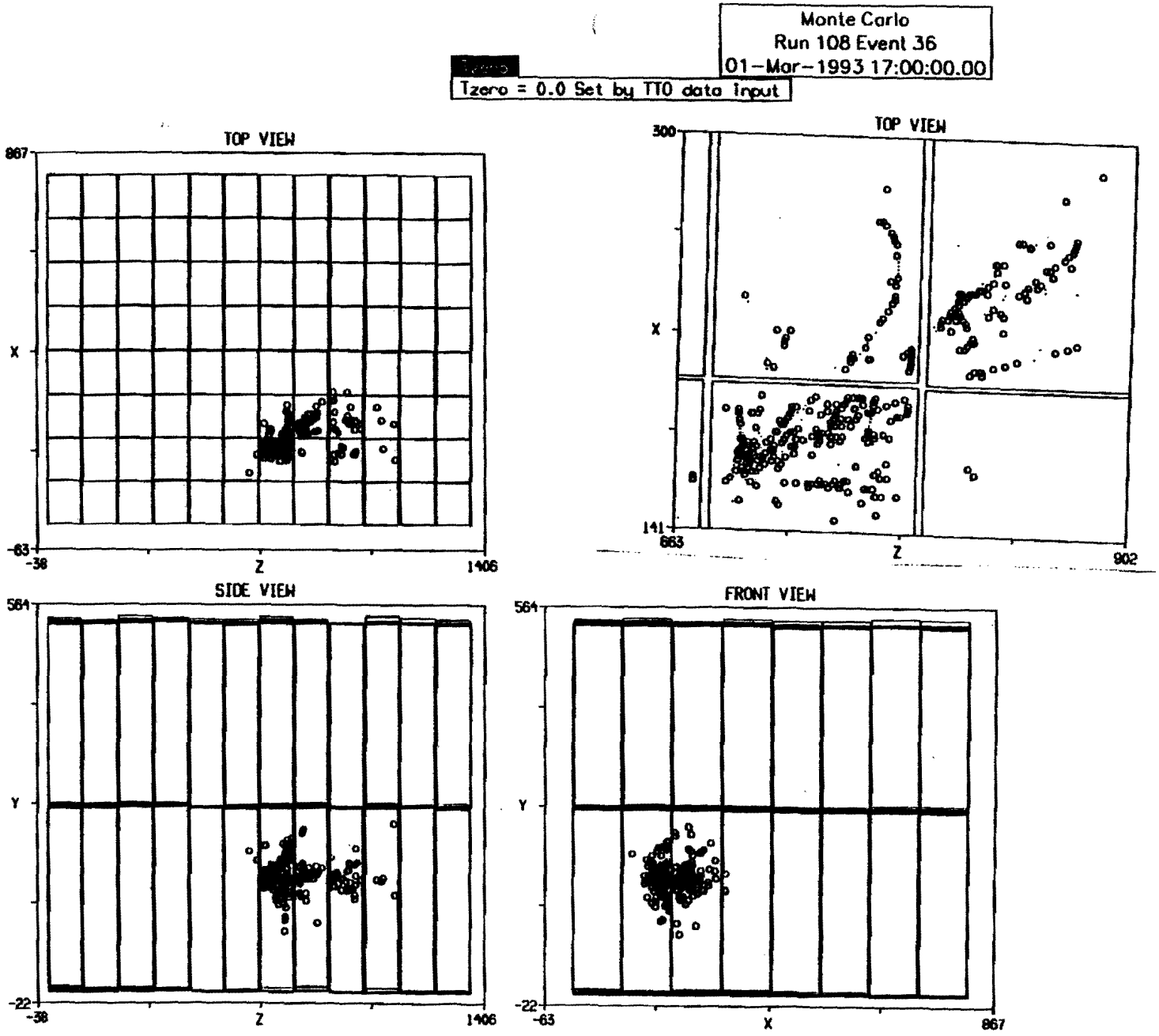

Figure 11: ν_μ neutral current event. In this event a 34 GeV ν_μ came in, and a 20 GeV neutrino and 14 Gev of hadrons were in the final state.

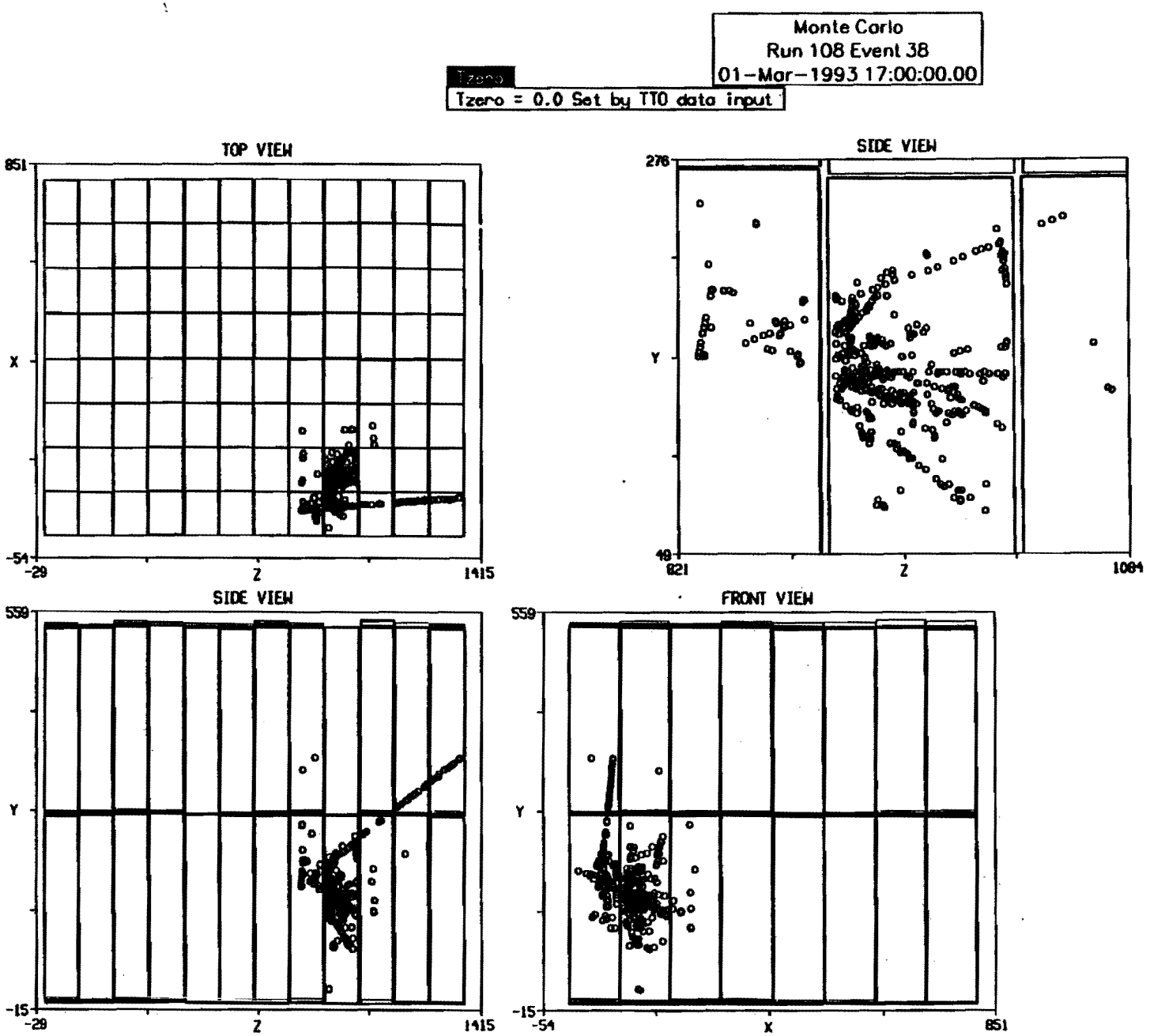

Figure 12: ν_μ charged current event. In this event a 19 GeV ν_μ made a 3.6 GeV μ^- and 15 GeV of hadrons.

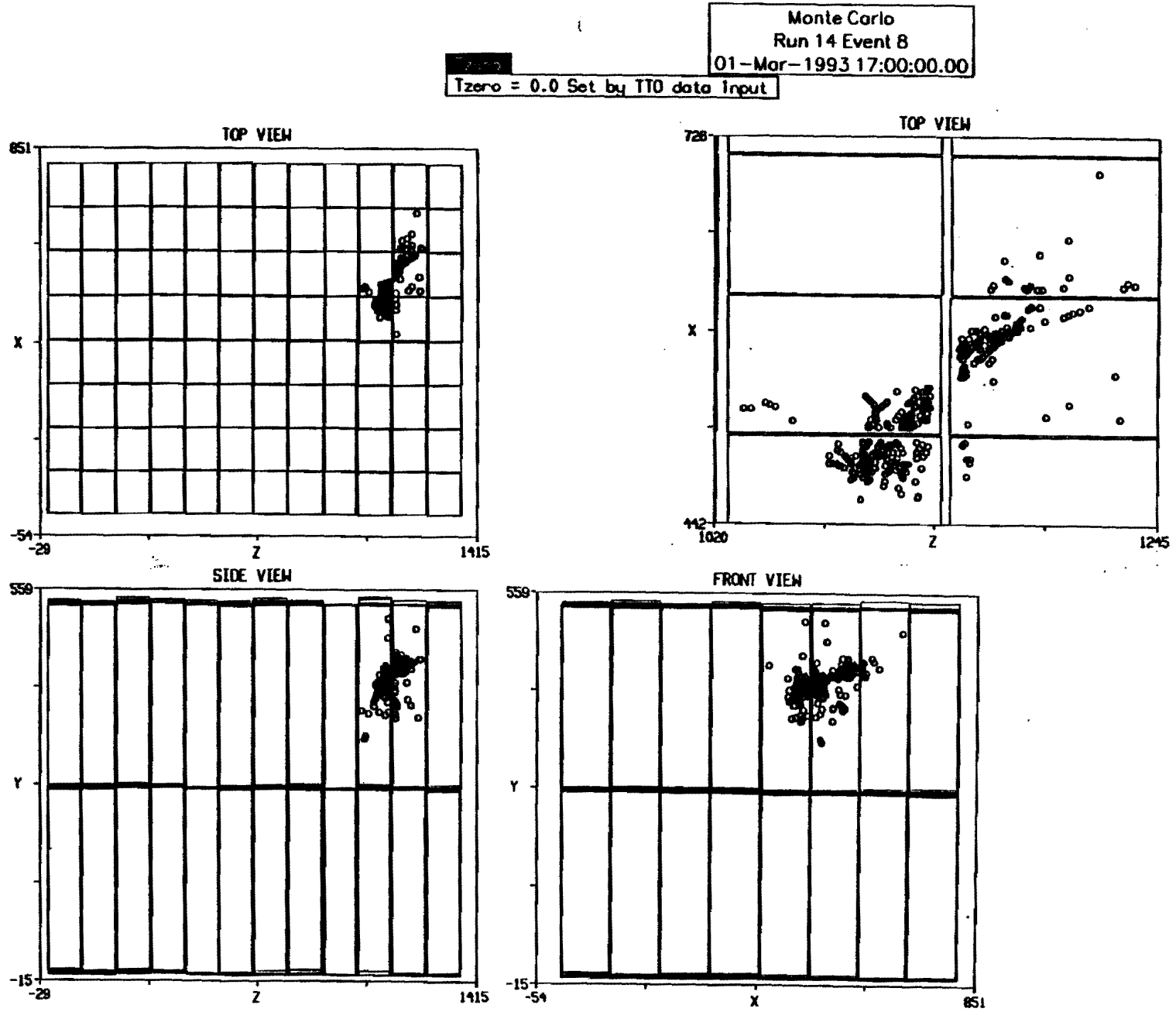

Figure 13: ν_τ charged current event in the Soudan 2 Monte Carlo. In this event a 16 GeV ν_τ made an 8 GeV τ^- and nine π's, $\tau \rightarrow \pi^-\pi^0\pi^0\nu_\tau$

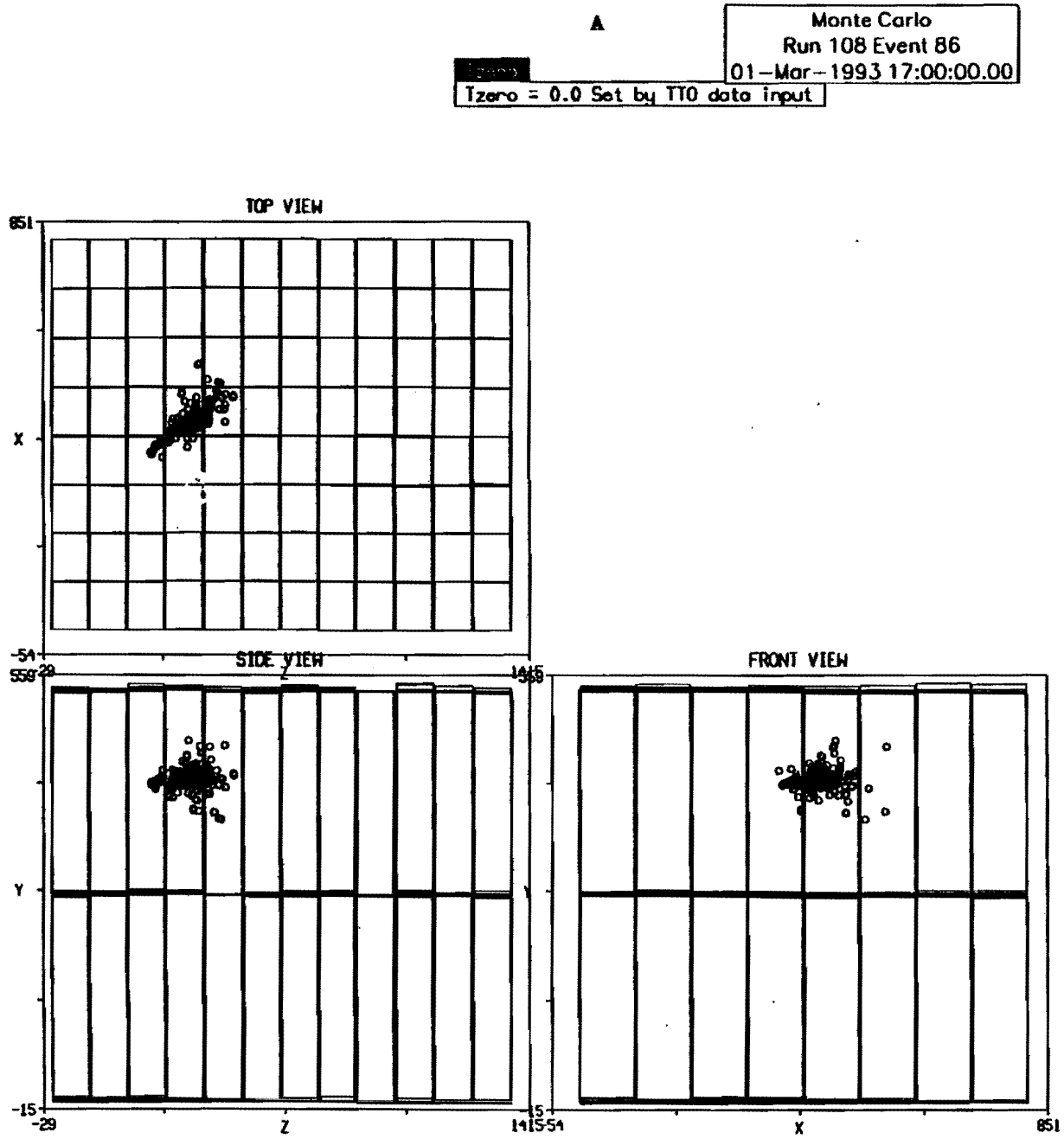

Figure 14: ν_e charged current event in the Soudan 2 Monte Carlo. This event was a 27 GeV $\nu_e p \rightarrow e^- \Delta^{1232++}$.

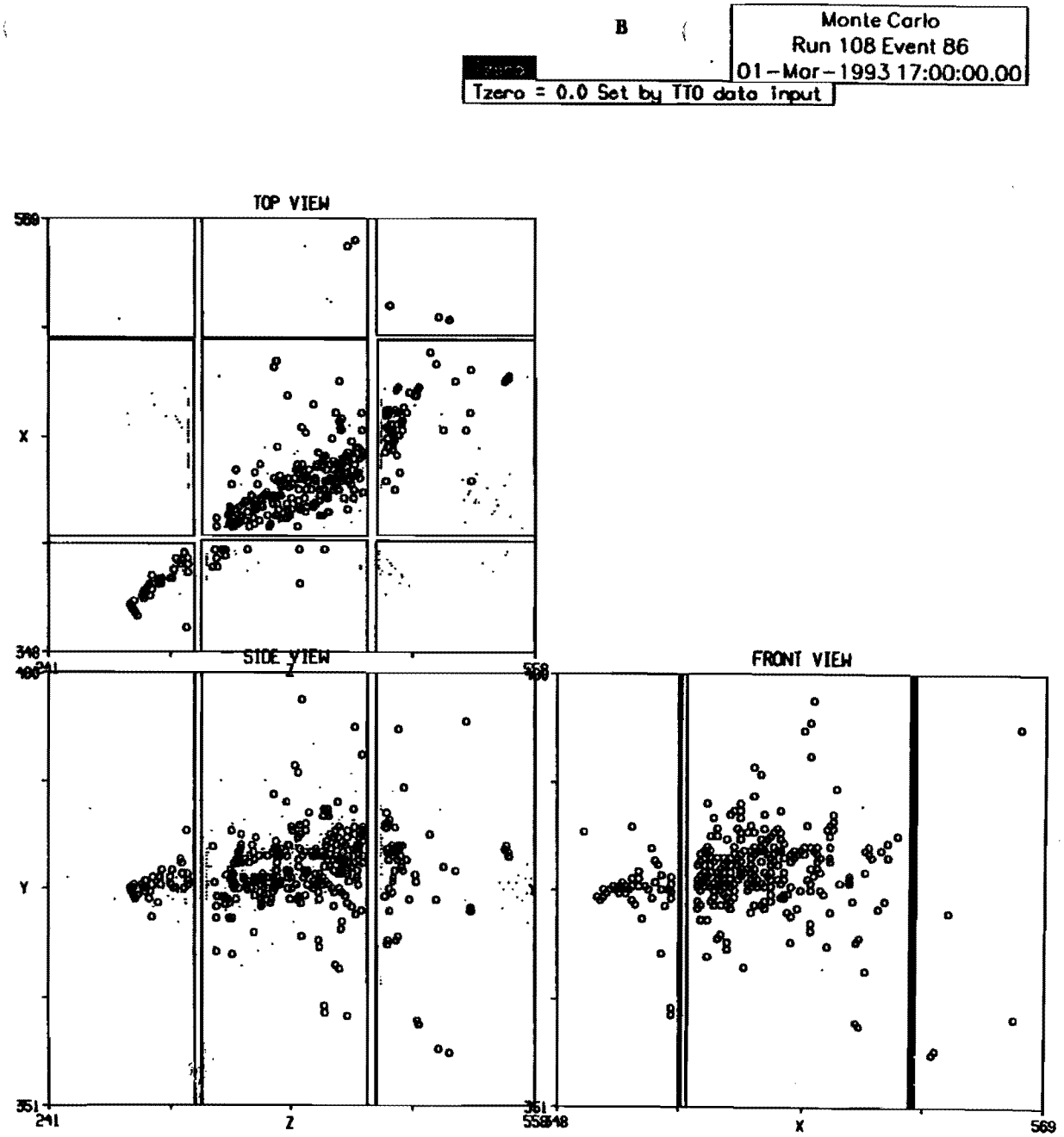

Figure 14: ν_e charged current event in the Soudan 2 Monte Carlo. This event was a 27 GeV $\nu_e p \rightarrow e^- \Delta^{1232++}$.

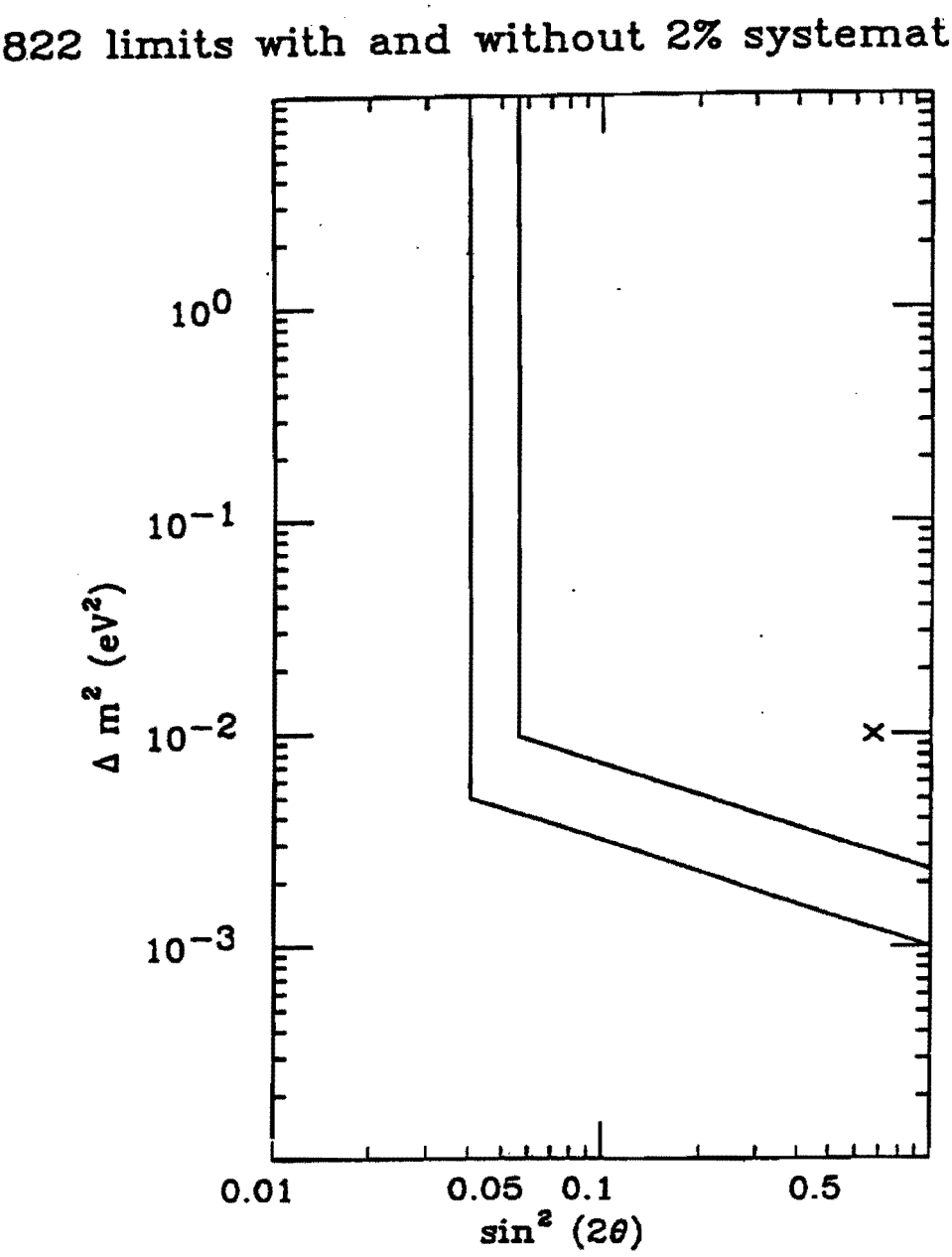

Figure 15: Approximate 822 limits using $R_{\text{"}\nu_e\text{"}/\text{"}\nu_e\text{"}}$

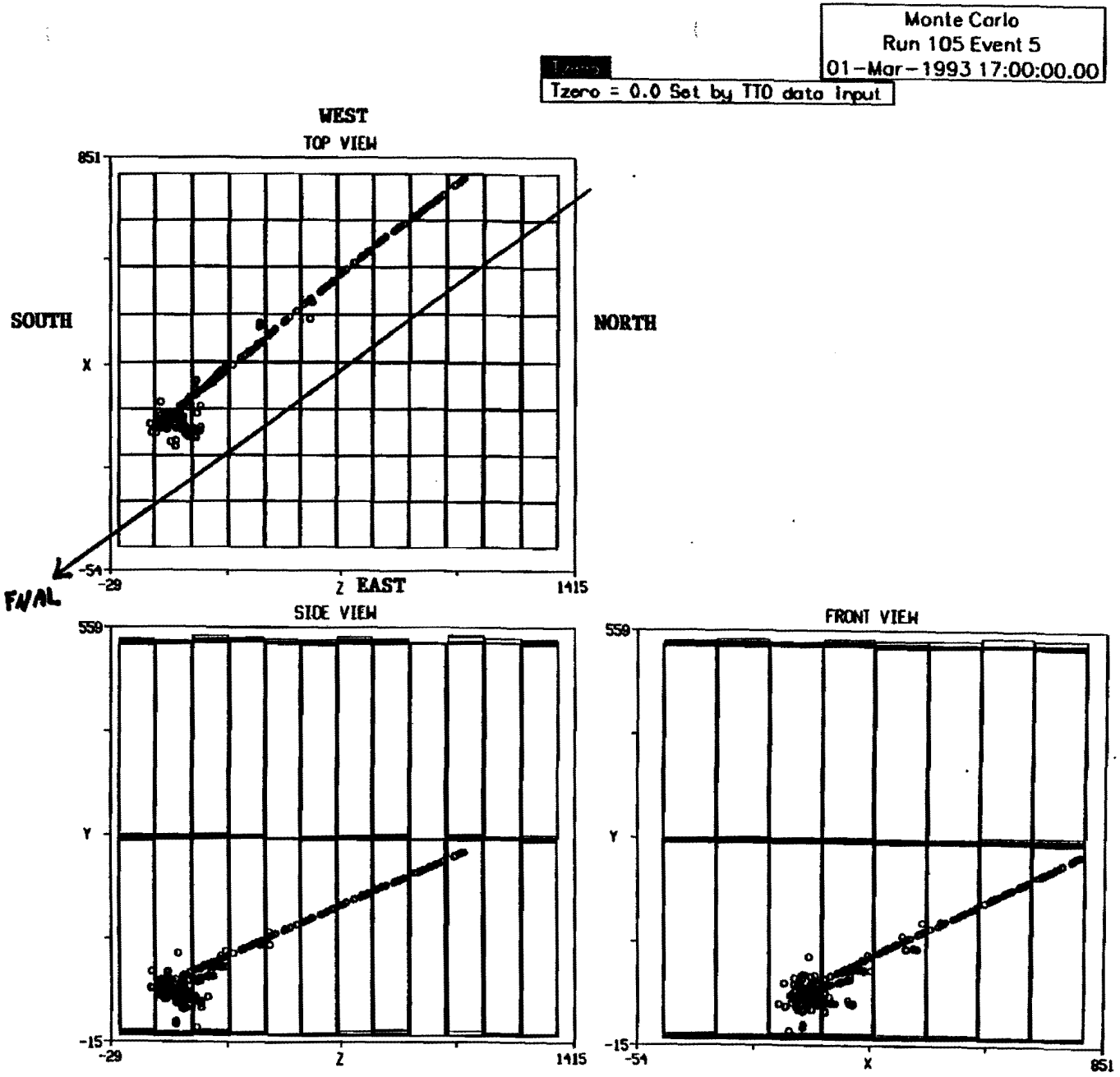

Figure 16: A charged current event showing the direction of Fermilab

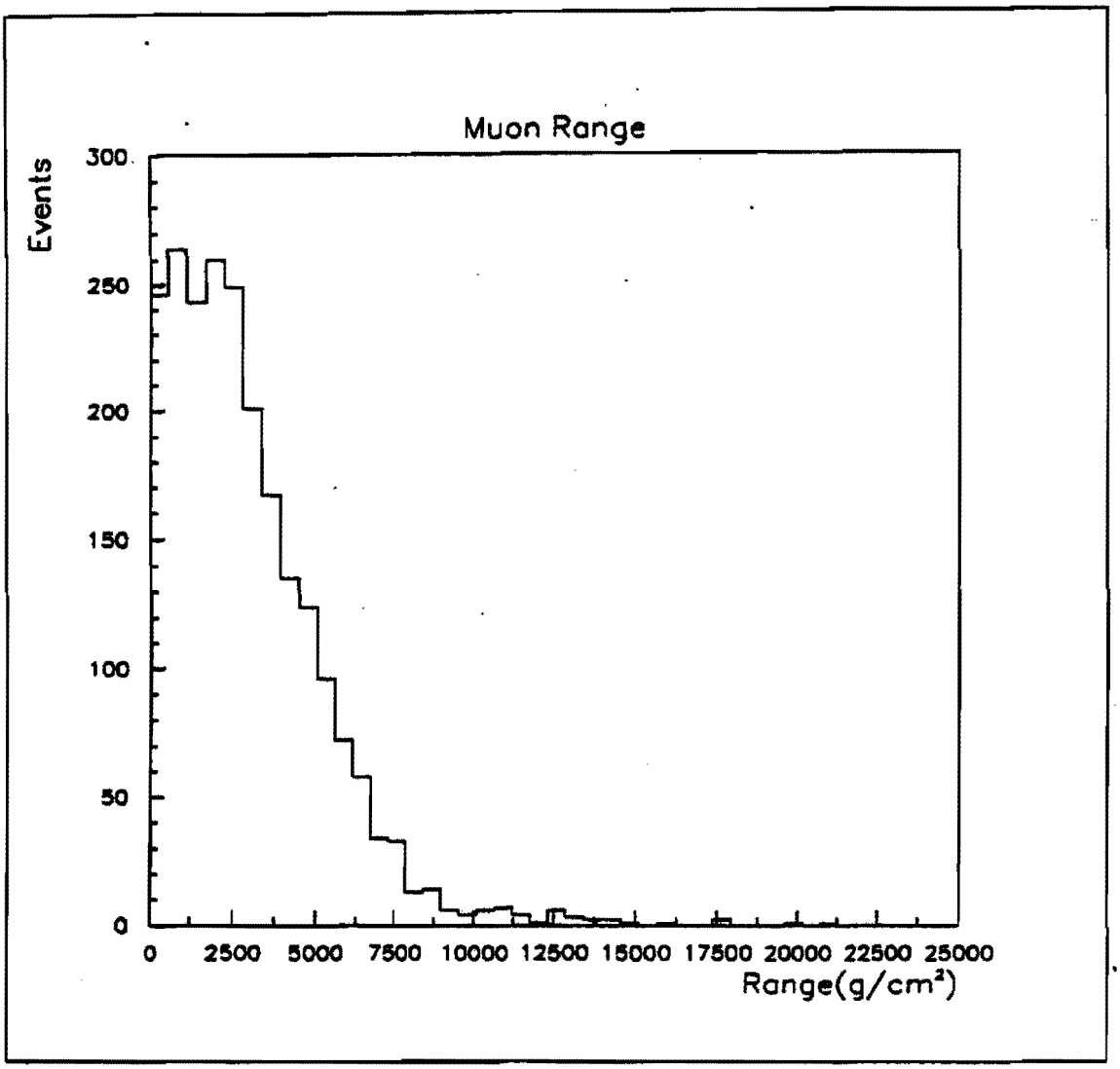

Figure 17: Muon momentum distribution of ν_μ charged current events expressed in muon range

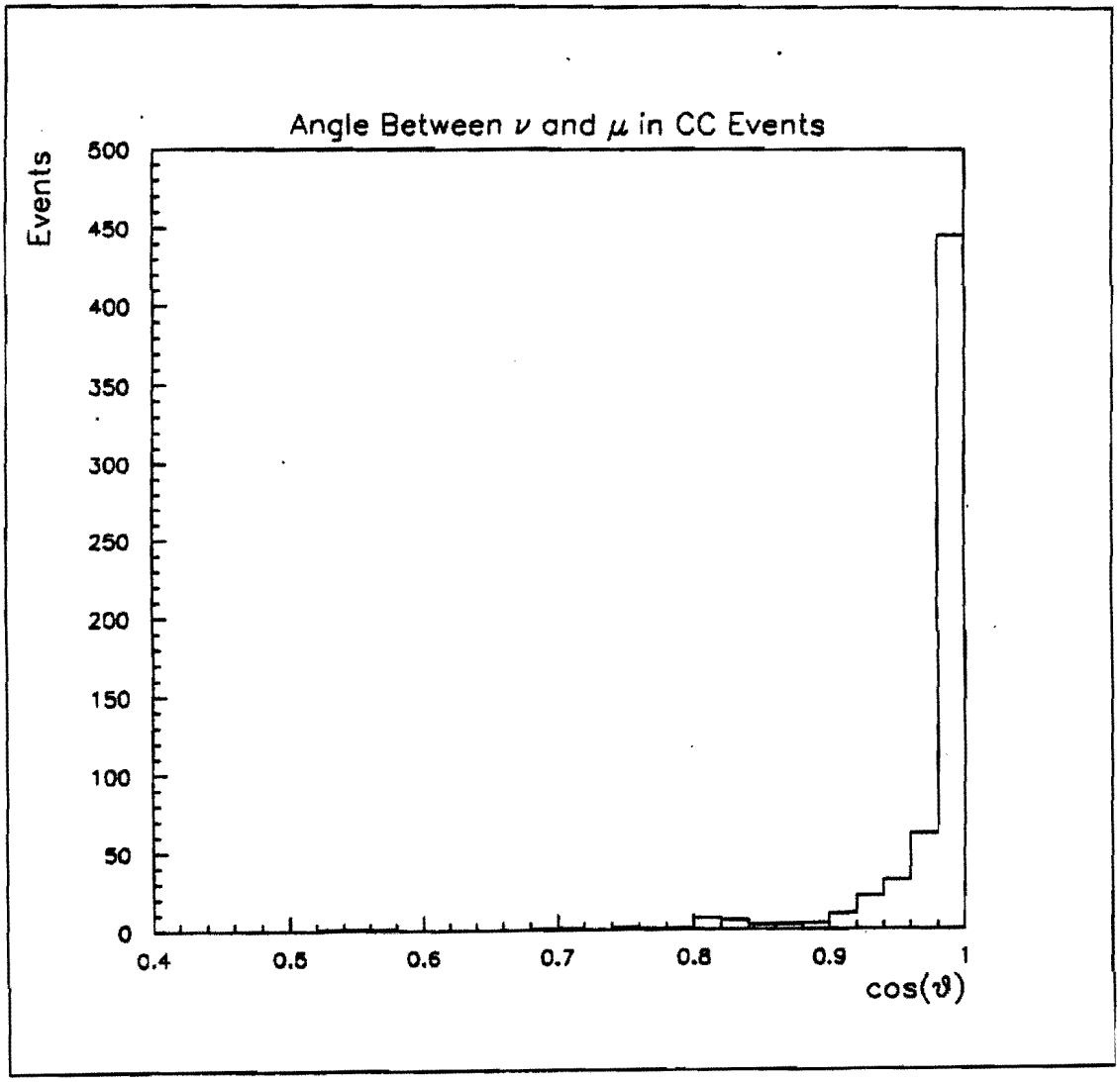

Figure 18: Angle of the muon track with respect to Fermilab, the neutrino direction, for charged current events

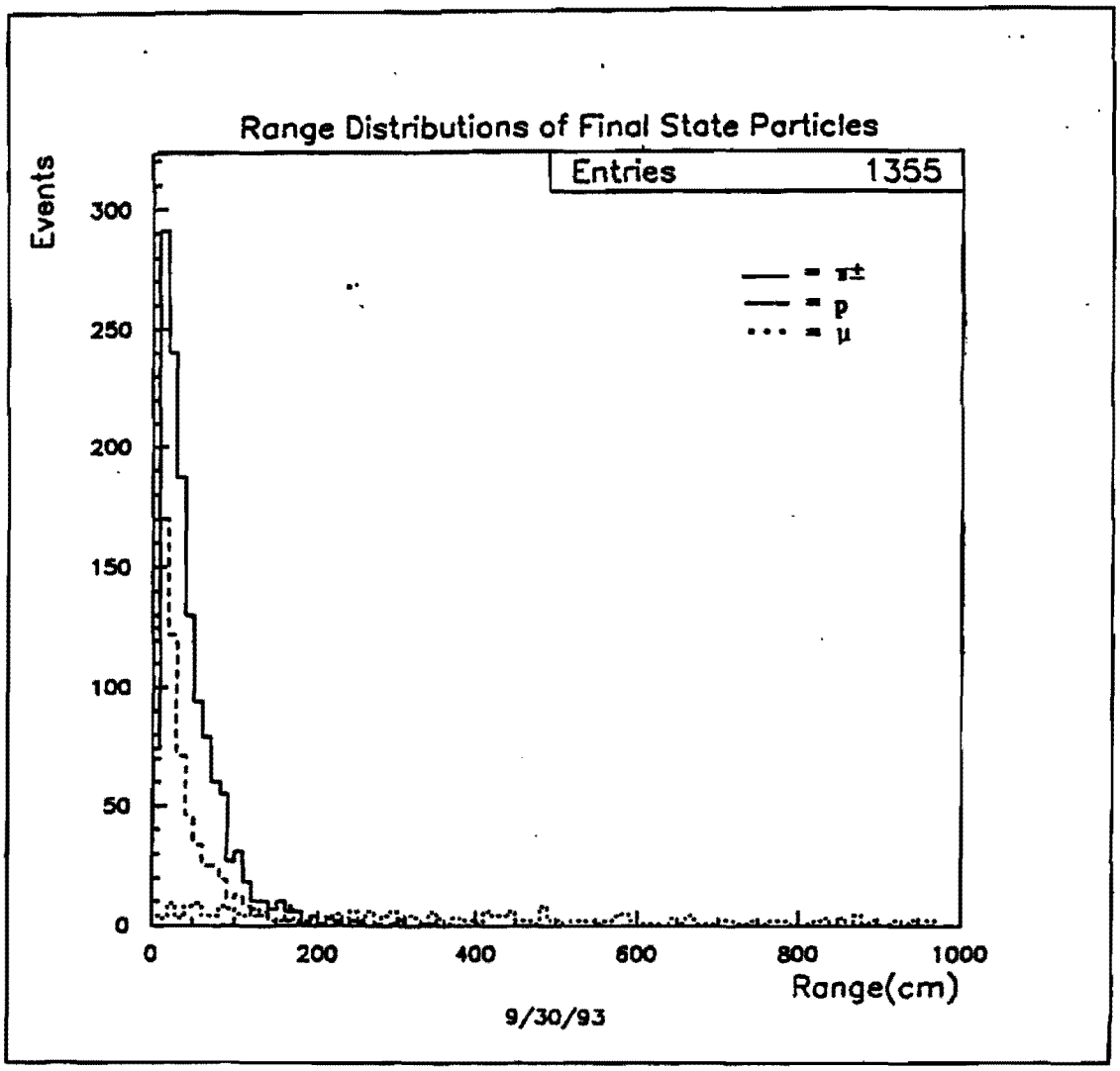

Figure 19: Length of the longest hadron in the detector for neutral current events

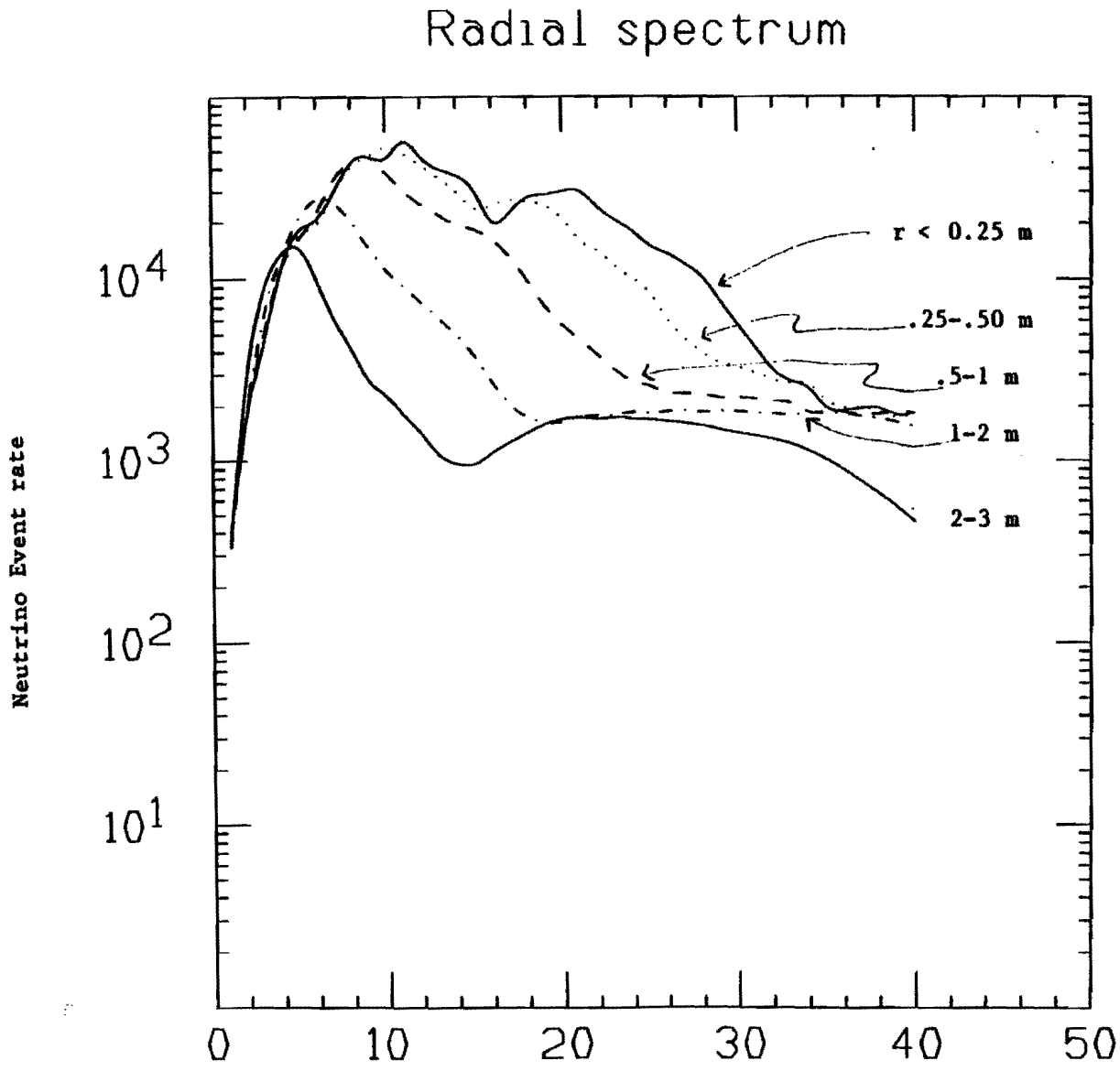

Figure 20: Radial dependence of the neutrino energy spectrum at the near detector location

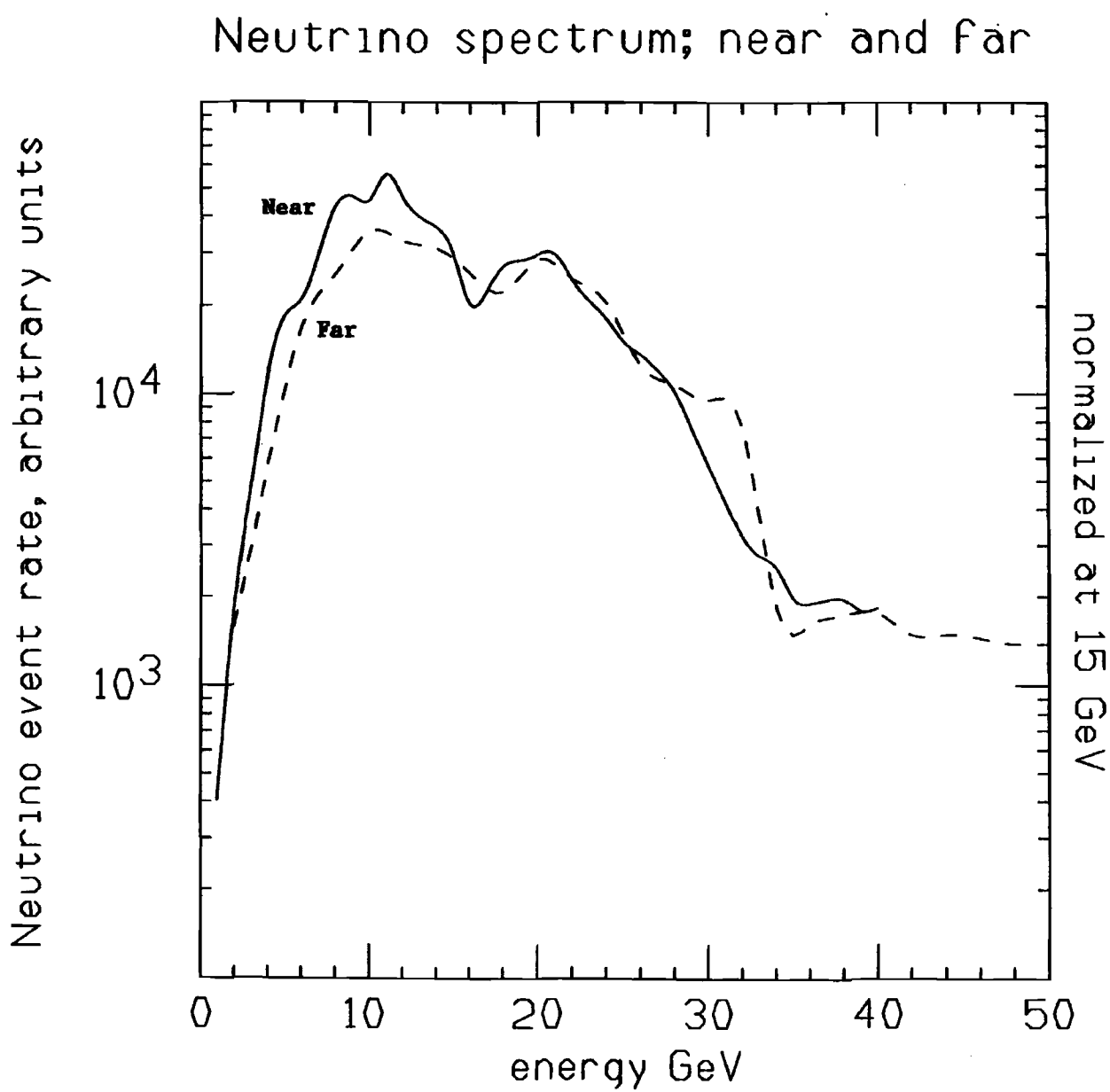

Figure 21: The neutrino event rate from the center 25 cm (radius) of the beam at the near detector and the far detector NUADA

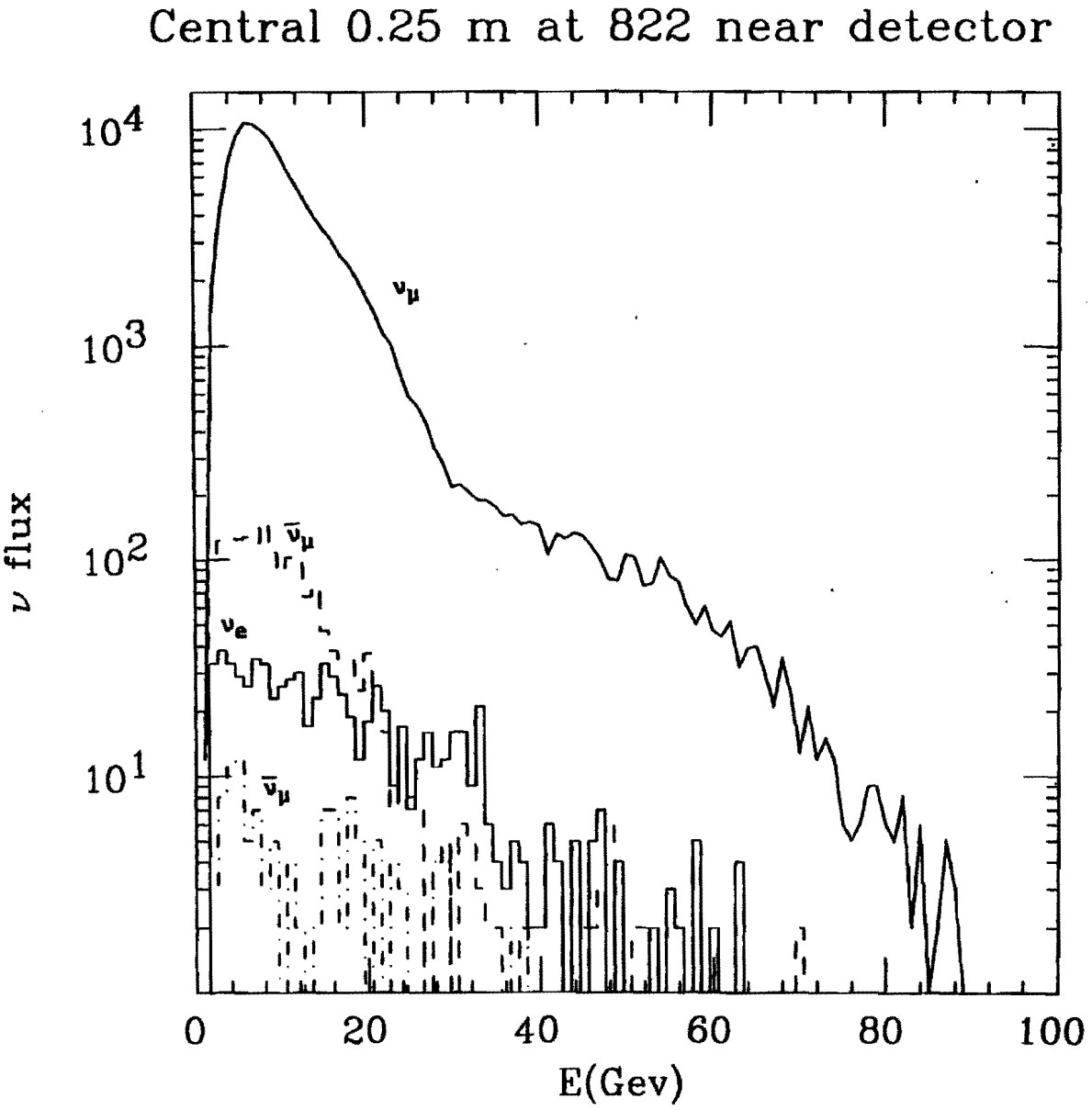

Figure 22: Near Neutrino event rate predicted by the 803 horn Monte Carlo for all four neutrino types

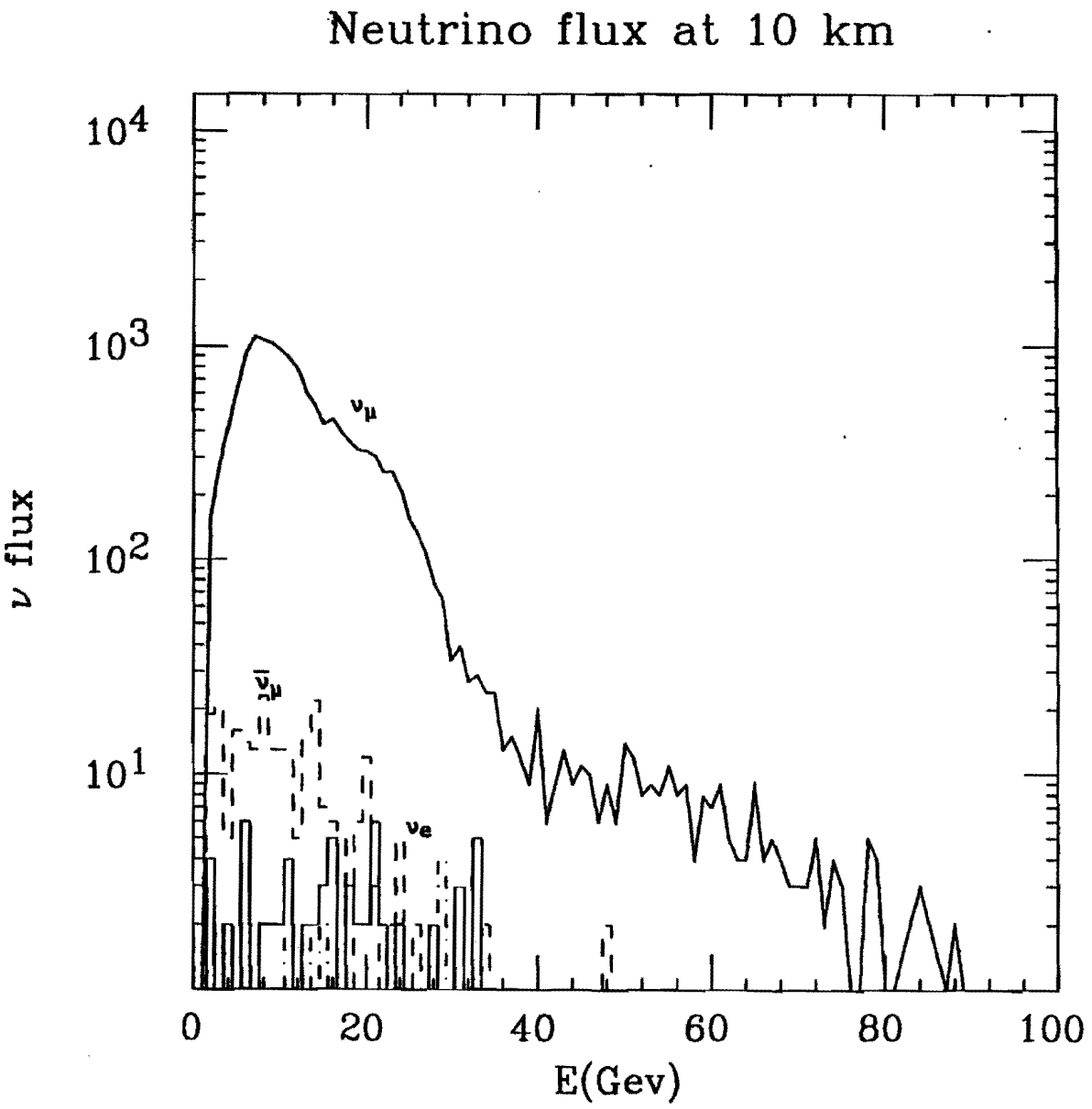

Figure 23: Far (10km) neutrino event rate predicted by an the 803 Monte Carlo

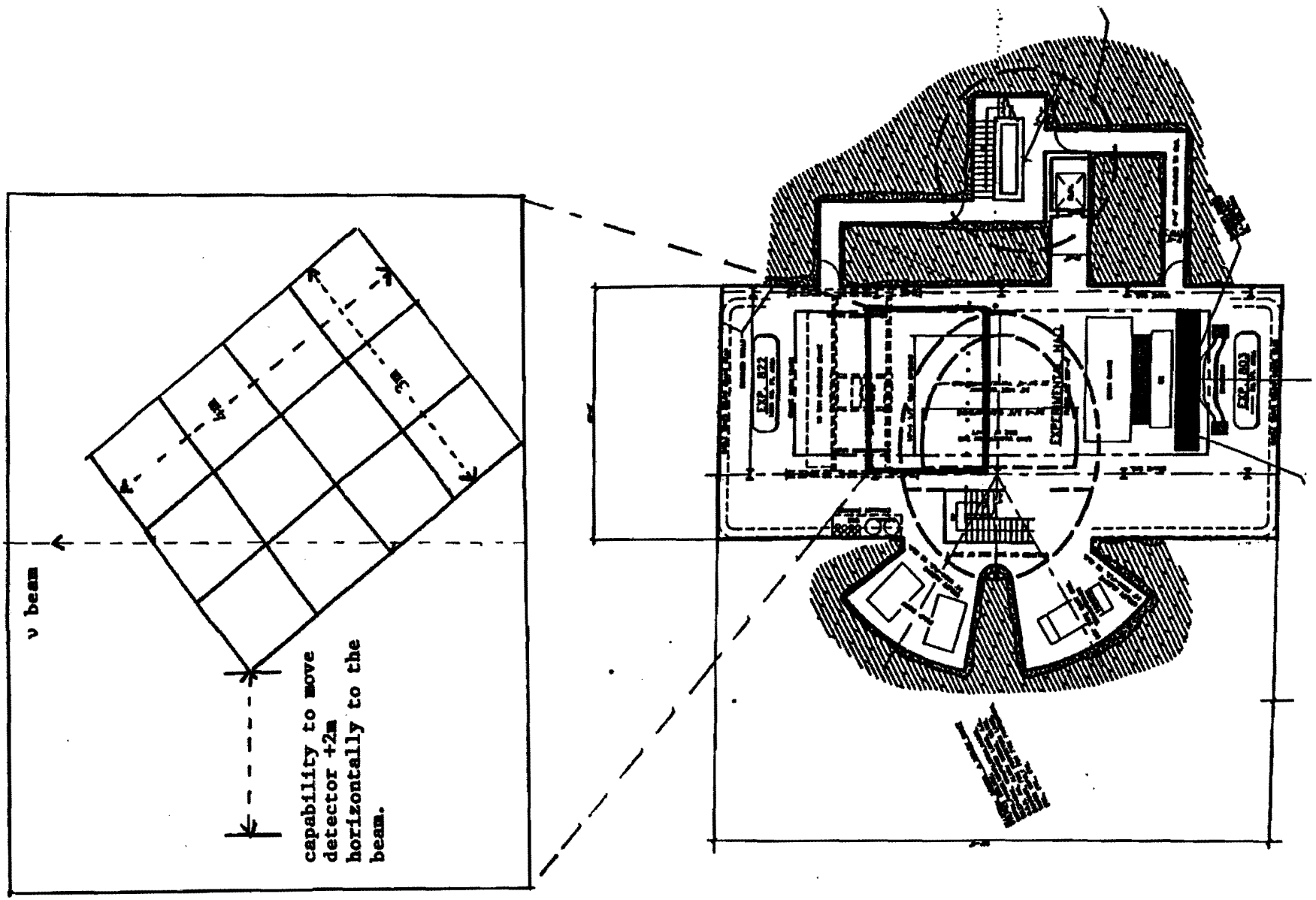

Figure 24: Sketch of the layout of the 822 near detector

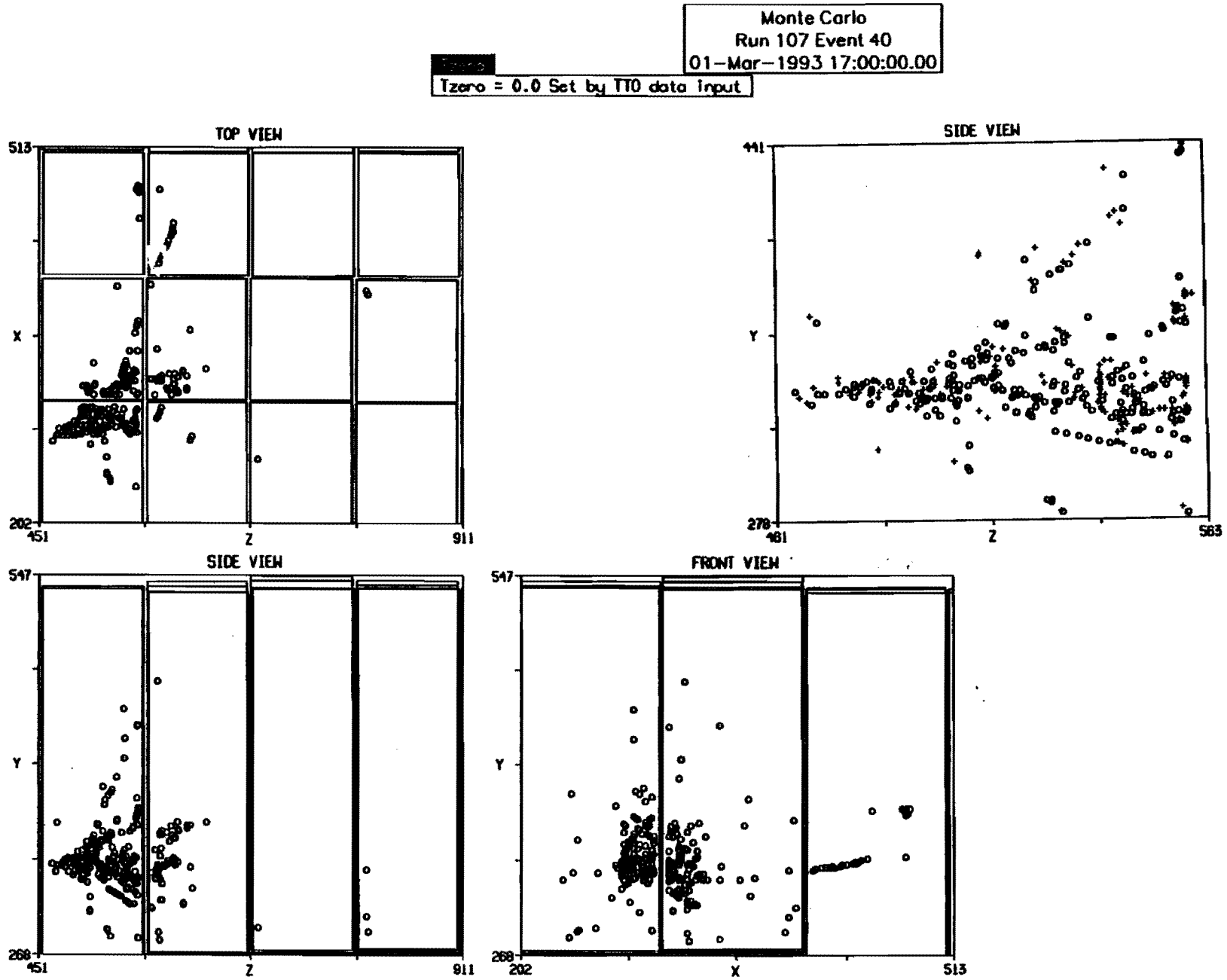

Figure 25: neutral current event in the near detector

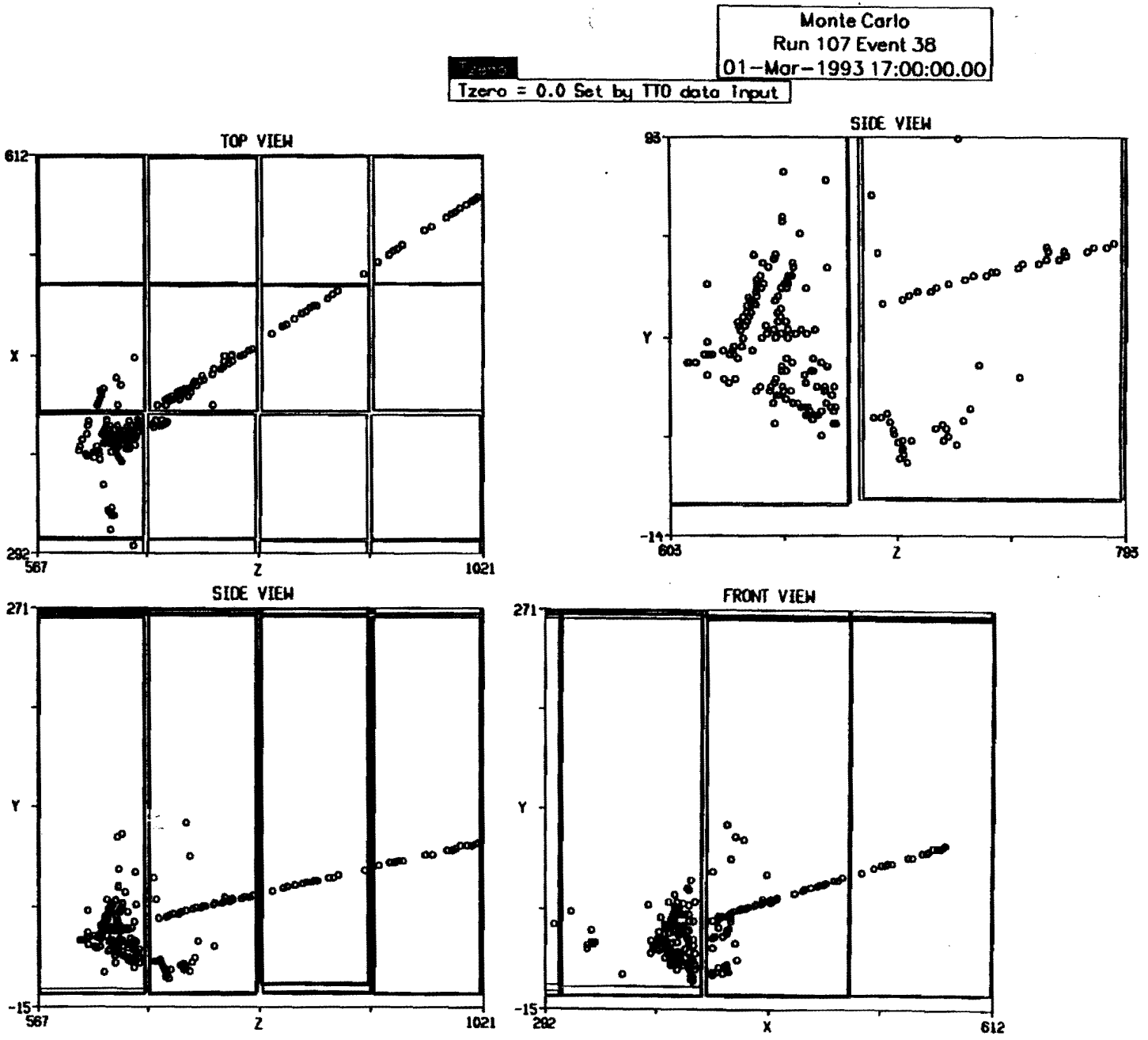

Figure 26: charged current event in the near detector

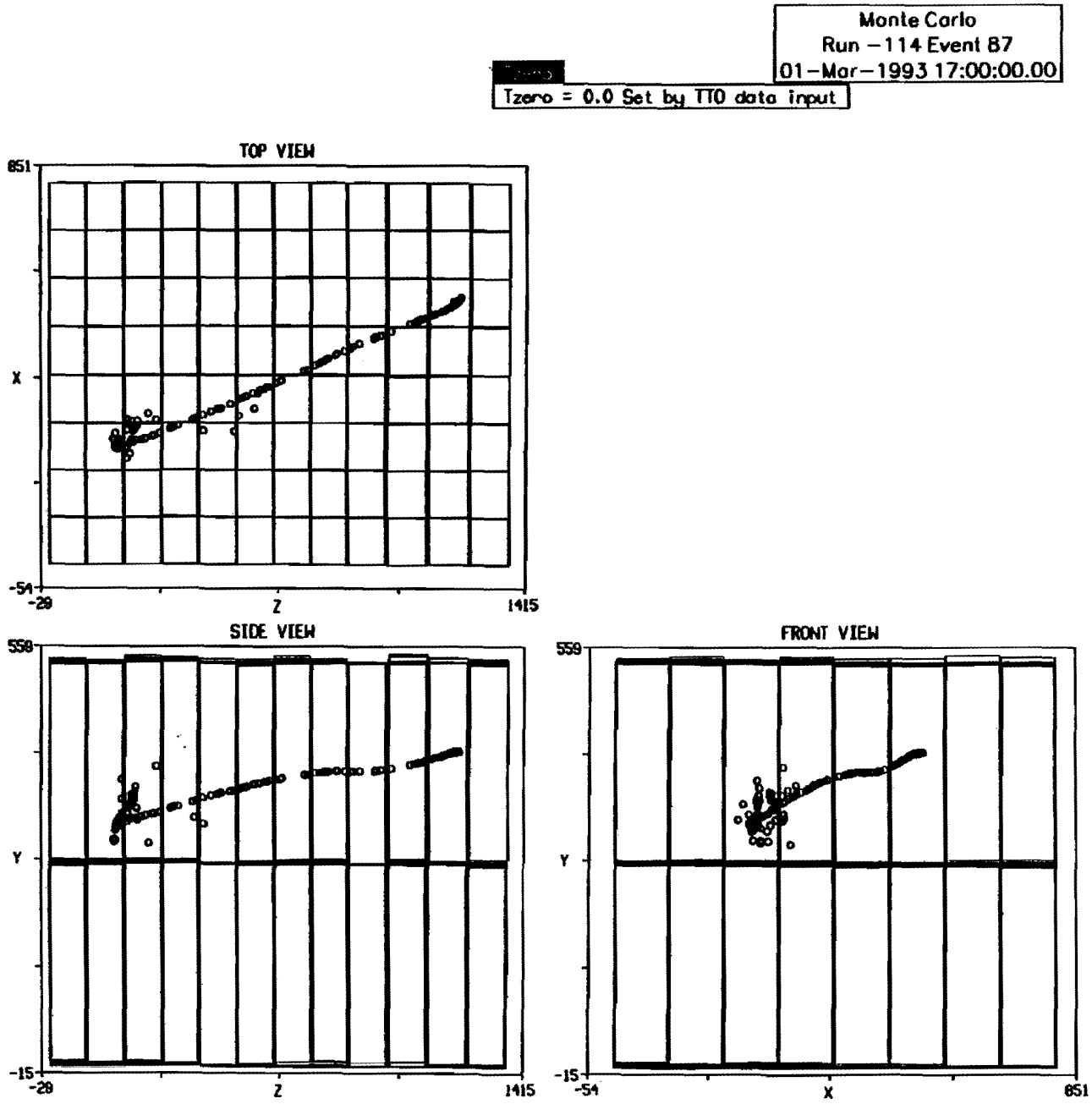

Figure 27: A charged current event with a 2.3 G μ^- which ranges out in Soudan 2

FERMILAB-Proposal-0822

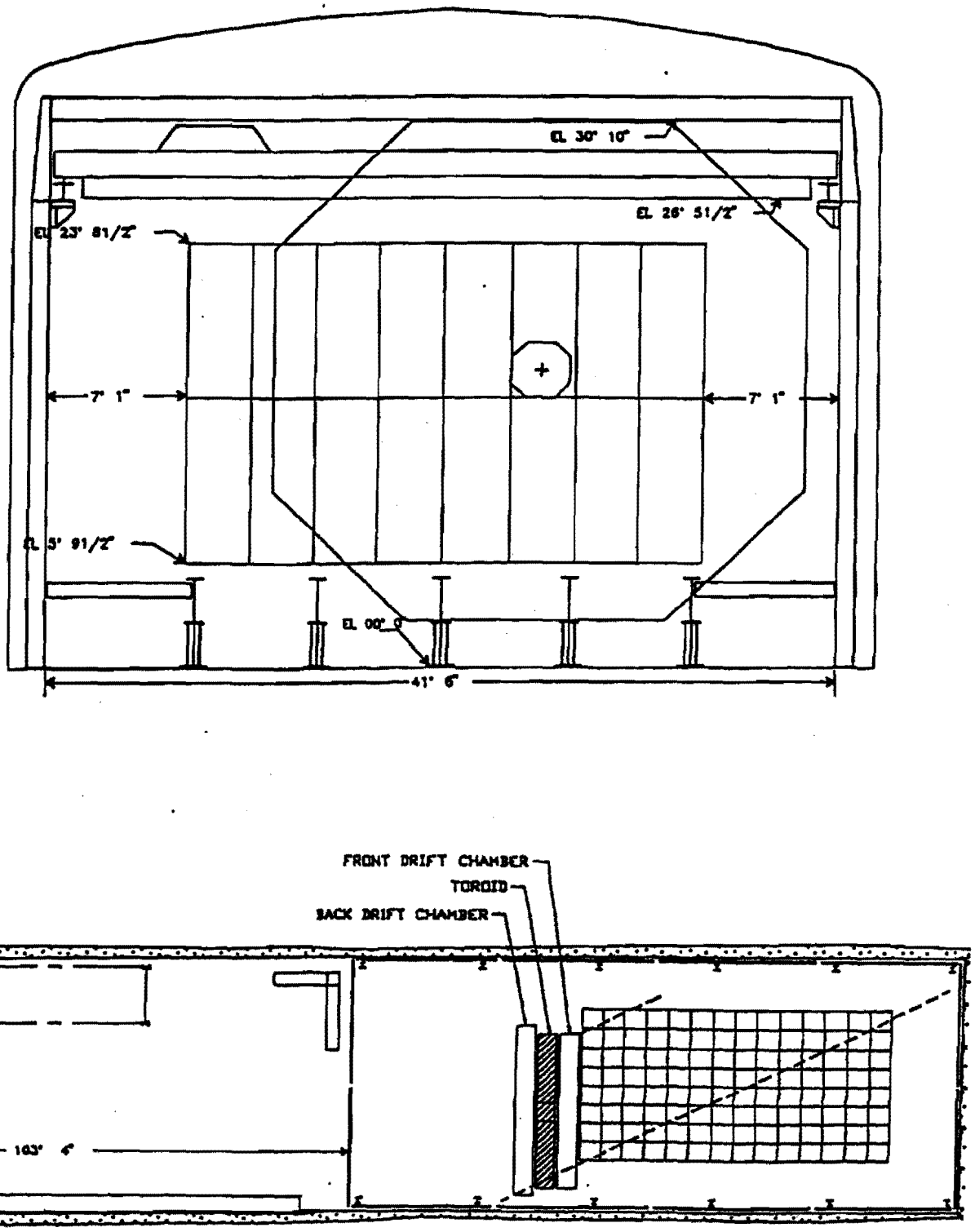

Figure 28: The upper view shows the elevation view of our toroid design with respect to the Soudan 2 detector. The dashed line in the lower plan view shows the Fermilab direction. North is to the left.

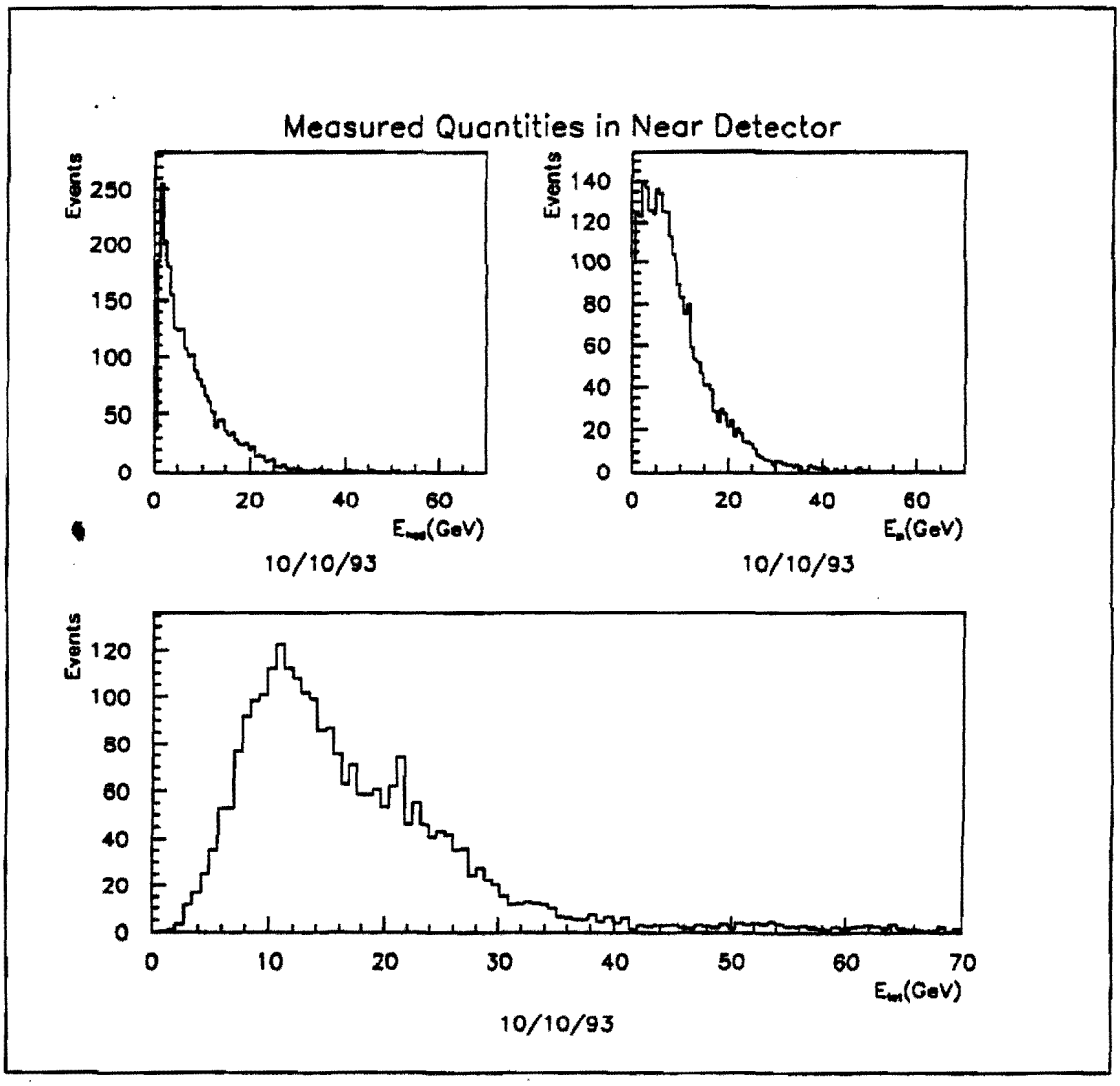

Figure 29: Smeared energy distributions in the near detector. E_μ, E_{had} and E_{tot} distributions are shown.

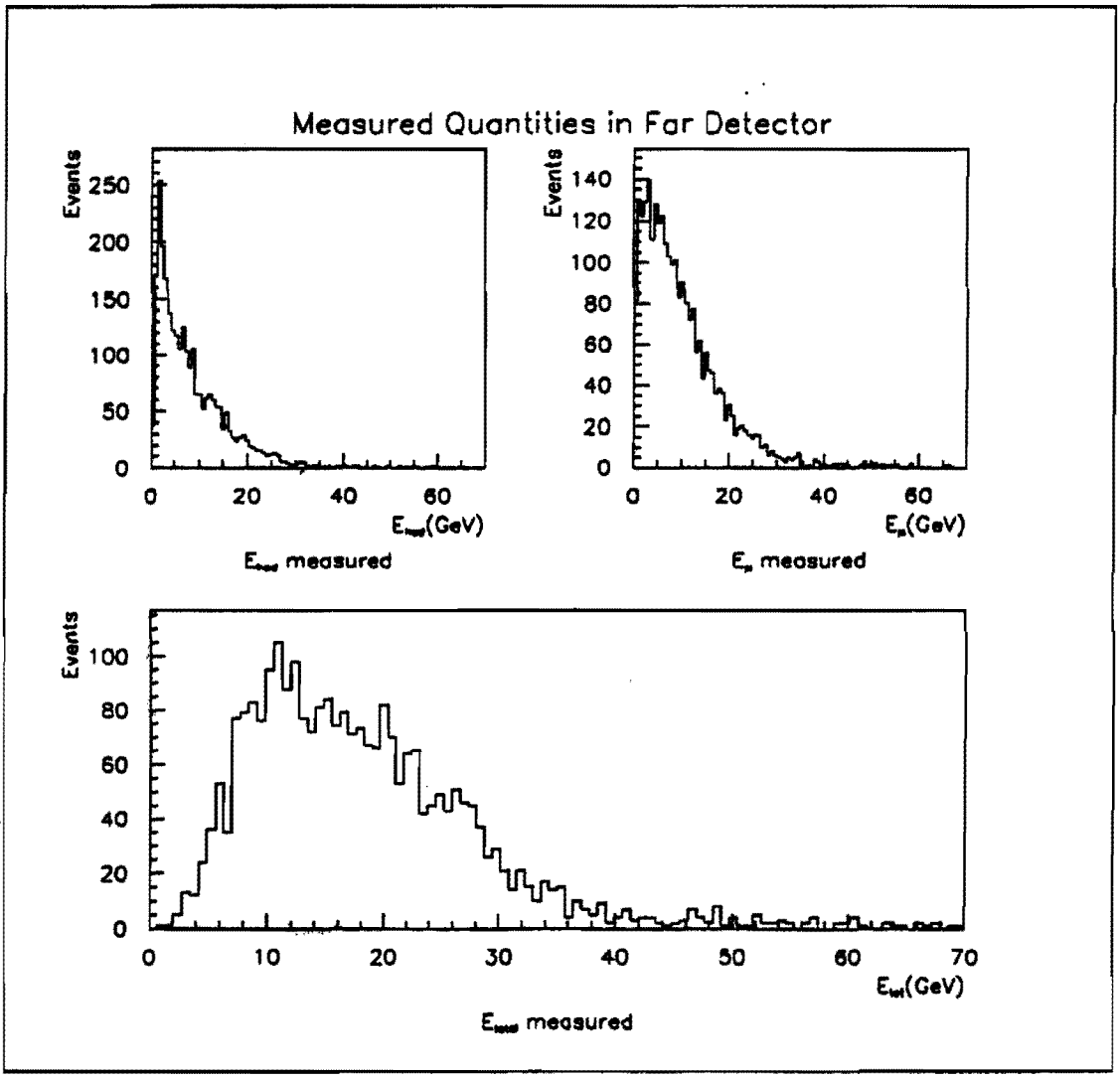

Figure 30: Smeared energy distributions in the far detector. E_μ, E_{had} and E_{tot} distributions are shown.

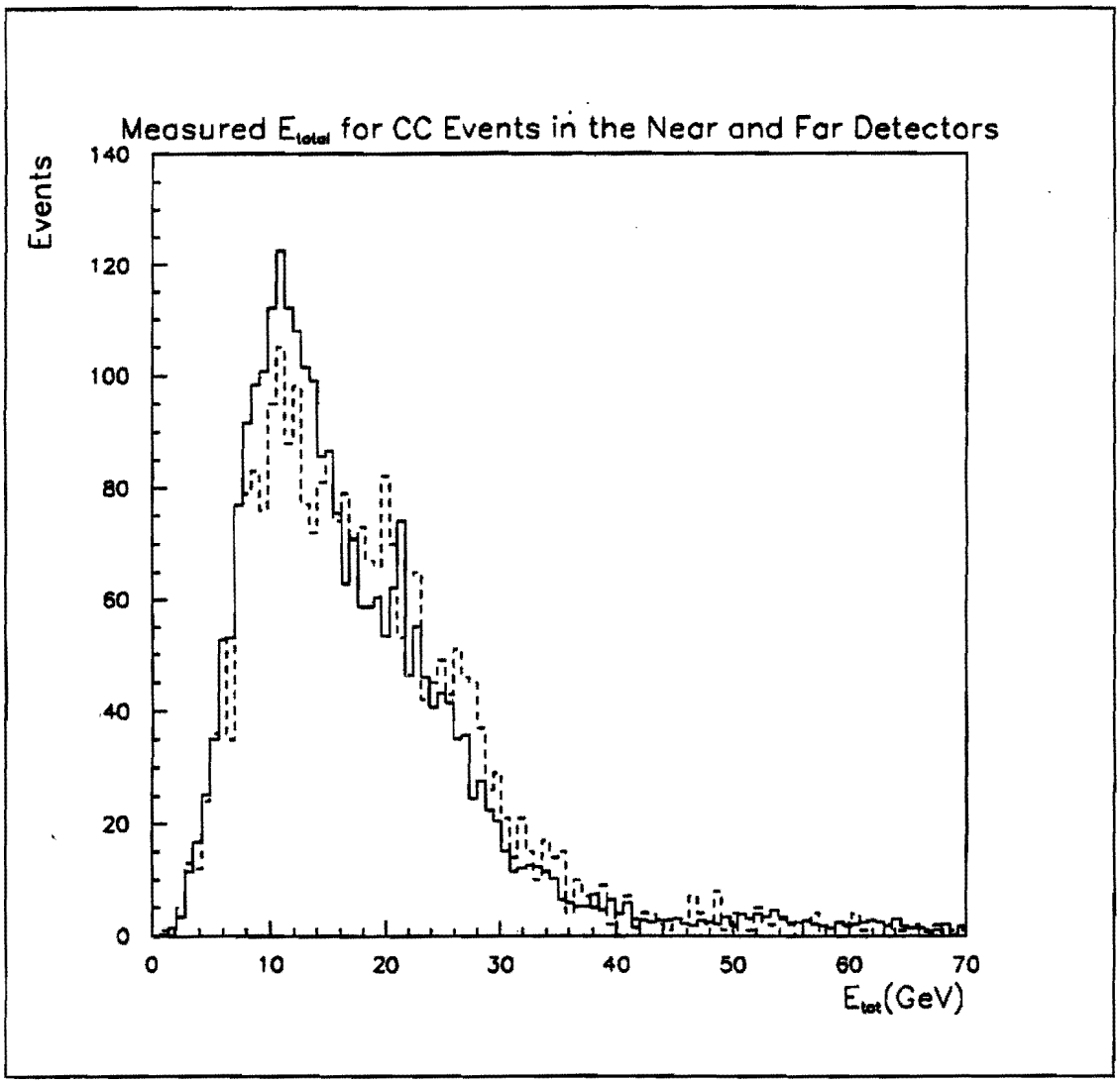

Figure 31: Comparison of the smeared E_{tot} distributions for the near(solid) and far(dashed) detector. The difference is due to low energy neutrinos from the decay of wide angle pions at the near detector.

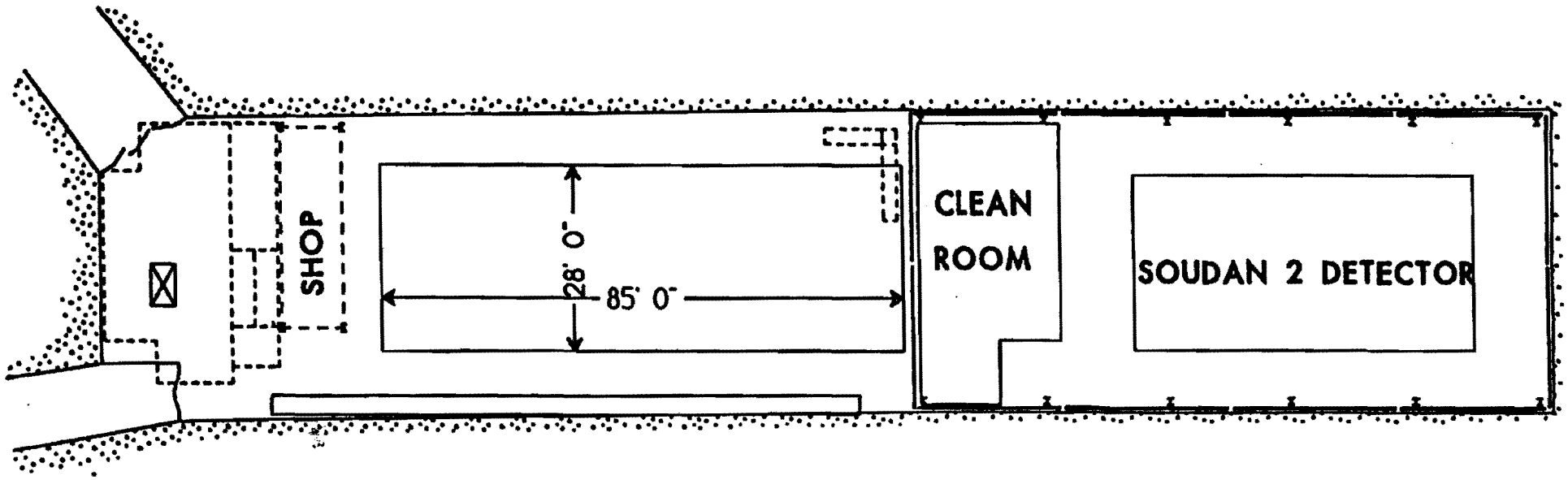

Figure 32: Floor plan for the Soudan 2 laboratory

mean density = $\frac{S*D_S + 2AD_A}{2A + G + S.}$

$D_S = 7.8 gm/cm^3$ $D_A = 3 gm/cm^3$

Set 2A = 5mm and G = 10mm.

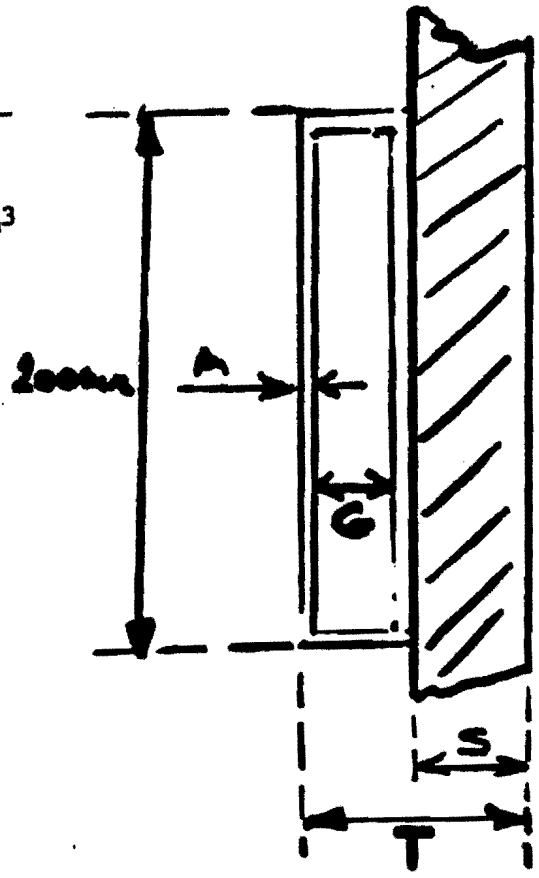

Figure 33: sketch of cavity filler options

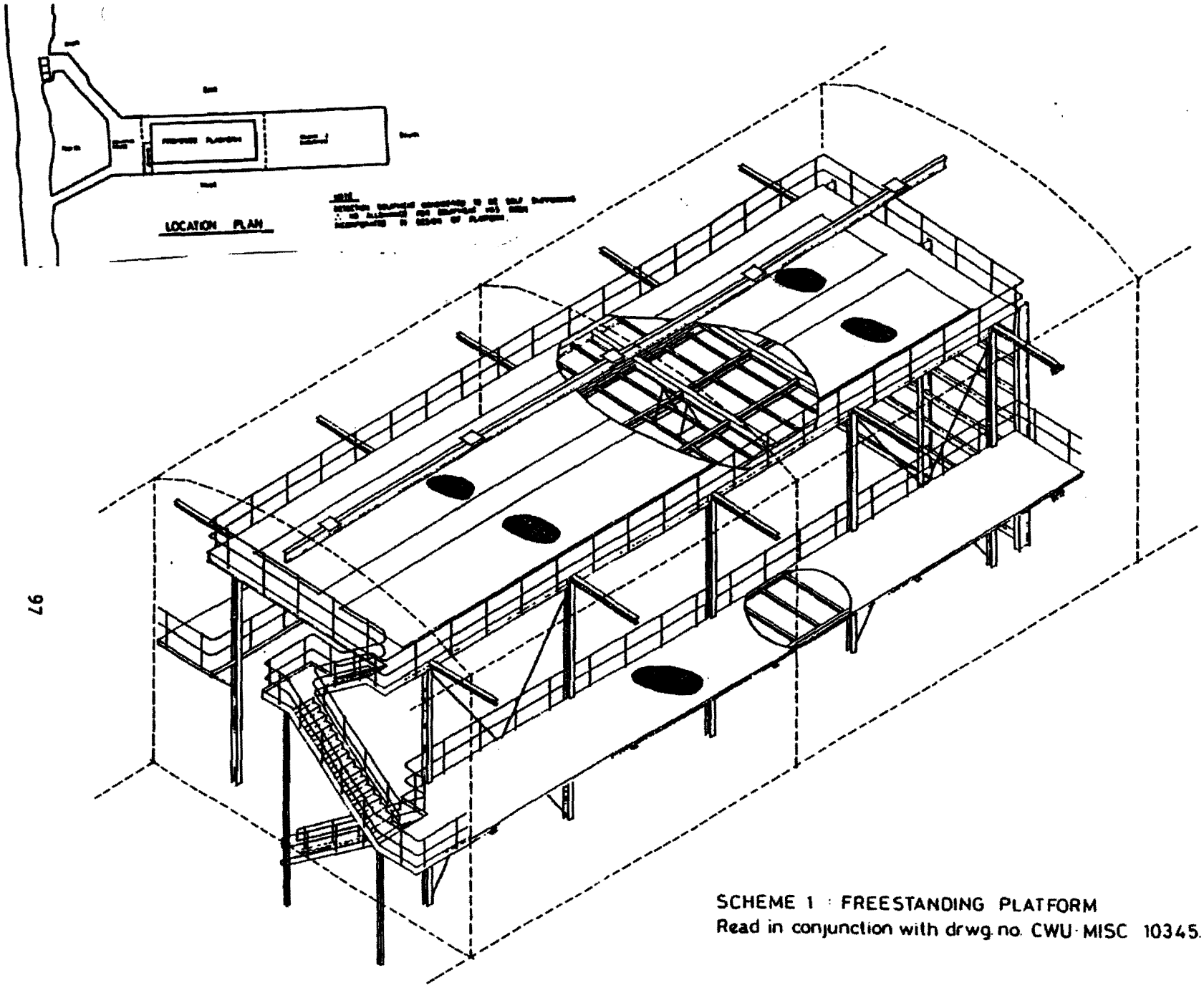

Figure 34: Cavity filler platform

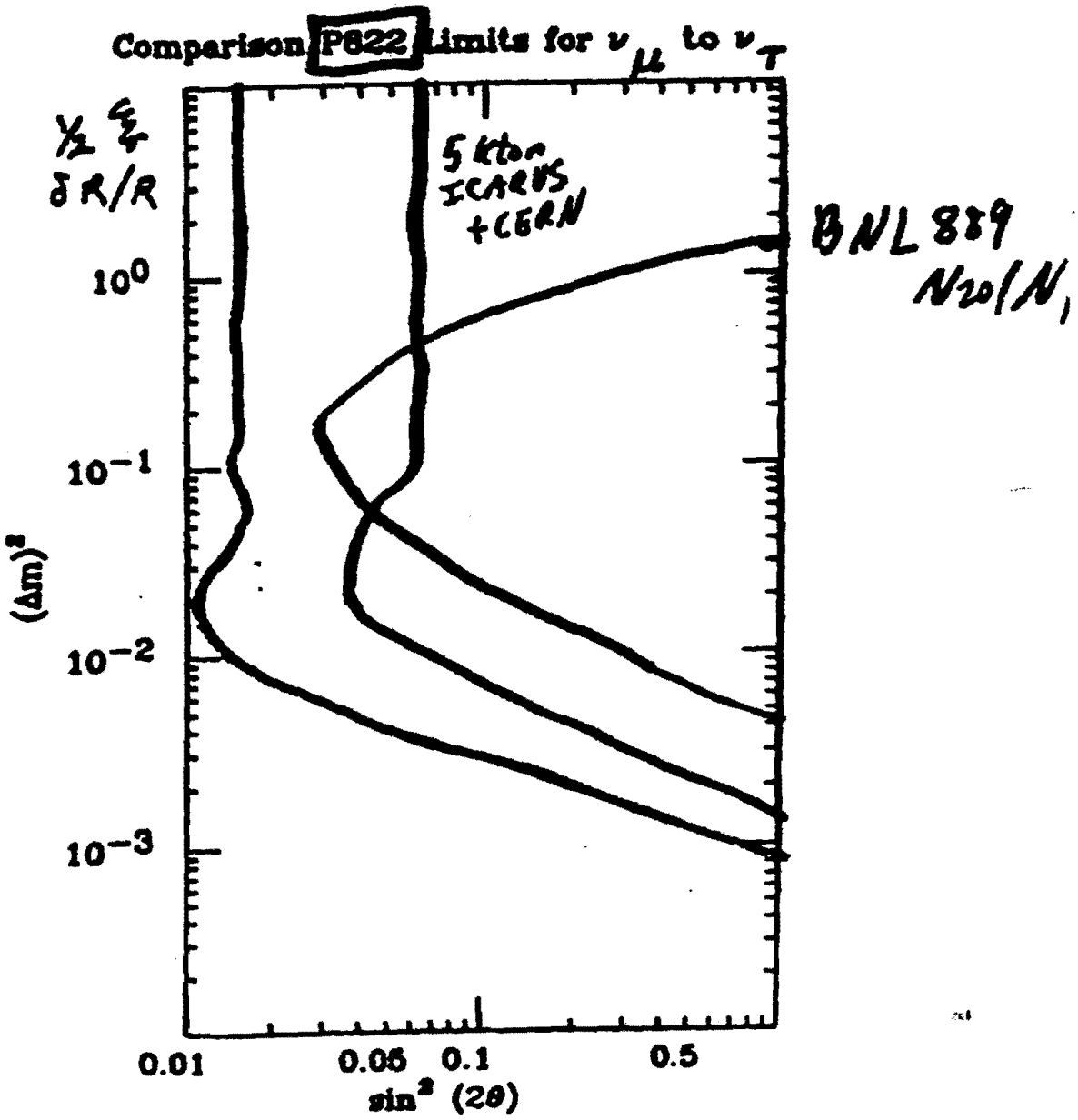

Figure 35: 822 limits with a cavity filler compared to other possible long baseline experiments

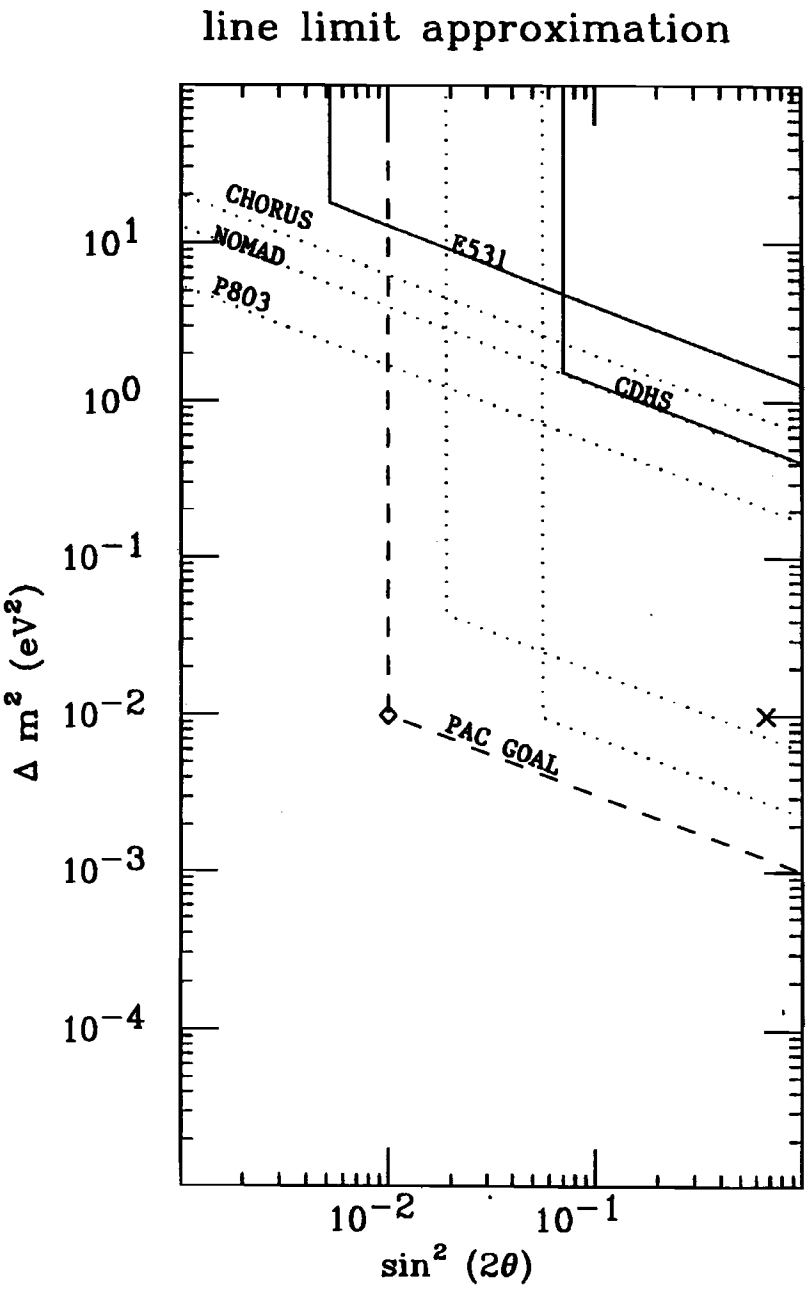

Figure 36: Limit curves using the approximations derived in Appendix A.

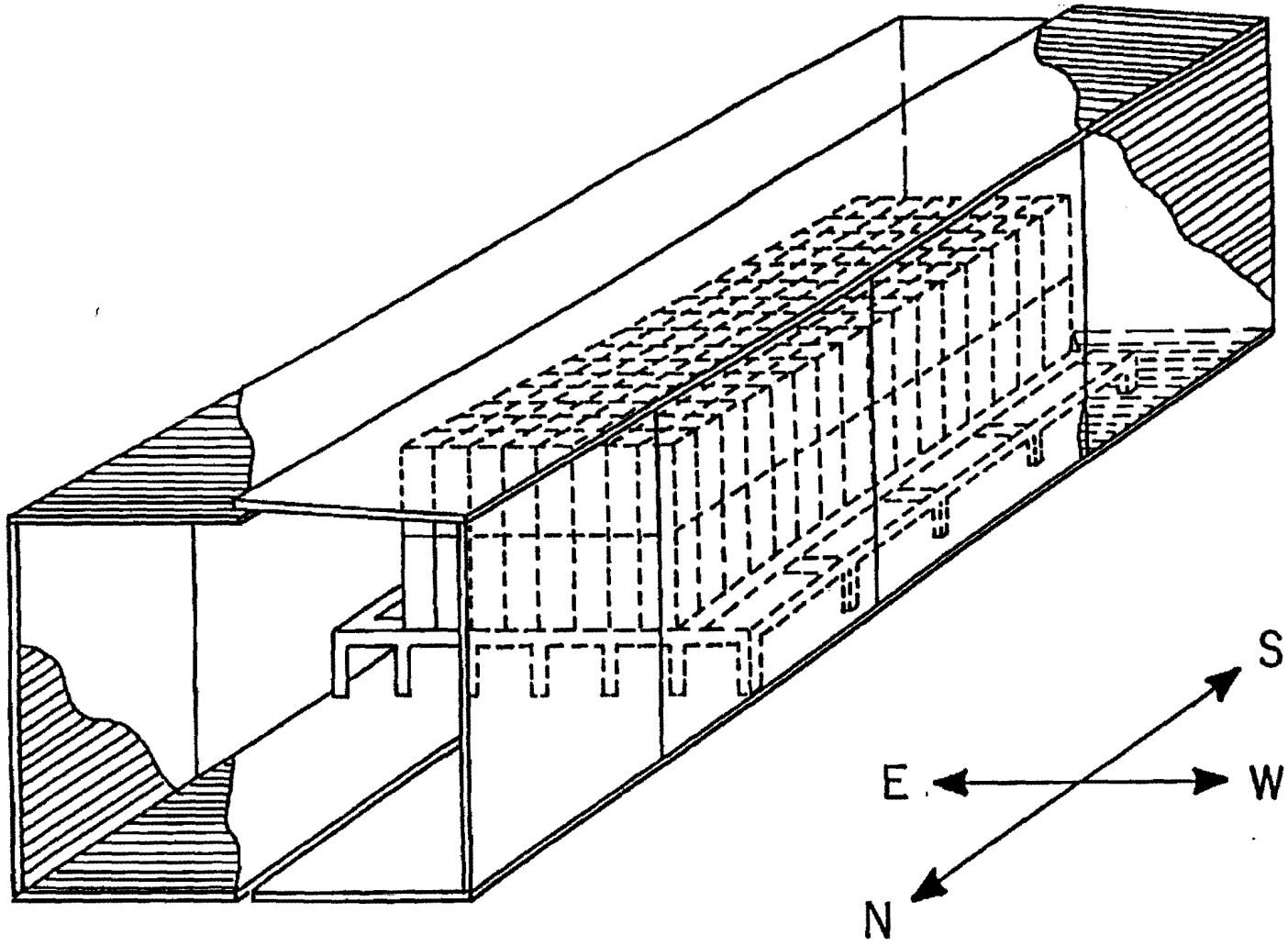

Figure 37: Soudan 2 main detector and active shield layout.

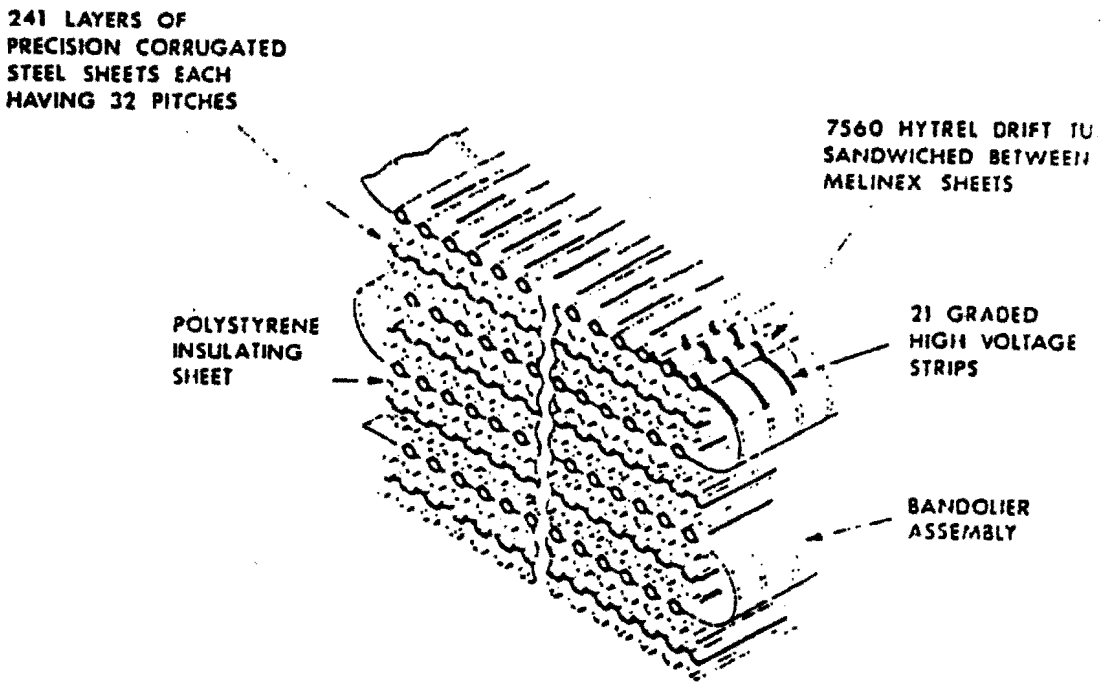

Figure 38: *Bandolier*, insulation sheets (inserts) and corrugated steel assembly (stack).

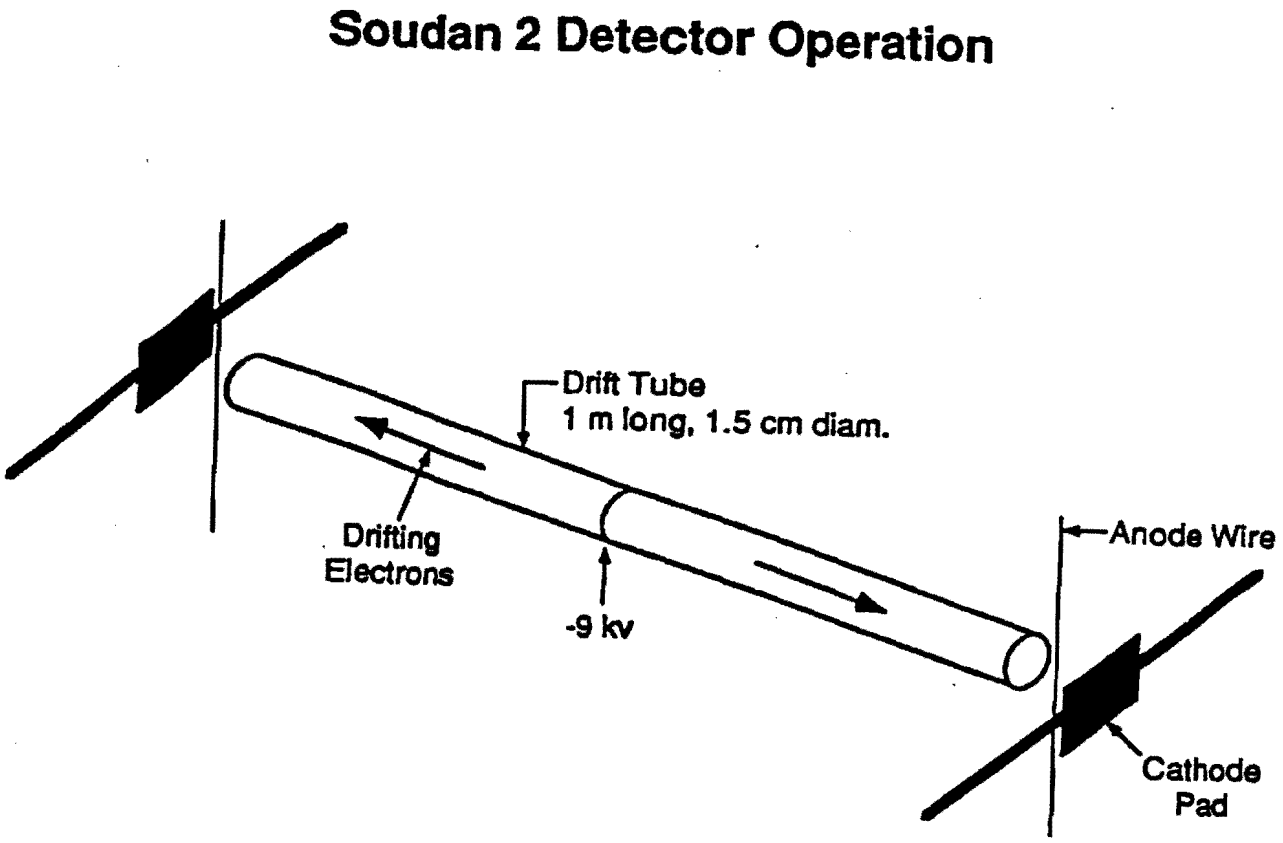

Figure 39: A single drift tube. The drift field is generated by the application of graded voltages on a series of 21 copper electrodes

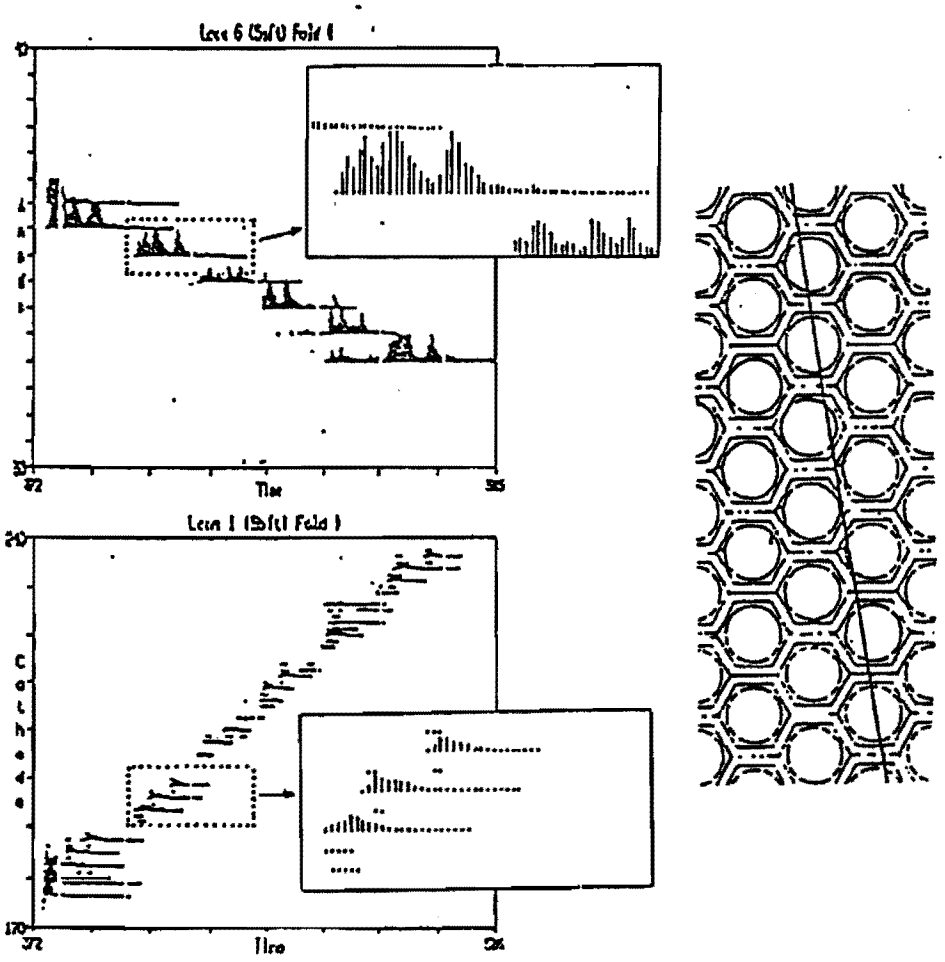

Figure 40: Segment of a muon track and fit

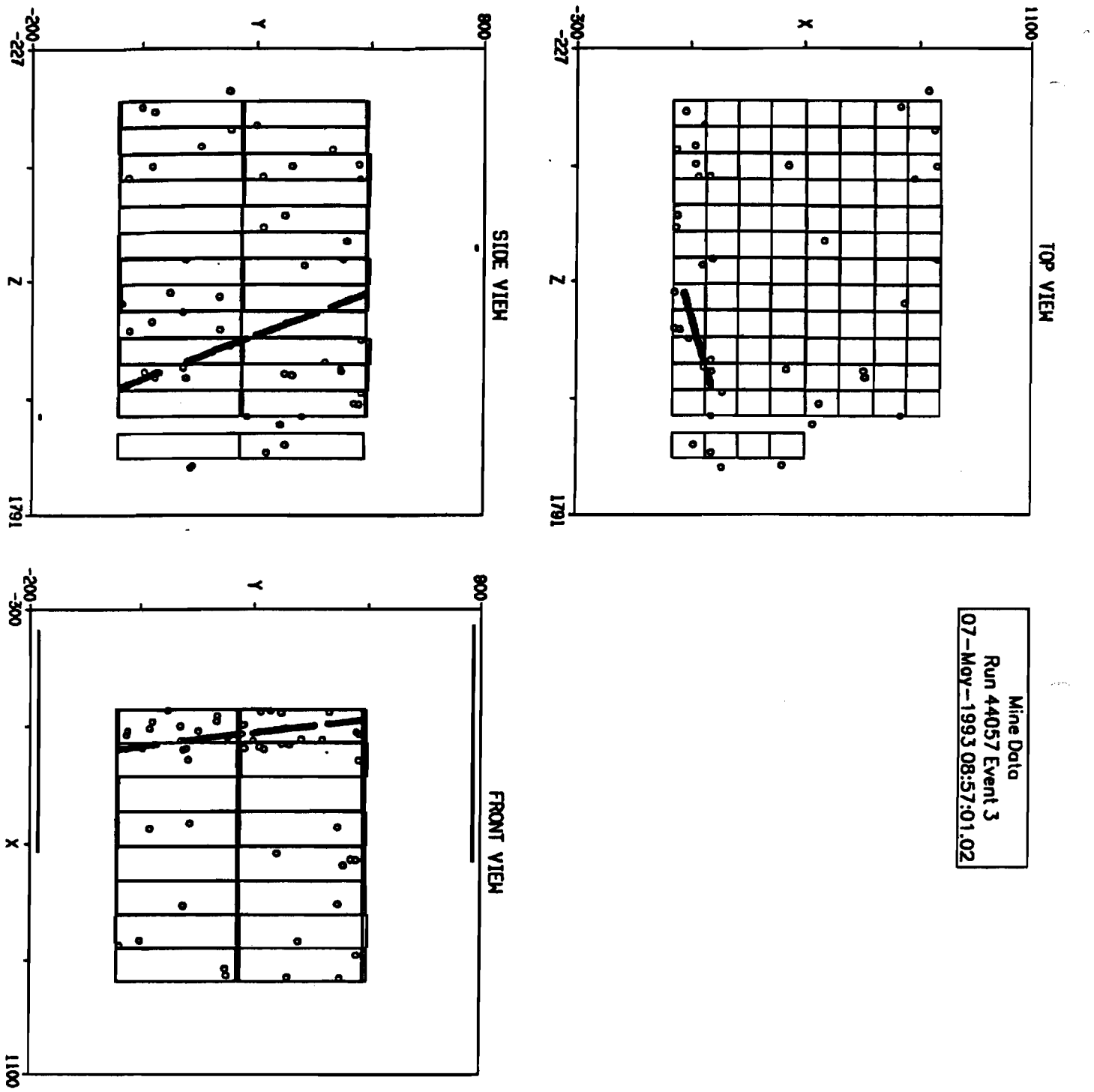

Figure 41: A cosmic ray muon in the Soudan 2 detector. The anode-time (x), cathode-time (y), and matched (z) views are shown

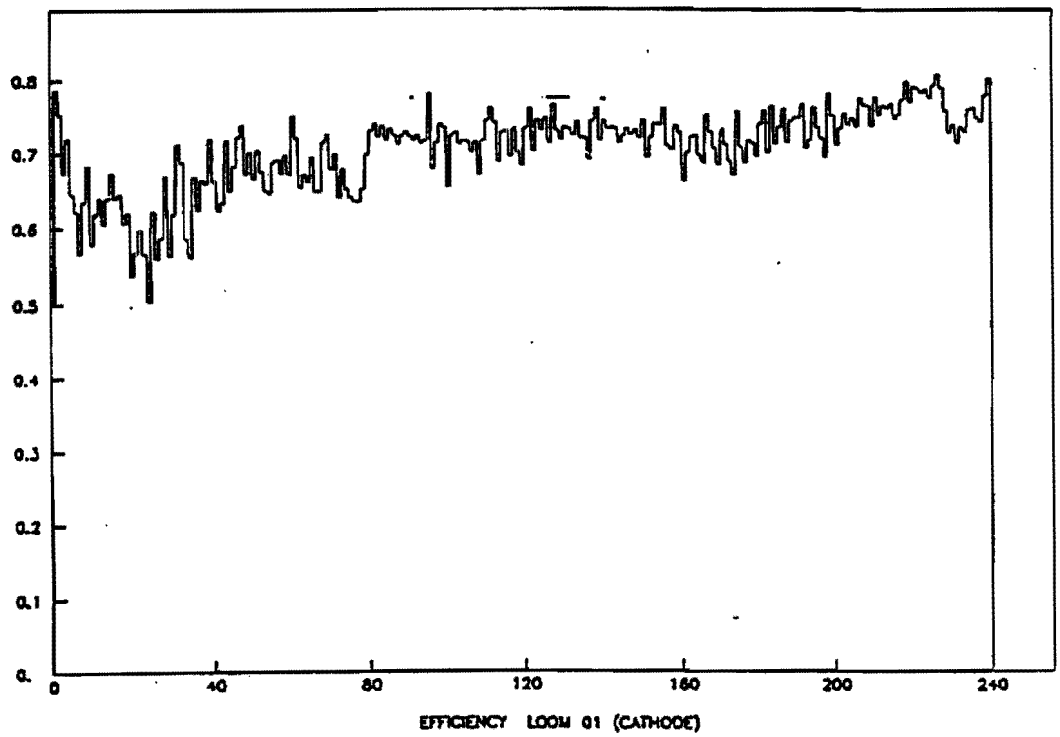

Figure 42: Typical mean tube efficiency variation with cathode numbers.

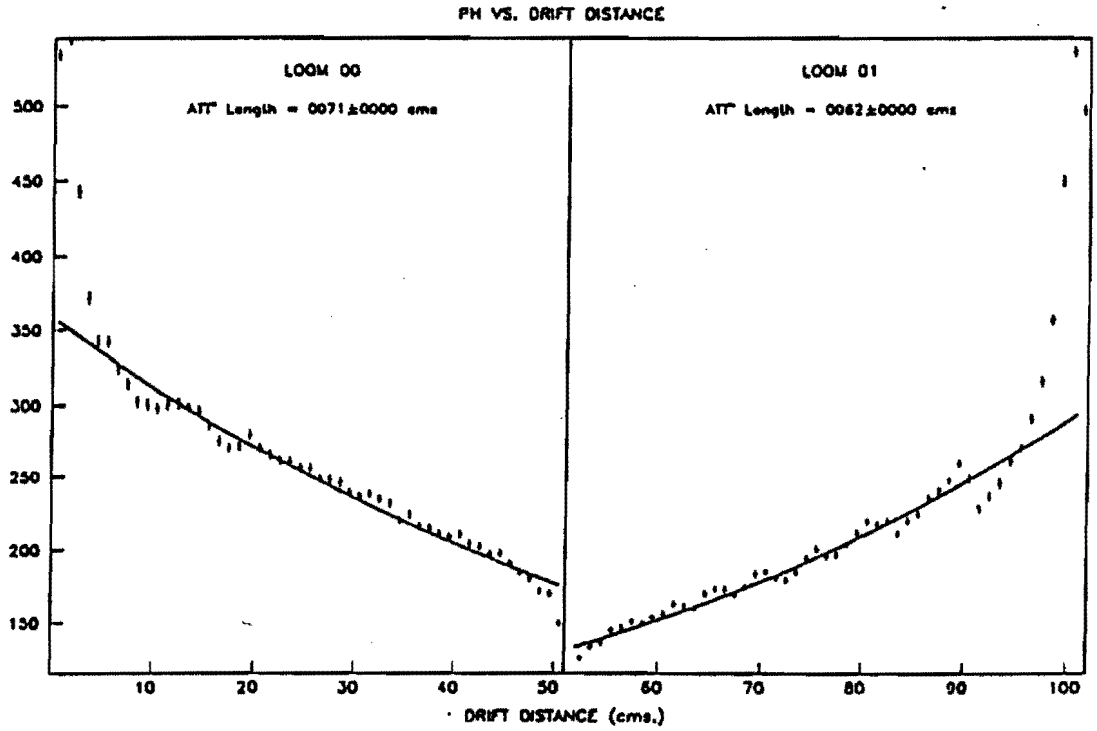

Figure 43: Typical pulse height variation along the drift direction.

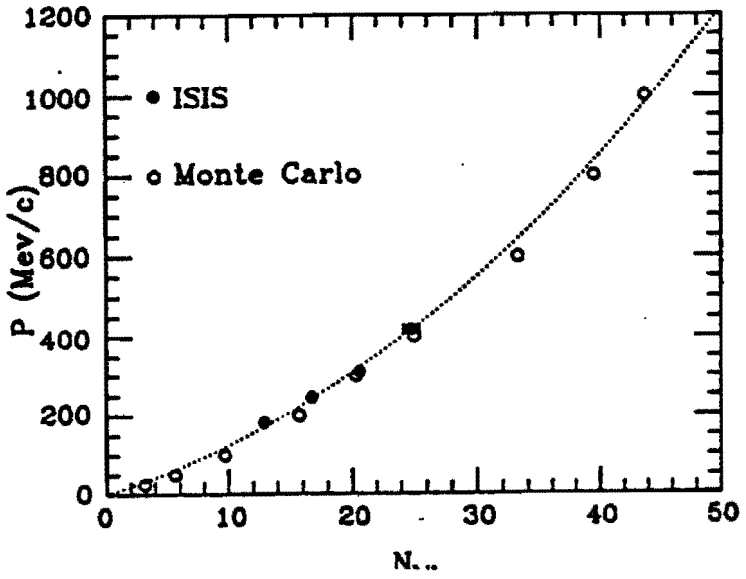

Figure 44: Electron shower energy versus number of hits from ISIS data and Monte Carlo simulations.

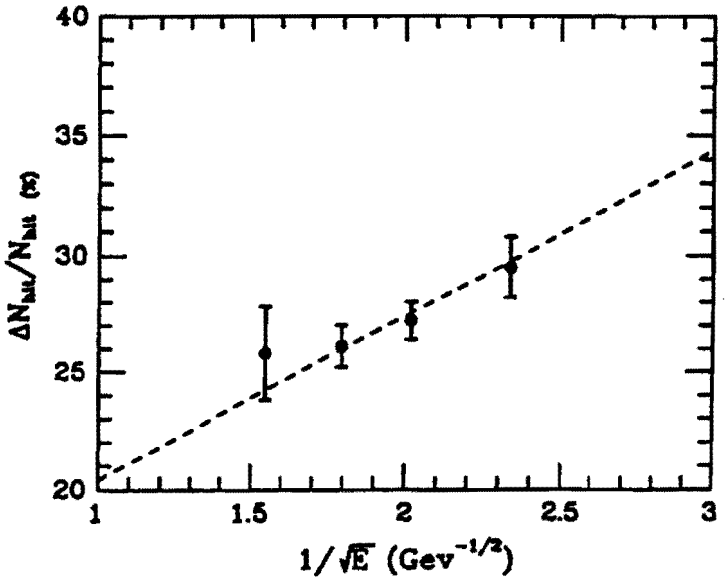

Figure 45: Energy resolution for electron showers.

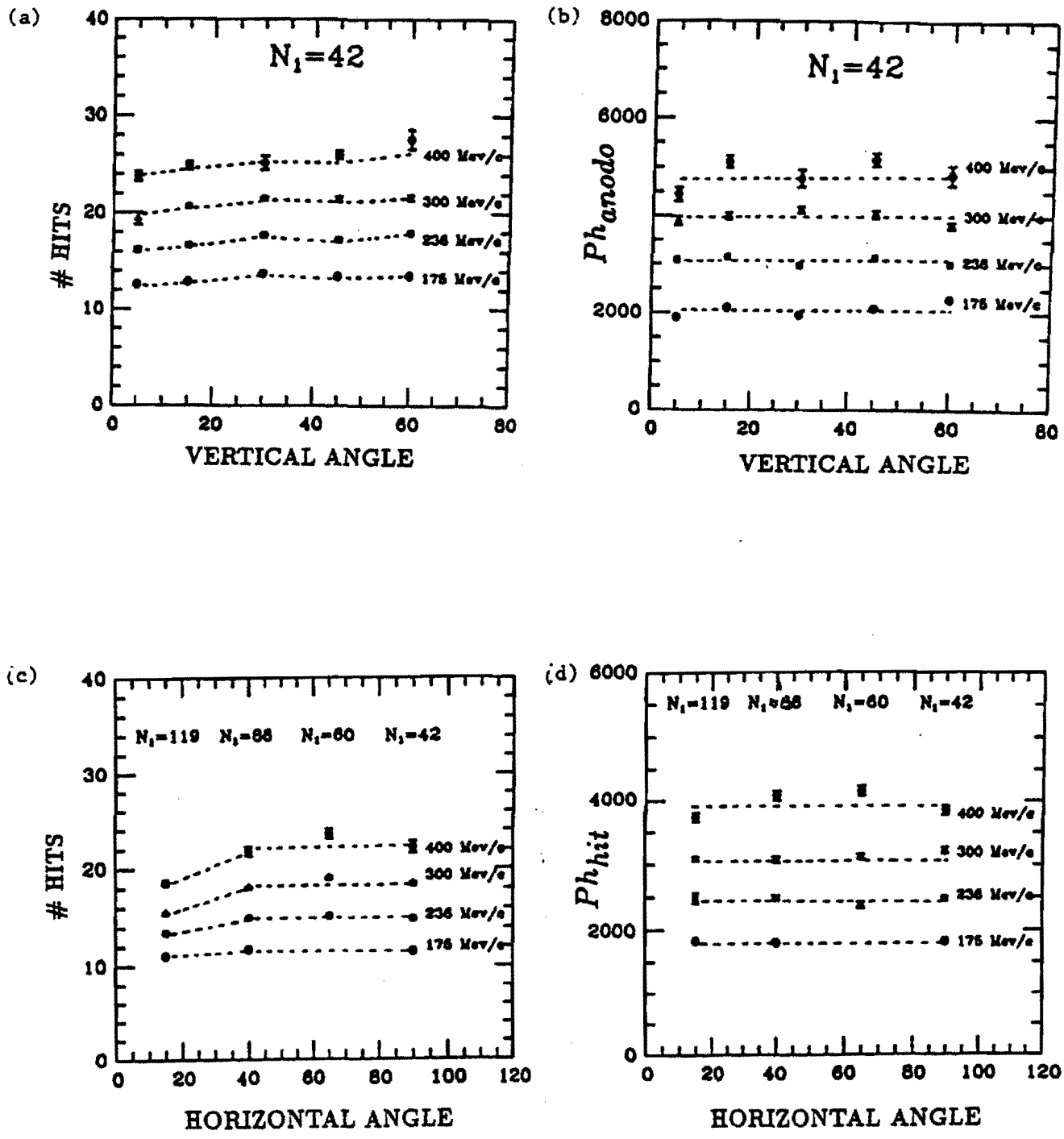

Figure 46: Mean number of hits (a) and mean total pulse height (b) for different beam momenta versus the vertical angle, and mean number of hits (c) and mean total pulse height (d) versus the horizontal angle.

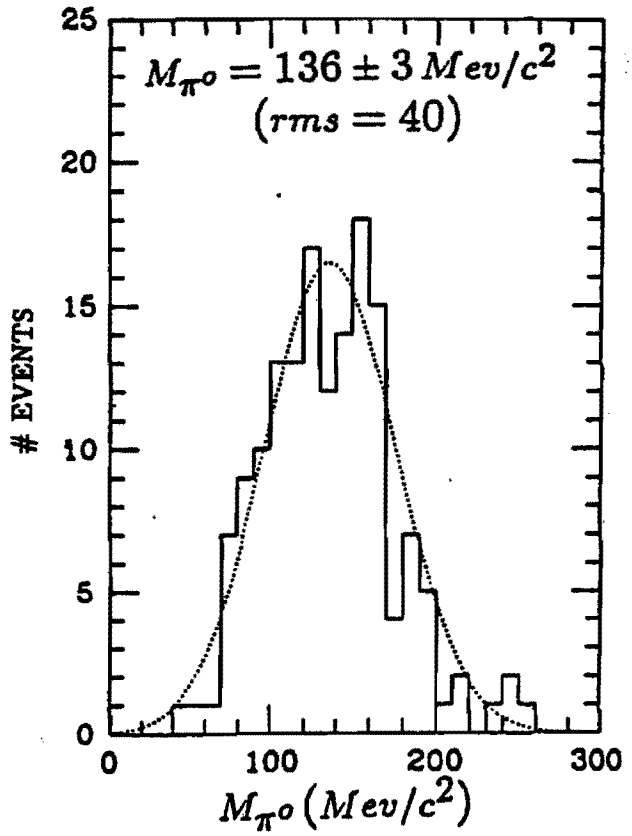

Figure 47: Invariant mass distribution for two shower events in the $\pi^{\pm}$ beam.

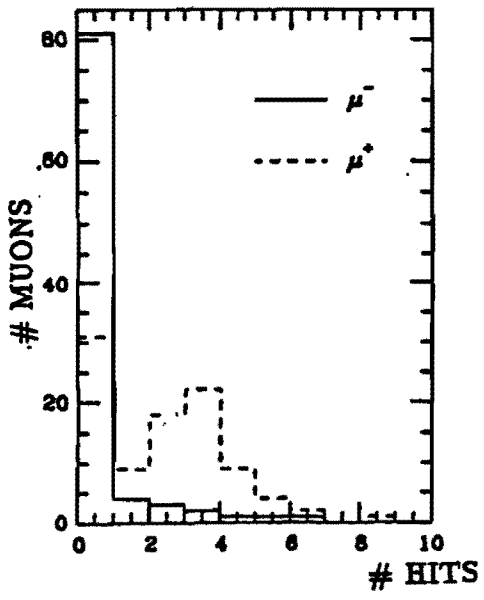

Figure 48: Number of shower hits at the end of $\mu+$ and $\mu-$ tracks.

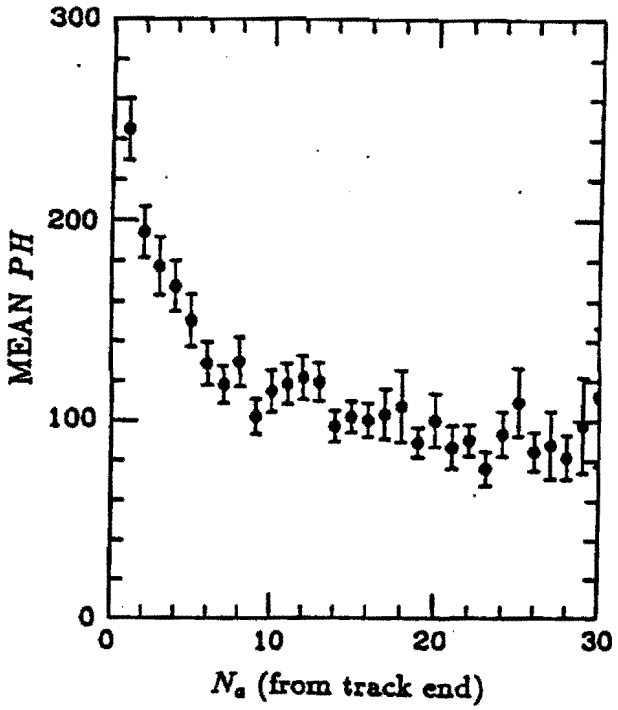

Figure 49: Mean pulse height versus anode number (measured from the last anode in the μ trajectory).

March 26, 1991

Taaji Yamanouchi
Director's Office
Fermilab
Box 500
Batavia Ill. 60510

Dear Taaji

Attached is the proposal from the P822 collaboration for a long baseline neutrino oscillation experiment for the Fermilab Main Injector era using the Soudan 2 nucleon decay detector. We are excited that the Main Injector seems to be proceeding and that these important areas of physics can be explored.

It is our understanding that the proposal will be sent to the PAC prior to the April 19th meeting. but that no presentation before the PAC is requested. We will be pleased to answer any questions which might arise either from the PAC or Fermilab staff in planning for neutrino running with the Main Injector.

The spokesman for this proposal is:

Maury Goodman
HEP 362
Argonne National Laboratory
Argonne, Ill. 60439
Telephone: 708-972-3646
Fax: 708-972-5076
Decnet: ANLHEP::MCG OR FNAL::MGOODMAN

We look forward to consideration of this proposal.

Sincerely yours,

Maury Goodman
High Energy Physics Division 362
Argonne, Illinois 60439

June 1993 Update to the 822 Proposal for a Long Baseline Neutrino Oscillation Experiment from Fermilab to Soudan

1 Introduction

The 822 Proposal for the long baseline neutrino oscillation experiment from Fermilab to Soudan was made in March 1991. The overall physics motivation and capabilities of the experiment to study neutrino oscillations remain essentially the same. However, several aspects of the proposal need to be updated. In this document, we will discuss the present status of the physics motivation for a long baseline neutrino oscillation search for $\nu_\mu \rightarrow \nu_\tau$, the experimental capabilities for an experiment in the Soudan mine, both in terms of possible limits that can be reached, and what discovery potential the experiment has for neutrino oscillations, and a comparison with other proposed experiments. A number of other important issues have been discussed in some detail in the Proceedings of the Long Baseline Workshop at Fermilab in 1991.[1]

An important possible upgrade to the Soudan 2 detector would be to take advantage of the empty space next to the Soudan 2 detector. We have worked out that an approximately 8 kiloton "cavity filler" could be constructed in that space. Using any of several conventional techniques, such a detector could be constructed in a routine fashion and for a reasonable cost. In this proposal update, we compare the capabilities of a long baseline experiment with and without a cavity filler.

2 Physics Motivation

Several neutrino oscillation experiments and proposals have been run or are being considered within the high energy physics and nuclear physics communities. Since the observed width of the Z boson favors only three flavors of light neutrinos,[2] it is reasonable to concentrate attention on the three possible modes $\nu_\mu \rightarrow \nu_e$, $\nu_\mu \rightarrow \nu_\tau$ and $\nu_e \rightarrow \nu_\tau$. A long baseline experiment with a primarily ν_μ beam can address the modes $\nu_\mu \rightarrow \nu_\tau$ and $\nu_\mu \rightarrow \nu_e$. We argue below that the mode $\nu_\mu \rightarrow \nu_\tau$ is most interesting to pursue.

A long baseline neutrino oscillation experiment from Fermilab's Main Injector to the Soudan Underground Physics Laboratory has a reasonable chance of discovering neutrino oscillations in the the mode $\nu_\mu \rightarrow \nu_\tau$. We emphasize this mode because:

- If the neutrino masses have the same generational hierarchy as the other quarks and leptons, and if the lepton version of the KM matrix has the same nearly diagonal structure as the quark KM matrix, then $\nu_\mu \rightarrow \nu_\tau$ is favored. This idea is developed below.

- Present experimental limits from accelerators and reactors are less restrictive on $\nu_\mu \rightarrow \nu_\tau$ than the other two modes.

- The solar neutrino data can be explained by $\nu_\mu \rightarrow \nu_e$ oscillations with the MSW effect. This range of Δm^2 for $\nu_\mu \rightarrow \nu_e$ cannot be reached with presently proposed accelerator

experiments, yet serves as a strong motivation for the notion of neutrino mass and mixing.

- The solar implied range of Δm^2 for $\nu_\mu \rightarrow \nu_e$ together with the normal neutrino mass hierarchy implies a m_{ν_τ} higher than $\sqrt{\Delta\, m^2\,(\nu_\mu - \nu_e)} \sim 10^{-4} eV^2$. This could be accessible to either the short baseline proposal 803 at small mixing angle and Δm^2 above a few eV^2, or to P822 at larger mixing angle and Δm^2 down to below $10^{-2} eV^2$.

- The apparent atmospheric neutrino ν_μ deficit could be explained by $\nu_\mu \rightarrow \nu_\tau$ oscillations in the parameter region accessible to P822.

- The demise of the 17 keV ν, which could have been evidence for $\nu_e \rightarrow \nu_\tau$, and which seemed to require complex scenarios for the neutrino sector.

Neutrino mass and neutrino oscillation experiments are well motivated without *any* of the above considerations. There is no compelling reason for zero neutrino mass. Thus a variety of accelerator and non-accelerator experiments to study neutrinos are being considered.

The NUMI program at Fermilab, by combining the short baseline P803 and the long baseline P822 offers such an opportunity. The availability of a neutrino beam using the Main Injector will provide an extremely large neutrino flux capable of giving large event rates at long distances, with a substantial fraction of the beam above ν_τ charged current threshold. This means that both an appearance search and disappearance experiment could be run simultaneously.

In the two neutrino approximation, the probability that one will oscillate into another is

$$P_{\nu_a \rightarrow \nu_b} = \sin^2 2\theta \, \sin^2(1.27\, \Delta m^2 \, \frac{L}{E_\nu}) \qquad (1)$$

with Δm^2 in eV^2, L in km and E_ν in GeV. $\Delta m^2 = |m^2_{\nu_a} - m^2_{\nu_b}|$ and θ is the mixing angle between ν_a and ν_b neutrinos. The masses and mixing angles are unknowns. An experiment which fails to find neutrino oscillations can set a limit in the usual parameter space. However, a skeptic can reasonably ask the following question,

> *The parameter space for neutrino oscillations is three semi-infinite plots of* Δm^2 *versus* $\sin^2 2\theta$. *Dozens of experiments have searched for and failed to find evidence for neutrino oscillations. Why should any new expensive experiment be built which can only exclude another finite area in parameter space?*

There are some general arguments which, though not compelling, indicate a particular region of parameter space in a particular mode as the most likely. First of all, all three neutrino masses are likely to be less than 20 eV, or they would overclose the universe. It is also interesting to note that if global symmetries are broken at the Planck scale, this implies a lower limit of m_ν of $10^{-5} eV$.[4]

Within this range, there would be three neutrino masses, m_{ν_e}, m_{ν_μ} and m_{ν_τ}. The quarks and leptons all exhibit a generational mass hierarchy, $m_u < m_c < m_t$; $m_d < m_s < m_b$; and $m_e < m_\mu < m_\tau$. Therefore it is likely (but by no means mandatory) that $m_{\nu_e} < m_{\nu_\mu} < m_{\nu_\tau}$.

We point out that specific models which have been published in the literature all seem to have this feature.[5] If no pair of neutrino masses is near degenerate, we would have

$$\begin{aligned} \Delta m^2(\nu_\mu - \nu_\tau) &= m^2_{\nu_\tau} \\ \Delta m^2(\nu_e - \nu_\tau) &= m^2_{\nu_\tau} \\ \Delta m^2(\nu_e - \nu_\mu) &= m^2_{\nu_\mu} \equiv \epsilon_1^2 m^2_{\nu_\tau} \end{aligned} \tag{2}$$

This last step is a definition of ϵ_1, which is smaller than 1.

Again with guidance from the quark sector, a lepton Kobayashi Maskawa Matrix is expected to have the following general form:

$$\begin{matrix} \sim 1 & \epsilon_2 & \epsilon_2^2 \\ \epsilon_2 & \sim 1 & \epsilon_2 \\ \epsilon_2^2 & \epsilon_2 & \sim 1 \end{matrix}$$

with ϵ_2 small compared to 1. To date, no evidence has been found for oscillations at accelerator experiments, so P is small. If we imagine changing L/E and repeating those experiments, then as we increase L and smaller E, we might find oscillations with $P \sim \theta^2 1.27 \Delta m^2 \frac{L}{E}$. If we now compare the probability of oscillation for the three modes for experiments at a fixed distance and energy, we find

$$\begin{aligned} P_{\nu_\mu \to \nu_\tau} &\propto \epsilon_2^2 \\ P_{\nu_e \to \nu_\tau} &\propto \epsilon_2^4 \\ P_{\nu_\mu \to \nu_e} &\propto \epsilon_2^2 \epsilon_1^2 \end{aligned} \tag{3}$$

With these rather general assumptions, the mode $\nu_\mu \to \nu_\tau$ is the most likely mode to be observable with accelerator neutrinos.

3 Atmospheric Neutrinos

When our 822 proposal was submitted in 1991, we argued that the possible atmospheric neutrino deficit was a strong argument for a long baseline neutrino oscillation experiment. At that time, the evidence for the deficit was based on 2.8 kiloton years of Kamioka data. Now, the same deficit is seen in over 13 kiloton years of H_2O Cerenkov data. It is reviewed here only briefly.

Several underground experiments which can measure the ratio of ν_μ to ν_e in the atmospheric neutrino flux see an apparent deficit of ν_μ compared to expectation. We define a ratio of ratios :

$$R \equiv \frac{(\nu_\mu/\nu_e)_{measured}}{(\nu_\mu/\nu_e)_{predicted}} \tag{4}$$

The experimental situation is summarized in Table 1.[7] If this deficit is interpreted as being due to neutrino oscillations, then there is a region of parameter space which is allowed. Restricting our interest to $\nu_\mu \to \nu_\tau$, we show that parameter space in Figure 1, together

with accelerator limits. The area shown is the area allowed at 90% Confidence level from an analysis of the first 2.76 kt-year of the Kamioka data. As the statistical significance for $R \neq 1$ has increased as Kamioka has taken more data, the "allowed" region has shrunk considerably. IMB has not publicly presented an oscillation analysis, but it is expected to be similar. To explain the entire effect as $\nu_\mu \rightarrow \nu_\tau$, one requires a large mixing angle. The entire area shown in figure 1 is no longer the result of a 90% CL, but remains an area of interest for the atmospheric neutrinos.

Limits have been presented based on the rate of upgoing muons and upgoing stopping muons.[8] However, any limits based on upward going muons should include large systematic errors due to uncertainties in the absolute flux of cosmic rays.[9],[10]

4 Experiment Capabilities

The design and capabilities of a wide band neutrino beam using the Main Injector were spelled out in the Fermilab Conceptual Design Report for the Main Injector Neutrino Program.[3] The specifics for extraction and beam design in the direction of Soudan 2 have been worked out by the Fermilab Main Injector groups and Research Division and will not be addressed in this document. A map of the beam and a cartoon sketch of a profile of the earth are shown in figure 2. The neutrino beam will go through the short baseline detector 803 and also a 40 ton near version of the long baseline detector at the Fermilab site. It will then traverse 730 km to the Soudan mine.

The Soudan 2 detector, when complete later this year, will have a mass of 960 tons. The cavity in the Soudan hall is $72m \times 14m \times 11m$, and we estimate that, depending on the required granularity, another detector of up to 8 kton could be constructed behind Soudan 2 with a similar capability for measuring nc/cc in the Fermilab beam.

Since the original proposal was written, the design intensity for the Main Injector has increased from 4 $10^{13}ppp$ every 2 seconds to $10^{14}ppp$ every 1.5 seconds. This leads to a factor of 3.3 increased neutrino event rate in the existing Soudan detector as shown in Table 2. A nine-month run with 100 hours per week of running has been assumed. We also show the event rate which could be obtained in four such nine month runs if we also build a 5 kiloton cavity filler.

These event rates can then be used to estimate limit curves. In Figure 3, the limit curves for the three tests discussed in the original proposal are shown for comparison. Restricting ourselves to the $R_{\text{"nc"}/\text{"cc"}}$ test, the limits shown in figure 4 compare what the two running periods would give, for two assumptions about the systematic error in $R_{\text{"nc"}/\text{"cc"}}$, $\frac{\delta R}{R}$ of 2% and 0%. We expect that with a fine grained short baseline detector, and the running experience of the 803 and 815 experiments, we estimate that we can achieve $\frac{\delta R}{R}$ between 0.5% and 2%.[1, 6] With similar assumptions about systematic errors, curves for the $R_{\frac{\mu}{\nu}}$ test are shown in figure 5.

Limit curves give some impression of the sensitivity of an experiment, but more telling is the capability to measure an effect. This is illustrated in Tables 2 and 3. In table 2 we show the expected event rates under the assumption of no neutrino oscillations (P=0), and assuming that the average probability is 0.1, 0.2 and 0.345. The latter value corresponds to the mean of the atmospheric ν_μ deficit. The exposure corresponds to one 9 month Main

Injector run and the existing Soudan 2 detector. If P = 0.345, we will see a 9.5 σ result in $R_{\text{"nc"}/\text{"cc"}}$, and independently an 8.8 σ result in $R_{\frac{\mu}{\nu}}$ and a 17 sigma result in $R_{near/far}$. (Errors are not Gaussian, but we assume that they are just for illustrative purposes.) The latter result is dominated by a 2% systematic error. All three results are statistically independent. In addition, there would be a shift in the neutral current hadronic energy spectrum from that expected with a significance greater than 3 σ.

Table 3 shows the numbers for four nine-month runs with an 8 kiloton cavity filler. As an example, if P = 0.1, we would see an 18 σ result in $R_{\text{"nc"}/\text{"cc"}}$, a 10 σ result in $R_{\frac{\mu}{\nu}}$, a 5 σ result in $R_{near/far}$, and a very significant shift in $E_{had}(nc)$. These four independent measurements provide a strong handle on whether any anomaly might be due to neutrino oscillations.

5 Comparison with other experiments

There are a variety of new and proposed neutrino oscillation experiments at accelerators around the world. Since the search for $\nu_\mu \rightarrow \nu_\tau$ oscillations is motivated in part by atmospheric neutrino experiments, and the time scale for running the experiment is large, we shall also consider the possible capabilities of new and proposed underground experiments studying atmospheric neutrinos.

We divide the consideration of other proposals/experiments into three classes; atmospheric neutrino experiments, "long baseline" accelerator experiments aimed at sensitivity to smaller values of Δm^2, and "short baseline" accelerator experiments designed to probe small mixing angles.

Between now and 1995, the only experiment likely to shed new light on the contained event ratio is Soudan 2. Kamioka will not double their statistics in the next several years. IMB, Frejus, and Kamioka may further analyse aspects of their existing data to see if they are consistent with a neutrino oscillation hypothesis. In two years, there will be a beam test of a water Cerenkov Detector at KEK using both Kamioka and IMB tubes. This will measure the trigger and pattern recognition efficiencies used in their analyses. The angular and energy distributions of atmospheric neutrinos will be important in distinguishing possible neutrino oscillation interpretations of the data.[1]

Between 1996 and 2000, Superkamiokande will come on line and greatly increase the statistics of contained events. At present, it seems unlikely that the effect will be explained away as a statistical aberration. However, greater statistics may be useful in various possible systematic effects.

A few proposals are directly competitive with the goals of P822, i.e. to search for $\nu_\mu \rightarrow \nu_\tau$ at low mass differences. These include Brookhaven 889 which plans a disappearance experiment along a 20km beam on Long Island. Fermilab Proposal 860 could build more detectors further from the debuncher and do a ν_μ disappearance experiment. CERN is thinking about aiming beams at Superkamiokande or the Gran Sasso laboratory. Existing detectors at Gran Sasso are not suitable for $\nu_\mu \rightarrow \nu_\tau$, so proposals are being considered for ICARUS, a liquid argon detector, and GENIUS, a planar calorimeter. A comparison of Brookhaven, CERN and P822 is made in table 4 and figure 6.

Also relevant to the question of possible atmospheric neutrino oscillations is the flux of upgoing muons, and the angular distribution of that flux. In addition to IMB and Kamioka,

this can be measured at MACRO, LVD, Baksan, and when they start to take data, at DUMAND and AMANDA.

Several experiments and proposals at accelerators emphasize other modes and other regions of parameter space than 822. At CERN, Chorus and Nomad will improve $\nu_\mu \rightarrow \nu_\tau$ limits at small mixing angle. If it gets significant running at Los Alamos, LSND could improve $\nu_\mu \rightarrow \nu_e$ limits at small mixing angle.

Experiment	Exposure	R'	90% *CL limits on* P_{av}
Kamiokande	6.10 kton-year	$0.60^{+.07}_{-.05} \pm 0.05$	$\mathbf{0.31} < P_{av} < 0.50$
IMB 3	7.70	$0.54 \pm 0.02 \pm 0.07$	$\mathbf{0.37} < P_{av} < 0.50$
Frejus	1.56	0.87 ± 0.21	$0.0 < P_{av} < \mathbf{0.40}$
NUSEX	~ 0.4	0.99 ± 0.40	$0.0 < P_{av} < 0.50$
PRELIMINARY			
Soudan 2	0.50	$0.55 \pm 0.27 \pm 0.10$	$\mathbf{0.24} < P_{av} < 0.50$

Table 1: Atmospheric neutrino exposures and results.

Example event rates

	P = 0	P = 0.1	P = 0.2	P = 0.345
$R_{\text{"nc"}/\text{"cc"}}$	$\frac{568}{1832} = .310 \pm .015$	$\frac{604}{1656} = .365 \pm .017$	$\frac{641}{1481} = .433 \pm .027$	$\frac{694}{1226} = .566 \pm .027$
$R_{\frac{\mu}{\nu}}$	$\frac{8800}{3000} = 2.93 \pm .06$	$\frac{7920}{2826} = 2.80 \pm .06$	$\frac{7040}{2652} = 2.66 \pm .06$	$\frac{5764}{2400} = 2.40 \pm .06$
$R_{near/far}$	$\frac{4\times10^7}{33000} = 1212 \pm 24$	$\frac{4\times10^7}{29700} = 1347 \pm 27$	$\frac{4\times10^7}{26400} = 1515 \pm 30$	$\frac{4\times10^7}{21615} = 1851 \pm 37$

Table 2: Expected ratios for several example probabilities of oscillation (.345 corresponds to the Kamiokande value at large L/E). Rates are for one 9 month run of the existing Soudan Detector.

References

[1] Proceedings of the Workshop on Long-Baseline Neutrino Oscillation, Fermilab , 17-20 November 1991. Maury Goodman editor.

[2] Adeva *et al.*, Phys. Lett. **B237** (1990).

[3] Conceptual Design Report: Main Injector Neutrino Program, 1991.

[4] S. Pakvasa, private communication; Akhmedov *et al.* Phys. Lett. **69** 3013 (1992).

[5] Dimopoulous, Hall and Raby Phys. Rev. **D47** R3697 (1993). ; K. S. Babu and R. N. Mohapatra, *Phys. Rev Let.* **70** 2845 (1993).

[6] Proposal for the 815 experiment, Fermilab, 1991.

[7] K. S. Hirata *et al.*, *Phys. Lett.* **B280**, 146 (1992); D. Casper *et al.*, *Phys. Rev. Lett.* **66**, 2561 (1991); Ch. Berger *et al.*, *Phys. Lett.* **B227**, 489 (1989); M. Aglietta *et al.*, *Europhys. Lett.* **8**, 611 (1989); M. Goodman, Proceedings of the DPF conference, Fermilab 1992; H. Meyer, private communication.

[8] R. Svoboda *et al.*, LSU-HEPA-3-92.

[9] Frati *et al.*,UPR-218E, Dec 1992.

[10] Don Perkins, OUNP-93-03 (unpublished).

[11] Donald Roback Ph.D thesis, *Measurement of the Atmospheric Neutrino Flavor Ratio with the Soudan 2 Detector*, University of Minnesota, 1992 (unpublished).

Example event rates

	P = 0	P = 0.1	P = 0.2	P = 0.345
$R_{"nc"/"cc"}$	$\frac{20410}{65840} = .310 \pm .002$	$\frac{21722}{59524} = .365 \pm .003$	$\frac{23033}{53209} = .433 \pm .003$	$\frac{24935}{44052} = .566 \pm .004$
$R_{\frac{\mu}{\nu}}$	$\frac{88000}{107813} = .816 \pm .004$	$\frac{79200}{101558} = .780 \pm .004$	$\frac{70400}{95303} = .739 \pm .004$	$\frac{57640}{86234} = .668 \pm .004$
$R_{near/far}$	$\frac{10^9}{330000} = 3030 \pm 60$	$\frac{10^9}{297000} = 3367 \pm 67$	$\frac{10^9}{264000} = 3788 \pm 76$	$\frac{10^9}{216150} = 4626 \pm 93$

Table 3: Rates are for 4 9 month runs with a 8 kiloton cavity filler.

Table 4. Comparison
Fermilab 822 and Brookhaven 889

	Soudan 2 as is	822 cavity filler	BNL889
event rate far detector	3000 ν 8800 μ (from rock)	108,000 ν 330,000 μ	18,300 quasi
event rate near detector	40×10^6	$> 10^9$	638,000
date to completion	$\sim$ 2001	$\sim$ 2005	$\sim$ 2000
distances	1km 730 km	1km 730 km	1 km 3 km 20 km
masses	1. 40 ton, 2. 900 ton	1. 100 ton 2. 8 kton	1. 400 ton 2. 400 ton 3. 4.6 kton
mean energy	16 GeV	16 GeV	1 GeV
run time	1-9 month run	4-9 month runs	1-4 month run
type of experiment	appearance	appearance	disappearance
neutral current	yes	yes	$(\nu N \rightarrow \nu \pi^o N)$ (?)
$\nu_\tau CC$	yes	yes	no
detector	calorimeter	calorimeter	H_2O Cerenkov
site	underground	underground	surface
accelerator requirement	Main Injector	Main Injector	upgraded AGS
beam	new beam	new beam	new beam

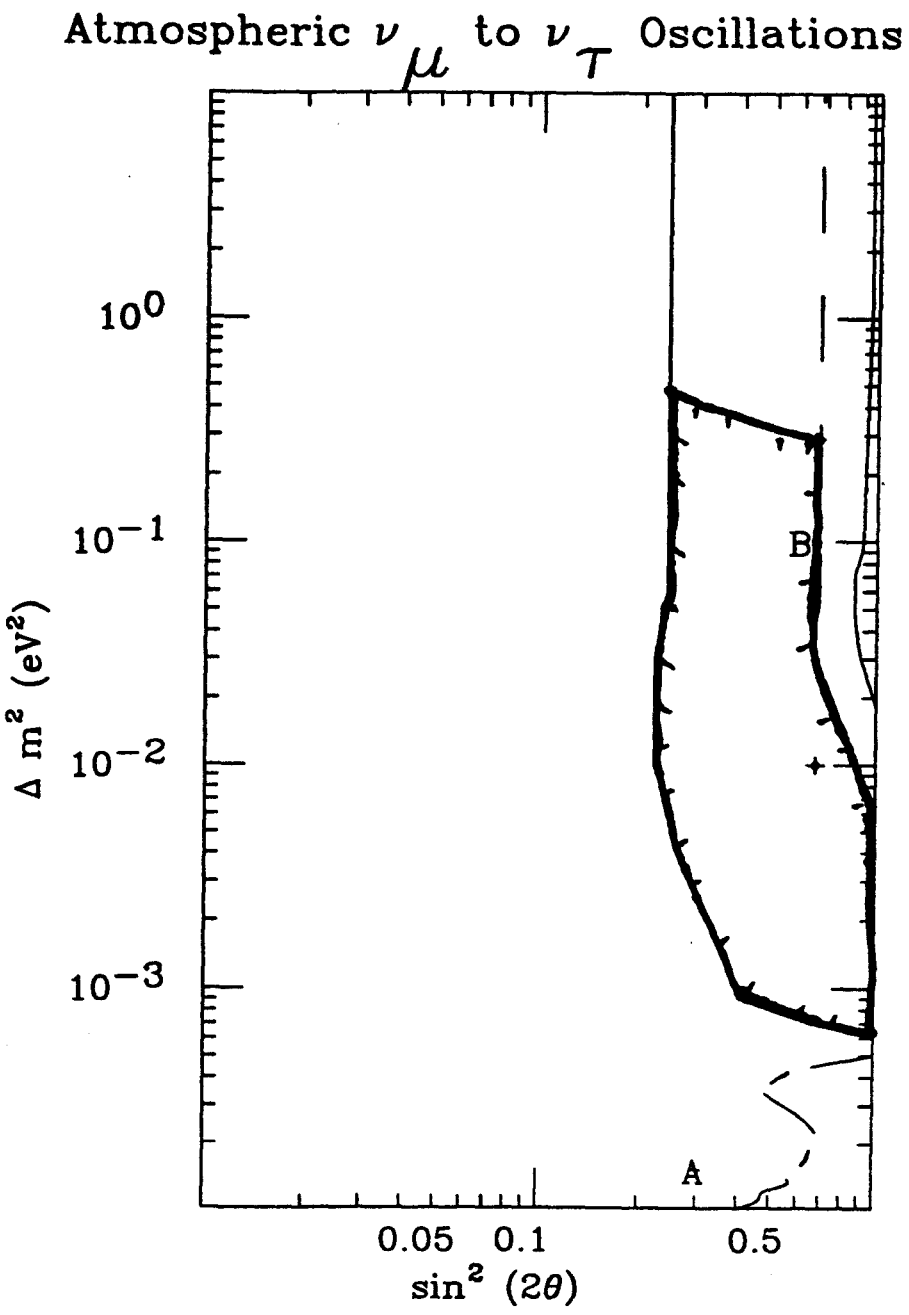

Figure 1. Region of Interest for the mode $\nu_\mu \rightarrow \nu_\tau$. The area shown is allowed at 90% CL by all accelerator experiments, the Frejus experiment, and the first 2.76 kiloton year analysis of the Kamiokande data.

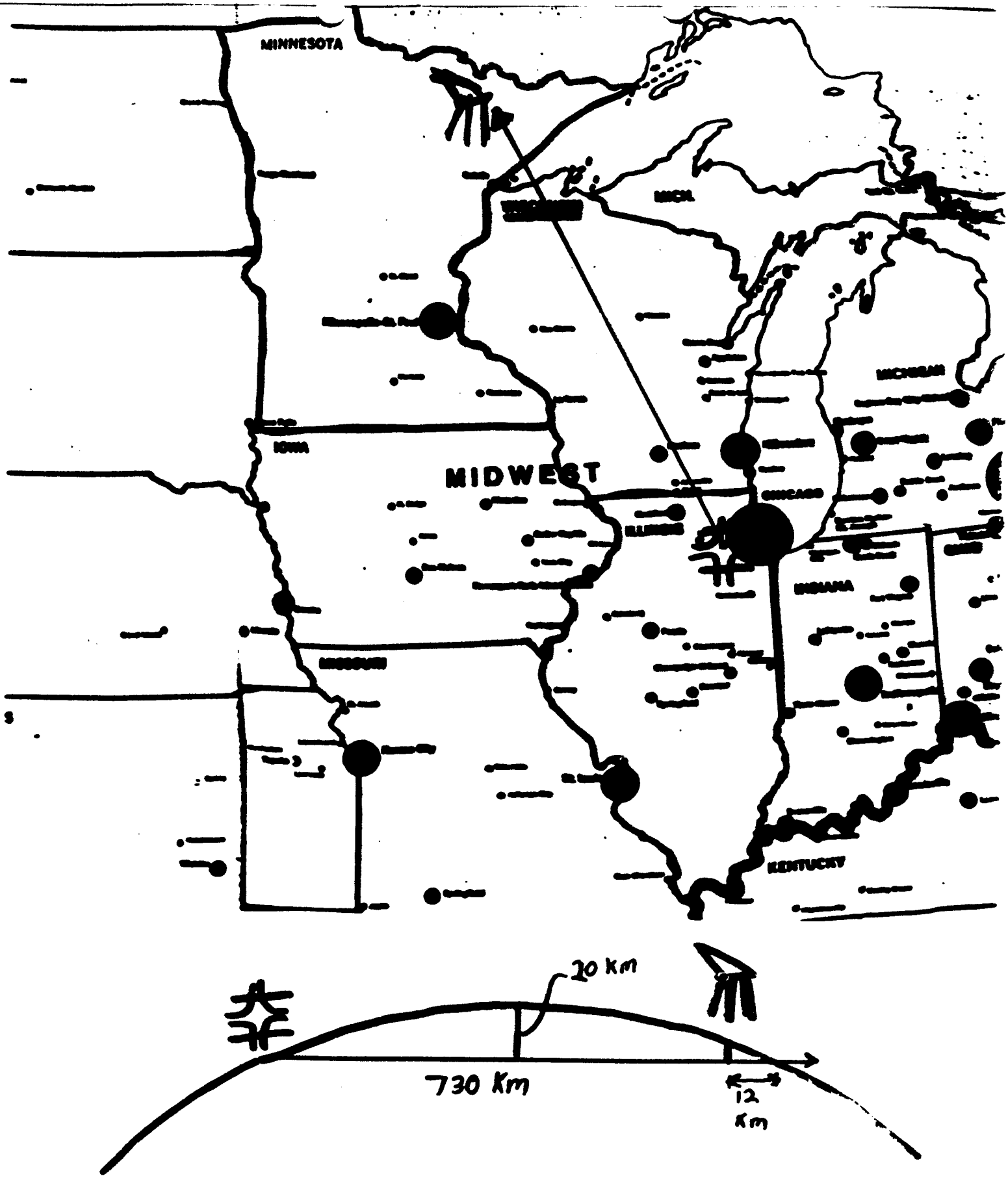

Figure 2. The approximate route of the beam from Fermilab to Soudan.

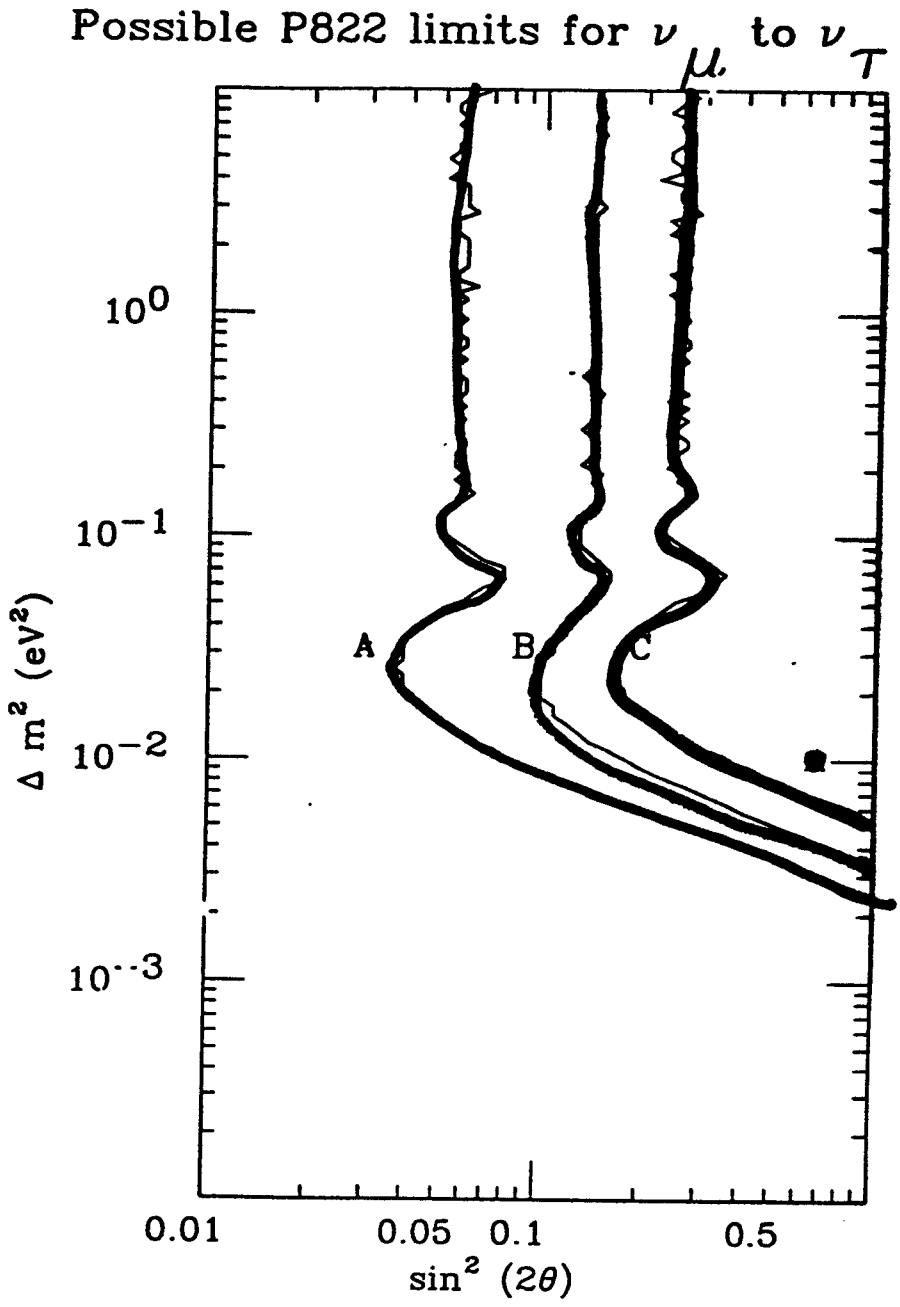

Figure 3. The limit curves from the original 822 proposal. Curve A was from the $R_{near/far}$ test. Curve B was from the $R_{\text{"nc"}/\text{"cc"}}$ test. Curve C was from the $R_{\bar{\nu}_e}$ test.

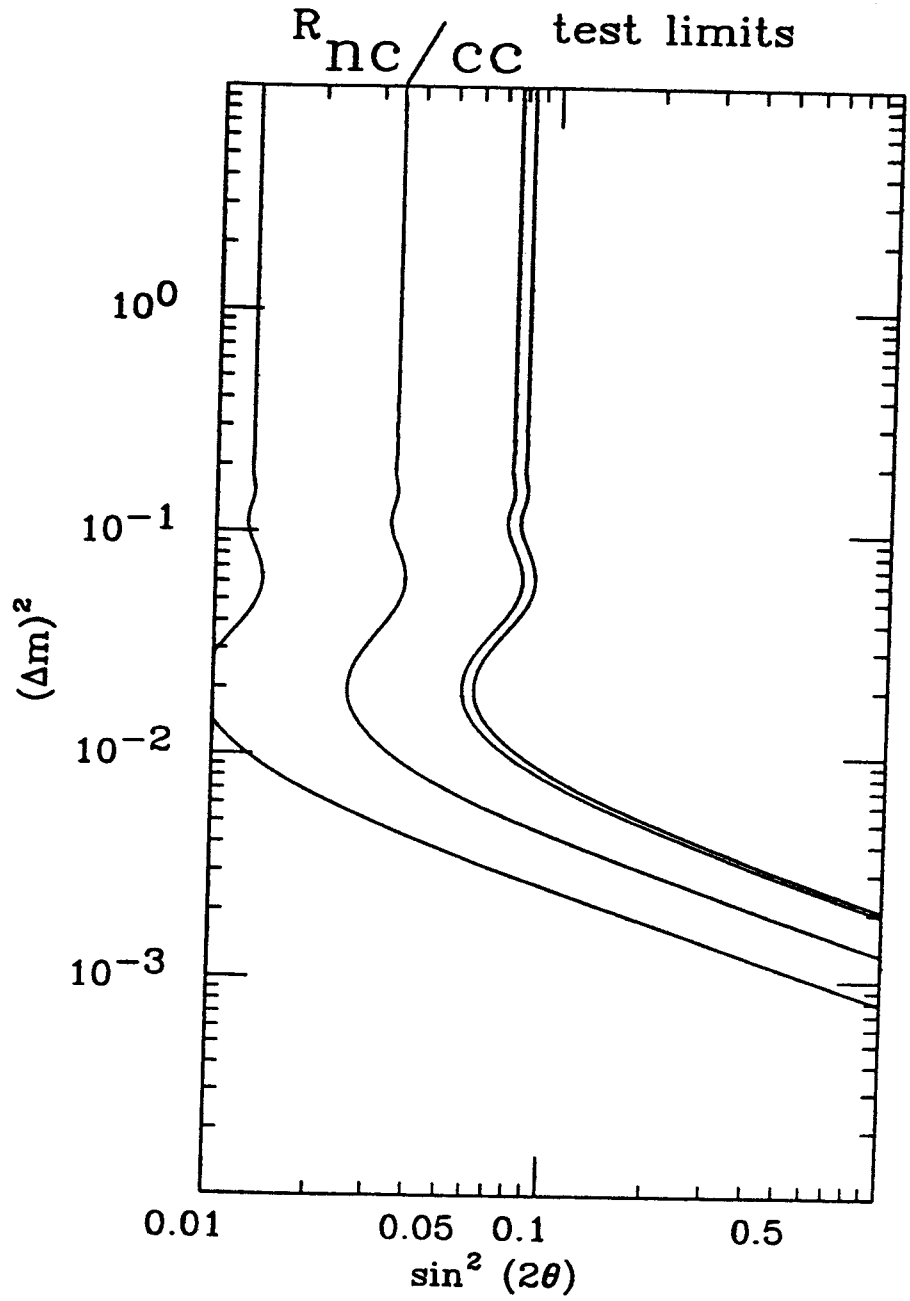

Figure 4. Estimated 90% CL limits we can set in the absence of a signal in 822 using the $R_{\text{"nc"}/\text{"cc"}}$ test. From left to right, the curves are for four nine-month runs and an 8 kiloton cavity filler assuming 0% and 2% systematic error, and one nine-month run and the existing Soudan detector assuming 0% and 2% systematic error.

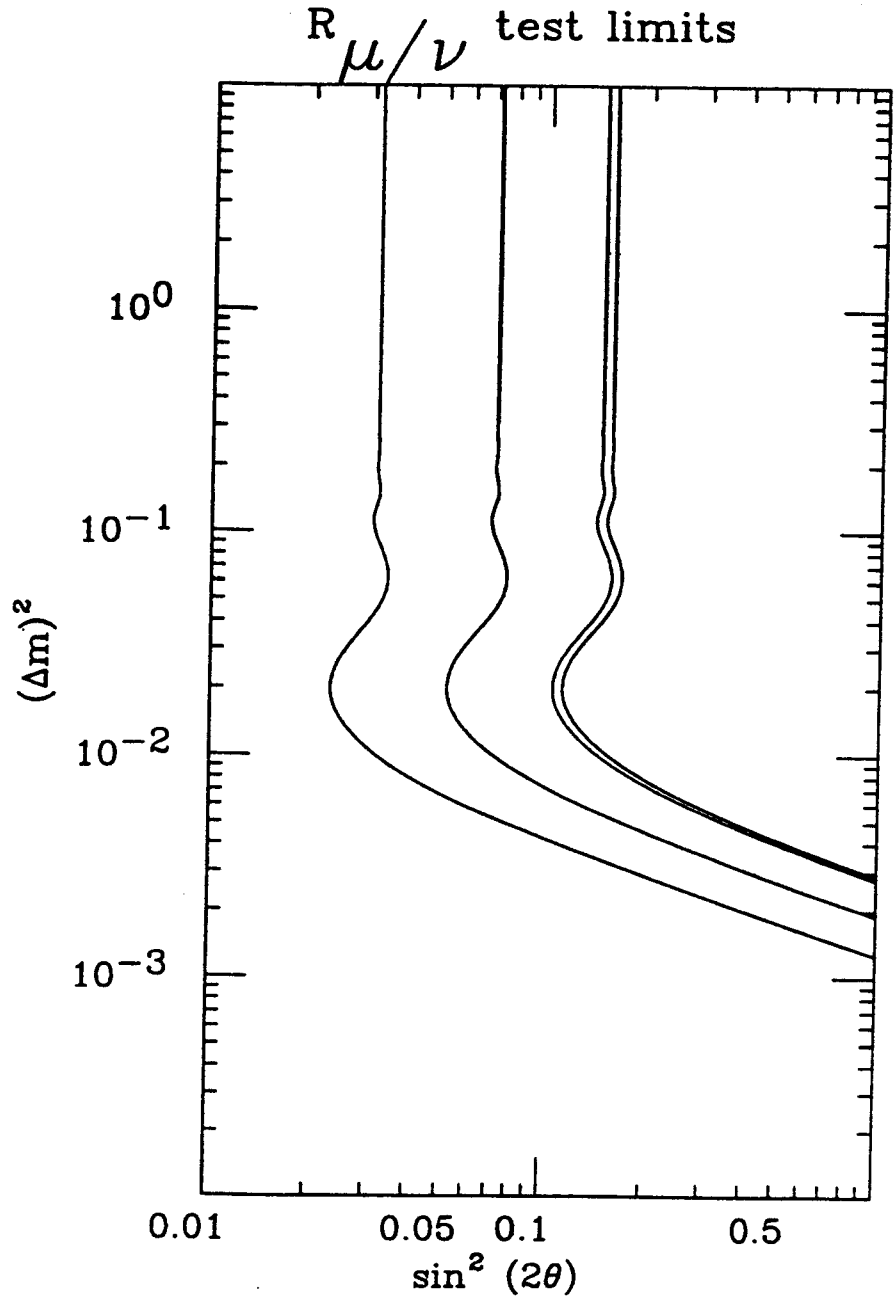

Figure 5. Estimated 90% CL limits we can set in the absence of a signal in 822 using the $R_{\bar{\nu}_e}$ test. From left to right, the curves are for four nine-month runs and an 8 kiloton cavity filler assuming 0% and 2% systematic error, and one nine-month run and the existing Soudan detector assuming 0% and 2% systematic error.

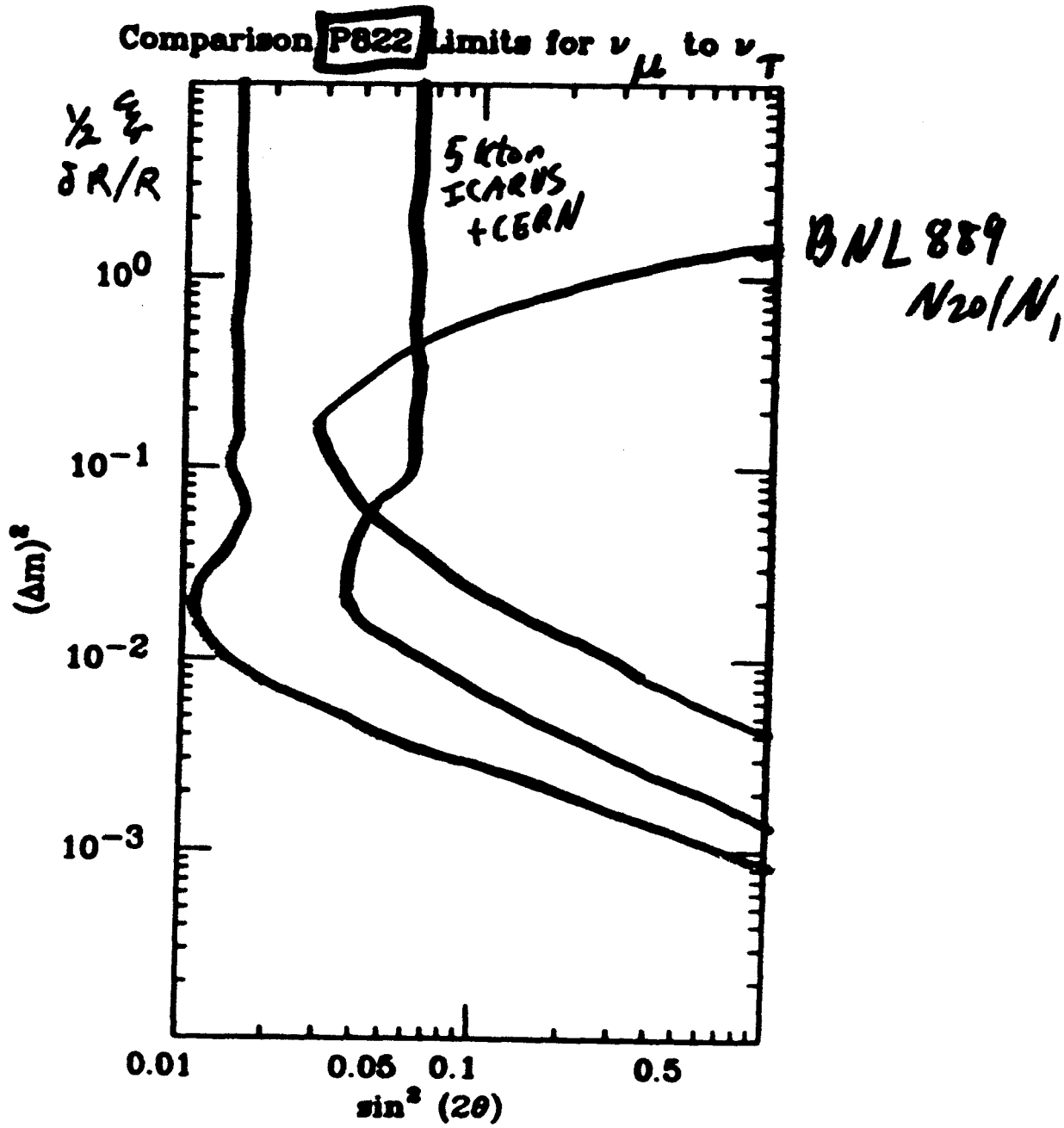

Figure 6. A comparison of 822 using a cavity filler and 0.5% systematic error with BNL 889 and an estimate from pointing a Cern beam at a 5 kiloton ICARUS detector at the Gran Sasso Laboratory.

Update to P822: Proposal for a long-baseline neutrino oscillation experiment from Fermilab to Soudan

8th March 1994

W.W.M. Allison[6], G.J. Alner[7], D.S. Ayres[1], L. Balka[1], W.L. Barrett[11], R.H. Bernstein[2], R.E. Blair[1], C. Bode[5], D. Bogert[2], P. Border[5], C.B. Brooks[6], V.A. Chechin[4], N. Christiansen[5], J.H. Cobb [6], D.J.A. Cockerill[7], R. Cotton[7], H. Courant [5], J. Dawson[1], D. Demuth[5], B. Ewen[10], T.H. Fields[1], H. Gallagher[1], G. Giller[6], M.C. Goodman[1], K. Heller[5], N. Hill[1], D.J. Jankowski[1], D. Johnson[2], T. Kafka[10], S. Kasahara[5], G. Koizumi[2], D. Krakauer[1], E.P. Kuznetesov[4], W. Leeson[10], P.J. Litchfield[7], F. Lopez[1], W. A. Mann[10], D. Maxam[5], M. L. Marshak[5], E.N. May[1], L. McMaster[10], R. Milburn[10], W. Miller[5], L. Mualem[5], A. Napier[10], W. Oliver[10], G.F. Pearce[7], D.H.Perkins[6], E.A. Peterson[5], L.E. Price[1], J. Repond[1], R. Rusack[5], K. Ruddick[5], J. Schneps[10], P. Schoessow[1], N. Sundaralingam[10], R. Talaga[1], J. Thron[1], T. Toohig[8], H. J. Trost[9], I. Trostin[3], V. Tsarev[4], G. Villaume[5], J. Volk[2], S. Werkema[2], and N. West[6]

Argonne[1] - Fermilab[2] - ITEP[3] - Lebedev[4]

Minnesota[5] - Oxford[6] - Rutherford[7] - SSC Lab[8]

Texas A&M[9] - Tufts[10] - Western Washington[11]

1 Introduction and summary

1.1 Introduction

In this document we address the issues raised by the PAC in their consideration of the P822 proposal for a long baseline neutrino oscillation experiment. They were:

1. The analysis strategy we propose to adopt and the systematic errors inherent in our measurement of the change in the ratio of apparent neutral current and charged current events due to neutrino oscillations between near and far Soudan 2 type detectors.

2. The gains to be obtained from a measurement of event energy at the two detectors.

3. The extension of the experiment with a new, more massive detector to reach the best possible sensitivity in Δm^2 and $\sin^2(2\theta)$.

One of the major features of the P822 proposal which distinguishes it from a below-τ-threshold experiment is that it offers a number of independent tests of neutrino oscillations e.g.:

- change in the fraction of apparent neutral current and charged current events between the near and far detectors
- change in the total energy spectrum of charged current events between the near and far detectors
- change in the hadronic energy spectrum of events without an identified muon between the near and far detectors
- deviations from the expected ratio of muons entering the far detector from interactions in the rock to the total event rate in the far detector
- change in the interaction rate in the far detector from that predicted by the rate in the near detector
- there is the potential to directly observe τ production

A crucial feature of a real signal in any test is that consistent effects must be seen in the other tests. We are thus shielded from the effects of systematic errors which might give a spurious result in any single test. Each of the tests has strengths and weaknesses in terms of statistical and systematic errors and the regions of Δm^2 and $\sin^2(2\theta)$ that it probes. In this document we will describe in detail the analysis strategy we have developed for two of the tests:

- The change of the fraction of charged current events between near and far detector offers the cleanest analysis in terms of systematic errors since many possible errors cancel.
- The change in the event energy spectrum between the two detectors provides an entirely independent oscillation test with quite different systematic errors which can separate the effects of Δm^2 and $\sin^2(2\theta)$.

Descriptions of the other tests are given in our previous proposals [1] and elsewhere [2].

These analyses can be done with the presently working 15M$ Soudan 2 detector with the addition of a downstream toroid. However, as we shall show below, a 1 kton detector at the distance of Soudan is limited by event rate and thus by statistical errors. The P822 collaboration is committed to doing the best experiment possible in the beam available from Fermilab. We believe that this involves a detector at the maximum possible distance, consistent with a sufficient event rate, in order to maximise the reach in Δm^2. This implies a larger detector than Soudan 2 in order to maximise the statistical precision and the reach in $\sin^2(2\theta)$. The larger detector also has the potential to provide the event rate which is necessary to enable cuts to be made which can separate τ production from the ν_μ background, thus exploiting the above-τ-threshold beam.

1.2 Summary

1. In section 2 we demonstrate an analysis strategy using the change in the fraction of charged current events from the near to the far detector which will enable us to set limits on neutrino oscillations in $\nu_\mu \rightarrow \nu_\tau$ in the Soudan 2 detector of $\sin^2(2\theta) \geq 0.14$ and $\Delta m^2 \geq 0.003\ eV^2$. For $\nu_\mu \rightarrow \nu_e$ the limit on $\sin^2(2\theta)$ would be 0.05. We show that systematic errors would limit this measurement at a $\sin^2(2\theta)$ of around 0.025 for $\nu_\mu \rightarrow \nu_\tau$ in a more massive Soudan 2 detector. Within these limits we have a high discovery potential. For example if neutrino oscillations exist with the Kamioka best fit parameters [3] the change in the fraction of CC events between near and far Soudan 2 detectors would yield an 8σ effect.

2. We reiterate that this experiment offers many checks of any apparent observation of oscillations. In section 3 we give an example of this by showing how oscillations can be observed by studying the difference in the measured CC total energy spectra between the near and far detectors which is *independent* of the above test. Observation of oscillatory behaviour in the energy spectra would be unambiguous evidence for neutrino oscillations. For the Kamioka parameters an additional, independent 6σ effect would be observed.

3. We are enthusiastic in wishing to extend the measurements that we can make in Soudan 2 to smaller mixing angles and to the direct observation of τ leptons. This will require the construction of a new, massive detector. We have entered into preliminary talks with several groups with a view to forming a larger collaboration to design and build such a detector. Section 4 expands on some of the considerations involved in the design of such a detector.

4. We envisage that the presently proposed experiment in the fine grain Soudan 2 detector will be backed up by a new, much more massive but possibly coarser grained detector. We request the PAC to give stage 1 approval for this experiment using Soudan 2. Approval now would have the following very desirable effects:

    - It will enable the present P822 collaboration to focus on the details of mounting the near detector at Fermilab and the upgrades proposed for the Soudan laboratory

- It will aid us in enlarging our collaboration, in particular for the design and construction of the new detector
- It will remove the uncertainty on the siting and design of the beam for E803/P822. The sharing of the beam construction and accelerator operating costs between two components of a neutrino oscillation program is an important advantage of the Fermilab program.
- It will demonstrate Fermilab's commitment to a long-baseline program which is vital if a comparison is to be made between the Fermilab and Brookhaven programs.

2 Analysis strategy for a two station experiment

We describe below our analysis strategy for the test which we consider has the smallest systematic errors and thus potentially the greatest reach in $\sin^2(2\theta)$; a measurement of the change in the fraction of charged current events between the near and far detectors. We detail the event classification procedures, the analysis formalism for a two station experiment including the effects of event acceptance and misidentification, and a discussion of the systematic errors expected.

2.1 Event classification by software filter

In our proposal we showed, by physicist scanning, that it was relatively easy to separate charged current (CC) events from neutral current (NC) events in Soudan 2 by observing the penetrating muon characteristic of CC events. It would be possible to scan all the events expected in the far detector. However the large numbers of events produced in the near detector and the large number of Monte Carlo events needed to determine corrections, make it necessary to use a program based separation method, although it will doubtless be less efficient than human scanning. We have adapted the reconstruction programs used for the present Soudan 2 proton decay experiment. These search for three dimensional tracks, calculating the track length and flagging whether or not the tracks exit the detector. It should be emphasised that the typical 20 GeV neutrino events from Fermilab are very different from the 0.5 - 1.0 GeV events for which the programs are optimised. It will be seen that the performance is good but improvements will be made by tuning for this new event configuration.

Figures 1a and 1b show the detector configurations used in the Monte Carlo. Figure 1a depicts an 86 ton near detector of 20 modules arranged in 5 rows of 4 modules, staggered to follow the beam, which enters at the same angle as the beam in the far detector. Events are generated in a central 50cm x 50cm region of the target module (shown in the figure). We demonstrated in our October 93 proposal that the neutrino beam in this central part of the beam spot corresponds closely to the beam in the far detector. Figure 1b shows a far detector similar to that presently installed and running.

Figure 2 plots the generated length of the muons in Monte Carlo near and far detector CC events versus the length of the longest track reconstructed in the event. The correlation is good. We will use the length of the longest reconstructed track as a flag for a muon.

The critical experimental difference between the near and far detector is that in the near detector events must be selected in a small region near the centre of the beam whereas events will be spread uniformly through the far detector. Figure 3a shows the length of the longest reconstructed track in Monte Carlo near detector CC events and 3b the same quantity for NC events. It can be seen that NC events are strongly peaked to short maximum lengths whereas the CC events typically have the maximum potential length available with only a small tail of short lengths, mostly due to low energy muons which do not exit the hadron shower region. A cut of 3.5m on the track length provides a good separation between CC and NC events. Figures 4a and 4b show the equivalent plots for all events produced in the far detector. There is no longer a clear separation between NC and CC events because many CC events are produced near the edge of the detector without sufficient potential length for the muon to exceed the cut length. It would be possible to define a fiducial volume in the far detector which maximised the muon potential length and minimised the possibility of hadron tracks from a neutral current event leaving the detector. However this would unnecessarily restrict the target mass and the statistics of the experiment. Instead we prefer to define a selection procedure which uses all of the available events but includes a category of events in which the potential path length of the tracks is too small to be able to distinguish between charged and neutral current.

The selection categories are:

1. Events with a reconstructed track longer than L (3.5m) are defined as charged current.
2. Events with no reconstructed track longer than L, AND with no track exiting the detector are defined as neutral current.
3. Events with no reconstructed track longer than L, AND with any track exiting the detector are defined as "out of acceptance"
4. Events with no track reconstructed

The confusion matrix for the near detector (defined such that the elements sum to 1.0) is:

Generated	Defined NC	Defined CC	Out of acceptance	No tracks	Total
Neutral current	0.138	0.023	0.061	0.014	0.236
Charged current	0.029	0.693	0.042	0.0	0.764

and for the far detector:

Generated	Defined NC	Defined CC	out of acceptance	No tracks	Total
Neutral current	0.086	0.017	0.120	0.020	0.243
Charged current	0.018	0.409	0.317	0.013	0.757

From these tables we find that our combined trigger and pattern recognition efficiency is 97%. Our acceptance is 88% for the near detector events and 53% for the far detector. These numbers could be equalised by different definitions of the fiducial volumes in the two detectors. However the event distributions in the two detectors will still be different and must be compensated for by the Monte Carlo. This correction is the major source of systematic error in the event definition procedure and is discussed in detail in section 2.4.2.

Near and far detectors with closely equal acceptance could be artificially produced by defining a detector of the same size as the near detector around each far detector event and only using hits within this pseudo-near detector in event reconstruction. Any event which was too close to the far detector edge to allow construction of a pseudo-near detector would be rejected as out of acceptance. Unfortunately this would reduce the fiducial mass of the far detector to only about 25% of its total mass and thus severely restrict the statistical precision of the experiment. It will however be a good check that the Monte Carlo calculations of acceptances and event misidentifications do not produce large biases.

2.2 Use of a toroid to increase CC acceptance

We propose to add magnetised iron toroid spectrometers downstream of both the near and far detectors. A preliminary design for the far detector toroid was given in our proposal. The major purpose of the toroids is to measure the change in the total visible energy of CC events between the near and far detectors, thus offering an independent test of neutrino oscillations (see section 3). However the toroid will provide extra muon identification, particularly for those events produced near the downstream end of Soudan 2 where there is not sufficient potential track length to provide muon identification. Events are defined as CC if a track passes completely through the toroid. The toroid acceptance is 57% for far detector CC events. We will investigate the possibilities of improving the definition of neutral current events by reconstructing tracks into the toroid and ensuring that no muons are missed. Adding the toroid identification we have a final identification matrix for the far detector given by:

Generated	Defined NC	Defined CC	out of acceptance	No tracks	Total
Neutral current	0.086	0.017	0.120	0.020	0.243
Charged current	0.013	0.559	0.179	0.006	0.757

Because the restricted target volume in the near detector guarantees a long potential length for most muons, the toroid does not add appreciably to the near detector acceptance.

2.3 Formalism for a two station experiment

We consider an experiment using the selection procedure defined in section 2.1. The number of selected charged current events (N''_{cc}), neutral current (N''_{nc}) and out of acceptance (OA) events can be written as:

$$N''_{cc} = F_{cc}N'_{cc} + F_{nc}N'_{nc} \quad (1)$$
$$N''_{nc} = F_{cn}N'_{cc} + F_{nn}N'_{nc} \quad (2)$$
$$OA = (1 - F_{cc} - F_{cn})N'_{cc} + (1 - F_{nc} - F_{nn})N'_{nc} \quad (3)$$

where
F_{cc} is the fraction of Monte Carlo muon events with reconstructed tracks longer than L cms,
F_{nc} is the fraction of Monte Carlo non-muon events with reconstructed tracks longer than L cms,
F_{cn} is the fraction of Monte Carlo muon events with no track longer than L cms AND no exiting track,
F_{nn} is the fraction of Monte Carlo non-muon events with no track longer than L cms AND no exiting track,
N'_{cc},N'_{nc} are the true numbers of events with and without a muon in the detector.

We can define two ratios that we measure in the far detector

$$R'' = \frac{N''_{nc}}{N''_{cc}} \quad (4)$$
$$T'' = \frac{N''_{cc}}{N''} \quad (5)$$

Where N'' is the total number of events observed.
Then

$$R'' = \frac{F_{cn}N'_{cc} + F_{nn}N'_{nc}}{F_{cc}N'_{cc} + F_{nc}N'_{nc}} \quad (6)$$
$$= \frac{F_{cn} + F_{nn}R'}{F_{cc} + F_{nc}R'} \quad (7)$$

and

$$T'' = \frac{F_{cc}N'_{cc} + F_{nc}N'_{nc}}{N''} \quad (8)$$
$$= (F_{cc} - F_{nc})T' + F_{nc} \quad (9)$$

where R' and T' are the ratios that would be obtained with perfect acceptance and identification

In our proposal we presented an analysis in terms of R'' (NC/CC) which is the variable used in experiments such as CCFR. However the ratio T'' (CC/total) only depends on the separation of events with long muons from the rest, i.e. does not depend on F_{cn} and F_{nn}. Also the expressions obtained in the following analysis are simpler and easier to interpret for systematic errors if T'' is used instead of R''. Of course in the limit of perfect acceptance and separation it would not matter which ratio is used but for the practical case we prefer to work in terms of T''.

We now consider the effects of ν oscillations. We initially consider the case of $\nu_\mu \rightarrow \nu_e$ as the algebra is simpler. We define P_e as the probability of a ν_μ turning into a ν_e, integrated over the energy spectrum. We also assume that all ν_e interactions are classified as NC and initially that we have perfect separation. At the far detector we have:

$$N'_{cc} = N_{cc}(1 - P_e) \quad (10)$$

$$1 - P_e = T'/T \quad (11)$$

where N_{cc} is the number of events with a muon and T is the ratio $\frac{CC}{total}$ in the absence of oscillations. Including the experimental acceptances and using equation 9 we find

$$1 - P_e = \frac{(T'' - F_{nc})}{(F_{cc} - F_{nc})T} \quad (12)$$

We may do exactly the same analysis at the near detector. Here the oscillation probability is 0. Using lower case quantities for the near detector we find

$$t = \frac{(t'' - f_{nc})}{(f_{cc} - f_{nc})} \quad (13)$$

Of course because of the difference in the acceptances of the two detectors $F_{cc} \neq f_{cc}$ and $F_{nc} \neq f_{nc}$.

Assuming that the unoscillated ratios are the same at the near and far detectors, i.e. t=T, we can substitute for T in the far detector formula, giving

$$(1 - P_e) = \frac{(T'' - F_{nc})(f_{cc} - f_{nc})}{(t'' - f_{nc})(F_{cc} - F_{nc})} \quad (14)$$

P_e and its associated error may be deduced from this expression. It can be seen that it is simply the ratio of the measured T'', t'' ratios near and far divided by the ratio of the acceptances for CC muons near and far, all quantities being corrected for the misidentification of NC events. If $\nu_\mu \rightarrow \nu_e$ then the right hand side of equation 14 will be less than 1.0

If instead of $\nu_\mu \rightarrow \nu_e$ oscillations we assume $\nu_\mu \rightarrow \nu_\tau$ then we can carry out the same analysis except that we have to correct for the fact that the integrated ν_τ cc cross-section is lower than the ν_μ CC cross-section at these low energies by a factor η (0.24) and that a fraction B (0.17) of τ's decay into μ's. Both of these effects reduce the size of changes in T'' and R'' produced by $\nu_\mu \rightarrow \nu_\tau$ oscillations compared with $\nu_\mu \rightarrow \nu_e$ oscillations. We then obtain

$$P_\tau = \frac{(t'' - f_{nc})(F_{cc} - F_{nc}) - (T'' - F_{nc})(f_{cc} - f_{nc})}{(t'' - f_{nc})((1 - B\eta)(F_{cc} - F_{nc}) - (T'' - F_{nc})(1 - \eta))} \quad (15)$$

It can be seen that the effect is to replace the factor $(F_{cc} - F_{nc})$ in equation 14 by

$$(1 - B\eta)(F_{cc} - F_{nc}) - (T'' - F_{nc})(1 - \eta)$$

Using the values obtained below the ratio of these factors is 1:2.7 and this quantifies the difference in sensitivity between $\nu_\mu \rightarrow \nu_e$ and $\nu_\mu \rightarrow \nu_\tau$.

2.4 Statistical and systematic errors

Using the above formulae we can calculate the statistical and systematic errors that we anticipate in our experiment. We emphasise that by performing a two station experiment we are, in general, only sensitive to changes between the two detectors. We do not have to determine absolute values of T or R though it will clearly be a crucial check of our analysis that we find consistency in the near detector with both previously measured quantities and the values found by E803. We have identified the following sources of systematic error:

1. Errors in the Monte Carlo calculation of the correction factors F_{cc} etc.
2. Changes in T due to uncertainty in the charm cross-section
3. Changes in T due to changes in the ν_e contamination between the near and far detector
4. Changes in T between the near and far detector brought about by changes in the neutrino energy spectrum
5. Differences in backgrounds at the near and far detector.

We can calculate the effects of changes in T between the near and far detectors by substituting $T = t + dT$ in equation 12 instead of $T = t$. This results in a spurious oscillation probability given by

$$dP_e = -\frac{(f_{cc} - f_{nc})}{(t'' - f_{nc})} dT \tag{16}$$

Substituting the numbers listed in section 2.4.1, we find

$$dP_e = -1.3dT \tag{17}$$

The equation for dP_τ has the same correction factor as equation 15 and therefore

$$dP_\tau = 2.7dP_e \tag{18}$$
$$= -3.5dT \tag{19}$$

2.4.1 Statistical errors

We assume that the statistical errors in the near detector are negligible compared with all other errors and do not consider them further.

Since our October 1993 proposal there has been a revision of the expected proton flux given by Fermilab. We now assume 5×10^{13} protons every 1.9 seconds for 100 hours per week and two 9 month runs. This is 40% of the proton flux assumed in our proposal. As a result we

now expect 2400 neutrino interactions from an unoscillated beam in the far detector instead of 6000. For completeness we repeat in Table 1 the table from our October proposal giving the numbers of expected events for $\nu_\mu \rightarrow \nu_\tau$, various oscillation parameters and various tests using this new flux and acceptances. $R_{\frac{\mu}{\nu}}$ is the ratio of the number of muons entering the detector from ν interactions in the rock to the total number of interactions in the detector. $R_{near/far}$ is the ratio of the total event rate in the near detector to the rate of muons passing through the Soudan 2 shield, our highest statistics test. New limit curves are plotted in Figure 5.

	$P_\tau = 0$	$P_\tau = 0.1$	$P_\tau = 0.2$	$P_\tau = 0.345$
R''	$\frac{240}{1280} = .187 \pm .013$	$\frac{259}{1170} = .222 \pm .0015$	$\frac{278}{1050} = .264 \pm .018$	$\frac{306}{887} = .345 \pm .023$
$R_{\frac{\mu}{\nu}}$	$\frac{7040}{2400} = 2.93 \pm .07$	$\frac{6340}{2250} = 2.81 \pm .07$	$\frac{5630}{2110} = 2.67 \pm .07$	$\frac{4610}{1890} = 2.44 \pm .07$
$R_{near/far}$	$\frac{4.0\times10^7}{17600} = 2270 \pm 45$	$\frac{4.0\times10^7}{15800} = 2530 \pm 51$	$\frac{4.0\times10^7}{14100} = 2840 \pm 57$	$\frac{4.0\times10^7}{11500} = 3470 \pm 69$

Table 1: Rates using the existing detector, including effects from misidentification, charm and ν_e's. The column with P=0.345 corresponds to the Kamioka oscillation parameters

The statistical error (dT'') on T'' is given by the binomial form

$$dT'' = \sqrt{T''(1-T'')/N''} \tag{20}$$

The values of the acceptance parameters and measured values of the ratios at the near and far detectors are:

F_{cc}	F_{nc}	f_{cc}	f_{nc}	T''	t''
0.734	0.069	0.880	0.081	0.586	0.692

To calculate the expected error on P_e (dP_e) we can differentiate equation 14 with respect to T'' (for $\nu_\mu \rightarrow \nu_e$). This yields a value of $dP_e = 0.0195$. For P_τ we have to apply the extra factor of 2.7 and obtain $P_\tau = 0.0526$

2.4.2 Systematic errors due to misidentification and acceptance

We repeat here the expression for P_e.

$$(1 - P_e) = \frac{(T'' - F_{nc})(f_{cc} - f_{nc})}{(t'' - f_{nc})(F_{cc} - F_{nc})} \tag{21}$$

It can be seen that the expression is rather symmetric in the acceptance parameters F_{cc}, F_{nc}, f_{cc}, f_{nc}.

The misidentification of a neutral current event as a charged current event (F_{nc}, f_{nc}) depends on the programs finding a long track, either because a hadron track managed to penetrate that far without interacting or, more likely, that the programs continued a hadron track through an interaction. Systematic errors could arise if the physics of the hadron showers was not perfectly simulated or if the tracking in the Monte Carlo is not completely correct. However since an error depends on finding a track longer than actually existed, uncertainties in the detector acceptance will not produce large effects. As both F_{nc} and f_{nc} are small and the physics errors will cancel from near to far detectors we consider that the systematic errors they introduce are negligible. Effects due to changes in the length cut are considered below.

The acceptance for charged current events (F_{cc}, f_{cc}) depends both on the fraction of events with muons of length less than the cut-off and on the acceptance of the detector and analysis for tracks longer than the cut-off. It can be seen that

$$dP_e \propto d(\frac{f_{cc}}{F_{cc}}) \tag{22}$$

The systematic errors in the two quantities will tend to cancel. We have identified four effects which could lead to a systematic difference between the acceptance in the near and far detectors:

1. Different numbers of events with muons physically shorter than the muon length cut because of differences in the energy distribution.

2. Errors in the detector geometries simulated in the Monte Carlo which could result in errors in the numbers of events passing the length cuts

3. Systematic differences caused by the choice of the value of the muon length cut L.

4. Differences in the numbers of events which are improperly reconstructed because of the different module geometries at the two locations

We have studied the change in the average energy distribution from the Monte Carlo, comparing the central part of the beam in the near detector to the beam in the far detector. The average energy only changes from 17.31 GeV to 17.34 GeV. The change in the numbers of accepted muons for this small change in average energy produces a negligible systematic error of $dT = 0.00010$.

Since the two detectors are made of identical components differences due to Monte Carlo geometry errors will be small. The maximum error that we can envisage is that the modules

are shifted by the equivalent of a row of tubes. We estimate that this would produce a negligible systematic error of $dT = 0.00002$.

We have changed the value of the length cut L within the range 3.25m to 3.75 m (around the best value of 3.5m). Although the values of F_{cc} vary between 0.72 and 0.76 and f_{cc} between 0.87 and 0.91 the calculated value of P_e varies by only 0.0005. We thus adopt this as a measure of the systematic error on P_e for this effect

The largest uncertainty in acceptance between the near and far detectors is the difference in reconstruction failures due to the different geometries in the two detectors. From the scatter plot in Figure 2, 5.3% of events are misassigned due to reconstruction failures. The failures would be the same for tracks located in the same positions relative to the modules and detector boundaries in the two detectors and would cancel in the ratio $\frac{f_{cc}}{F_{cc}}$. However, the distribution of tracks will be different due to the fiducial volume selection on the events in the near detector. We conservatively assume that the Monte Carlo is unable to correct for 5% of these reconstruction failures. In Figure 2 approximately the same number of CC are misreconstructed as NC as vice versa. However again to take account of the worst case we assume that the events that the Monte Carlo is unable to correct give rise to a change in $\frac{f_{cc}}{F_{cc}}$ equal to the full size of the misreconstructed and uncorrected fraction, giving us a systematic error of $d(\frac{f_{cc}}{F_{cc}}) = 0.00265$. From equation 21, substituting the values of the acceptances, dP_e is approximately equal to $0.85d(\frac{f_{cc}}{F_{cc}})$.

Reconstruction failures represent the largest source of systematic error which we have considered. However this systematic error is much less than the statistical error, and it can reduced further by;

1. Improvements in the reconstruction of muons in the programs
2. Hadron and muon beam calibrations of the near detector.
3. Extensive study of the causes of reconstruction failures in the Monte Carlo.

2.4.3 Systematic errors due to uncertainty in charm cross sections

The neutral current to charged current ratio is well measured at high energy. [4] The contribution to the charged current cross section by charm has been measured with opposite sign dimuons.[5] At the low energies of this proposed experiment, however, charm cross sections are poorly measured and there are theoretical uncertainties in extrapolating to lower energy. This can be parameterised as an uncertainty in the charm quark mass in the slow rescaling model.[6]

If the neutrino energy distribution and acceptance for the near and far detectors were identical, then any uncertainty in the cross section would cancel in the comparison of the near to far detector. Our beam calculations show differences in the energy distribution between the central 0.25 m of the near detector and the far detector, and in addition there is some uncertainty in that difference. We will measure the energy distribution and the radial dependence of the energy distribution in the near detector and in E803 and thus be able to test and refine our beam calculations. However, in order to estimate our systematic error due to charm cross sections, we conservatively take the uncertainty in the energy distribution to be 100% of the difference we currently obtain between the near and far detectors.

We have modeled the uncertainty due to charm using two beam Monte Carlos, and two calculations of the uncertainties in the charm cross sections. The results are given in Table 2. The two beam calculations came from the NUADA program used at Fermilab and the Monte Carlo program written by the E803 collaboration (PBEAM). The two calculations of the charm cross sections as a function of energy are given in Figure 6. The dashed curves are a parameterisation of the neutrino induced charm cross-sections from the E803 proposal [8]. The low, medium and high curves assume a charm mass of 1.9 GeV, 1.5 GeV and 1.1 GeV respectively. These curves bracket the high energy dimuon data. Another calculation due to Phillips [9] using more up-to-date structure functions and with a charm mass varying between 1.8 and 1.2 GeV is shown in the solid curves. The charm quark mass is better known than is implied by this large mass interval, but this range brackets the dimuon data and it can be argued that this parameterisation allows for additional variations which arise from strange sea and structure function uncertainties.

Table 2 shows the charm contribution to the charged current cross sections using the neutrino fluxes at the far detector and using the central part of the beam in the near detector. The numbers are the results of the calculation of the ratio

$$\frac{\int \sigma^{charm}(E)\phi_\nu(E)dE}{\int \sigma^{cc-total}(E)\phi_\nu(E)dE} \tag{23}$$

where $\phi_\nu(E)$ is the neutrino flux as a function of energy. The contribution to the systematic error is:

$$\frac{dT}{T(1-T)} = \frac{\int \Delta\sigma^{charm}(E)\Delta\phi_\nu(E)dE}{\int \sigma^{cc-total}(E)\phi_\nu(E)dE} \tag{24}$$

where $\Delta\sigma^{charm}(E)$ is the uncertainty in the charm cross section, and $\Delta\phi_\nu(E)dE$ is the uncertainty in the energy distribution.

Also shown in the table are the calculated charm fractions for the entire target of the 803 experiment. Since the target is transversely large compared to the central part of the beam at the near detector, the average neutrino event energy is lower and the contribution from charm is lower. We will verify our Monte Carlo predictions by comparing them with the charm contribution as a function of radius in the E803 emulsion.

Using the most conservative result in the table (0.42%), we assign a systematic error due to the uncertainty in charm cross sections to be dT = 0.00077. If the beam Monte Carlos are verified so that the uncertainties in the energy distribution can be reduced, there is still a systematic error from these estimated uncertainties in the cross section of 0.1% which leads to dT = 0.00020.

2.4.4 Systematic error due to electron neutrinos

Electron neutrinos interact with the same neutral and charged current cross sections as ν_μ's, but will all be classified as neutral current interactions in our analysis. The systematic error in the two station analysis arises from the uncertainty in the difference of the electron neutrino components at the near and far detectors. The contributions from various neutrinos by neutrino type were shown in figures 22 and 23 of our October 1993 proposal[1]. In the near central detector, $0.76\% \pm 0.03\%$ of the events were due to ν_e and $\bar{\nu}_e$, with the error due

PBEAM Monte Carlo; E-803 $\sigma's$

	high	mid	low
near	1.77%	1.21%	0.75%
far	2.19	1.51	0.96
E803	1.58	1.08	0.66
(near-far)	0.42	0.30	0.21

NUADA Monte Carlo; E-803 $\sigma's$

	high	mid	low
near	1.82%	1.24%	0.77%
far	2.08	1.42	1.01
E803	1.50	1.01	0.60
(near-far)	0.26	0.18	0.13

PBEAM Monte Carlo; Phillips' $\sigma's$

	high	mid	low
near	1.41%	0.92%	0.59%
far	1.83	1.22	0.80
E803	1.24	0.80	0.51
(near-far)	0.42	0.30	0.20

Table 2: Predicted charm cross sections as a fraction of the total charged current cross section.

to Monte Carlo statistics. In the far detector, they contributed $0.65\% \pm 0.07\%$ of the events. We take as the present uncertainty 200% of this difference, which is 0.22% of the events. This leads to a systematic error dT = 0.00167. The large uncertainty in the difference of fluxes is currently dominated by the statistics of the monte carlo.

We can estimate how accurately we can expect to extrapolate the ν_e's in the near detector to those in the far detector. From our beam Monte Carlo, 80% of the ν_e come from K_{e3} decays, 5% from $K_L's$ and 15% from $\pi's$. Figure 7 shows the energy dependence of the neutrino event rate in the near detector for 5 radial slices of a near detector, from 0-0.25 m to 2-3 meters. This is the same plot as Figure 20 in the revised proposal, but the contributions from π and K decay are shown separately. The energy distribution of neutrinos from π decay varies considerably in different angular regions of the beam. However, because of the larger transverse momentum available in the K decays, the energy distribution of neutrinos from K decay is much less variable. Thus the extrapolation of the ν_e portion of the beam to the far detector will be less sensitive to misalignments and energy spectrum differences than the ν_μ part.

2.4.5 Systematic error due to changes in the energy spectrum between the near and far detectors

Variations in energy spectrum between the near and far detectors were discussed with regard to the charm cross sections above. We have run our detector monte carlo to determine the difference in the generated R and T values integrating over the differences in the energy distributions. Using the uncertainties in energy distribution from NUADA, there is a corresponding uncertainty in dT = 0.00004. Using the PBEAM Monte Carlo, we found dT = 0.00009.

A second source of systematic can be generated by uncertainties in the ν_μ cross sections

if the near and far energy distributions are not identical. The major uncertainty in the ν_μ charged current cross section was charm production discussed above. Most other uncertainties tend to cancel. We have studied the effects of uncertainties in the low Q^2 deep inelastic cross-sections and the parameterisation of the resonance production and quasi-elastic cross-sections. We find that the changes produced in T due to these uncertainties are small. The cross-sections for resonance production and quasi-elastic scattering are parameterised in terms of form factors whose main uncertainty lies in the value of the axial-vector mass, which has a world-average value of 1.032±.036 GeV. The uncertainty in this parameter, when folded in with the differences in energy spectrum for the near and far detectors produces a change in T of 0.0002. Most high statistics neutrino measurements of deep inelastic scattering have been made at much higher energies than those of this experiment. As a result, there is some ambiguity in the low Q^2 region, which lies outside the range where the parton distributions are well constrained. One approach is to extrapolate the Q^2 evolution of the parton distributions outside the range of the Q^2 cuts on the data that went into constructing the parton distributions. We have estimated the uncertainties due to this by continuing the extrapolation of the CTEQ1M parton distributions from 4.0 GeV^2 to 1.0 GeV^2. The uncertainty in T resulting from such an extrapolation is 0.0003.

A third source of systematic errors is misalignment of the beam which could change the energy spectrum incident on the far detector. The center of the beam has a higher mean energy than the outer parts because of the kinematics of the decays producing it. We have, of course, the best of beam monitors, the near detector. We expect to be able to determine the centre of the beam in the near detector relative to the optical centre of the horn to better than 5cm, thus determining the beam direction to 100 μradians. This gives an error in the beam centre at Soudan of 70m. Satellite surveying will give the geographical positions to the same or better precision. This is much smaller than the angle subtended by the centre part of the beam that we are using in the near detector. Thus any error due to misaiming will be much less than the error due to energy differences already discussed, and will be negligible.

Although alignment of the beam is not a problem for the two detector T test, it is crucial for the near/far disappearance test discussed in earlier proposals. We plan to use the standard Fermilab neutrino beam instrumentation and we will obviously cooperate closely with E803 in beam monitoring. In addition we are considering installing beam profile monitors in the near detector area, in deep wells at the Fermilab site boundary, and on the surface near the Soudan mine, in order to guarantee that the pointing of the beam is understood and is stable with time.

2.4.6 Errors due to background events

The background of events within the Fermilab beam spill will be different at the near and far detectors. At Soudan we have measured the rate of events with contained vertices arising from atmospheric neutrino interactions or interactions of cosmic ray muons in the rock. Applying the Fermilab beam duty cycle gives a completely negligible background. The near detector is close to the surface and in a much noisier environment and thus backgrounds could be a problem. The CCFR experiment has measured its neutral current background within the beam spill as 800 events with a detector threshold of 20GeV. If we extrapolate this to a threshold of 0.5 GeV, appropriate to our detector, using a cosmic ray spectral index of

2.6 we would obtain a background of 2%. However this is an upper limit to any background as our near detector will be some distance underground and is much smaller than CCFR. The rate of non beam associated background events can of course be measured to very high precision by monitoring at off-spill times. We conclude that errors due to this source will be negligible.

2.4.7 Limits on $\sin^2(2\theta)$

Having estimated the above errors on P we can translate them into limits on $\sin^2(2\theta)$ via the usual equation:

$$P = \sin^2(2\theta)\,\sin^2(1.27\,\Delta m^2\,\frac{L}{E_\nu}) \tag{25}$$

For illustration we will give the limits on $\sin^2(2\theta)$ in the limit of saturated oscillations, i.e. where the $\sin^2$ term involving Δm^2 integrates to 0.5

To calculate a 90% confidence limit on $\sin^2(2\theta)$ we must multiply dP by a factor of 1.3 to convert from σ to 90% confidence and a factor of 2 for the above integral, a total factor of 2.6.

Table 3 summarizes the contributions of the above effects to the errors and limits.

Contribution	dT	dP_e	dP_τ	$\sin^2(2\theta)$ $\nu_\mu \rightarrow \nu_e$	$\sin^2(2\theta)$ $\nu_\mu \rightarrow \nu_\tau$
Statistics	0.0100	0.0195	0.0526	0.0507	0.1368
MisID-energy cut	0.00010	0.00013	0.00035		
MisID-Δ(Acceptance)	0.00002	0.00003	0.00008		
MisID-reconstruction fail		0.00225	0.00608		
Length cut		0.00050	0.00135		
ν_e	0.00167	0.00220	0.00594		
Charm	0.00077	0.00099	0.00268		
Energy spectrum-PBEAM	0.00009	0.00009	0.00025		
M_A	0.00020	0.00026	0.00070		
Q^2 cutoff	0.00030	0.00039	0.00105		
Total Systematics		0.00336	0.00928	0.00874	0.02413
Statistics and Systematics		0.0198	0.0534	0.0515	0.1388

Table 3: Summary of statistical and systematic error

The systematic errors have been added in quadrature. It can be seen that at the present levels of statistics our experiment is not limited by systematic errors but that the systematic errors would have to be very carefully controlled if a detector with an order of magnitude more mass was constructed.

3 Limits from total visible energy measurements

The addition of a toroidal momentum analysing magnet downstream of the existing Soudan 2 detector and a similar magnet behind the near detector would greatly enhance the capability of the experiment. For a CC event the energy of the muon, E_μ, would be measured by the toroid and the hadronic energy, E_{had}, would be measured calorimetrically in the detector modules allowing $E_\nu = E_{mu} + E_{had}$, the energy of the interacting neutrino, to be obtained. A comparison of the near and far energy spectra of CC interactions would not only be a valuable check on systematic effects due to misunderstanding of the beam but would also provide *unambiguous* evidence for oscillations. In particular, given a non-zero value of $\sin^2(2\theta)$, oscillations in the event rate as a function of energy would be visible and the value of Δm^2 could be determined. This is in contrast to the measurement of T'' where only a contour in the Δm^2,$\sin^2(2\theta)$ plot is found. A comparison of the *shapes* of the energy spectra measured in the near and far stations would allow oscillations to be detected, or $\sin^2(2\theta)$ - Δm^2 limits to be set *independently* of the absolute normalisation of the exposures in the two detectors.

The momentum resolution of the toroidal magnet system discussed in the proposal is expected to be:

$$\frac{\Delta p_\mu}{p_\mu} = 20\%$$

for muons exiting the detector with $p_\mu > 2.0\ GeV/c$. It has an acceptance of 57% for all muons from CC events in the far detector.

The hadronic energy resolution of the calorimeter modules has been determined by simulations to be

$$\frac{\Delta E_{had}}{E_{had}} = \frac{90\%}{\sqrt{E_{had}/1GeV}}$$

for the hadronic component of the final states of neutrino interactions from the Main Injector beam. On average $E_\mu = E_{had} = E_\nu/2$ and the effective resolution is $\Delta E_\nu/E_\nu \sim 17\%$ at $E_\nu = 20\ GeV$, where the event rate is maximum.

In two nine-month runs with 5×10^{13} *ppp* on target 500 identified and fully measured CC events are expected. Figures 8 and 9, which include the energy resolution of the calorimeter and toroidal magnet, compare the near and far energy (E_ν) spectra, normalised to the same number of events, for $sin^2(2\theta) = 1.0$ and $\Delta m^2 = 0.01$ and $0.1\ eV^2$ respectively. The error bars indicate the expected errors for a sample of 500 CC events in the far detector. Oscillations would be clearly visible[1].

Comparison of the shapes of the near and far energy spectra for CC events can be made using maximum likelihood or, equivalently, a Fourier analysis of the $1/E_\nu$ distributions[10]. The

[1]Energy distributions are shown for the sake of convention. The data would be more advantageously displayed as distributions of reciprocal energy, $dn/d(1/E_\nu)$, since the 'wavelength' of oscillations is constant as a function of $1/E_\nu$.

disappearance limits in the Δm^2 - $sin^2(2\theta)$ plane obtainable from such a test and assuming $\nu_\mu \rightarrow \nu_e$ are shown on Figure 10. The solid line shows the limits obtainable if the absolute normalisation of the exposures of the two detectors is known and the total numbers of CC events in the near and far detectors are compared. This comparison could indicate a non-zero value of $\sin^2(2\theta)$ but would give no information on Δm^2. The dashed line on Figure 10 indicates the limits obtainable from a comparison of the *shapes* of the near and far *spectra only*, i.e. with a free overall normalisation. This limit curve turns over at high Δm^2 due to the finite energy resolution of the calorimeter + toroid system. Also shown on the same Figure is the limit curve obtained by combining these two tests. Systematic uncertainties in $\phi_\nu(E_\nu)$ between the near and far detectors will primarily reduce our ability to set limits or detect oscillations only in the region of small Δm^2 and $\sin^2(2\theta) \sim 1$.

As an example of the additional power that the momentum analysing magnet would add to the experiment, even with the modest statistics of 500 fully measured CC events, an 8 standard deviation deficit would be observed in the number of CC events in the far detector and an *independent* 8 standard deviation effect would be obtained from a comparison of the shapes of the near and far E_ν spectra for $\Delta m^2 = 0.01\ eV^2$ and $\sin^2(2\theta) = 1$.

For the same exposure 880 CC events with fully contained hadronic energy and the muon identified (of which 500 would be fully measured) are expected. The disappearance limits which could be achieved by a comparison of the numbers of such CC events in the near and far detectors are shown in Figure 11. The greater reach in $\sin^2(2\theta)$ is due to the increase in the number of events counted. The hadronic energy in a neutrino interaction is, on average, $E_\nu/2$ although there are large fluctuations due to the flat $y = E_{had}/E_\nu$ distribution. A measurement of E_{had} in the calorimeter for CC events would, therefore, be a crude measurement of E_ν and some information on Δm^2 could be obtained from a comparison of the E_{had} distributions observed in the near and far detectors. The dashed line on Figure 11 shows the limits which would be achieved by this comparison with free overall normalisation between the two detectors. These are less stringent than those obtained from the comparison of the $E_\nu = E_{had} + E_\mu$ distributions discussed above because of the flat y distribution.

From the foregoing we conclude that the addition of a muon momentum analysing system to both the near and far detectors would be a powerful enhancement to this experiment. It would provide control of systematic effects and allow limits to be obtained, or neutrino oscillations detected, independently of the normalisation of the relative exposures of the near and far detectors.

4 The design of a new massive detector

From the analysis in Section 2 it can be seen that systematic errors become a major consideration in an experiment aiming at limits on $\sin^2(2\theta)$ for the mode $\nu_\mu \rightarrow \nu_\tau$ much below 0.03. The present P822 proposal using the Soudan 2 detector has statistical limits some way above this value and would clearly benefit from increased mass. Costs dictate that any new, much more massive detector will be much coarser grained than Soudan 2. Detector R&D

is needed to design a massive detector which costs significantly less per ton than Soudan 2 without dramatically increasing the systematic errors of the experiment.

A major advantage of the Fermilab beam compared with that from the AGS at Brookhaven is that the beam energy is above τ threshold. Thus it is in principle possible to verify that oscillations have taken place into ν_τ by a more direct identification of τ leptons than the change in N_{cc}/N. We are investigating several possible identification criteria:

- High and missing p_t in the decay $\tau \rightarrow \mu$
- High energy electrons from the decay $\tau \rightarrow e$
- High hadronic energy from the decay $\tau \rightarrow hadrons$

Separation of τ leptons will involve strong cuts to isolate regions of phase space populated by ν_τ but not by ν_μ interactions. Although Soudan 2 would almost certainly be more powerful at separating such events than any affordable new detector, the number of charged current ν_τ interactions in a two year run is only about 200, even for maximal mixing. In any given τ decay channel there will be rather few events. An important goal in the design of a massive detector is to obtain sufficient events to enable these cuts to be applied while maintaining enough resolution to separate τ events from background.

It is clear that these goals places strong constraints on the design of a new detector. One possible configuration is thick steel plates separated by Resistive Plate Chambers (RPC's) [1]. A similar proposal has been made by the Caltech group in the GENIUS proposal for a ν oscillation experiment from CERN to Gran Sasso [11]. RPC's can achieve nsec timing and can be instrumented with narrow readout strips for good spatial resolution. The Caltech group has carried out tests of an RPC calorimeter in a test beam at CERN[13]. Alternatively slower, but more conventional, detectors such as drift chambers, possibly interspersed with RPCs for timing, are also under consideration. To repeat our energy spectrum analysis in a new detector and also to measure muon p_t requires magnetic analysis. In a big detector this would have to be much more closely integrated into the detector than the proposed Soudan 2 toroid and requires extensive study.

Such a detector would also considerably extend our knowledge of atmospheric neutrinos. The statistics on atmospheric neutrino interactions above 1 GeV are very limited from current detectors, both because of overall event rate and because these high energy events are not contained within the detectors. It is not currently clear whether or not the deficit of ν_μ observed around 500 MeV neutrino energy is also present above 1 GeV. If the deficit is due to oscillations then there will be a characteristic energy variation. If it is due to other physics (e.g. proton decay as suggested by reference [12]) or experimental errors then new data above 1 GeV may be crucial. To demonstrate that high energy neutrino events originate inside the detector requires good timing to discriminate between entering and leaving tracks. Fast RPC's could provide this. This physics would provide a second string to the bow of a large underground detector of the kind needed to extend P822.

A preliminary design for a massive detector was described in our October 1993 proposal document. This still remains valid but much work remains to be done to fully address the highly desirable goals described above. We have initiated discussions with several groups with a view to forming a new collaboration to design and build such a detector.

5 Conclusions

5.1 Request for stage 1 approval

This document provides detailed answers to the PAC's questions about P-822. The case for a high energy (above τ threshold) long baseline experiment is compelling, particularly in comparison to the low energy experiment already approved at Brookhaven. The discovery of neutrino oscillations, and nonzero neutrino masses, would have profound implications for our views of physics and of cosmology. We therefore request that the PAC recommend stage 1 approval of this experiment.

The collaboration is enthusiastic about the prospect of improving the mixing angle sensitivity of our experiment by the construction of a new massive far detector, which could also have the additional potential for better identifying tau neutrino events and for studying high energy atmospheric neutrino interactions. A positive PAC response to our request for stage 1 approval would greatly aid our pursuit of these additional goals with an enlarged collaboration. It would also demonstrate Fermilab's firm commitment to a comprehensive program of short and long baseline experiments to discover neutrino oscillations.

5.2 Future plans

After stage 1 approval of this proposal, the collaboration plans to pursue the following tasks:

1. Develop detailed analysis strategies for the other neutrino oscillation tests listed in section 1 (as we have already done in sections 2 and 3 for the first two tests). In particular we will investigate the possibilities for direct detection of τ's in Soudan 2
2. Continue design studies of a new massive far detector, with emphasis on:
   - Identification of τ events
   - Identification of high energy atmospheric neutrino events,
   - Detailed development of RPC and drift chamber detector options,
   - Cost estimates.
3. Begin engineering design and performance optimisation studies of near and far toroid spectrometers.
4. Prepare for test beam studies of Soudan 2 calorimeter modules at Fermilab, to study their response to high energy charged particles and Fermilab backgrounds.

List of Figures

References

[1] FERMILAB PROPOSAL P–822; Proposal for a Long Baseline Neutrino Oscillation Experiment from Fermilab to Soudan, Allison *et al.*, October 1991; revised October 1993.

[2] Neutrino oscillations: past, present, and future, J. Schneps, 15th Int. Conf. on Neutrino Physics and Astrophysics (Neutrino 92), Grenada, Spain, June 7-12, 1992. (Tufts report TUHEP-92-03)

[3] K.S. Hirata et al. Phys. Lett. **B280**, 146 (1992); **B205**, 416 (1988).

[4] Arroyo *et al.*, NEVIS R1498, Submitted to Phys. Rev. Lett. 1994.

[5] S. A. Rabinowitz *et al.*, Phys. Rev. Lett. **70** (1993) 134; C. Foudas *et al.* Phys. Rev. Lett. **64** (1990) 1207; B. Strongin *et al.* Phys. Rev. **D43** (1990) 2057; H. Abramowicz *et al.*, Z. Phys. **C15** (1982) 19.

[6] R. Brock, private communication. Also see R. Phillips, *Nucl. Phys* **B212**, p109, 1983.

[7] Conceptual Design Report: Main Injector Neutrino Program, 1991.

[8] FERMILAB PROPOSAL P–803, Muon Neutrino to Tau Neutrino Oscillations, Kodama *et al.*, October 1990 and revisions.

[9] R. Phillips, private communication.

[10] J. H. Cobb, Neutrino Oscillation Limits from Total Energy Measurements, Soudan 2 Internal Note, unpublished

[11] D. Michael, proposal for the GENIUS detector (unpublished).

[12] W.A. Mann, T. Kafka and W. Leeson, Phys. Lett. **B291**, 200 (1992).

[13] D. Michael, private communication.

List of Tables

a)

b)

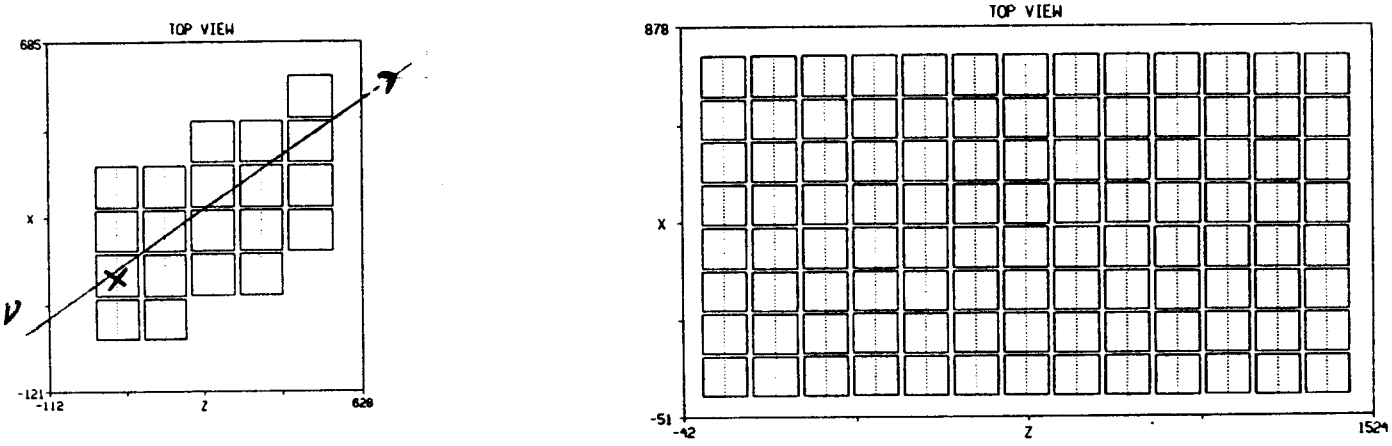

Figure 1: a) The far detector configuration; b) The near detector configuration. Vertices in the near detector were generated in the center of the beam in the marked module. Scales are in cm.

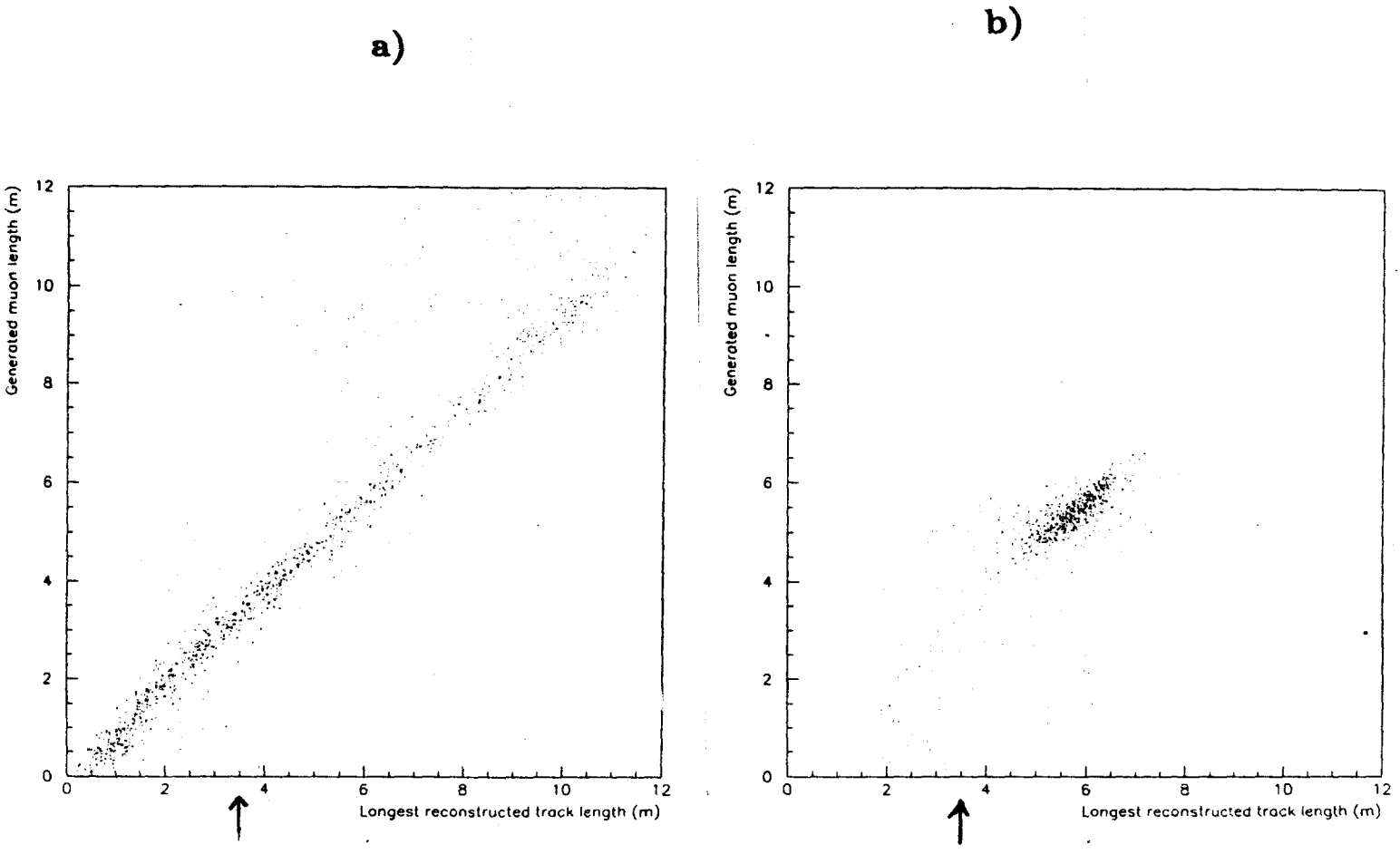

Figure 2: Generated versus reconstructed μ track length for a) the far detector; b) the near detector.

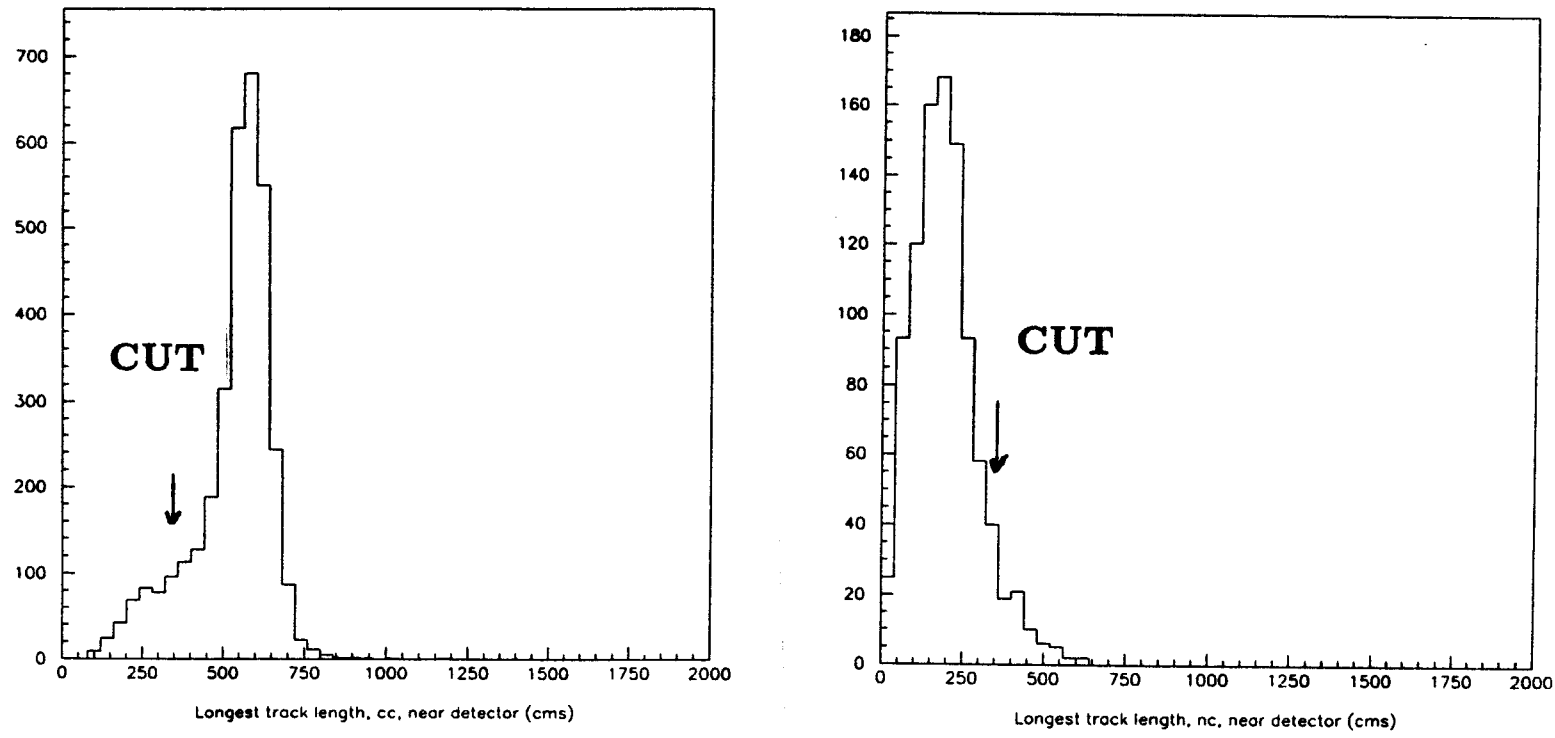

Figure 3: Longest track length for a) CC events in the near detector; b) NC events in the near detector.

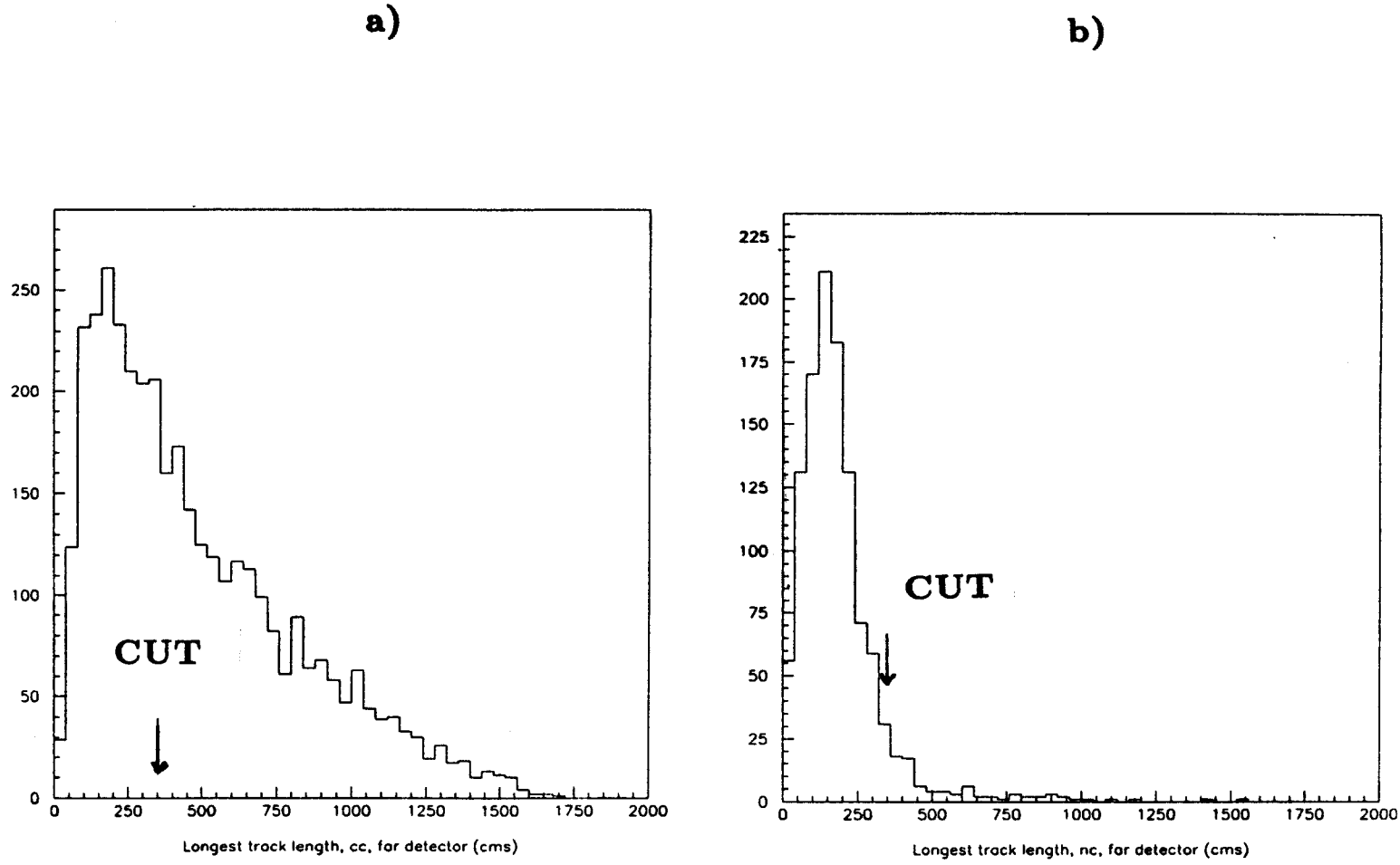

Figure 4: Longest track length for a) CC events in the far detector; b) NC events in the far detector.

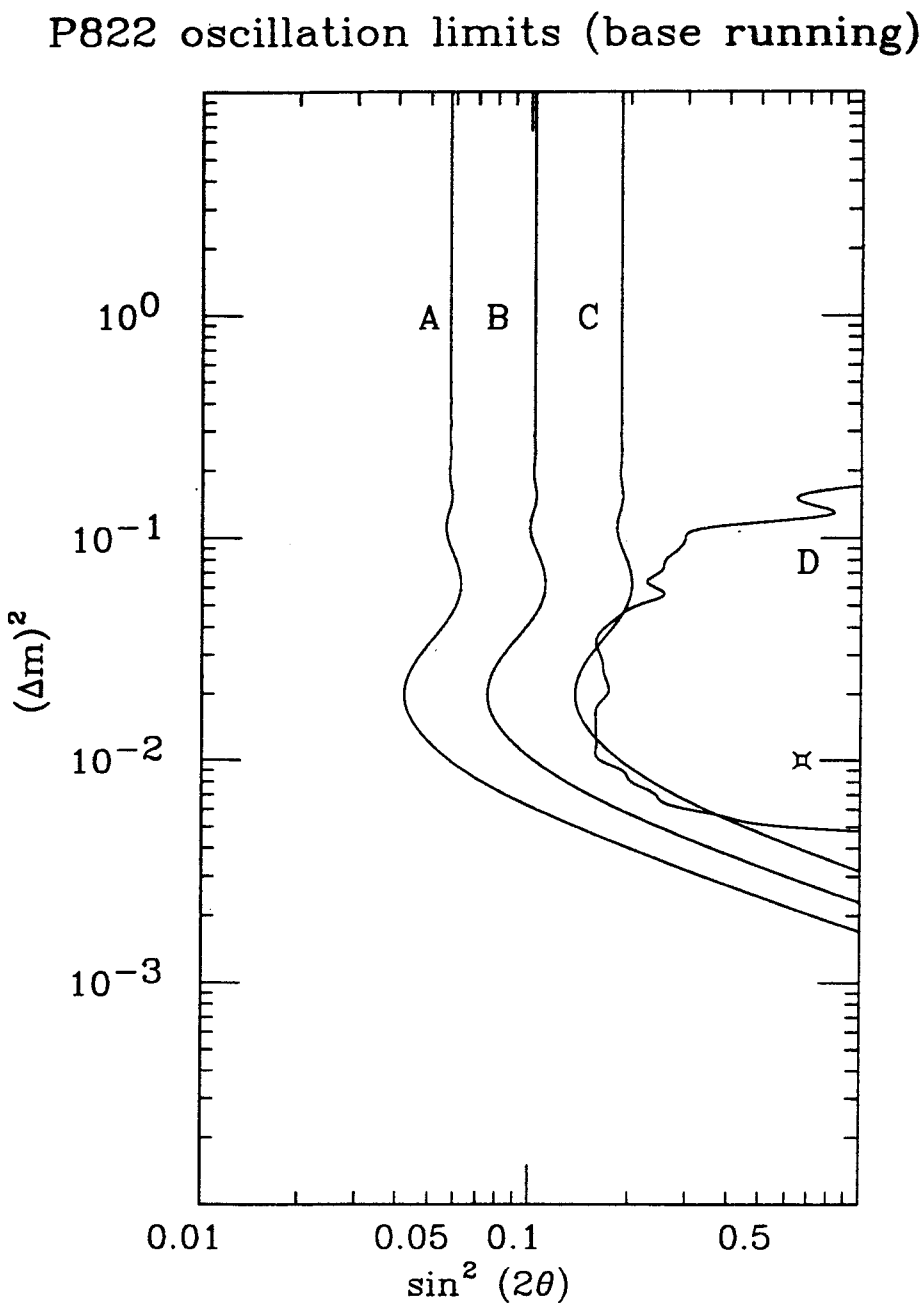

Figure 5: Limits on $\nu_\mu \rightarrow \nu_\tau$ for 822 with 2 9 month runs corresponding to $7.5 \times 10^{20} pot$. Curve A is for the near/far test, B is the CC/tot test from equation 14, C the μ/ν test, and D the energy slope test.

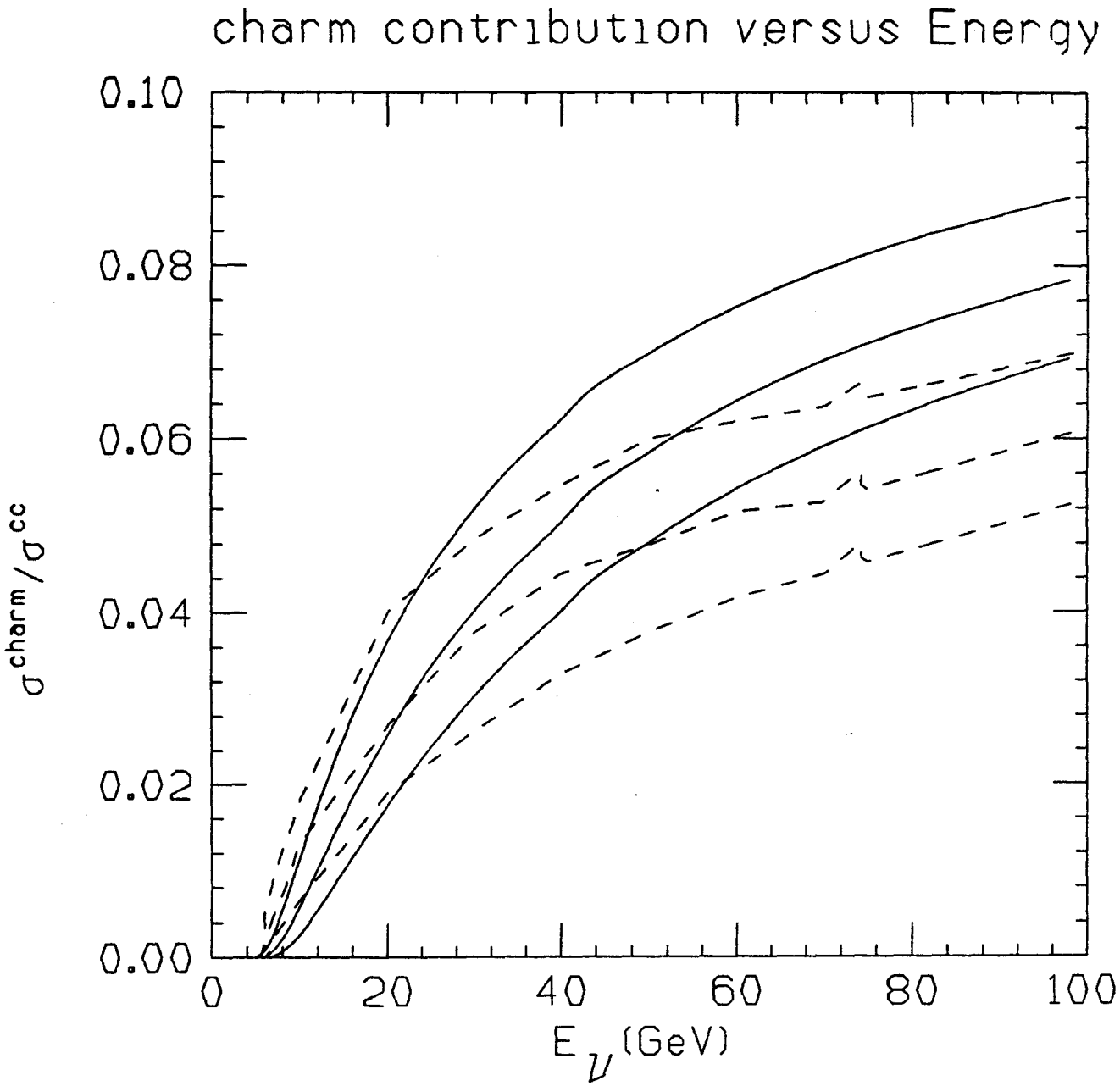

Figure 6: Two estimates of the charm cross section. The dashed lines are a parameterisation of a calculation in the 803 Monte Carlo. The solid line is an independent calculation by R. Phillips. Each calculation is done for 3 charm quark masses as described in the text.

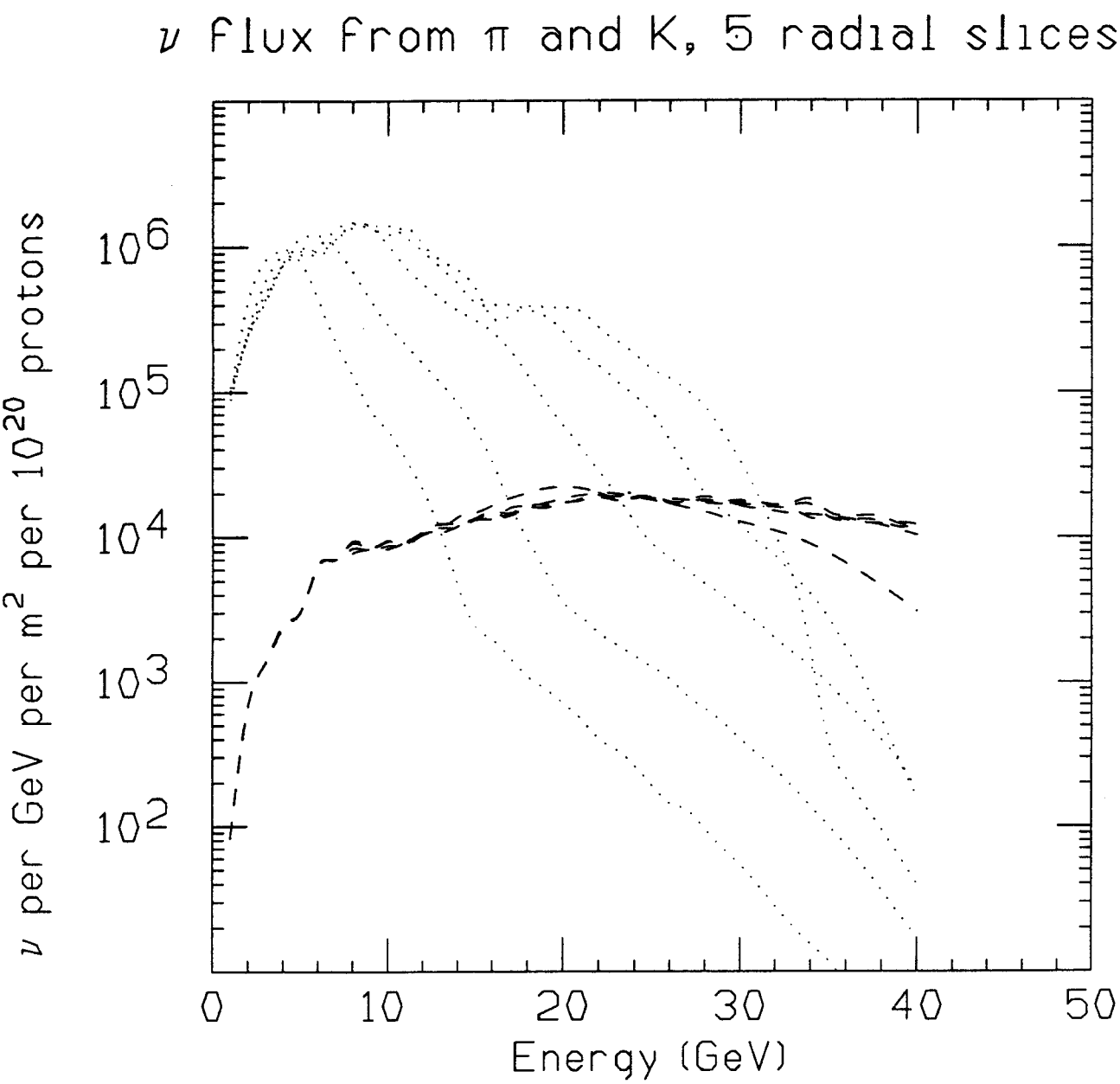

Figure 7: Energy dependence of the neutrino beam for 5 radial slices at the near detector. Neutrinos from π decay are shown with a dotted line, those from K decay with a dashed one. The softest spectrum is for 0-0.25 m, followed by 0.25m to 0.5m; 0.5m to 1m; 1m-2m; and 2m-3m.

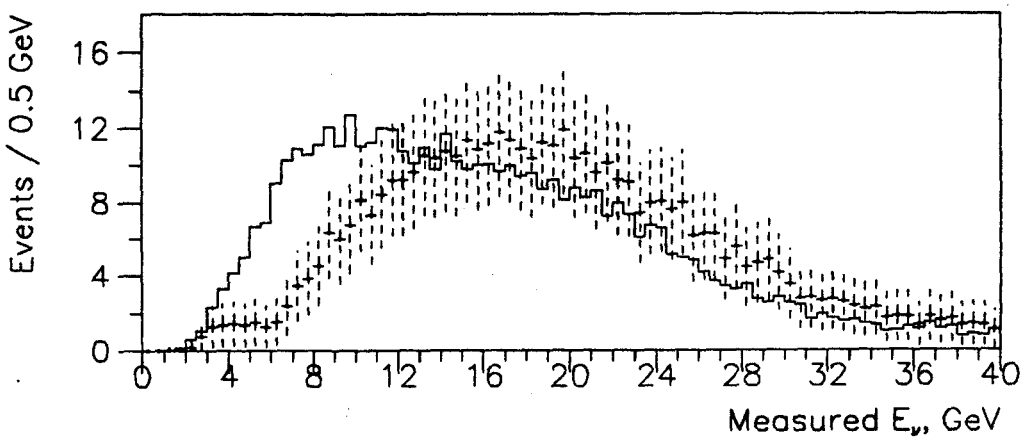

Figure 8: Measured E_ν spectrum for CC events in the far detector (points) compared with the measured E_ν spectrum in the near detector, normalised to 500 events for $\Delta m^2 = 0.01\ eV^2$, $\sin^2(2\theta) = 1$.

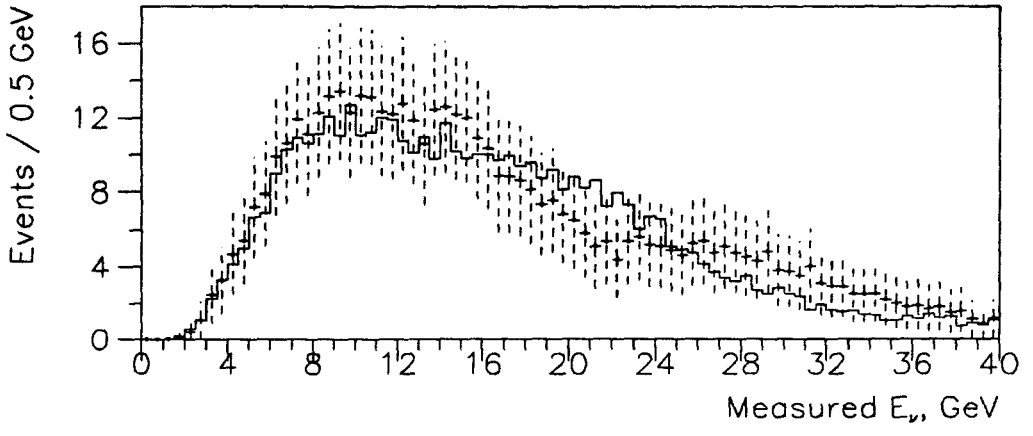

Figure 9: As Figure 9 but for $\Delta m^2 = 0.1\ eV^2$.

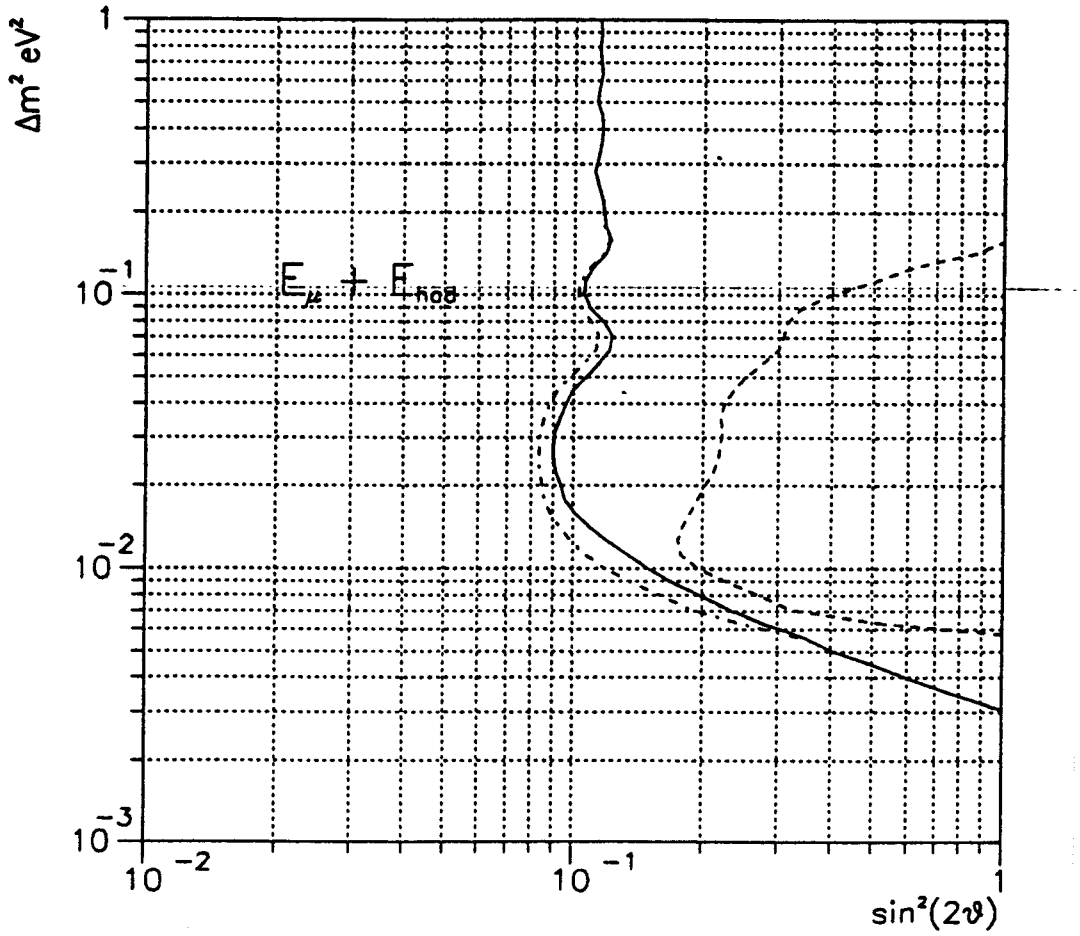

Figure 10: ν_μ disappearance limits, assuming $\nu_\mu \rightarrow \nu_e$, obtained from (a) a comparison of the numbers of CC events in the near and far detectors (solid line), (b) independently from a comparison of the *shapes* of the far and near E_ν spectra for CC events (dashed line) with E_μ measured by the toroid, and (c) the limits obtained by combining these *independent* tests (dot - dash line).

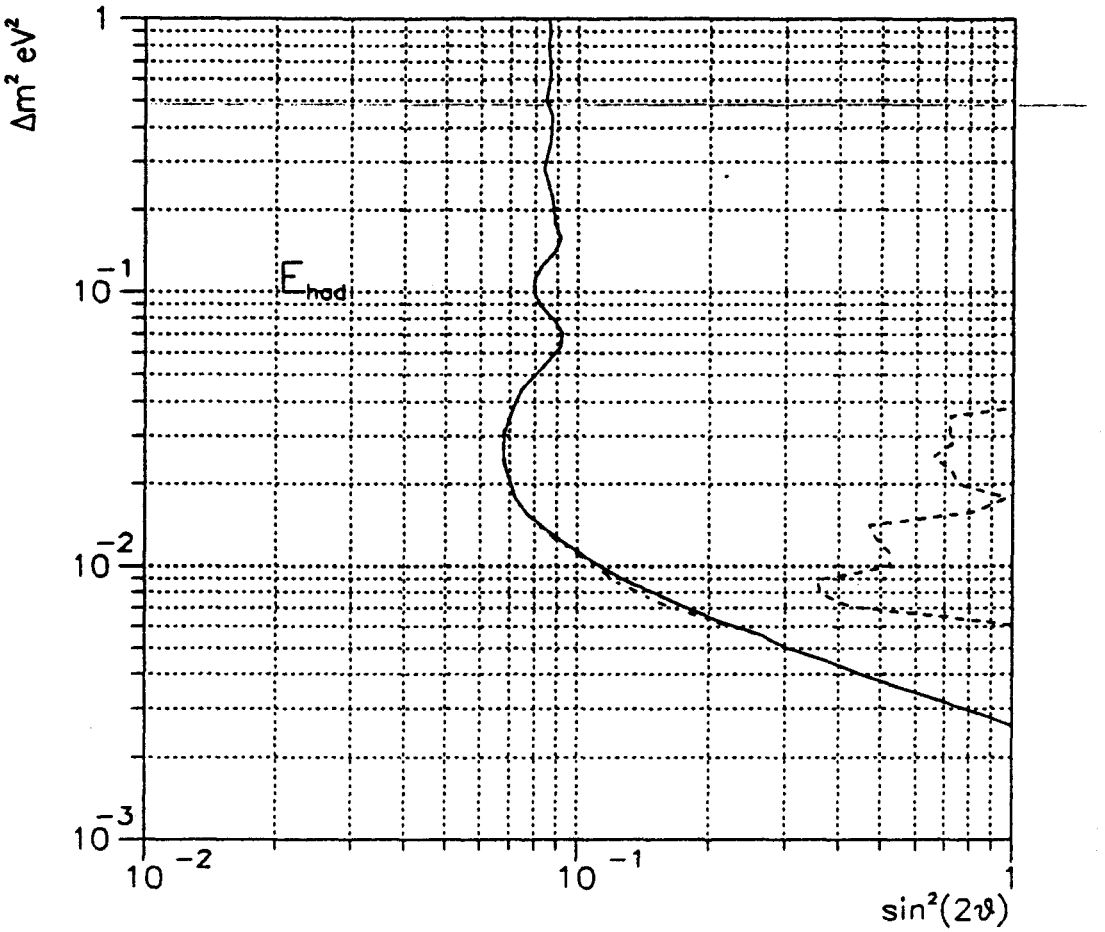

Figure 11: As for Figure 11 but with 880 identified CC events and E_{had} only measured; i.e. without a measurement of E_μ.